

**Differential Targeting of Glucose Transporter
Isoforms in *Leishmania enriettii***

by

Erik Lee Snapp

A Dissertation

Presented to the Department of

Molecular Microbiology and Immunology

and

the Oregon Health Sciences University

School of Medicine

in partial fulfillment of the requirements for the degree of

Doctor of Philosophy

April 23, 1999

School of Medicine
Oregon Health Sciences University

CERTIFICATE OF APPROVAL

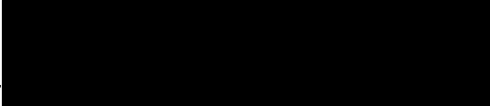
This is certify that the Ph.D. thesis of

Erik Lee Snapp

has been approved



Professor in charge of thesis



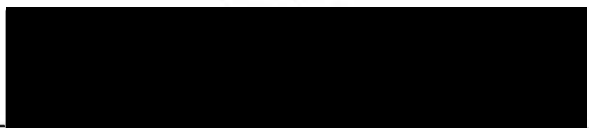
Member



Member



Member



Associate Dean for Graduate Studies

TABLE OF CONTENTS

	<u>Page</u>
TABLE OF CONTENTS	i
ACKNOWLEDGMENTS	vii
LIST OF TABLES	viii
LIST OF FIGURES	viii
NOTE ON NOMENCLATURE	xii
ABSTRACT	xiii
Chapter 1: Introduction	1
I. The Order Kinetoplastida	4
A. Characteristics	4
1. The Kinetoplast and RNA Editing	7
2. <i>trans</i> Splicing	8
3. The Glycosome	9
B. Bodonids and Trypanosomatids	10
1. Trypanosome Species (<i>T. brucei</i> and <i>T. cruzi</i>)	13
2. <i>Leishmania</i>	14
A. <i>Leishmania donovani</i>	15
B. <i>Leishmania enriettii</i>	15
C. Life Cycle of <i>Leishmania</i>	16
D. Leishmaniasis	21
1. Cutaneous Leishmaniasis	23
2. Mucosal Leishmaniasis	23
3. Visceral Leishmaniasis	24
E. Chemotherapy	25

II. The Plasma Membrane	26
A. Flagellar Pocket	27
B. Pellicular Plasma Membrane	28
C. Flagellar Membrane	28
III. Types of Membrane Proteins and their Distribution on the Trypanosomatid Plasma Membrane	31
A. General Classification of Integral Membrane Proteins	31
B. GPI Anchored Proteins	35
C. Acylated and Prenylated Proteins	36
IV. Protein Targeting Mechanisms	38
A. Targeting Based on a Protein Sequence Motif	40
1. Sorting Signals Based on Protein Secondary Structure	40
2. Primary Amino Acid Sequence	40
a. The SKL Glycosomal/Peroxisomal Targeting Sequence	41
b. The Tyrosine-based Membrane Protein Sorting Signal	44
B. Anchoring and Retrieval/Retention Mechanisms (Sequence Based)	44
1. Retrieval (KDEL and KK for ER) (LL for Endocytosis)	45
a. ER Retrieval Sequences	45
b. LL Endocytic Motif	46
2. Anchoring	46
C. Physical Properties of the Protein	47
D. Post-translational Modifications	48
1. Carbohydrate Modifications	49
2. Phosphorylation	50

3. GPI Modifications	51
V. Cytoskeleton	52
A. Higher Eukaryotic Cytoskeletons	55
1. Actin/Spectrin/Ankyrin	55
2. Microtubules: Structure and Function	55
a. General Properties of Microtubules	56
b. Disrupting and Stabilizing Drugs	57
B. The Trypanosomatid Cytoskeleton	57
1. Actin in Trypanosomatids	58
2. Trypanosomatid Microtubules	58
a. Differences Between <i>Leishmania</i> and Higher Eukaryotic Microtubules	59
3. Formation of New Microtubules During Cell Division in Trypanosomatids	60
C. Microtubule Organization in <i>Leishmania</i>	60
1. Subpellicular	61
2. Flagellar Cytoskeleton and Motility	62
a. Axoneme	64
b. Paraflagellar rod	64
3. Flagellar Pocket	65
VI. The Mammalian Glucose Transporter Superfamily	65
A. Structure	66
B. Function and Biochemistry	67
C. Mobilization of GLUT4	69
VII. Trypanosomatid Hexose Transporters	70
A. Regulation (Amastigote and Promastigote)	72
B. Biochemistry (Uptake Studies, Substrates, Inhibitors, and K_m s)	72

C. Isoforms of PRO1 (ISO1 and ISO2)	74
1. Gene Arrangement and Expression	75
2. Biochemistry	75
3. Targeting and Localization	80
D. Other Trypanosomatid Transporters of the Mammalian Glucose Transporter Superfamily	81
1. Other Hexose Transporters	81
a. <i>L. mexicana</i> GLUT1, 2, and 3	81
b. Trypanosome Hexose Transporters	83
c. D2	83
2. MIT	84
 VII. Specific Aims	 85
1. To characterize the flagellar targeting sequence(s) of ISO1	85
2. To characterize targeting and restriction of ISO2 to the pellicular plasma membrane.	86
 Chapter 2: Cytoskeletal Association is Important for Differential Targeting of Glucose Transporter Isoforms in <i>Leishmania</i>.	 88
Abstract	89
Introduction	90
Materials and Methods	93
Results	98
Discussion	105
Figures and Figure Legends	109

Chapter 3: Characterization of a Flagellar Membrane	
Protein Targeting Motif in <i>Leishmania enrietti</i>	132
Abstract	133
Introduction	134
Materials and Methods	137
Results	144
Discussion	153
Figures and Figure Legends	157
Chapter 4: Discussion	182
Future Directions	193
Summary	195
References	200
Appendices	233

ACKNOWLEDGMENTS

This thesis would not have been possible without the patience, wisdom, and encouragement of my advisor, Scott Landfear. All graduate students should have an advisor as attentive and dedicated as Scott. My committee members made significant contributions to the progress of my research. Caroline, thank you for suggesting to look at cytoskeletal tethering. Eric, thank you for suggesting the statistical analysis of the flagellar mutants. Also, thank you for being the most demanding (and funniest) faculty member at OHSU. Buddy, thank you for not holding too much of a grudge against me for stealing your lab manager from you. Thanks to Richard Burchmore, Andreas Seyfang, and Armando Jardim for helpful and challenging discussions. Thanks to Marina Ignatushchenko, Marco Sanchez, Gayatri Vasudevan, Alexey Merz (for the N-propyl-gallate), Aurelie Snyder, Ilja Boor, and Chris Langford for helping with everything from teaching me techniques to being good friends. Special thanks to Rick Landes, Kim Goldsmith, Mary Jane Hendrickson, Syndi Timmers, and Michael and Kari Leon for helping me keep my sanity. Thanks to my mother, Sheryl, for actually encouraging me to study parasites. Thanks to my mother-in-law, Marjorie, for keeping me well fed during graduate school. Finally, thanks to my wife, Sarah, for proof reading my qualifier, "lending" me reagents, understanding my mushroom hunting and computer game addictions, and for encouraging my interest in cell biology. I look forward to many years of dinner time conversations about emerging infectious diseases.

This thesis is dedicated to the memory of my father, Richard Lee Snapp.

LIST OF TABLES	<u>Page</u>
3-1. Mutagenic Oligos for Characterization of the Necessary Amino Acid Sequence for the Flagellar Targeting of <i>ISO1</i>	140
3-2. Oligos to Generate <i>ISO1::ISO2</i> Chimeras	140
3-3. Oligos to Generate Internal Deletions of <i>ISO1</i>	140
3-4. Relative Flagellar Intensities	180
3-5. Relative Flagellar Pocket Staining.	181

ILLUSTRATIONS

Chapter 1: Introduction

1-1. General Features of a <i>Leishmania</i> Promastigote	5
1-2. Trypanosomatid Phylogeny	11
1-3. <i>Leishmania</i> Life Cycle	17
1-4. Integral Membrane Protein Topologies	33
1-5. Glycosomal Targeting Signal Degeneracy	42
1-6. Cytoskeletal Elements	53
1-7. Trypanosomatid Flagellum Cross Section	63
1-8. Comparison of NH ₂ -terminal Hydrophilic Domains of ISO1 and ISO2	76
1-9. Amino Acid Compositions of the NH ₂ -terminal Hydrophilic Domains of ISO1 and ISO2	77
1-10. Comparison of Predicted Secondary Structures of the NH ₂ -terminal Domains of ISO1 and ISO2.	78
1-11. Amino Acid Composition of D2.	82

Chapter 2

2-1. Schematic Diagram Showing the Putative Membrane Topology of PRO1 Glucose Transporter Isoforms, ISO1 and ISO2.	109
2-2. Immunoblots of Triton X-100 Extracted <i>L. enriettii</i> Fractions.	110
2-3. Confocal Micrographs of Triton X-100 Extracted <i>L. enriettii</i> Cytoskeletons.	112
2-4. Immunoblot of Chlorpromazine Treated Detergent Extraction Fractions of <i>L. enriettii</i> .	114
2-5. Immunoblot of Epitope Tagged ISO1 and ISO2 Detergent Extraction Fractions.	116
2-6. Confocal Micrographs of Detergent Extracted Cytoskeletons of Epitope Tagged ISO1 and ISO2 Expressing Cells.	118
2-7. Confocal Micrographs of Cells Expressing ISO1::D2 or ISO2::D2 Chimeras.	120
2-8. NH ₂ -terminal Deletions of ISO1.	122
2-9. Confocal Micrographs of Detergent Extracted Cytoskeletons of ISO1 NH ₂ -terminal Deletion Expressing Cells.	125
2-10. Immunoblots of Detergent Fractions of Cells Expressing D2 or MIT.	128
2-11. Confocal Micrographs of Detergent Extracted Cytoskeletons of Cells Expressing D2 or MIT.	130

Chapter 3

3-1. Chimera Strategy	157
3-2. Internal Deletion Strategy	159
3-3. Analysis of Immunofluorescent Staining on the Flagellum and Flagellar Pocket.	161
3-4. Confocal Immunofluorescence Microscopy Images of ISO1 (1-35)::ISO2 Chimera Expressing Cells.	163

3-5 Confocal Immunofluorescence Microscopy Images and Immunoblot of Cells Expressing Internal Deletion Mutants of ISO1.	164
3-6. Confocal Immunofluorescence Microscopy Images of Alanine Replacement Mutants of ISO1.	167
3-7. Histograms of Relative Flagellar Intensities of ISO1 Alanine Replacement Mutants.	169
3-8. Confocal Immunofluorescence Microscopy Images of Double Alanine Replacement Mutants of ISO1.	171
3-9. Immunoblot of ISO1 Double Alanine Mutants.	172
3-10. Immunoblot of Single Alanine Mutants.	174
3-11. Localization of <i>L. enriettii</i> ISO1 Expressed in Other <i>Leishmania</i> Species	176
3-12. Alignment of ISO1 Flagellar Targeting Motif to Other Trypanosomatid Flagellar Proteins.	178
 Appendices	
AP-1. Topology of ISO2 and the regions of ISO2 recognized by the P1L and anti-GLUT2 antibodies.	236
AP-2. Immunofluorescence of permeabilized and nonpermeabilized ISO2 expressing <i>L. enriettii</i> .	237
AP-3. Immunoblot of the Detergent Extraction of GP63.	240
AP-4. Triton X-100 Extractions.	242
AP-5. Other Detergent Extractions.	244
AP-6. SDS Extractions.	245
AP-7. NaCl Extractions.	246
AP-8. COOH-terminal Deletions of ISO and ISO2	248

AP-9. Alignment of ISO1 and Yeast Glucose Sensor Domains.	251
AP-10. Comparison of the Predicted Secondary Structures of ISO1 and the SNF3.1 Sensor Domain.	253
AP-11. Gallery of Wild Type ISO1.	255
AP-12. Gallery of P22A	256
AP-13. Gallery of P23A	257
AP-14. Gallery of R24A	258
AP-15. Gallery of R25A	259
AP-16. Gallery of T26A	260
AP-17. Gallery of G27A	261
AP-18. Gallery of T28A	262
AP-19. Gallery of T29A	263
AP-20. Gallery of S30A	264
AP-21. Gallery of H31A	265
AP-22. Gallery of A32G	266

A Note on Nomenclature: This thesis uses the genetic nomenclature described by Clayton *et al.* [Clayton, 1995 #828]. Briefly, all genes are designated by italicized uppercase letters (i.e. *ISO1*). Proteins are designated by the same uppercase letters but are not italicized (i.e. ISO1). Fusion proteins are designated 5' to 3'. A fusion of ISO1 and D2 would be written as ISO1::D2. Plasmid constructs are designated in square parentheses and are italicized (e.g. [*pX63 HYG ISO1*]).

ABSTRACT

This thesis describes targeting signals and mechanisms that direct integral membrane proteins to the flagellar and pellicular plasma membranes of *Leishmania* parasites. *L. enriettii* expresses two isoforms of a glucose transporter, ISO1 and ISO2. The two isoforms are identical except for their NH₂-terminal cytoplasmic domains, which lack similarity to each other. ISO1 targets to the flagellar membrane, while ISO2 targets to the pellicular plasma membrane. Because the isoforms discretely localize and differ only in their NH₂-terminal cytoplasmic domains, we exploited ISO1 and ISO2 as a model system to study differential targeting of integral membrane proteins in a contiguous membrane.

The first aim characterizes the flagellar targeting sequence for ISO1. We demonstrated that the NH₂-terminal hydrophilic domain of ISO1 is **sufficient** to retarget a pellicular plasma membrane protein to the flagellar membrane. To identify the sequences within ISO1 that are necessary for flagellar targeting, we created a series of NH₂-terminal deletions and mapped a necessary targeting sequence to the region near amino acids 20-25. A chimera of the first 35 amino acids of ISO1 added to ISO2 was **sufficient** to target this fusion protein to the flagellar membrane. Together, these results suggest that essential flagellar targeting information is located between amino acids 20-35. Individual alanine replacement of amino acids 22-32 did not prevent flagellar targeting of ISO1. However, single mutations in amino acids 25-29 (RTGTT) did alter the relative distribution of ISO1 between the flagellum and the flagellar pocket, suggesting

that these residues play an important role in flagellar targeting. This flagellar membrane targeting motif is the first characterized for any eukaryote. The flagellar targeting signal is functional in several species of *Leishmania* and is likely to be utilized by a variety of flagellar membrane proteins.

The second aim was to characterize the targeting of ISO2 by investigating mechanisms that could direct or restrict ISO2 to the pellicular plasma membrane. Specifically, we tested whether ISO1 or ISO2 associates with the parasite cytoskeleton. The microtubule based cytoskeleton of *Leishmania* was extracted with nonionic detergents, and immunoblots revealed that ISO1 fractionates with the supernatant of the detergent extraction, while ISO2 fractionates with the cytoskeletal pellet. Immunofluorescence microscopy of detergent extracted cytoskeletons revealed intense staining of ISO2 over the subpellicular microtubules, but only background levels of staining of flagellar microtubules. Consequently, ISO2 is tethered to the subpellicular cytoskeleton. Cytoskeletal tethering was also demonstrated for two other *Leishmania* transporters in other species of *Leishmania*. Tethering anchors and may restrict ISO2 and other membrane proteins away from the flagellar membrane. Thus, flagellar targeting and cytoskeletal tethering represent two distinct but complementary mechanisms that result in the discrete distribution of two similar glucose transporters. The work presented in this thesis offers an example of how a unicellular organism is able to elaborate highly differentiated domains of its surface membrane in order to confer distinct biological functions upon different components of the plasma membrane.

Chapter 1: Introduction

Parasitic protozoa represent an important resource for the study of eukaryotic cell biology (21). For example, *L. major* has been used to help characterize the TH1 and TH2 Helper T cell responses of the mammalian immune system (38). In other cases, new biological phenomena have been identified first in protozoa. The tethering of surface proteins *via* glycosphosphatidyl inositol (GPI) anchors (227) was first discovered in African trypanosomes, and later observed in mammalian cells. Because parasitic protozoa represent some of the most evolutionarily ancient eukaryotic cells (22, 234), these organisms also provide the opportunity to study the origins of various eukaryotic cell phenomena. For example, the kinetoplastid glycosome organelle has strong similarities to the higher eukaryotic peroxisome (104). Apoptosis or programmed cell death, a process previously believed to be restricted to multicellular organisms, has been observed in both trypanosomes and *Leishmania* (7, 150, 241). Each of these observations coupled with recent advances in molecular biology techniques for these parasites offers the possibility of learning about the essential components required for these cellular processes. With this perspective, this thesis will focus on the question of how cells create differential distributions of integral membrane proteins in a contiguous membrane using the parasitic protozoan *L. enriettii* as a model organism.

Through studies of protein targeting to cellular organelles, neurons, and polarized epithelial cells, it has become clear that several different mechanisms exist, acting in concert, to organize proteins into discrete cellular subdomains.

Protein sorting often requires a specific targeting signal that can include the primary amino acid sequence, post-translational modifications such as phosphorylation or acylation, and/or a specific three-dimensional conformation. Targeting mechanisms such as receptor binding, vesicular sorting, interaction with cellular motor proteins such as dynein and kinesin, and cytoskeletal tethering all act alone or in concert to create a specific spatial and temporal distribution of a given protein.

Relatively few studies of protein targeting in protozoa, primarily because molecular biology tools such as recombinant DNA expression vectors have only been developed relatively recently for these protozoa. To date the only characterized targeting sequences in kinetoplastids include the glycosomal targeting signal SKL, a mitochondrial import sequence, and an ER localization signal (10, 85, 104, 161, 162, 214).

In this thesis, the differential targeting of two glucose transporter isoforms (ISO1 and ISO2) in *L. enriettii* is characterized. The two isoforms differ dramatically in their NH₂-terminal cytoplasmic domains. ISO1 has a 130 amino acid domain with a predicted pI that is close to neutrality, while ISO2 has a 48 amino acid domain with a predicted acidic pI. The transporters have similar transport properties, but target to different domains within the contiguous plasma membrane. ISO1 localizes to the flagellar membrane and flagellar pocket, while ISO2 localizes to the pellicular plasma membrane and flagellar pocket (177). The studies in this thesis identify a flagellar targeting sequence that appears homologous to sequences in other unrelated flagellar membrane proteins from

other species of *Leishmania* and related trypanosomes. The flagellar targeting motif is the first characterized for any flagellar or ciliary membrane protein in any species of eukaryotic cell. In addition, these studies demonstrate that at least three pellicular plasma membrane transporters from different species of *Leishmania* associate with the parasite cytoskeleton. Two distinct and complementary mechanisms work together to create the discrete distributions of two glucose transporters in a contiguous membrane. The mechanisms appear to be applicable to other membrane proteins in other species of *Leishmania* and trypanosomes.

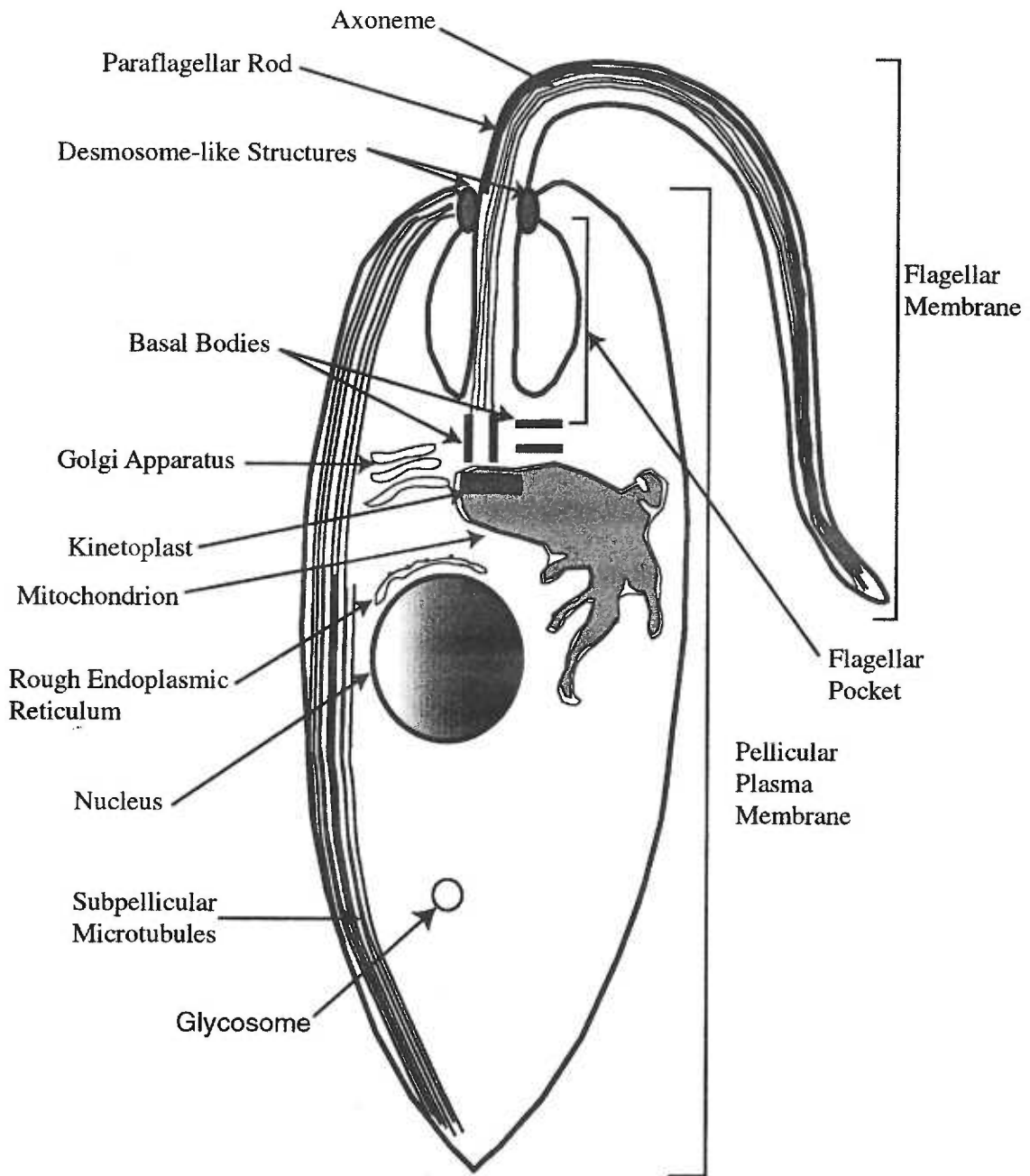
I. The Order Kinetoplastida

Studies in this thesis use the trypanosomatids *Leishmania* and also draw upon work of others in various species of *Trypanosoma*. Both genera belong to the order Kinetoplastida. In the following sections, the characteristics of trypanosomatids and their associated pathologies in mammals will be described.

A. Characteristics

The taxonomic tree of the order *Kinetoplastida* includes single celled protozoa distinguished by the key characteristics of the order including one or more flagella (present during at least one life stage), a specialized glycolytic organelle referred to as the glycosome, an unusual cytoskeleton composed of a corset of highly crosslinked microtubules, genes that are apparently transcribed polycistronically and *trans* spliced with a separate spliced leader sequence, and a specialized organelle within the mitochondrion referred to as the kinetoplast (234). Figure 1-1 illustrates the features of a representative promastigote (insect

Figure 1-1. General Features of a *Leishmania* Promastigote. The figure highlights key domains and organelles of a *Leishmania* promastigote. Features identified on the left side of the figure indicate organelles and cytoskeletal elements. Features identified on the right side of the figure delineate the subdomains of the plasma membrane.



stage) trypanosomatid, *Leishmania*. The following sections describe the distinguishing features, which include the kinetoplast, RNA editing, *trans* splicing, and the glycosome.

1. The Kinetoplast and RNA Editing

Kinetoplastids have an unusual mitochondrial structure composed of globular and tubular extensions. Within the double membrane of the mitochondrion resides a nucleoid referred to as the kinetoplast, which contains concatenated mini and maxi circles of kinetoplast DNA (kDNA)(234). The kinetoplasts of different genera vary from a single capsular region within the mitochondrion to multiple capsules to noncapsulated DNA dispersed throughout the mitochondrion (234). The common features of kinetoplasts include 25-50 maxicircles (each approximately 20-38 kilobases) and thousands of minicircles (each approximately 0.46-2.5 kilobases) of specialized DNA referred to as kDNA (210). The maxi circles encode essential mitochondrial genes (210). However many maxicircle genes do not contain contiguous open reading frames (ORFs) for functional proteins. The mRNAs from the transcribed maxicircle genes are corrected by “guide RNAs” encoded by the both maxi and minicircles (210). The guide RNAs provide the template for the removal or addition of uridines to the mRNA wherever necessary to create an in frame message (101). The extent of RNA modification is impressive. The *T. brucei* mitochondrial genome includes 12 genes that have 3030 uridines inserted or deleted by editing (101). It is unclear why the parasites would evolve and retain such an elaborate and apparently inefficient RNA editing system. Simpson and Maslov speculate

that editing is a remnant of the “RNA world” or developed in early mitochondria due to unknown regulatory demands (209). Sommer *et al.* have demonstrated that mRNA editing occurs in mammalian cells, although on a much more modest scale and by a completely different mechanism (212). These authors found a single nonencoded amino acid that substitutes for the encoded amino acid of the glutamate receptor channels.

2. *trans* splicing

Another unusual eukaryotic RNA processing reaction first identified in trypanosomatids is *trans* splicing. A 39 nucleotide leader encoded by an exon is added *via* a splicing reaction involving two separate RNA molecules (146, 169). The spliced leader or mini-exon consists of a 39 nucleotide 5'-most sequence of the 85 to 140 (depending on the species) nucleotide transcript (3, 147). The *trans* splicing reaction differs from the *cis* splicing reaction, because it fuses exons on two separate RNA molecules rather than fusing exons in the same molecule of RNA (3). The addition of this spliced leader or mini-exon is necessary for the creation and resolution of mRNA from polycistronic mRNA precursors in trypanosomatids (3). *trans* splicing is coupled to addition of the poly (A) tail and appears to define the site of poly (A) addition between two adjacent mRNAs in the polycistronic precursor (124). Interestingly, *trans* splicing has been demonstrated in *Caenorhabditis elegans*, *Euglena*, and flatworms (113, 180, 223). While no *trans* spliced mammalian mRNAs have been identified, Eul *et al.* have demonstrated that thymidine kinase-negative rat 2 cells are capable of *trans* splicing SV40 viral T1 antigen mRNA (68).

3. The Glycosome

The kinetoplastid peroxisome equivalent, the glycosome (see Figure 1-1), contains the glycolytic enzymes that convert glucose to phosphoglycerate, the purine salvage enzyme HGPRTase, CO₂ fixation enzymes, enzymes involved with β -oxidation of fatty acids, and some pyrimidine biosynthetic enzymes (161, 162). The targeting of soluble glycosomal enzymes strongly resembles the peroxisomal targeting sequence in higher eukaryotes (104). Enzymes necessary for the completion of glycolysis exist in the cytosol, as in most higher eukaryotes (162). Glycosomes lack DNA, have a single lipid bilayer, and range in size from 0.2-0.3 μm (162). Concentrating glycolytic enzymes into the glycosome allows kinetoplastids to achieve some of the highest rates of glycolytic flux for any cell type and reduces the amount of protein required to less than 10% of total cellular protein (versus up to 65% in yeast) (162).

Blattner *et al.* demonstrated that *T. brucei* glycolytic enzymes must be restricted to the glycosome during at least one life cycle stage. Expression of phosphoglycerate kinase (PGK) during the bloodstream stage proved lethal to the parasites (24). The authors speculate that the extraglycosomal distribution of the enzyme disrupts the glycolytic flux by changing the equilibrium of ATP between the cytosol and glycosome (24). The enzyme in the cytosol could outcompete the glycosomal enzyme and deplete the source of glycosomal ATP, which would shut down the first steps of glycolysis and thus inhibit the entire process (24).

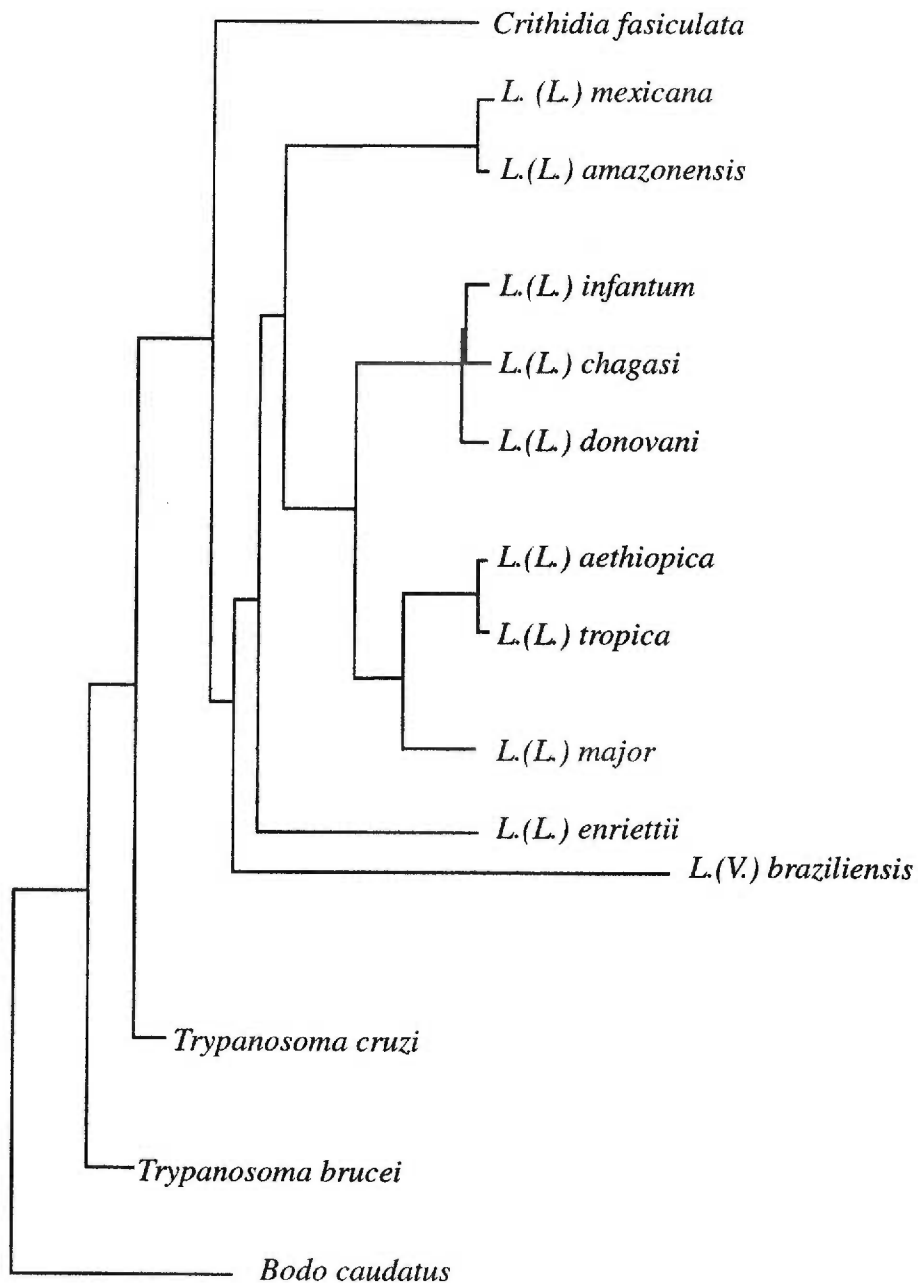
B. Bodonidids and Trypanosomatids

Vickerman and others hypothesize that the earliest kinetoplastids branched from the most primitive eukaryotes shortly after the appearance of mitochondria (234). Kinetoplastids include two major families, the *Trypanosomatidae* and the *Bodonidae*, (or suborders *Trypanosomatina* and *Bodonina*) (182) which are both single celled flagellates that contain a kinetoplast within their mitochondria (234). The *Bodonidae* are mostly free-living cells, while the *Trypanosomatidae* primarily exist as obligate parasites (182, 234).

Members of the Trypanosomatid family include parasites of insects, fish, amphibians, plants, reptiles, birds, mammals, and even other protozoa (234). Trypanosomatid species include the human pathogens trypanosomes and *Leishmania*. Trypanosomatids have digenetic life cycles that alternate between invertebrate vectors, including insects and leeches, and vertebrates ranging from eels and marine fish to reptiles, birds, and mammals (182). Trypanosomatids have a single flagellum, present during at least one life cycle stage and unlike *Bodonidae*, lack a cytopharynx (182). Indirect evidence exists for sexual interaction for trypanosomatids, but only binary fission has been characterized as the mode of reproduction (182). This thesis will focus on trypanosomatids, specifically *Leishmania* and trypanosomes.

Figure 1-2 represents the phylogeny of *Leishmania* in relation to the trypanosomatids *Trypanosoma cruzi*, *Trypanosoma brucei*, and *Crithidia fasciculata* in relation to the *Bodo caudatus*. The phylogeny is based on the DNA

Figure 1-2. Trypanosomatid Phylogeny. Two separate trypanosomatid phylogenetic trees based on DNA and RNA polymerase subunits and small and large ribosomal RNA subunits were combined to delineate the relatedness of *T. brucei*, *T. cruzi*, several species of *Leishmania*, and *Crithidia fasciculata*, with *Bodo caudatus* as the outgroup for the rRNA based tree and *Endotrypanum monterogeii* as the outgroup for the polymerase based tree. The key points of this figure include 1) *T. brucei* represents one of the most ancient trypanosomatids, 2) *Leishmania* includes two subgenera- *Leishmania* and *Vianna*, 3) *Leishmania* includes three major species groupings - *mexicana*, *donovani*, and *tropica*, and 4) *Leishmania enriettii* can not be classified within the major species groupings. The tree is based on trees by Maslov *et al.* and Croan *et al.* (47, 137).



(not to exact scale)

polymerase α catalytic subunit and the small subunit of ribosomal RNA (47, 137).

Figure 1-2 does not conform to an exact scale, but rather represents relative relationships between the species and genera. The placement of *L. enriettii* is arbitrarily between the *L. (Leishmania) tropica* complex and *L. (Viannia) braziliensis*. A search of the literature has not revealed a phylogenetic relationship for *L. enriettii*, other than the designation of the species being a *Leishmania* subspecies rather than a *Viannia* subspecies.

The trypanosomatid phylogeny highlights two key points. First, there are three major groupings of *Leishmania* (*mexicana*, *donovani*, and *tropica*) with other unclassified individual species, such as *L. (L.) enriettii*. The *Leishmania* groupings correspond to geographical distribution between the New and Old World. Croan *et al.* propose that Old World *Leishmania* evolved from New World *Leishmania* species (47). Second, the two major trypanosome human pathogens, *T. cruzi* and *T. brucei* are not very closely related. Numerous differences in host milieu (intra- vs. extracellular), insect vector, geographical distribution, and pathogenicity support evidence for an early divergence between the two species. In the following sections, important characteristics of trypanosomatids relevant to this thesis will be described.

1. Trypanosome Species (*T. brucei* and *T. cruzi*)

All trypanosomes have at least 2 distinct life stages including an invertebrate (leeches, Hemiptera, or Diptera) vector stage (promastigote) and a vertebrate (Bird, Mammal, Amphibian, or Teleost) host stage (amastigote) (137). The evolutionary emergence of members of the trypanosomatid family remains

speculative. Maslov *et al.* propose that trypanosomes began as parasites of leeches or insects (probably both simultaneously) and independently evolved lifestages that parasitize vertebrates (137).

T. brucei and *T. cruzi* both cause significant diseases in humans but differ in several important ways. The New World species, *T. cruzi*, is restricted to Central and South America, while the Old World species, *T. brucei*, is localized to Africa. The parasites have different insect vectors; the *Triatoma*, reduviid bugs for *T. cruzi* and *Glossina*, and the tsetse fly, for *T. brucei* (44). More significantly, *T. brucei* is free living in the bloodstream of the mammalian host, while *T. cruzi* is an intracellular parasite of endothelial cells of the spleen and liver, as well as all types of muscle cells (182).

2. *Leishmania*

Leishmania form the most recent genus of trypanosomatid evolution (69, 234). These parasites exist throughout the subtropical regions of the world. The two types of hosts include the gut of the insect vector phlebotomine sandflies (belonging to the genera *Phlebotomus* and *Lutzomyia*) and the phagolysosomes of host macrophages in vertebrate hosts. While *Leishmania* have differentiated significantly during their proposed evolution from trypanosomes, certain characteristics have remained and are relevant to this thesis. In particular, *Leishmania* and trypanosomes both have a distinct flagellum with integral membrane proteins specific to the flagellum, a flagellar pocket, and a microtubule corset cytoskeleton (see Figure 1-1). For the purpose of this thesis, the cell

biology of the trypanosomes and *Leishmania* are similar enough to merit comparisons of putative protein targeting sequences and mechanisms.

Leishmania species differ in size, associated disease, host range, and nutritional requirements. Identifying classification is made on the basis of antisera reactivity, lectin binding, DNA hybridization, host specificity, and comparison of electrophoretic mobility of isoenzymes secreted into culture media (44). Old world *Leishmania* species include *L. donovani*, *L. tropica*, and *L. major*. New World species include *L. mexicana*, *L. brazilenesis*, *L. amazonensis*, and *L. chagasi*. The New World species are further subdivided and include numerous parasites of mammals and reptiles (47). The two species used in the thesis studies are *L. enriettii* and *L. donovani*.

A. *L. donovani*

Donovan and Leishman independently described the *Leishmania* protozoan in 1903, as the causative agent of Dum-Dum fever, also known as Kala Azar or visceral leishmaniasis (80). The amastigote form of the parasite is also known as the Leishman-Donovan (L-D) body (182). The eponymous species, *L. donovani*, primarily causes a visceral infection of the macrophages of spleen, liver, lymph nodes, intestine, and bone marrow (182). Dogs provide the main parasite reservoir in all countries except India, in which humans act as the disease reservoir (182).

B. *Leishmania enriettii*

Medina first observed *L. enriettii* amastigotes in domestic Hartley guinea pigs (*Cavia porcellus*) in 1946 in Brazil (116). Naturally occurring infections of

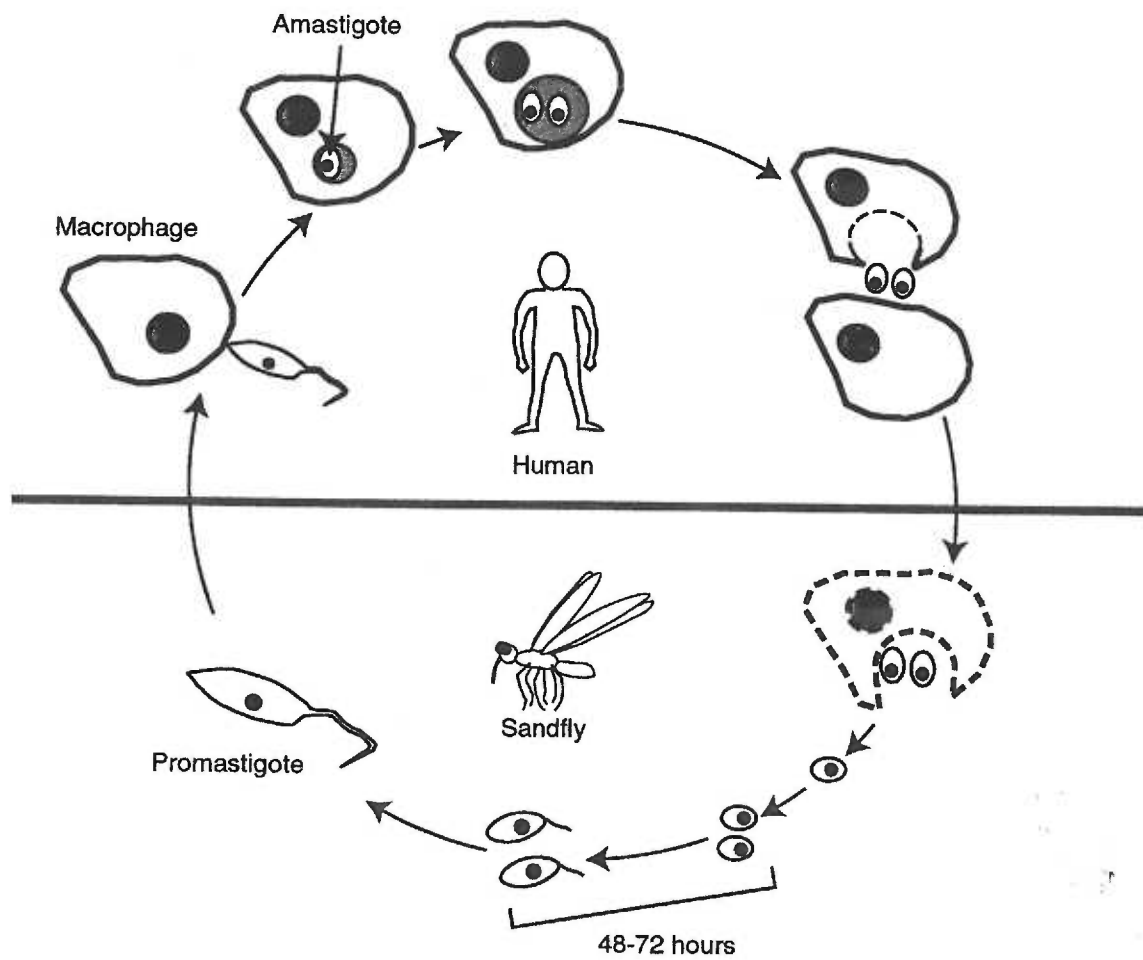
guinea pigs have been reported in 1946, 1967, and 1991 in Brazil (116). The parasite is highly specific in its host range and is unable to productively infect the closely related wild guinea pig (*Cavia aperea*) or a variety of other mammals including mice, dogs, and humans (116). The inability of *L. enriettii* to infect humans has made the parasite useful for laboratory studies because of the minimal risk to workers. The sandfly vector and natural host for *L. enriettii* remain unknown.

Instead of *L. enriettii*, most laboratories prefer to study *L. major*, *L. donovani* or *L. mexicana*, which have the advantages of defined sandfly vectors and medical relevance. *L. mexicana* also can be grown as axenic amastigotes, which greatly facilitates studies of the mammalian stage of the parasite (18).

C. Life Cycle of *Leishmania*

The dimorphic life cycle (Fig 1-3) of *Leishmania* consists of a flagellated sandfly stage (promastigote) and nonflagellated intracellular vertebrate host stage (amastigote). The highly motile promastigote stage has a characteristic elongated bullet shaped cell body with a significant invagination, the flagellar pocket, at one end. In contrast the flagellum regresses into the flagellar pocket of the amastigote. The amastigote cell body has a rounded shape and lacks motility. Both life stages reproduce by binary fission (182). Initially, the promastigote begins as a nectomonad, which is the most elongated stage of the parasite and is either free swimming or attached to the insect midgut by insertion of the flagellum between the epithelial cilia of the gut (5, 17). Whether specific flagellar proteins help mediate the insertion is not clear. The parasites mature into

Figure 1-3. *Leishmania* Life Cycle. *Leishmania* parasites are present as the flagellated promastigote form in the gut of the phlebotomine sandfly host. Over time, the promastigote matures into an infection competent metacyclic form that is transmitted to the mammalian host during a sandfly blood meal. Mammalian host macrophages clear the parasites from the bloodstream and isolate the parasites into phagolysosomes. The parasites transform from the flagellated oblong form to the smaller spherical amastigote form within the phagolysosome. Following transformation, the amastigotes divide by fission, eventually overwhelming and killing the host macrophage, and proceed to infect new macrophages. The life cycle is completed when another sandfly takes a bloodmeal. Host macrophages lyse within the sandfly gut, liberating amastigotes, which divide and transform into the elongated flagellated promastigote form.



haptomonads or broad cells with expanded flagellar membranes connected to the insect foregut by hemidesmosome-like attachments (5, 17). Next the parasite transforms into rounded or oval paramastigotes (5). After 4-5 days, the metacyclic parasites (which are competent to infect mammals) migrate to and clog the sandfly esophagus and pharynx (17, 182). It appears that the sandfly pumps the blockade of promastigotes in and out to clear the proboscis during a bloodmeal obtained from a mammal (182). Such behavior may enhance the chance of successfully infecting a mammalian host.

In the bloodstream of the mammalian host, macrophages rapidly clear parasites, which unwittingly serves the dual purposes of protecting the parasite from the lethal complement components of mammalian sera and shuttling the parasite to its preferred environment in the mammalian host (140).

Phagolysosome sequestered parasites undergo a transformation from the morphologically distinct elongated and flagellated metacyclic promastigote to the nonflagellated rounded amastigote form (5, 140). Amastigotes range from 2.5 to 5 μm wide and comprise some of the smallest nucleated cells known (182).

Parasites divide and eventually prove lethal to the macrophage, inducing lysis, which permits the amastigotes to infect other macrophages. The inhospitable environment of the phagolysosome has a pH of 4.7-5.2, is oxidative (contains nitric oxide, hydrogen peroxide, and superoxide anion), and is low in glucose and proline (140, 187). Amastigotes feed primarily on non-esterified fatty acids (140).

The life cycle is completed when another sandfly takes a bloodmeal from an infected host. Within the gut of the sandfly, the blood meal is enveloped in the peritrophic membrane which is secreted by the midgut epithelium (17).

Macrophages lyse and release amastigotes, which first divide and then transform into promastigotes over the next 24-48 hours (5, 83, 123). Transformation of *L. mexicana* from promastigotes to amastigotes *in vitro* requires the presence of non-esterified fatty acids, the primary energy source for amastigotes (83). The gut of the sandfly has a pH that is close to neutrality, a temperature that is determined by the ambient environment, and contains the nutrients proline and glucose that are obtained from blood meals and glucose rich plant sap (195). The glucose meal has been shown in some studies to be important for enhancing the development of parasite competence for infection of mammalian hosts (195, 196, 239).

The description of the life cycle highlights the extreme differences in environments (pH, temperature, nutrients, and oxidative potential) that the parasite encounters between its two hosts. Adaptation to each environment requires differential gene regulation to allow the parasite to express appropriate sets of proteins to take advantage of the differences in available nutrients, to protect against different host defenses, and to acquire competence to infect the next host.

Several groups have demonstrated that mRNA levels of a variety of genes differ in relation to the life stage of *Leishmania* (14, 34, 35). However, gene regulation in *Leishmania* differs significantly from other eukaryotes. RNA polymerase II transcribed genes do not appear to have regulatory promoters (14,

242). Instead, gene regulation appears to be primarily post-transcriptional. The genes of *L. mexicana* promastigote and axenic amastigote specific proteins are transcribed at similar levels during both life cycle stages (34). Burchmore and Landfear have shown that while mRNA levels differ markedly between the two life stages for the *L. mexicana* glucose transporter (GT) genes, the relative rates of glucose transporter gene transcription are similar in promastigotes and amastigotes (34). The authors propose that regulation may occur at the level of mRNA stability (34). However, Wong *et al.* have identified a regulatory element in *L. enriettii* that affects the strandedness of transcription of genes and thus affects levels of mRNA (242).

D. Leishmaniasis

Trypanosomatid protozoa include some of the most important pathogens of man, particularly within the subtropical regions of the world. Leishmaniasis has afflicted humans for centuries. Peruvian ceramic masks from A.D. 400-900 resemble modern day espundia victims (80). *Trypanosoma* and *Leishmania* both register on the World Health Organization/Tropical Disease Research six most important tropical diseases (20). The World Health Organization latest epidemiological survey begins with the statement "It is clear that official data are frequently a gross underestimate of the reality as official data are obtained almost exclusively through passive case detection"(1). *Leishmania* infections are estimated at over 500,000 cases of visceral leishmaniasis and over 1,000,000 cases of cutaneous leishmaniasis annually (1). By recent estimates, 80,000 people die from leishmaniasis every year and as many as 350 million people are at risk

for exposure to leishmaniasis (1, 8). Because of the high mortality associated with leishmaniasis and other parasitic diseases, medical research leading to protection of people from these devastating diseases is of great importance. The urgency is compounded due to a real trend in increased incidence of leishmaniasis throughout the world. WHO cites resource harvesting and road construction in forests, economic migration, and urbanization for sources of increased exposure to infected sandflies. In addition, co-infection with HIV is now considered an “emerging disease” that threatens intravenous drug users (1).

While leishmaniasis is confined primarily to developing nations, industrialized nations such as the United States are not free from *Leishmania*. For example, 27 nontravel related *Leishmania* infections have been recorded in Texas over the last 93 years (142). A wood rat (*Neotoma micropus*) reservoir and sandfly vector (*Lu. anthophora*) have been identified for the Texas strain of *Leishmania* (142). Travel and military ventures also expose citizens of industrialized nations to *Leishmania*. For example, nine cases of visceral leishmaniasis in Americans have been associated with Desert Storm (20).

Leishmania infections of humans result in three disease types: cutaneous, mucosal, and visceral leishmaniasis. The diseases range in severity from self-healing ulcerations to grossly deforming lesions of the mucosa to life threatening immunosuppression (20, 44). All of the diseases result from infection of macrophages found in different locations in the host. Parasites not only impair the killing ability of infected macrophages but also induce a general immunosuppression of the host (44, 80). The macrophages can be induced to kill

Leishmania by treatment with cytokines, especially interferon- γ (140), which induces production of nitric oxide, the primary anti-leishmanial activity of the macrophage (79).

1. Cutaneous Leishmaniasis

Cutaneous leishmaniasis results from infections of *L. major* and *L. aethiops* in Africa and Asia and by *L. mexicana* and *L. braziliensis* in Central and South America (44). Parasites infect macrophages of the dermis and mucosa resulting in manifestations ranging from a single lesion to diffuse ulcerations that can cover the entire body (80). Infections vary from self-limiting sores to disfiguring scars (44). In cases of co-infection with HIV, normally cutaneous disease causing species have been observed to disseminate and cause visceral disease (44). Thus, even the mildest forms of leishmaniasis can have life threatening consequences.

2. Mucosal Leishmaniasis

Mucosal leishmaniasis is observed primarily in the Americas and results from *L. braziliensis*, *L. guyanensis*, and *L. panamensis* infections (44). The disease involves infection of macrophage permeated deep mucosa of the nasopharyngeal regions. Often the patient lacks an observable initial lesion, and pathogenesis may not develop for two to 35 years after the initial infection (44). Infection of the mucosa and mucocutaneous junctions results in mucosal granulomas that lead to either an enlarged nose and mouth or ulcerative mutilation that can destroy most of the palate (44, 136). Espundia (from the Portuguese word for sponge, because of the sponge-like appearance of the patient's skin)

refers to the severe form of mucosal leishmaniasis caused by *L. braziliensis* (44). Patients often suffer from and may die from nasal or pharyngeal obstructions (44).

3. Visceral Leishmaniasis

Of all of the diseases caused by *Leishmania*, visceral leishmaniasis ranks as the most serious form. *L. infantum* and *L. donovani* cause visceral leishmaniasis in Asia and Africa, while *L. chagasi* is the causative agent in the Americas. Untreated patients usually die, while the death rate in treated individuals varies from 1-11% (20). Disease onset usually occurs from two to four months following the initial infection (44), but incubation times of three weeks have been reported (44). Patients suffer from fever, pain, splenomegaly, hepatomegaly, exhaustion, and anorexia (44). In India and Burma, late stage infections lead to a pronounced darkening of the skin which is the origin of the Indian name for visceral leishmaniasis, “kala-azar” or black skin (44). Late stage disease involves secondary bleeding and significant immunosuppression that leads to secondary infections including pneumonia, tuberculosis, measles, and septicemia, which often lead to the death of the untreated patient (44, 136). Poor nutrition and coinfection with other parasites, such as malaria, further suppress the patient’s ability to mount an effective immune response against *Leishmania*. Prior immunosuppression, such as HIV infection, leads to higher parasite loads in patients and a poor response to treatment (44). Other forms of visceral leishmaniasis exist, including inapparent to mild flu-like disease, which was often seen in U. S. soldiers that were deployed in Desert Storm (20).

E. Chemotherapy

Treatment of visceral leishmaniasis includes three major drugs, which all have significant toxicity, require injections, and have become less effective with the rise of drug resistant parasites. The drugs include pentavalent antimony (Pentostam or Glucantime), pentamidine, and Amphotericin B. The mode of action has not been defined for any of the drugs. Because of the devastating impact of leishmaniasis, the absence of inexpensive highly effective drugs with low toxicity makes the outlook for disease control poor. Furthermore, no effective vaccines exist.

Pentostam, the primary treatment for visceral leishmaniasis (44) has numerous side effects including pancreatitis, neuropathy, and cardiotoxicity which can lead to sudden death (20). An additional complication is that drug toxicities such as liver or bone marrow dysfunction resemble the effects of Kala Azar (136). Pentostam treated patients have a 20% relapse rate with two months after discharge from the hospital (20).

An alternative drug, Pentamidine, has a 99% cure rate with a 21% relapse rate (20). Pentamidine is preferable to antimony for treating cutaneous leishmaniasis, because less toxic low doses of Pentamidine can be used to treat the disease (20). Side effects include hyperglycemia and tachycardia (20). To reduce toxicity and to treat drug resistant strains, pentamidine often is used in combination with antimony (20).

Another alternative for the treatment of antimony resistant parasites is the antifungal, Amphotericin B (deoxycholate), an ergosterol-like compound that

mimics a membrane component of *Leishmania* (20). Amphotericin B has near 100% cure rates for visceral leishmaniasis (20). Side effects include decreased renal function and infusion related effects such as fever and rarely cardiac arrest (20). In many regions with antimony resistant leishmaniasis, amphotericin B has become the drug of choice for visceral disease (20).

Other drugs have been tested for anti-leishmanial activity. However, none to date has the efficacy of the toxic frontline drugs, and there are reports of drug resistance to the primary drugs. Clearly, new therapies with high specificity and low toxicity are needed. Study of the basic biology of *Leishmania* may yield insights that could form the basis for new therapies.

II. The Plasma Membrane

The plasma membrane consists of a lipid bilayer and numerous membrane proteins. The membrane acts as a barrier and the interface between the cell and the environment. The parasite plasma membrane contains lipids typical of eukaryotes, including: 48% phospholipids (choline, ethanolamine, and inositol based phospholipids), 31% sterols (ergosterol and cholesterol), and 20% triglycerides (primarily unsaturated fatty acids)(2). *Myo*-inositol anchored glycolipids including lipophosphoglycan, LPG and GPI anchored proteins, especially GP63, cover the majority of the plasma membrane (80). The dense coating of LPG and GP63 assists in promastigote entry into macrophages, attachment to the sandfly midgut, and may protect the parasite from degradation within macrophage phagolysosomes (5, 17, 80, 140, 175).

The plasma membrane, while continuous, can be divided into three distinct domains with differentially localized proteins (74, 166, 177). The three membrane domains include the flagellar pocket, the pellicular plasma membrane, and the flagellar membrane (9).

A. Flagellar pocket

The flagellar pocket membrane separates the flagellar membrane from the pellicular plasma membrane (Fig. 1-1). Aside from the desmosome-like structures that attach the pellicular plasma membrane to the flagellar membrane, no obvious structures, such as tight junctions, define the flagellar pocket. As no obvious physical barrier exists between the flagellar pocket and both the pellicular plasma and flagellar membranes, the mechanism for the localization and retention of proteins, such as the GPI-linked transferrin receptor, remains unclear (78). The pocket “contains an electron dense carbohydrate-rich matrix of unknown structure (163).” The adhesion zone, that defines the flagellar pocket boundaries, allows molecules as large as antibodies and LDL to pass from the surrounding environment into the flagellar pocket space (163).

Unlike the majority of the cell surface, the flagellar pocket lacks underlying crosslinked microtubules (61). The exposed membrane is the only known site of endo- and exocytosis for *Leishmania* (61, 163, 240). In fact, the flagellar pocket exhibits one of the highest rates of exocytosis of any organism (45). Integral membrane proteins bud in vesicles from the Golgi and are added to the surface of the flagellar pocket (163).

B. Pellicular plasma membrane

The pellicular plasma membrane (Fig. 1-1) makes up about 70-80% of the total plasma membrane and covers the region from the anterior tip to the desmosome-like structures that connect to the flagellum (9, 45). The pellicular plasma membrane covers the subpellicular microtubule array that defines the bullet-like shape of the promastigote. Dwyer *et al.* demonstrated that the pellicular plasma membrane physically attaches to the subpellicular microtubules, probably by linker proteins (62). Although the pellicular plasma membrane attaches to the cytoskeleton, the membrane is not static. Bulow *et al.* used Fluorescence Recovery After Photobleaching (FRAP) to demonstrate that the plasma membrane continuously flows and can randomize cell surface components, such as VSG (in *T. brucei*) in 40 minutes (163). Presumably, integral membrane proteins also flow in the membrane, ultimately returning to the flagellar pocket for endocytosis and degradation.

C. Flagellar membrane

The flagellar membrane (Fig. 1-1) encases the axoneme and the paraflagellar rod of the parasite flagellum and covers about 20-30% of the cell surface (9, 45). Several studies demonstrated that the kinetoplastid flagellar membrane protein population differs from the proteins in the pellicular plasma membrane (65, 74, 166, 177, 244). The *Leishmania* pellicular plasma membrane attaches to the flagellar membrane through a single row of dense bodies that “are basically similar in structure to epithelial cell desmosomes,” as observed by electron microscopy (234). The desmosomes differ from the annulus ring found

in spermatozoa, in that the desmosome ring does not form a continuous barrier (15, 233). Particles as large as antibodies and LDL readily diffuse through the desmosome-like structures and enter the flagellar pocket space (163). Without an obvious physical barrier to block exchange of proteins between the flagellar membrane and the flagellar pocket, it is unclear what mechanism sorts and retains membrane proteins in each membrane domain.

A potential clue comes from studies of surface membrane lipid compositions. Although no formal studies have been published, some reports suggest that the trypanosomatid flagellar membrane lipid composition differs from that of the pellicular plasma membrane (9). Interestingly, studies on the cilia and flagella (of other protozoa, such as *Tetrahymena*, *Euglena*, and *Paramecium*) do demonstrate a lipid composition distinct from the rest of the cell surface (102). In particular, flagella and cilia contain a sterol ratio as much as 1.5 times higher than the rest of the cell (102). The functional significance of sterols in the membrane is theoretical. Yeagle proposes that the ability of cholesterol to flip-flop between leaflets in the membrane could assist shape changes by rapidly modifying the relative amounts of membrane material on each side of the leaflets (245). Furthermore, cholesterol reduces membrane permeability (245). Thus, an organelle that constantly bends and deforms could better maintain membrane integrity with a high cholesterol/sterol content. Another significant property of cholesterol is that it can modulate transporter activity (245). Cilia of *Tetrahymena* and *Paramecium* also contain quantitatively higher concentrations of amide linked fatty acids in sphingolipids and ether

linked fatty alcohols in glycerolipids (102). However, sterols have a high affinity for sphingolipids and repel phosphatidylethanolamine (245). Thus, the increased level of sterols could play a role in determining the concentrations of other lipids in the flagellar membrane. Because the kinetoplastid flagellum architecture and functions resemble those of cilia and flagella of other organisms (i.e. all share the same basic microtubule axoneme and make similar beating motions), studies of the membranes of the flagella and cilia of other organisms may prove relevant to kinetoplastids. Thus, it is plausible that kinetoplastid flagellar membrane lipids differ from those in the pellicular plasma membrane. Furthermore, the mechanisms that generate the distinct lipid and protein compositions may be analogous between organisms. Because the flagellar protein and lipid composition (at least in the ciliary and flagellar membranes of other protozoa) differ distinctly from the rest of the cell surface, it is reasonable to consider the flagellar membrane as a *bona fide* subdomain of the plasma membrane.

At least two possible nonexclusive mechanisms could generate the differences in flagellar lipid composition. First, lipid modifying enzymes have been localized to flagella and cilia (102). Second, cellular trafficking mechanisms (i.e. vesicular sorting) could enrich flagella and cilia for specific lipids, just as vesicular sorting enriches the GPI-anchored membrane protein content of the apical membrane of polarized epithelial cells (227). If sorting mechanisms exist for the lipid components, such machinery also could sort

integral membrane proteins to the flagellar membrane. However, a potential caveat is that vesicles have not been observed in flagella or cilia (27).

III. Types of Membrane Proteins and Their Distribution on the Trypanosomatid Plasma Membrane

Membranes serve as the barrier and interface between the cell and the external environment. To sense and interact with the external environment, cells utilize proteins that span or associate with the plasma membrane. Membrane proteins fall into two major groups, integral membrane proteins and lipid modified proteins that associate with either the cytoplasmic or extracellular membrane leaflets (Fig. 1-4). Another group of proteins associates with the membrane by interacting with integral membrane proteins. This section will describe the types of membrane proteins and give examples of each in trypanosomatids.

A. General Classification of Integral Membrane Proteins

Integral membrane proteins primarily originate from the endoplasmic reticulum (ER). The protein inserts into the ER membrane during co-translation (for higher eukaryotes) by interaction with a group of Sec proteins and the ribosome (126, 185). Sec 61 forms a pore to feed the newly synthesized protein into the ER (88, 185). Co-translation of membrane proteins into the ER membrane involves association of the ribosome with the Sec61p complex and requires GTP (138).

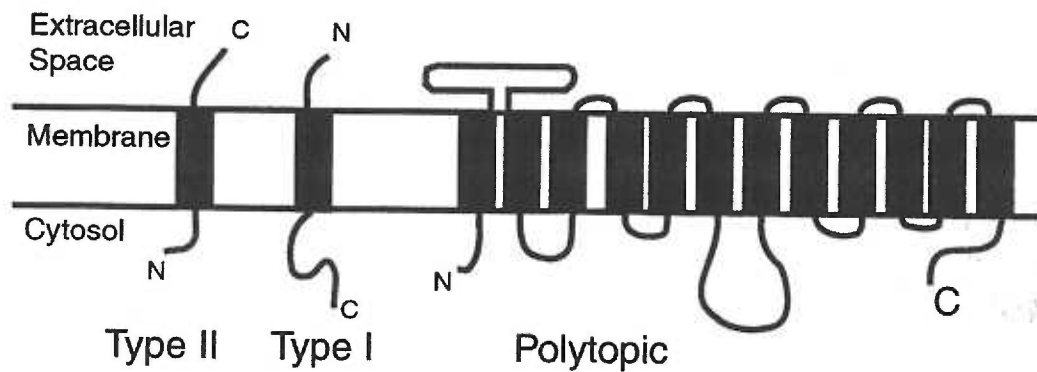
In yeast, and sometimes in higher eukaryotes, membrane protein insertion occurs post-translationally (138). The post-translational insertion process is ATP

dependent (and evidence exists for ATP enhancement of translocation in co-translational mechanisms) (56) and requires the assistance of the ER molecular chaperone BiP to prevent misfolding of the protein (as the protein is imported into the ER lumen) (138) for post-translational protein insertion. Following successful folding of the integral membrane protein, further modifications, such as glycosylation or acylation, occur in the ER and in the Golgi complex, as the protein traffics to its destination. Integral membrane proteins arrive on the plasma membrane after transport through the Golgi and Trans Golgi Network *via* vesicles or tubules. The final orientation of the protein in the plasma membrane places the ER lumen side of the protein on the external face (or extracellular space). Consequently, a protein that begins with the NH₂-terminus in the lumen of the ER will adopt a plasma membrane conformation with the NH₂-terminus on the external face of the plasma membrane.

The integral membrane proteins fall into three categories: Type I, Type II, and polytopic membrane proteins. Type I proteins insert into the ER membrane NH₂-terminus first, with the COOH-terminus exposed to the cytoplasmic face (88, 126, 185). Insertion involves a recognition event in which an NH₂-terminus signal sequence becomes bound to the Signal Recognition Particle (SRP) (185). The SRP bound protein docks with the ER translocation proteins and feeds the newly translated protein through the Sec channel in the ER membrane (185). Upon completion of insertion, the signal peptidase cleaves the NH₂-terminal signal sequence (185). The COOH-terminus contains a stop transfer/anchor sequence that prevents the feeding of the entire protein into the ER lumen (185).

Figure 1-4. Integral Membrane Protein Topologies. Single

transmembrane domain proteins are divided into Type I and Type II proteins. On the cell surface, Type I NH₂-termini are exposed in the extracellular space, while Type II NH₂-termini are exposed to the cytosol. Polytopic membrane proteins adopt a variety of conformations. The predicted topology of a member of the mammalian glucose transporter superfamily is illustrated on the right. The transmembrane domains of the proteins, illustrated in this figure, are predicted to be α -helices.



Type II proteins have a final orientation with the COOH-terminus in the ER and the NH₂-terminus in the cytosol (185). Most Type II proteins contain a combination signal peptide/anchor (not at the NH₂-terminus, but the signal can be located nearly anywhere else in the protein) that is not cleaved (126, 185). Proteins with a non-cleaveable signal anchor can adopt either a Type I or Type II conformation. Orientation of the signal anchor appears to be determined by a combination of the position of the signal peptide and the relative number of positive charges on either side of the transmembrane domain. The side of the protein with the most positively charged amino acids within 15 residues of the transmembrane domain tends to be the luminal side (84). Thus, a protein lacking a cleaveable signal sequence but inserted with the NH₂-terminus in the ER lumen would be Type I (185).

A third class of integral membrane proteins, polytopic membrane proteins, contains multiple transmembrane domains. The work in this thesis will focus on this latter class of membrane proteins. Polytopic membrane proteins lack a cleaveable signal sequence (126). Protein orientation depends on a variety of factors, and the mechanisms remain controversial (193). In some cases, the same polytopic membrane protein can have multiple conformations, even in the same cell type (126, 247). Figure 1-4 includes an illustration of the predicted topology of a member of the mammalian glucose transporter superfamily.

Computer algorithms such as GES (Goldman, Engelman, and Steitz) or Kyte-Doolittle can generate hydropathy plots to predict protein topology in the membrane (64, 114). However due to frequent exceptions to the algorithm rules,

predicted topologies still require experimental confirmation. Topology in eukaryotic cells can be determined by proteolysis protection assays, immunofluorescence microscopy or immunogold electron microscopy with domain specific antibodies, cysteine-reactive chemical agents, or glycan scanning mutagenesis (91).

As alluded to above, different subdomains of the trypanosomatid plasma membrane contain characteristic resident integral membrane proteins. For example, all integral membrane proteins are hypothesized to initially appear on the flagellar pocket membrane, the site of most surface membrane traffic in kinetoplastids (163). In some cases, proteins such as the trypanosomatid transferrin receptor or LDL receptor remain localized to the flagellar pocket membrane by an unknown mechanism (78, 217). Other integral membrane proteins, such as the MIT *myo*-inositol transporter, diffuse or target over the entire plasma membrane (59). Other trypanosomatid integral membrane proteins segregate to either the pellicular plasma membrane (i.e. ISO2 glucose transporter and the D2 hexose transporter) or to the flagellar membrane (i.e. the ISO1 glucose transporter and ESAG4, a trypanosome adenylate cyclase) (121, 166, 177). The targeting signals that direct the differential trafficking of flagellar and pellicular plasma membrane proteins are the main focus of this thesis.

B. GPI-anchored Proteins

Besides transmembrane domains, proteins can associate with a lipid bilayer *via* attachment of lipid residues directly to the protein. Glycosyl phosphatidyl-inositol (GPI) attachment to a protein that lacks transmembrane

domains can target modified proteins to the extracellular leaflet of the plasma membrane. The primary example of this targeting in *Leishmania* is GP63 (a glycoprotein with an approximate molecular weight of 63 kD), one of the most abundant surface proteins in these parasites (5). Another important GPI anchored trypanosomatid protein is the variable surface glycoprotein (VSG) of *T. brucei* (61). VSG is present at 10^7 copies over the plasma membrane of *T. brucei* (61), and provides a protective coat for this parasite. In trypanosomatids, the primary form of GPI attachment occurs by a COOH-terminal amide bond between an asparagine and an ethanolamine linked by a phosphodiester bond to the terminal mannose unit of the GPI (227). Trypanosomatid GPI anchors associate with the membrane through a dimyristoyl glycerol (227)

In addition to providing a physical link to the lipid bilayer, GPI anchors can be important for differential targeting of proteins. In polarized epithelial cells, GPI anchored proteins preferentially sort to the apical membrane (129). Sorting occurs at the TGN and by a poorly understood mechanism creates a different lipid composition for the apical membrane as opposed to the basolateral membrane.

C. Acylated and Prenylated Proteins

A complementary group of acyl lipid modifications (i. e. myristoylation and palmitoylation) and prenyl lipid modifications (farnesylation) promotes protein association with the inner/cytoplasmic membrane leaflet, presumably *via* the insertion of amino acid bound lipids into the membrane (143). The primary amino acid sequence specifies the acyl addition sites; myristate attaches by an

amide bond to a glycine adjacent to the NH₂-terminal initiating methionine, while palmitate attaches by a thioester linkage to a cysteine (143). Prenylation of proteins appears to play a similar role in membrane localization and protein interactions. The prenylation specifying sequences have been determined for mammalian proteins (CxxQ/S/M, CC, and CxxL/F on the COOH-terminus of the protein, where x is any amino acid), but remain unknown for trypanosomatids (246). In higher eukaryotes, the cysteine is modified with the prenyl addition (246). Evidence exists for prenylation in trypanosomes and *Leishmania* and a gene for a farnesyltransferase has been cloned recently from *T. brucei* (246). No role for prenylation in targeting to different membranes has been demonstrated for trypanosomatids.

In some cases acylation may indirectly promote membrane localization. For example, the acyl group on the mammalian p60^{src} protein brings the protein into proximity to associate with an integral membrane protein (143). Chow *et al.* demonstrated that acylation alters protein conformation to promote protein-protein interactions (41). The picorna virus capsid protein VP4 contains a myristic acid that stabilizes interaction between VP4 and another capsid protein VP3 (41, 143). In other cases, the role of the lipid modification remains unknown. For example, the mammalian transferrin receptor contains a transmembrane domain, and mutation of the cysteine normally associated with the palmitate has no effect on membrane localization of the protein (98).

At least one example of acylation has been characterized in trypanosomatids. Godsel *et al.* demonstrated that myristoylation and

palmitoylation of the *T. cruzi* Flagellar Calcium Binding Protein (FCaBP) are necessary for membrane association of the protein (74). Mutating the glycine at position two (the site of myristoyl addition) or the cysteine at position five (the site of palmitoyl addition) to alanine prevents the protein from associating with the cytoplasmic leaflet of the flagellar membrane (74). FCaBP lacking either modification is cytosolic. In addition, Godsel *et al.* propose that the acyl groups provide the targeting specificity for FCaBP and possibly other flagellar membrane proteins (74). Some proteins may use such a mechanism. For example, sea urchin sperm flagellar creatine kinase has myristoylated and nonmyristoylated forms (179). Both forms localize to the flagellum, but only the myristoylated form associates with the flagellar membrane (179). Given that both forms localize to the flagellum, a mechanism separate from membrane association may direct flagellar targeting. In the case of trypanosomatids, ISO1 and other known flagellar membrane proteins, such as the *T. brucei* Receptor Adenylate Cyclases, do not have acylation consensus sequences. Furthermore, at least three of the known FCaBP's contain a sequence with significant similarity to a motif in ISO1 that is necessary for flagellar localization. The nature and similarity of the sequences will be discussed in Chapters 3 and 4 of this thesis.

IV. Protein Targeting Mechanisms

Protein distribution in the cell results from a dynamic process in which signals and mechanisms target and/or retain proteins (153). Protein localization is not static within the cell and requires either tethering or retrieval for retention once the protein has been delivered to the cellular domain dictated by the protein's

targeting motif(s). The half life of the protein also affects the steady state concentration of the protein in a cellular domain.

Directing proteins to a specific site involves a combination of targeting motifs (either an amino acid sequence or a post-translational modification) and sorting mechanisms that usually involve a receptor recognizing the targeting motif followed by movement of the receptor by vesicles and/or motor proteins.

Targeting information ultimately resides within the protein sequence. The protein can contain a primary amino acid targeting sequence, a sequence that stipulates a targeting post-translational modification (such as phosphorylation or glycosylation), a sequence motif that dictates the relative half-life of the protein in a particular cell location, or even a physical property of the folded protein (i.e. a transmembrane helix that retains a protein in the Golgi complex). The spatial context of targeting information (whether the targeting machinery can access the motif) determines whether a protein gets directed to its proper destination. If a targeting motif misses a key interaction with a receptor protein, aberrant targeting could result. To ensure an adequate concentration of a necessary protein in a specific cellular location, the cell may use quality control mechanisms (i.e. degrading mistargeted proteins), or proteins may contain multiple redundant targeting motifs. This section describes different types of targeting domains and mechanisms of protein targeting and localization.

A. Targeting Based on a Protein Sequence Motif

The following section will describe targeting mediated by receptors that recognize specific protein motifs. Both motifs recognized *via* a secondary structure or a primary amino acid sequence will be considered.

1. Sorting Signals Based on Protein Secondary Structure

Some protein targeting sequences adopt a specific three-dimensional secondary structure, such as an α -helix. One of the best studied examples is the mitochondrial import sequence. Mitochondrial proteins are translated outside the mitochondrion and require a mechanism to import the proteins into the mitochondrion. Similar to Type I integral membrane proteins, several mitochondrial membrane proteins contain a cleaveable 7-9 amino acid signal sequence at the NH₂-terminus (85, 130). Numerous studies have demonstrated that the NH₂-terminal domain adopts a basic amphipathic helix conformation in the proximity of phospholipids (130). Several integral membrane proteins and cytosolic chaperones function together to import proteins containing the NH₂-terminal signal sequences (130). Häusler *et al.* have demonstrated that trypanosomatids encode mitochondrial proteins that contain consensus NH₂-terminal signal sequences (85).

2. Primary Amino Acid Sequence

A second type of protein sequence based targeting involves receptor recognition of a region of the primary sequence. Several examples exist in the

literature, and the specific cases of the glycosomal import signal and the tyrosine containing clathrin binding motif will be addressed here.

a) The SKL Glycosomal/Peroxisomal Targeting Sequence

The glycosome resembles the higher eukaryotic peroxisome and actually uses the same protein import signal, SKL (104). While the mechanism for protein import remains undetermined for glycosomes, analogous studies of peroxisomes, especially in yeast, provides some insight.

In yeast, the cytosolic protein Pex5p binds to the SKL signal directly and then binds to an SH3 domain on the peroxisomal integral membrane protein Pex13p (66). How these proteins act to translocate the SKL containing protein into the peroxisome is unknown. Curiously, protein import has been demonstrated for prefolded proteins, and no evidence exists for protein unfolding, although a 70 kD chaperone appears to be important for the translocation process (66, 237).

Regardless of the actual mechanism, the targeting sequence requirements have been well characterized for peroxisomes and glycosomes. Sommer *et al.* demonstrated that a COOH-terminal SKL sequence is necessary for the import of glycosomal *T. brucei* phosphoglycerate kinase and for import of luciferase into the glycosome (213, 214). While the primary sequence and its position provide the necessary targeting information, a series of mutagenesis studies, using firefly luciferase, demonstrate the considerable degeneracy of the sequence. When two of the three amino acid positions were kept constant, substitutions that still promoted glycosomal import included A/C/G/H/N/P/T at the S position,

Figure 1-5. Degeneracy of the SKL Glycosomal Targeting Signal. The figure illustrates which amino acids can substitute for each position of the SKL COOH-terminal glycosomal targeting sequence, as determined by Sommer *et al.* (213).

S	K	L
A	H	I
C	M	M
G	N	Y
H	Q	
N	R	
P	S	
T		

H/M/N/Q/R/S at the K position, and I/M/Y at the L position (213). Some degeneracy in the sequence such as threonine for serine or arginine for lysine has precedence in nature. For example, the *T. brucei* and *T. cruzi* glycosomal glyceraldehyde-3-phosphate dehydrogenases contain AKL and ARL at their respective COOH-termini (105, 145). However, substitutions of an aromatic tyrosine for leucine or a neutral serine for a basic lysine do not seem intuitive. The authors rationalized the degeneracy as: 1) the serine position requiring a small amino acid, 2) the lysine position requiring an amino acid capable of hydrogen bonding, and 3) the leucine position must be hydrophobic (213). However seemingly similar amino acids such as phenylalanine did not have the same ability as tyrosine to substitute for leucine, while asparagine and histidine seem difficult to classify as “small” amino acids”. The results indicate that, in some cases, a necessary targeting sequence can be quite degenerate.

An important consideration for the studies of Sommer *et al.* is that firefly luciferase is a peroxisomally targeted protein in its native context (213). Blattner *et al.* propose that the glycosomal targeting sequence degeneracy can be explained in terms of stringent context requirements (25). In support of Blattner *et al.*'s hypothesis, Gould *et al.* found that removal of part of the NH₂-terminus of firefly luciferase or insertion of four amino acids in the NH₂-terminus could disrupt peroxisomal targeting, despite an intact SKL COOH-terminus signal (77). While the SKL sequence is clearly important for targeting, comprehensive sufficiency studies with a normally cytoplasmic protein will be required to define the essential glycosomal targeting sequence(s).

b) The Tyrosine-based Membrane Protein Sorting Signal

The best characterized targeting sequence and its receptor is the tyrosine containing motif that directs clathrin-mediated endocytosis and post-Golgi secretory pathways (43). The two best characterized motifs are NPXY and YXX Φ , where X is any amino acid and Φ is a bulky hydrophobic amino acid (135). The efficiency of lysosomal and endosomal targeting can be influenced by the sequence context. For example, a glycine before the YXX Φ sequence enhances lysosomal targeting of LAMP-1 (135). The tyrosine was predicted to force the motif into a tight β -turn conformation that permits interaction with the μ 1 and μ 2 of the clathrin associated complexes, AP-1 and AP-2 (159). However, contrary to expectations, the recent crystal structure of TGN38 bound to the μ 2 subunit of AP-2 demonstrates that the tyrosine motif adopts an extended conformation (164).

While a gene for clathrin has not been cloned from trypanosomatids, clathrin-like coated vesicles have been purified and partially characterized (204), which raises the possibility that tyrosine sorting signals and clathrin coat based sorting may occur in trypanosomatids.

B. Anchoring and Retrieval/Retention Mechanisms (Sequence Based)

Once a protein targets to its destination, retention in the cellular subdomain requires additional targeting information. Retrieval mechanisms exist as a form of quality control to ensure that the majority of a protein species remains concentrated in a specific subdomain. Even if some proteins stray/escape, the retrieval machinery interacts with targeting motifs to return the

protein to its resident subdomain. Anchoring mechanisms use a different approach to achieve the same result. Proteins are tethered and effectively restricted to their resident subdomain.

1. Retrieval (KDEL and KK for ER) (LL for Endocytosis)

a) ER Retrieval Sequences

The endoplasmic reticulum (ER) is the site of initiation for vesicular trafficking of newly translated proteins (4). Very high levels of vesicular budding occur on the ER, which functions to transport integral membrane and soluble proteins into the Golgi complex. However, resident ER proteins (whose function primarily occurs in the ER) often sort indiscriminately into the vesicular traffic (131). Rather than wastefully express higher levels of the ER proteins to maintain a sufficient level of ER resident proteins, a mechanism exists to recycle/retrieve the ER proteins back into the ER. Retrieval requires either a COOH-terminal -KDEL (or -RDEL or -KEEL) sequence for soluble proteins or a COOH-terminal KK motif (-KxKxx or -KKxx) for integral membrane proteins (131). The -KDEL sequence binds to a specific receptor (ELP-1 in humans and ERD2 in yeast), while the KK motif binds to a COP I complex (which is involved in both vesicular formation and anterograde transport to the Golgi complex and retrograde transport back to the ER) (131).

In *T. brucei*, a study by Bangs *et al.* demonstrated that at least one ER retention signal is evolutionarily conserved (10). The *T. brucei* homologue of the chaperone BiP contains a COOH-terminal -MDDL sequence that is sufficient to retain VSG, a protein that normally localizes to the plasma membrane (10). The

MDDL sequence is strongly reminiscent of the -KDEL sequence of higher eukaryote ER proteins (10).

b) LL Endocytic Motif

Certain integral membrane proteins, such as CD3 γ and δ chains, CD4, the insulin receptor, and the mannose-6-phosphate receptors, lack the tyrosine motif that specifies clathrin coated vesicle sorting, yet still sort to clathrin vesicles (82, 230). Instead, a dileucine (LL or IL) in the cytoplasmic domain can replace the tyrosine motif (125). Marks *et al.* have demonstrated that proteins containing the LL motif use a receptor distinct from the receptor for tyrosine motif containing proteins (135). The receptor for the LL motif is AP-3, a protein that may associate with clathrin, although it is associated with a nonclathrin sorting pathway in yeast (55, 90, 158). No dileucine motif containing proteins have been identified in trypanosomatids (but the targeting mechanisms for relatively few membrane proteins have been characterized).

2. Anchoring

In contrast to the dynamic mechanisms of protein targeting and localization, cytoskeletal anchoring restricts movement of the protein. Two examples of anchoring that have been well characterized in eukaryotic cells include binding of integral membrane proteins such as the anion exchanger 1 (AE1) and the Na^+/K^+ -ATPase to spectrin (*via* ankyrin) and binding of the neuronal glycine receptor (*via* gephyrin) to microtubules (57, 107). In both cases the integral membrane proteins tether to cytoskeletal elements by a linker protein.

In the case of trypanosomatids, two groups of cytoskeleton anchored proteins have been characterized. The first are MAPs, Microtubule Associated Proteins, which bind to subpellicular or flagellar microtubules *via* a series of proline rich repeats. Identification of MAPs is complicated by the inherent difficulties of demonstrating a genuine interaction with “sticky” microtubules. Some so-called MAPs have been retracted because later studies demonstrated that microtubule association was spurious (170, 183). *Bona fide* MAPs include p41, 52K, SCB210, Gb4, and P320 all of which remain of unknown function (109).

The second group of cytoskeletally anchored proteins are integral membrane transporter proteins including: the D2 hexose transporter, the ISO2 glucose transporter, and the MIT *myo*-inositol transporter (211). Characterization of the cytoskeletal interaction is discussed in Chapter 2 (211) of this thesis. How these transporters interact with the cytoskeleton remains unclear. It seems unlikely that the interaction with microtubules or other cytoskeletal elements is direct, because the transporters do not contain any known microtubule binding motifs, such as proline rich regions with three to four ~30 amino acid repeats (60). We hypothesize that ISO2, MIT, and D2 interact indirectly with the parasite cytoskeleton, much like the glycine receptor and AE1 protein, *via* a linker protein (i.e. a MAP).

C. Physical Properties of the Protein

In addition to traditional targeting sequences that interact with some form of receptor, another form of targeting has been proposed. The inherent physical properties of the protein in the context of its cellular milieu may be sufficient to

retain the protein at a particular locus, without any post-translational modifications or protein-protein interactions.

One possible mechanism for targeting integral membrane proteins involves the length of the transmembrane domain. In the case of Golgi apparatus proteins, the 15 amino acid transmembrane domain is shorter than the typical 20 amino acid transmembrane domain of most plasma membrane proteins (31). The shorter transmembrane domain may trap proteins in the Golgi lipid bilayer, which contains shorter lipids than the plasma membrane (31). The model proposes that the charged amino acids on each side of the transmembrane domain of a Golgi protein would prevent a stable integration into the thicker plasma membrane, because the submersion of hydrophilic residues in the lipid bilayer would be energetically unfavorable (31, 131). Thus, Golgi integral membrane proteins would be incapable of being distilled from the thinner lipid bilayer of the *cis* and *medial* Golgi into the more plasma membrane-like thicker *trans* Golgi and Trans Golgi Network (TGN). Although the transmembrane domain of certain Type II integral membrane proteins is necessary and sufficient for Golgi retention, the domain can be replaced with a series of 17 leucines and still target to the Golgi complex (156). The evidence strongly suggests that proteins can be targeted and retained by mechanisms other than protein-protein interactions.

D. Post-translational Modifications

Post-translational modifications complement targeting information present in the primary, secondary or tertiary structure of the protein. Modifications such as carbohydrate addition increase the repertoire of targeting motifs/signals

available to cells. Other modifications, such as phosphorylation, add a reversible mechanism for regulating protein localization.

1. Carbohydrate Modifications

Resident lysosome proteins usually contain two or more mannose-6-phosphates on one or two different branching N-linked oligosaccharides (4, 89). All N-linked sugars are added in the ER (4). In the early or *cis* Golgi complex, proteins containing a N-X-S/T (where X is any amino acid except proline) sequence (necessary for N-linked glycosylation) and a mannose, in the context of a spatial recognition motif, bind to a GlcNAc phosphotransferase, which adds a GlcNAc-phosphate to a mannose oxygen at the 6 position (4). Subsequently, a GlcNAc phosphoglycosidase removes the GlcNAc to create a mannose-6-phosphate (4).

After passing through the Golgi apparatus, the modified proteins enter the TGN by binding to one of two mannose-6-phosphate receptors, MPR 46 or MPR 300 (4, 89). The receptor bound lysosome proteins become concentrated in clathrin coated vesicles and by a poorly understood mechanism become sorted to lysosomes (89). Finally, the acid pH of the lysosome induces ligand dissociation from the receptors, and the receptors recycle to the TGN (89). Cells that do not express the MPRs secrete over 70% of normally lysosomal soluble enzymes (51). However, other lysosomal targeting mechanisms exist.

The targeting motif for the mannose-6-phosphate modification has been well characterized for cathepsin D and cathepsin L. Baranski *et al.* and Cantor *et al.* demonstrated that two separate domains of cathepsin D confer specificity for

mannose phosphorylation (12, 36). Based on the x-ray crystal structure, Baranski *et al.* and Cantor *et al.* determined that the two domains are solvent exposed (12, 36). Cuozzo *et al.* further defined the mannose phosphorylation sequence as consisting of a pair of solvent exposed lysines separated by 34 angstroms (49). Mutation of lysines 203 and 293 to alanines inhibited phosphorylation by 42% and 13% separately and 70% together (49). In addition, Cuozzo *et al.* defined other amino acids within the microdomains surrounding the two lysines that are necessary for mannose phosphorylation (49). None of the amino acids is consecutive, which emphasizes that the recognition sequence requires a 3-dimensional structure composed of spatially isolated amino acids.

Another example of carbohydrates involved in targeting occurs with the mammalian GLYT1 glycine transporter. Experiments which either blocked addition of carbohydrate by tunicamycin or removed sites of N-glycosylation by mutagenesis revealed that the nonglycosylated transporter does not traffic to the plasma membrane (160). The GPI-anchor also affects protein targeting and is discussed in greater detail in Section III B.

2. Phosphorylation

Protein phosphorylation governs many functions within the cell, ranging from regulation of signaling pathways to altering protein conformation/function to altering protein localization (4). The latter effect occurs through either interaction with a protein to directly bind the phosphorylated/dephosphorylated site or by alteration of the protein conformation to expose a targeting signal. For example, the guanine nucleotide binding protein, Rab 4, can associate with endosomes by

an isoprenylation modification (26). Phosphorylation of Rab 4 prevents addition of the isoprenyl group, and Rab 4 remains cytosolic and not associated with endosomes (26). In other cases, proteins directly interact with phosphorylated protein sequences. For example, numerous signaling pathways utilize receptor proteins containing a SH2 domain (Src homology domain 2) that binds to phosphotyrosine containing motifs. Proteins such as Src-like kinases are normally cytoplasmic, but become bound to the PDGF (platelet-derived growth factor) Receptor, a plasma membrane protein, upon autophosphorylation of the receptor following PDGF binding (26).

When attempting to predict phosphorylation sites, consensus sequences do not always correspond to actual phosphorylation sites. The putative phosphorylation motifs must be accessible to the kinase in question, which may depend on localization and cell type.

3. GPI Modifications

Several post-translational lipid modifications play roles in altering protein localization from cytosolic to membrane associated. Acyl and prenyl modifications (which tend to direct proteins to the cytoplasmic surface of the plasma membrane) have not been proven conclusively to target proteins to specific membrane domains. However, GPI-modifications clearly play an important role in the targeting of apical membrane proteins in polarized epithelial cells and recently have been shown to be essential for secretory transport and plasma membrane surface localization of VSG in *T. brucei* (11, 139, 141).

In polarized epithelial cells, GPI linked proteins preferentially sort to the apical membrane (139). It remains unclear whether sorting involves the GPI anchor or the lipids associated with the anchor. However, GPI anchored proteins do sort into “rafts” in artificial membranes, and recent studies by Varma and Mayor and Friedrichson and Kurzchalia confirm that cholesterol dependent GPI anchored protein rafts exist *in vivo* (72, 208, 229). Detergent extraction of rafts indicates that the lipid composition is enriched for cholesterol, GPI-attached lipids, and sphingolipids (208). Sorting into rafts in the TGN has been proposed as a mechanism for apical membrane protein sorting in epithelial cells (208).

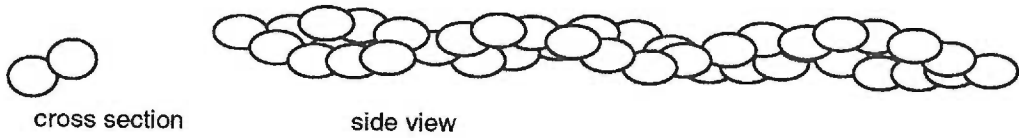
McDowell *et al.* recently demonstrated that GPI anchors increase forward trafficking of nonintegral membrane proteins, such as VSG, five-fold (141). The group found that VSG lacking a GPI anchor tended to accumulate in the endoplasmic reticulum, even though the protein appeared to fold properly (141). It remains unclear whether sorting occurs by a receptor mediated process or in a raft dependent mechanism.

V. Cytoskeleton

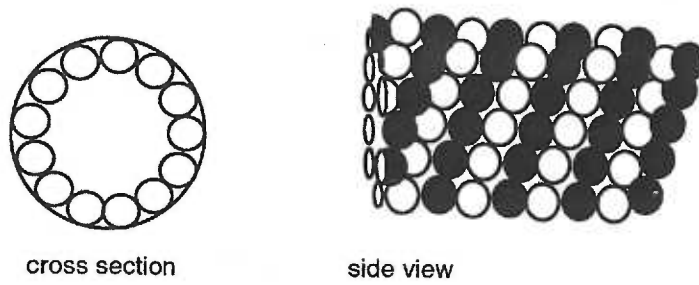
The roles of the cytoskeleton include cell shape, motility, and organizing the cell by serving as a kind of scaffold. In the case of higher eukaryotes, cell shape derives from different cytoskeletal elements, which include microfilaments (actin based) and microtubules (tubulin based). Other cytoskeletal proteins exist, but only those involved in formation of microfilaments and microtubules will be discussed here.

Figure 1-6. Cytoskeletal Elements. A. The structural differences between actin filaments and microtubules are compared. Actin polymerizes to form two intertwined helices that constitute the microfilament. α - (dark spheres) and β -tubulin (white spheres) dimers typically polymerize to form a 13-filament microtubule. B. Distribution of actin and microtubules in epithelial cells and trypanosomatids. In epithelial cells, microtubules localize to the interior of the cell, while actin microfilaments line the cytoplasmic face of the plasma membrane. In trypanosomatids, microtubules line the cytoplasmic face of the plasma membrane, and microfilaments have not been localized.

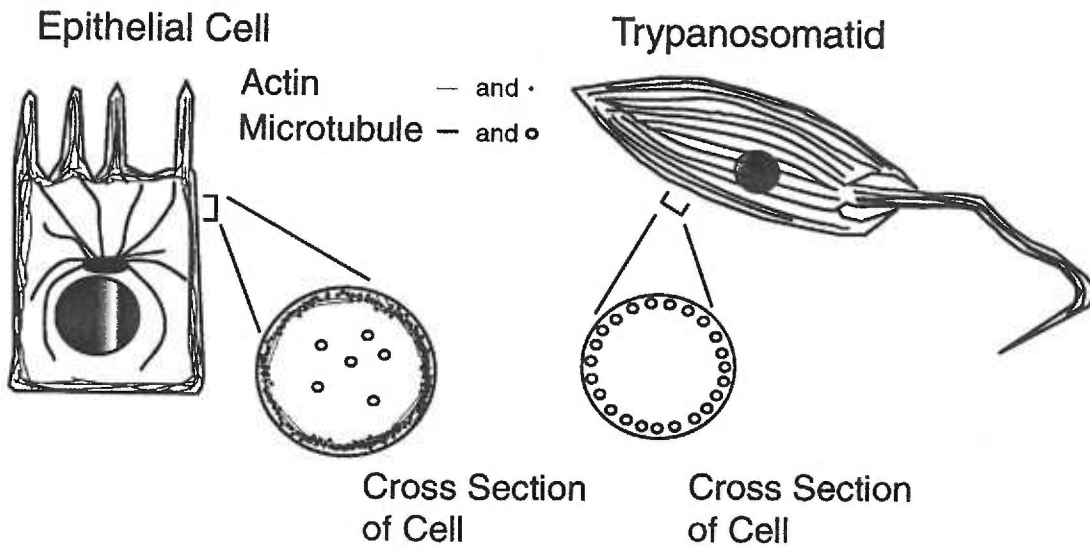
A.
Actin



Microtubule



B. Distribution of Actin and Microtubules in



A. Higher Eukaryotic Cytoskeletons

1. Actin/Spectrin/Ankyrin

The cytoplasmic face of the plasma membrane of many higher eukaryotic cells consists of an elaborate mesh-like network of actin, spectrin, and ankyrin (see Figure 1-6A)(4, 30). Actin consists of 8 nm thick filaments composed of actin monomers that vary in length depending on the cell type (4). Actin monomers polymerize in the presence of ATP which is hydrolyzed during the formation of oligomers (4). Actin polymerizes in a polar fashion, with a plus and a minus end, with the plus end polymerizing ten times faster than the minus end (4).

The tetrameric protein spectrin contains two binding sites for F-actin oligomers, and each oligomer associates with five or six spectrin filaments (30). Together, the two components form the web underneath the plasma membrane. Ankyrin binds to spectrin and binds the plasma membrane by attaching to integral membrane proteins such as the Anion Exchanger 1 (AE1) and the Na^+/K^+ -ATPase (30).

In addition to organizing cell shape, actin serves as a regulatory barrier to endocytosis and exocytosis, organizes some integral membrane protein distributions (i. e. AE1 and Na^+/K^+ -ATPase), and aids in cell locomotion in conjunction with the molecular motor protein myosin (30, 148).

2. Microtubules: Structure and Function

Another major cytoskeletal element, the microtubule, is also a polymer. In contrast to actin, microtubules are composed of heterodimers of α - and β -tubulin

that polymerize in the presence of GTP and magnesium to form hollow tubules (see Figure 1-6A)(4). Microtubules have plus and minus ends, similar to actin, but *in vivo* the minus end is usually attached to microtubule organizing centers (235). γ -tubulin forms an elongating tubule ring to create the microtubule organizing centers which α -and β -tubulin use as a platform for polymerization (199). α -tubulin interacts directly with the γ -tubulin ring (235). When microtubules polymerize, strands form which end with the β -tubulin at the plus end (235). The $\alpha\beta$ heterodimers form “protomers” that organize as 13 parallel strands that form the hollow tube structure (see Figure 1-6A) (235). Unlike actin, microtubules are relatively stiff and rigid (4).

Microtubules have three major roles in higher eukaryotic cells.

Microtubules form the mitotic spindle that separates chromosomes during mitosis, provide the framework/tracks for the Golgi apparatus and trafficking vesicles, and contribute to cell shape (4, 128, 235). Microtubules help create the rigid internal cellular framework that the actin/spectrin network surrounds (4).

a. General Properties of Microtubules

Microtubules and actin differ significantly in their properties. Within the cell, actin appears flexible, while microtubules appear rigid. However, in response to shearing force, actin is very rigid, while microtubules deform easily (4). In higher eukaryotes, most microtubules are highly dynamic and turnover frequently by polymerization and depolymerization (4).

b. Disrupting and Stabilizing Drugs

The dynamic nature of microtubules makes them susceptible to a variety of drugs. Colchicine, an alkaloid derived from saffron, binds free tubulin, but not polymerized tubulin, which results in the depolymerization of microtubules (4). Vinblastine and nocodazole have similar effects (4, 132). In contrast, taxol binds polymerized microtubules and stabilizes them (4). In higher eukaryotes, taxol causes the pool of free tubulin to polymerize and (like colchicine and vinblastine) prevents the completion of mitosis (4).

In addition to pharmacological treatments, higher eukaryotic microtubules readily depolymerize *in vitro* and at low temperatures (near 0°C) (201). However, trypanosomatid microtubules are very resistant to depolymerization by either low temperatures or by drugs such as colchicine, vinblastine, and nocodazole (201).

B. The Trypanosomatid Cytoskeleton

Trypanosomatid cytoskeletons differ significantly from higher eukaryotes. Instead of an actin/spectrin mesh, trypanosomatids derive their cell shape from a corset of subpellicular microtubules and a flagellar axoneme (Figure 1-6B). The rigid microtubules confine surface exocytosis and endocytosis to the flagellar pocket, which is not bounded by microtubules. In addition, trypanosomatid microtubules differ in several respects from higher eukaryotic microtubules, as discussed below.

1. Actin in Trypanosomatids

The kinetoplastid microtubule corset effectively substitutes for actin in lining the cytoplasmic face of the plasma membrane. *T. cruzi* actin has been shown by immunoblotting to be approximately 43 kD and has a diffuse homogeneous distribution throughout the cell, as seen by immunofluorescence (152). In *Leishmania*, there appears to be more intense immunofluorescence staining at the apical pole and the globular tip of the flagellum (50). While an actin gene has been cloned for *Leishmania*, and the presence of actin has been demonstrated in the cell by immunoblotting and immunofluorescence localization, detailed localization of actin by electron microscopy has proven elusive (53, 109, 152). At present, no role for actin has been identified for trypanosomatids.

2. Trypanosomatid Microtubules

An unusual corset of parallel microtubules defines the bullet shape of the promastigote and the more rounded shape of amastigotes (184). The cytoskeleton of trypanosomatids lacks internal cytoskeletal components (such as cytoplasmic microtubules or intermediate filaments), although the microtubule-based mitotic spindle is present during cell division (67). Seebeck *et al.* speculate that the trypanosomatids lack the internal cytoskeleton scaffolding to allow cell deformation in the shearing environment of the mammalian host bloodstream (201). However, trypanosomatids evolved long before multicellular organisms.

The *Leishmania* α - and β -tubulin genes are arranged in two separate clusters of 7-15 tandem repeats of α tubulin and 8-9 tandem repeats of β -tubulin (117). Expression is regulated, in *L. enriettii*, post-transcriptionally, at the level of mRNA accumulation (118). The transition from amastigote to promastigote includes a dramatic increase in the mRNA levels of both genes (118). In contrast, mRNA levels of both genes appear to be the same for both life stages in *L. mexicana* (71).

a. Differences Between *Leishmania* and Higher Eukaryotic Microtubules

Trypanosomatid microtubules contain three major post-translational modifications: detyrosination, acetylation, and glutamylation (109). Acetylation occurs on lysine 40 of α -tubulin, before or just after insertion into the microtubule (192). While some labile structures, such as the mitotic spindle, contain acetylated α -tubulin, the modification primarily correlates with enhanced microtubule stability (201). Detyrosination can occur on the COOH-terminal α - or β -tubulin tyrosine after addition of the subunit to the growing microtubule (109). The function of detyrosination remains unknown. The third type of modification, glutamylation occurs extensively on both α - and β -tubulin (197). Glutamylation involves addition of lateral chains of six to 15 glutamyl residues to β - and α -tubulin, respectively (197). The side chain attaches to glutamic acid 445 of α - and 435 of β -tubulin (197). Schneider *et al.* speculate that polyglutamylation enhances interactions between MAPs and microtubules (as has been shown for the mammalian MAP, Tau), which could partially account for the extreme stability of protozoan microtubules and cytoskeletons (197).

Unlike higher eukaryotic organisms, trypanosomatid microtubules are highly stable and resistant to traditional microtubule disrupting conditions, including cold (201), colchicine and nocodazole (132, 188). Cotreatment with 1M NaCl and 1mM CaCl₂ solubilizes trypanosome subpellicular microtubules (183). However, neither of these conditions disrupt *Leishmania* microtubules (211). 10mM CaCl₂ will disrupt *Leishmania* microtubules into an amorphous mass (211). The anti-psychotic tricyclic compound chlorpromazine (Thorazine) visibly disrupts (but does not solubilize) *Leishmania* microtubules in living parasites, but the drug is extremely toxic to *Leishmania* (200, 211). The extreme stability of trypanosomatid microtubules makes their purification difficult (201).

3. Formation of New Microtubules During Cell Division in Trypanosomatids

Trypanosomatids create daughter cells by binary fission. The microtubules of the new cell form in-between the stable microtubules of the parent cell (205, 206). New microtubules are distinguished by still retaining the COOH-terminal tyrosine and are detyrosinated over time (206). The cell divides along the posterior/anterior axis, beginning at the flagellum, and the nuclei segregate before the second distinct cell body forms (205). Subpellicular microtubule inheritance is semi-conservative, with each resulting cell containing new and old microtubules (109).

C. Microtubule Organization in *Leishmania*

In trypanosomatids, microtubules are organized into four different structures, the subpellicular microtubule corset, basal bodies, the mitotic spindle, and the flagellar axoneme (109). The microtubules of each structure have

different properties. For the purposes of this thesis, only subpellicular and axonemal microtubules will be discussed.

1. Subpellicular

The subpellicular microtubule corset of kinetoplastids defines the bullet-like cell shape of the promastigote form. The kinetoplastid-type subpellicular microtubule corset is also seen in some apicomplexans, such as *Plasmodium* sporozoites, merozoites, and ookinetes (188), but not in higher eukaryotic cells. The corset microtubules sit directly beneath the pellicular plasma membrane and consist of approximately 100 helically arranged microtubules (29, 62, 198). The microtubules directly associate with the membrane and remain attached following shearing of whole cells by a Dounce homogenizer (62). The microtubules organize in parallel with the plus end at the posterior of the cell and the minus end at the anterior (site of flagellar attachment) of the cell (184). The microtubules are organized in a regular spacing of 18-22 nm (in closely related trypanosomes) and associate tightly with each other *via* bridge forming MAPs (243). The crosslinked microtubules exclude vesicular transport from the pellicular plasma membrane and restrict the fusion of vesicles to the flagellar pocket (163) region of the surface membrane. The subpellicular microtubules are significantly more stable than the microtubules of higher eukaryotes (201). The overall stability of the cytoskeleton allows for isolation of the intact network by nonionic detergent extraction (183).

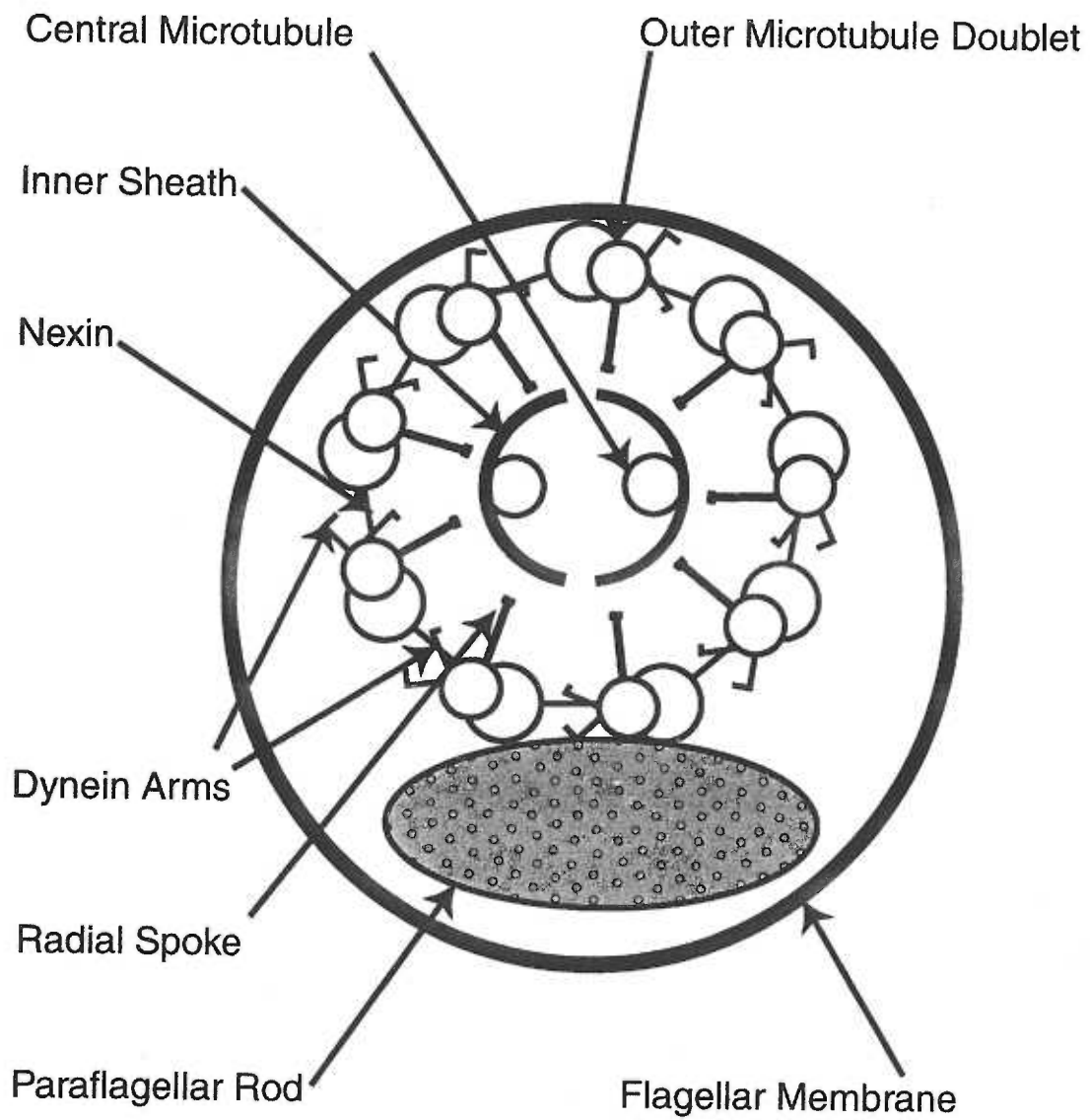
Subpellicular microtubules differ biochemically from flagellar microtubules. First, trypanosome subpellicular microtubules can be disrupted by

1 M NaCl or 1 mM CaCl₂, while the flagellar microtubules remain intact (183). However, the subpellicular microtubules of *Leishmania* are resistant to up to 1 M NaCl and more than 4 mM CaCl₂ (211). Second, subpellicular microtubules have varying amounts of detyrosinated tubulin (the posterior tip and newly forming microtubules contain mostly tyrosinated tubulin), while flagellar microtubules are primarily detyrosinated (206). Sherwin and Gull demonstrated that detyrosination occurs as new flagella grow during the cell cycle (206). In contrast, the subpellicular microtubule corset contains intercalated growing microtubules that have not been detyrosinated yet (206). The difference in overall amounts of detyrosinated tubulin relates to the relative assembly rates of subpellicular and flagellar microtubules. Trypanosome flagella assemble over four hours, while subpellicular microtubules extend at rates 60 times faster than flagellar microtubules and thus accumulate tyrosinated tubulin (206). Microtubules rich in detyrosinated tubulin have slower turnover rates and are more resistant to the depolymerizing effects of drugs and cold (206).

2. Flagellar Cytoskeleton and Motility

The flagellum of *Leishmania* and other kinetoplastids strongly resembles cilia and flagella of other eukaryotes (201). Eukaryotic flagella do not share proteins or structures found in prokaryotic flagella, despite the same name for the two structures. The backbone of the flagellum consists of two components, the microtubule axoneme and the paraflagellar rod.

Figure 1-7. Trypanosomatid Flagellum Cross Section.



a. Axoneme

The *Leishmania* flagellum contains a 9-2 microtubule based axoneme (Fig. 1-7), common to most eukaryotic flagella and cilia. Flagellar microtubules direct their positive poles toward the distal end (anterior) of the flagellum (the opposite orientation of the subpellicular microtubules) (109). The structure consists of nine doublets of microtubules in a circular arrangement beneath the flagellar membrane, with two microtubules in the center of the circle. The doublets are composed of a standard 13 strand microtubule and a partially open 11 strand microtubule (Fig. 1-7)(4). Each doublet connects to two dynein arms which can reach the adjacent doublet (218). The central microtubules connect to a structure referred to as the inner sheath. Flagellar microtubules are even more stable than subpellicular microtubules (183, 205).

Kinetoplastids generate tip to base waves that can be generated at any point along the flagellum (218). The sinusoidal waves result from the bending of the axoneme (4, 218). To bend, the dynein arms attached to one microtubule move along an adjacent microtubule (218). Dynein arm movement requires ATP hydrolysis (218).

Kinetoplastids propel themselves flagellum first and rotate about an axis parallel to direction of the cell (218). Rotation occurs counterclockwise when viewed from the base of the flagellum to the tip (218).

b. Paraflagellar Rod

The paraflagellar rod (PFR) of trypanosomatids contains two major proteins, PFR-1 and PFR-2 in *L. mexicana* or PFR-A and PFR-C in *T. brucei*, and

several unidentified components (54, 149). Specific axoneme microtubules (microtubule doublet 7 in trypanosomes) associate with the PFR (184).

Knockouts of the PFR genes revealed that the paraflagellar rod is essential for motility (16, 191). In knockout mutants, the flagellum develops normally, but the beating motion does not propel the parasite (16, 191).

3. Flagellar pocket

The flagellar pocket does not contain any obvious cytoskeletal elements. In fact, the flagellar pocket is the only domain of the plasma membrane free from interactions with microtubules. The lack of packed stable microtubules beneath the flagellar pocket membrane may account for the fact that this domain is the only known site of endocytosis, exocytosis, and addition of plasma membrane proteins to the cell surface.

VI. The Mammalian Glucose Transporter Superfamily

Glucose serves as a nearly universal carbon energy source for plants, animals, and prokaryotes. Organisms obtain glucose either through synthesis or transport. Cells incapable of photosynthesis must rely on transport to bring glucose from the extracellular environment across the plasma membrane into the cell. Prokaryotic and eukaryotic cells have evolved a “superfamily” (the Major Facilitator Superfamily) of twelve transmembrane domain transporters to obtain nutrients (such as glucose), excrete toxins and waste products, and regulate cell ion concentrations (167). The “sugar porter family” forms the foundation of the facilitator superfamily (167), which includes active (which requires energy and/or cotransport of ions) and facilitative (uptake by facilitative diffusion) hexose

transporters. The mammalian erythrocyte glucose transporter, GLUT1, provides the standard model for the facilitative glucose transporters (154). The key characteristics include: 1) twelve predicted transmembrane α -helical domains, 2) cytoplasmic amino and carboxy termini, 3) a large intracellular loop between transmembrane domains 6 and 7, and 4) a large extracellular loop between transmembrane domains 1 and 2, and 5) the ability of the transporters to specifically transport the D-enantiomer of glucose and some other hexoses (75, 225).

Active glucose transporters, such as the SGLT1 (sodium-dependent glucose transporter 1) transporter, have been biochemically characterized, and their genes have been cloned (86). However, members of the active glucose transporter family contain several differences that distinguish them from facilitative glucose transporters. SGLT1 has eleven predicted transmembrane domains (as opposed to twelve for facilitative glucose transporters), lacks a large extracellular loop between transmembrane domains one and two, cotransports sodium with glucose, and lacks sequence homology to the facilitative glucose transporter superfamily members (86). The active glucose transporters will not be considered further, because the glucose transporters relevant to this thesis belong to the facilitative glucose transporter superfamily.

A. Structure

Based on computer hydropathy prediction programs (75, 155), the GLUT proteins contain twelve predicted 21 amino acid transmembrane helix domains. Protease digestion studies, in conjunction with immunoblotting, support the

predicted topology (52, 154). The most convincing evidence for the predicted topology comes from glycosylation scanning studies. N-linked-glycosylation sites were genetically engineered into predicted cytoplasmic and extracellular domains of GLUT1 (91). Because N-glycosylation usually only occurs on the extracellular domains of proteins, Hresko *et al.* predicted that hydrophilic loops that became glycosylated would face the extracellular space. While the attempts to discern the topology in a cell free dog pancreatic microsome system were ambiguous, expression of mutants in *Xenopus* oocytes confirmed the predicted 12 transmembrane domain topology (91).

Most higher eukaryotic hexose transporters contain an N-glycosylation site on the large extracellular loop between transmembrane domains one and two (172). Feugas and co-workers have demonstrated that the glycans are critical for glucose transport (70). However, the bacterial and lower eukaryotic hexose transporters do not contain putative glycosylation sites. The exact role for the glycans in transport has not been resolved.

The members of the glucose transporter superfamily (eukaryotic and prokaryotic) appear to divide into two segments of six transmembrane domains each. Bibi and Kaback showed that the *E. coli lac* permease gene can be divided into two separately transcribed domains that, when co-expressed, still produce a functional transporter (23).

B. Function and Biochemistry

Heterologous expression systems, such as *Xenopus laevis* oocytes, have made it possible to characterize the biochemistry and mechanisms of the

mammalian glucose transporters (76, 104). A key property of oocytes is that they lack background glucose transport on the cell surface. To assay transporter activity, mRNAs of the gene of interest are microinjected into oocytes, and three to five days later the oocytes are tested for the ability to transport radioactive substrates. Considerable evidence confirms the validity of using heterologous expression systems and their relevance to *in vivo* properties of transporters. For example, K_m values for GLUT1 and GLUT4 are in close agreement with values from native and *in vitro* systems (76). 2-deoxy-D-glucose uptake K_m values measured for heterologously expressed mammalian glucose transporters are 6.9 ± 1.5 mM (172) for GLUT1 and either 4.6 ± 0.3 mM (172) or 1.8 mM (104) for GLUT4. The lower K_m of GLUT4 (depending on source of the value) may help ensure that the transporter operates near V_{max} under conditions of high blood glucose to rapidly divert blood glucose into stored energy (76). The oocyte system also can be used to identify substrates, inhibitors, and other transport parameters.

While the six functional facilitative hexose transporters identified in humans (GLUT1-5 and GLUT7) have similar amino acid sequences and predicted structures, the transporters differ in tissue distribution, cellular localization, and substrate specificity. GLUT1 localizes to the plasma membrane and is found in all tissues (76, 172). GLUT4 is found in white and brown adipose tissue, as well as cardiac and skeletal muscle and localizes to insulin responsive intracellular vesicles (172). GLUT4 translocates to the plasma membrane in response to insulin stimulation (172). GLUT5 is a fructose transporter localized to the apical

membrane of intestinal enterocytes and to the plasma membrane of spermatozoa (52, 154).

C. Mobilization of GLUT4

GLUT4 has 65% sequence identity to GLUT1 (172), but the transporters differ significantly in K_m values. In skeletal muscle, heart, and adipose cells, GLUT1 and GLUT4 are expressed simultaneously (96), but have different surface distributions in response to insulin stimulation. In unstimulated adipose cells, GLUT1 makes up the majority of facilitative glucose transporters on the cell surface, while GLUT4 resides within intracellular vesicles. Insulin stimulates the recruitment or mobilization of GLUT4 to the plasma membrane (172). Because GLUT4 levels increase up to 15-20-fold in response to insulin stimulation, compared to 2-fold for GLUT1, the process of mobilization of a high K_m transporter provides an effective regulation of glucose uptake in response to extracellular glucose levels (172).

The mechanism for insulin regulation of GLUT4 targeting has been the studied extensively. Nonetheless, the components of mobilization and the targeting motifs of GLUT4 remain only partially characterized. Several regions of GLUT4, ranging from the NH_2 -terminus to a variety of intracellular loops to the $COOH$ -terminus, have been proposed to contain targeting information (95). Piper *et al.* identified a sequence in the NH_2 -terminus of GLUT4 that appeared to be responsible for targeting to intracellular tubules (176). Studies by Garippa *et al.* contradicted the interpretation of Piper *et al.* and instead demonstrated that the NH_2 -terminus of GLUT4 functions to regulate the relative rate of protein

internalization at the plasma membrane (73). A mutagenesis study by Verhey and Birnbaum reported that, in fibroblast cells, the targeting sequence is a dileucine motif in the COOH-terminus of GLUT4 (230, 231). However, Verhey later determined that the COOH-terminal dileucine motif does not play a role in the rapid translocation to the plasma membrane in 3T3-L1 adipocytes, a cell type more physiologically similar to normal adipocytes which are insulin responsive and, unlike fibroblasts, do translocate GLUT4 (232). While the exact targeting motif has remained elusive, Verhey *et al.* have presented the most convincing data to date that the COOH-terminal 30 amino acids are sufficient for the insulin responsive translocation of GLUT4 in 3T3-L1 adipocytes (232). Studies by Wang *et al.* identified an aspect of the insulin regulated retargeting. Insulin directly or indirectly induces a conformational change in GLUT4 that exposes the COOH-terminus (238), which supports other evidence that the COOH-terminus of GLUT4 contains the insulin responsive targeting motif. The study of GLUT4 illustrates the complexities inherent in any attempt to characterize a protein targeting motif. Cell type, gene expression levels, type of mutant (alanine replacement or chimera), and effects of mutations on protein folding/turnover all influence localization of a protein and add to the difficulties of investigating targeting motifs.

VII. Trypanosomatid Hexose Transporters

Glucose serves as a critical energy source for most insect stage trypanosomatids (224). Most trypanosomatids generate ATP from glucose *via* glycolysis followed by the Krebs cycle and the mitochondrial respiratory chain

(224). The bloodstream forms of *T. brucei* lack a functional respiratory chain and instead rely on high rates of glucose transport and glycolysis to generate ATP. Genes for members of the mammalian glucose transporter family have been cloned from *L. enriettii*, *L. donovani*, *L. mexicana*, *T. brucei*, *T. cruzi*, and *T. vivax* (32, 34, 35, 120, 216, 224, 236). All trypanosomatid transporters whose genes have been cloned appear to transport glucose in a facilitative (nonenergy dependent) manner (224), although proton symport has been suggested by some workers (248).

During the sandfly stage of *Leishmania*, the primary carbon energy sources consist of proline from sandfly bloodmeals and glucose from both bloodmeals and plant sap (28). Despite their role in *Leishmania* transmission via the bloodmeal, sandflies mainly feed on glucose rich plant sap. In addition to serving as an energy source, glucose may play an important role in the transformation of promastigotes into infection competent metacyclics (195).

To obtain glucose from the environment of the sandfly gut, the *Leishmania* parasites use transporters that belong to the mammalian glucose transporter superfamily. Cairns *et al.* and Langford *et al.* cloned and characterized the first trypanosomatid glucose transporter genes (35, 119). This transporter from *L. enriettii* is called PRO1 for **promastigote stage specific protein** (35). The following section describes the characterization of the biochemistry, molecular biology, and cell biology of PRO1.

A. Regulation in Amastigotes and Promastigotes

Comparison of glucose uptake between *L. mexicana* amastigotes and promastigotes demonstrates that promastigotes readily transport glucose and related hexoses, while amastigotes transport hexoses at a ten fold lower V_{\max} than promastigotes (33). Down-regulation of transport could be due to lower expression of the transporter, higher turnover of the transporter, or by a regulatory mechanism (such as phosphorylation) that could alter protein structure and curtail transport. Of these possible mechanisms, Langford *et al.* have determined that mRNA expression of the major promastigote hexose transporter (PRO1) of *L. enriettii* is down-regulated dramatically in amastigotes (119).

PRO1 was initially identified by differential hybridization as a developmentally regulated gene in *L. enriettii* (35). The promastigote expression and amastigote down-regulation of PRO1 correlates well with the availability of glucose in the *Leishmania* diet. The phlebotomine sandfly vector feeds on glucose rich plant sap, in addition to blood, while the macrophage phagolysosome lacks significant quantities of glucose (35). As appears to be the case for other *Leishmania* genes, regulation of glucose transporter expression (at least for the PRO1 homologues in *L. mexicana*) occurs at the post-transcriptional level, specifically message stability (34).

B. Biochemistry (Uptake Studies, Substrates, Inhibitors, and K_m 's)

Zilberstein and Dwyer measured 2-deoxy-D-glucose and proline uptake by *L. donovani* in combination with various transport inhibitors and concluded that

glucose and proline transport in *Leishmania* are protonmotive force driven processes (248). They also demonstrated that transport does not involve symport of sodium (as is seen in some higher eukaryote transporters) or use ATP (248). However, a series of chemostat studies using D-glucose by ter Kuile and Opperdoes questioned the interpretation that glucose accumulated against a concentration gradient. Ter Kuile and Opperdoes demonstrated that glucose transport across the plasma membrane of *Leishmania* is not energy dependent, does not require proton symport, but that conversion of glucose to metabolites did require energy (219).

Glucose uptake studies in *Leishmania* promastigotes provide different K_m values depending on the substrate and correction for hexokinase activity. Burchmore and Hart measured 2-deoxy-D-glucose uptake in *L. mexicana* and calculated a K_m of 0.024 mM and a V_{max} of $2.21 \text{ nmol min}^{-1} (\text{mg protein})^{-1}$ (33). Ter Kuile and Opperdoes measured glucose uptake in a chemostat and, after correcting for hexokinase activity, determined that *L. donovani* transports glucose with a K_m between 0.4 and 0.9 mM (221).

The cloning of the PRO1 glucose transporter made it possible to test transporter properties in a heterologous system and to perform voltage clamp experiments to test whether a protonmotive force is required for glucose transport. The heterologous *Xenopus* oocyte expression system was used to determine the K_m ($0.285 \pm 0.06 \text{ mM}$) of 2-deoxy-D-glucose uptake by PRO1, a value that agrees most closely with the calculated K_m of ter Kuile and Opperdoes. The transporter also can use fructose and mannose (119). The pharmacological inhibitors

Cytochalasin B and phloretin (inhibitors of mammalian facilitative glucose transporters), phloridzin (an inhibitor of mammalian sodium-dependent glucose transporters), and FCCP (an uncoupler of oxidative phosphorylation) moderately inhibit 2-deoxy-D-glucose transport in mRNA injected oocytes and wild type parasites (119). Forskolin (an inhibitor of mammalian facilitative glucose transporters) does not affect transport (119). Oubain (an inhibitor of the Na⁺/K⁺-ATPase) had no effect on transport, which indicates that transport is not sodium dependent (119). Voltage clamp experiments failed to demonstrate the presence of a current during 2-deoxy-D-glucose transport (119) consistent with the notion that PRO1 is a facilitative transporter. Another transporter in the glycolytic pathway, such as a yet unidentified glycosomal glucose transporter, might be energy dependent.

C. The Isoforms of PRO1, ISO1 and ISO2

Southern analysis of the genomic arrangement of *PRO1* indicated the presence of approximately eight copies of the gene (216). Sequencing the first copy of *PRO1* identified a unique isoform of the transporter (215), while the other copies appear to be identical to the originally sequenced form of *PRO1* (215). The two isoforms are identical in sequence, except for their cytoplasmic NH₂-terminal domains. The original PRO1 is now referred to as ISO2 and has a 48 amino acid NH₂-terminal cytoplasmic domain. The new isoform, referred to as ISO1, has a 130 amino acid NH₂-terminal cytoplasmic domain (Fig. 1-8). The names refer to the relative order of *ISO1* and *ISO2* on the chromosome. The

following section describes the biochemistry, molecular biology, and cell biology of the two isoforms.

1. Gene arrangement and Expression

The *PRO1* locus consists of one copy of *ISO1* followed by approximately seven copies of *ISO2* in a tandem repeat (120). The two isoforms have different 5'-untranslated regions (UTR) and share the same 3'-UTR (215). Expression is regulated during the life cycle for both isoforms (215). Low levels of mRNA and protein for each isoform are seen in amastigotes, while promastigotes express high levels of mRNA and protein for both isoforms (177, 215).

2. Structure and Biochemistry

A comparison of the sequences of ISO1 and ISO2 fails to demonstrate any obvious similarities between the two NH₂-terminal domains (Fig. 1-9). The NH₂-terminus of ISO2 has a high content of acidic amino acids (27.66% acidic residues and 17.03% basic amino acids) that results in a predicted pI of 4.23. The NH₂-terminus of ISO1 has a predicted pI of 6.69 (with 7.7% acidic amino acids and 11.55% basic amino acids). In addition the NH₂-terminus of ISO1 has a 27.69% serines and threonines and a total polar amino acid content of 43.08%, while ISO2 has a 12.77% serine/threonine content and a 21.28% total polar amino acid content. Other potentially significant differences between the NH₂-termini include: 1) ISO2 lacks leucine, isoleucine (ISO1 has a 10% leucine/isoleucine content), cysteine (ISO1 has one), tyrosine (ISO1 has two), glycines (ISO1 has 5), and histidines (ISO1 has 6), and 2) ISO1 has more than twice the proline content of ISO2 (13.85% versus 6.38%). The differences give rise to dramatic differences

Figure 1-8. Comparison of NH₂-terminal Hydrophilic Domains of ISO1 and ISO2.

ISO1	MSYYPPKSQDQGQLPLKTFSSPPRRTGTTSHAAHNCVAES
ISO1	ETLPTTPPLPSFLRGNDVQLPKTASVAHSLTTSPPSVNNLSP
ISO1	PGAGPHTHHRIANPINPASTEDDTTFSTTSASQDPP
ISO2	MSDRVEVNERRSDSVSEKEPARDDARKDVTDDQEDA
ISO1	RESSLFSSLNIR
ISO2	PFMTANNARVM

Figure 1-9. Amino Acid Compositions of the NH₂-terminal Hydrophilic

Domains of ISO1 and ISO2.

Amino Acid Composition: ISO1

Non-polar:	No.	Percent
A	9	6.92
V	4	3.08
L	10	7.69
I	3	2.31
P	18	13.85
M	1	0.77
F	4	3.08
W	0	0.00
	37.7	

Polar:	No.	Percent
G	5	3.85
S	20	15.38
T	16	12.31
C	1	0.77
Y	2	1.54
N	7	5.38
Q	5	3.85
	43.08	

Acidic:	No.	Percent
D	6	4.62
E	4	3.08
	7.7	

Basic:	No.	Percent
K	3	2.31
R	6	4.62
H	6	4.62
	11.55	

Estimated pI = 6.69

Amino Acid Composition: ISO2

Non-polar:	No.	Percent
A	5	10.42
V	5	10.42
L	0	0.00
I	0	0.00
P	3	6.25
M	3	6.25
F	1	2.08
W	0	0.00
	34.05	

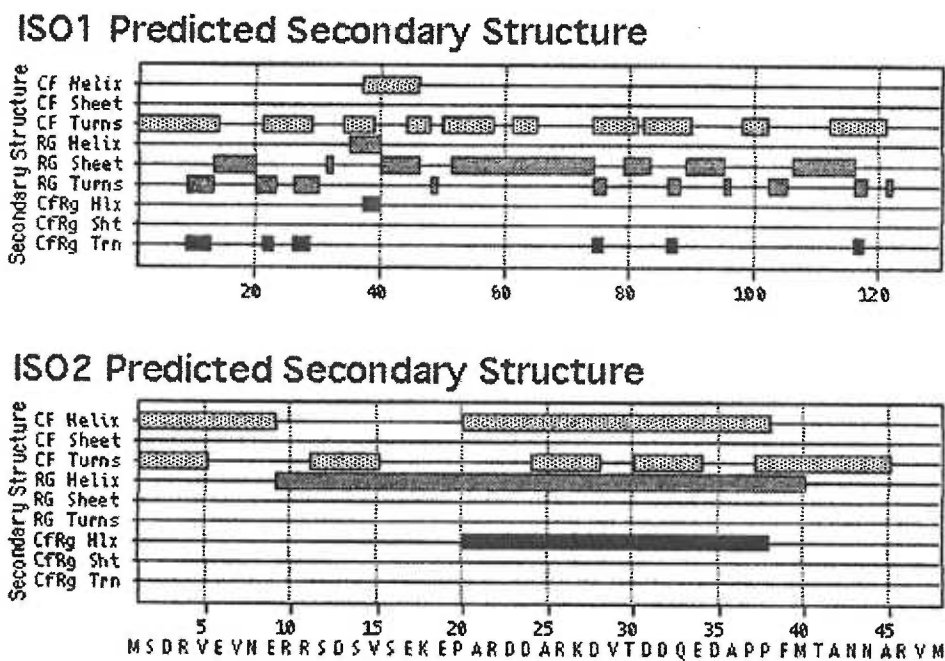
Polar:	No.	Percent
G	0	0.00
S	4	8.33
T	2	4.17
C	0	0.00
Y	0	0.00
N	3	6.25
Q	1	2.08
	21.28	

Acidic:	No.	Percent
D	8	16.67
E	5	10.42
	27.66	

Basic:	No.	Percent
K	2	4.17
R	6	12.50
H	0	0.00
	17.03	

Estimated pI = 4.23

Figure 1-10. Comparison of Predicted Secondary Structures of the NH₂-terminal Domains of ISO1 and ISO2. The MacVector 5.0 protein analysis toolbox secondary structure prediction programs were used to predict the secondary structures. CF refers to Chou-Fasman and RG refers to Robson-Garnier algorithms. CfRg is the consensus of the two algorithms. Numbering below the boxes refers to the position of amino acids.



in the predicted secondary structures for the two NH₂-termini (Fig. 1-10). Depending on which algorithm is used, ISO1 has a higher content of turns, a possible β -pleated sheet, and few if any helices. In contrast, ISO2 has one or two predicted helices, no sheets, and turns predicted only by the Chou Fasman algorithm. The difference in proline content could account for differences in numbers of predicted turns and helices. However, the main point of these analyses has been to demonstrate that the NH₂-termini of the two isoforms lack any similarities, aside from both being predicted to be on the cytoplasmic side of the plasma membrane.

Aside from these NH₂-terminal domains, the two isoforms are identical, which gives rise to the obvious question: why does the parasite have two glucose transporter isoforms? The first hypothesis considered possible differences in transport properties. Langford *et al.* used the *Xenopus* oocyte expression system to measure the relative K_m's and substrate specificities of each isoform. Both isoforms share similar K_m's for 2-deoxy-D-glucose uptake (0.65±0.26 mM for ISO1 and 0.29±0.06 mM for ISO2) (119). Expression of both isoforms together in oocytes gave a K_m of 0.46±0.22 mM for 2-deoxy-D-glucose uptake compared to the K_m of 0.053±0.006 mM for wild type *L. enriettii* (119). The oocyte glucose transport K_m values differ by an order of magnitude from parasite values. The authors rationalize the discrepancy between the parasite and oocyte K_m's by arguing that 2-deoxy-D-glucose uptake studies in the parasite probably measure substrate uptake and phosphorylation by hexokinase rather than transport *per se* (122). Hexokinase phosphorylation of glucose appears to be rate limiting in

Leishmania, but not in oocytes (119, 219). Thus, glucose uptake experiments by ter Kuile and Opperdoes correct for hexokinase in *L. donovani* and result in K_m values between 0.4 to 0.9 mM, which agree with the oocyte expression values obtained for ISO1 and ISO2 (122, 219).

3. Targeting and Localization

Another hypothesis to account for the presence of two isoforms proposed that each isoform targets to different subdomains of the cell. To address this possibility, each isoform was modified with an epitope tag from the COOH-terminus of the mammalian glucose transporter, GLUT2 (177). Confocal immunofluorescence and immunoblotting experiments demonstrated that epitope tagged ISO2 localizes to the pellicular plasma membrane, while epitope tagged ISO1 localizes to the flagellar membrane (177). Because the two isoforms target to different domains, it is unlikely that the epitope tag interferes with targeting. Why the parasite has a flagellar glucose transporter remains unclear, especially since the majority of glycolytic enzymes localize to membrane bound glycosomes in the cell body (162) so that glucose transported into the flagellum cannot be utilized until it has reached the cytoplasm. The possible roles of the flagellar glucose transporter will be addressed in the Discussion section of this thesis.

However, because the two isoforms differ only in their NH_2 -terminal cytoplasmic domains and each isoform targets to a distinct subdomain of the plasma membrane, we utilized these two isoforms as a model system for studying differential targeting of integral membrane proteins in a contiguous membrane.

D. Other Trypanosomatid Transporters of the Mammalian Glucose

Transporter Superfamily

In addition to PRO1, other glucose transporters and twelve transmembrane domain transporters have been cloned and characterized in trypanosomatids. Two *Leishmania* transporters in particular are relevant to this thesis, the D2 hexose transporter and the MIT *myo*-inositol transporter.

1. Other Hexose Transporters

The other trypanosomatid hexose transporters strongly resemble PRO1 at the level of amino acid sequence and predicted secondary structure (224). The section below briefly describes the salient characteristics of the other hexose transporters.

a. *L. mexicana* GT1, GT2, and GT3

Recently, Burchmore and Landfear cloned the genes encoding the *L. mexicana* homologues of PRO1 (34). The three isoforms exhibit greater than 90% amino acid identity between LMGT1, LMGT2, and LMGT3 and between 78-85% amino acid identity to PRO1 (34). *LMGT2* mRNA is expressed primarily in the promastigote stage, while the mRNAs for the other two isoforms are constitutively expressed in both promastigote and amastigote stages, but at significantly lower levels than *LMGT2* (34). The genes are present as single copies in a tandem cluster (34). LMGT1 contains a longer NH₂-terminus than the other isoforms (45 amino acids longer) (34). Localization has not yet been determined for any of the isoforms.

Figure 1-11. Amino Acid Composition of D2.

Nonpolar:	No.	Percent
A	9	8.41
V	2	1.87
L	9	8.41
I	3	2.80
P	11	10.28
M	5	4.67
F	3	2.80
W	0	0.00
		39.24

Polar:	No.	Percent
G	4	3.74
S	17	15.89
T	7	6.54
C	0	0.00
Y	0	0.00
N	6	5.61
Q	4	3.74
		35.52

Acidic:	No.	Percent
D	6	5.61
E	11	10.28
		15.89

Basic:	No.	Percent
K	6	5.61
R	3	2.80
H	1	0.93
		9.34

Estimated pI=4.28

b. Trypanosome Hexose Transporters

Hexose transporters genes have been cloned from *T. brucei*, *T. vivax*, and *T. cruzi* (224). As with *Leishmania* hexose transporters, the trypanosome transporters are facilitative and have K_m s (0.1-0.5 mM) comparable to ISO1 and ISO2 (224). None of the transporters has been localized by electron microscopy or immunofluorescence. The trypanosome transporter NH₂-termini are similar in length to ISO2 and do not contain sequences resembling ISO1.

c. D2

The D2 transporter from *L. donovani* is encoded by a single copy gene and is expressed exclusively in the promastigote stage (120). The protein has 45% amino acid identity to PRO1 (120). The NH₂-terminus of D2 is similar to ISO1 in length (103 amino acids *versus* 130 for ISO1), and the amino acid composition of the NH₂-terminus has features similar to both ISO1 and ISO2 (Fig. 1-11). However, the NH₂-terminus of D2 has a predicted acidic pI of 4.28, similar to ISO2. The transport properties differ significantly from PRO1. In *Xenopus* oocytes, D2 has a much higher K_m of 150 mM for 2-deoxy-D-glucose (about 500-fold greater than ISO1 or ISO2 and higher than any other known hexose transporter) (121). The D2 transporter potentially functions to take advantage of high glucose levels when sandflies take a glucose rich plant sap meal. Alternatively, D2 could recognize some other unknown substrate with glucose serving as a poor substrate analog. However, examination of many other sugars or related compounds failed to reveal any other substrates, except for fructose and

mannose, compounds which are also substrates for the other known trypanosomatid glucose transporters.

D2 localizes to the pellicular plasma membrane and the flagellar pocket (121). The transporter also localizes to a distinct uncharacterized dot, as seen by immunofluorescence, that may be the Golgi apparatus (121). Immunoblotting and Southern blots suggest that *L. enriettii* contains a homologous gene (unpublished results).

2. MIT

Langford *et al.* cloned the gene for another putative member of the facilitative hexose transporter superfamily from *L. donovani*, referred to as *D1* (120). The *D1* transporter originally was considered most similar to an arabinose transporter (120). However, *D1* was subsequently shown to have significant amino acid homology to a yeast *myo*-inositol transporter (*ITR1*) and does in fact transport *myo*-inositol (59). Unlike the *Leishmania* hexose transporters, the MIT *myo*-inositol transporter (*D1*) is an active transporter that cotransports protons (59).

MIT expression occurs in both amastigote and promastigote life stages of the parasite (120). The *MIT* gene is present as a single copy (120). Most relevant to this thesis is the fact that the transporter localizes over the entire plasma membrane (flagellar, flagellar pocket, and pellicular plasma membrane), although flagellar membrane localization is weak compared to the rest of plasma membrane and is concentrated toward the base of the flagellum (59).

VII. Specific Aims

Specific Aim 1: To characterize the flagellar targeting sequence(s) of ISO1

We postulated that the NH₂-terminal domain of ISO1 contains the necessary information for flagellar targeting. We created chimeric proteins using the pellicular plasma membrane targeted hexose transporter, D2 and replaced the NH₂-terminus of D2 with the NH₂-terminus of ISO1 or ISO2. Confocal immunofluorescence microscopy revealed that the ISO2::D2 chimera targets to the pellicular plasma membrane, like the wild type D2 protein. However, the ISO1::D2 chimeric protein targets to the flagellar membrane, demonstrating that the NH₂-terminus of ISO1 is **sufficient** to retarget a pellicular plasma membrane protein to the flagellar membrane.

To begin characterizing the sequences of the NH₂-terminus necessary for flagellar targeting, we used PCR to generate a series of NH₂-terminal deletion mutants. Deletion mutants missing the first 10 or 20 amino acids still target to the flagellar membrane. The 25 amino acid deletion mutant targets to both the flagellar and pellicular plasma membranes, although most of the staining is in the pellicular plasma membrane, while the 30 amino acid deletion mutant localizes exclusively to the pellicular plasma membrane and flagellar pocket. Thus, a **necessary** flagellar targeting sequence maps to the sequence near amino acid 25. Internal deletions of various increments of downstream amino acids from 30 to 130 were created to test whether other sequences of ISO1 are necessary for flagellar targeting.

A complementary approach to creating chimeras between the NH₂-termini of ISO1 and ISO2 was used to identify regions of ISO1 **sufficient** for flagellar targeting. An ISO1::ISO2 chimera containing the first 35 amino acids of ISO1 added to the NH₂-terminus of ISO2 is sufficient to retarget ISO2 to the flagellar membrane. Thus the shortest sequence of ISO1 so far proven to be capable of retargeting ISO2 is 1-35.

To define the essential amino acids of the flagellar targeting sequence, we mutagenized amino acids 22 through 32 and replaced them with alanines or glycines. No single amino acid substitution was sufficient to prevent flagellar targeting of ISO1. However, single mutations in any of amino acids 25 to 29 did display quantitatively altered flagellar targeting patterns relative to wild type ISO1, which suggests that amino acids 25 to 29 are important for flagellar targeting. We hypothesized that redundancies may exist in the targeting sequence and that individual amino acid substitutions are insufficient to abrogate flagellar targeting, although such mutations may affect to some degree the efficiency of flagellar targeting.

Specific Aim 2: To characterize targeting and restriction of ISO2 to the pellicular plasma membrane.

The nature of ISO2 localization to the pellicular plasma membrane could involve multiple mechanisms including and not limited to: 1) a targeting signal to direct ISO2 to the pellicular plasma membrane, 2) passive diffusion from the flagellar pocket into the pellicular plasma membrane, 3) a physical barrier or active process that excludes ISO2 from the flagellar membrane, and/or 4) a

mechanism that retains ISO2 in the pellicular plasma membrane. The second specific aim of this thesis was to characterize the nature of pellicular plasma membrane targeting of ISO2.

We tested the hypothesis that ISO1 or ISO2 might differentially associate with the parasite cytoskeleton. *Leishmania* subpellicular microtubules have been shown to be physically attached to the pellicular plasma membrane. We performed nonionic detergent extractions, followed by immunoblots of the detergent insoluble cytoskeletal pellet versus the detergent soluble supernatant. Immunoblots demonstrated that ISO1 fractionates exclusively with the supernatant, while ISO2 quantitatively fractionates with the cytoskeletal pellet. Confocal immunofluorescence microscopy of detergent extracted cytoskeletons from wild type *L. enriettii* and epitope tagged isoform expressing parasites confirmed the immunoblot results. Thus, parasite cytoskeletons displayed intense staining for ISO2 over the subpellicular microtubules, but only background staining of flagellar microtubules, and the cytoskeletons did not show any staining for ISO1. These results indicate that ISO2 is tethered to the pellicular microtubules, but that ISO1 is not stably attached to the cytoskeleton. Furthermore, the phenomenon of cytoskeletal tethering was demonstrated for other integral membrane proteins including the D2 hexose transporter and the MIT *myo*-inositol transporter, both from another species, *L. donovani*. Interestingly, NH₂-terminal deletion mutants of ISO1 that retarget to the pellicular plasma membrane also tether to the subpellicular microtubules, indicating that this isoform contains all of the structural information required for tethering.

Chapter 2

Cytoskeletal Association is Important for Differential Targeting of Glucose Transporter Isoforms in *Leishmania*.

Erik L. Snapp and Scott M. Landfear

Department of Molecular Microbiology and Immunology, Oregon Health
Sciences University, Portland, Oregon 97201

published in J. Cell Biol. 139: 1775-1783. 1997.

Address correspondence to Scott M. Landfear, Department of Molecular Microbiology and Immunology, Oregon Health Sciences University, 3181 S.W. Sam Jackson Park Road, Portland, OR 97201. Tel: (503) 494-2426. Fax: (503) 494-6862.

Abstract

The major glucose transporter of the parasitic protozoan *Leishmania enriettii* exists in two isoforms, one of which (ISO1) localizes to the flagellar membrane while the other (ISO2) localizes to the plasma membrane. These two isoforms differ only in their cytosolic NH₂-terminal domains. Using immunoblots and immunofluorescence microscopy of detergent extracted cytoskeletons, we have demonstrated that ISO2 associates with the microtubular cytoskeleton that underlies the cell body membrane, whereas the flagellar membrane located ISO1 does not associate with the cytoskeleton. Deletion mutants that remove the first 25 or more amino acids from ISO1 are retargeted from the flagellum to the pellicular plasma membrane, suggesting that these deletions remove a signal required for flagellar targeting. Unlike the full length ISO1 protein, these deletion mutants associate with the cytoskeleton. Our results suggest that cytoskeletal binding serves as an anchor to localize the ISO2 transporter within the plasma membrane and that the flagellar targeting signal of ISO1 diverts this transporter into the flagellar membrane and away from the pellicular microtubules.

Introduction

Differential targeting of integral membrane proteins plays a critical role in defining specialized compartments and structures in eukaryotic cells.

Considerable attention has been given to the mechanisms of protein targeting in yeast and higher eukaryotic cells. One well characterized mechanism for selective retention of integral membrane proteins involves association of the protein with the cytoskeleton. Band 3 (or AE1, anion exchanger 1), a mammalian reticulocyte anion exchanger associates with ankyrin (19, 57), which binds directly to the cytoskeletal protein β -spectrin. Ankyrin acts as a tether, effectively securing Band 3 to the cytoskeleton. The cytoskeletal tethering has been shown to be critical for maintenance of erythrocyte cell morphology and for the restriction of AE1 to the polarized apical or basolateral cell surface of epithelial cells (6, 58). In epithelial cells, the Na^+/K^+ -ATPase associates with ankyrin in a similar manner (100, 110, 151, 157). In neurons, the glycine receptor associates with gephyrin, a protein which binds to microtubules (107). Cytoskeletal tethering functions to localize and concentrate the glycine receptor at postsynaptic sites where these receptors function in neurotransmission (106, 108). Thus cytoskeletal association of specific integral membrane proteins is likely to be widespread among different cell types and organisms and is a major mechanism for restricting proteins to discrete membrane subdomains.

The plasma membrane of trypanosomatid protozoa such as trypanosomes and *Leishmania* species can be divided into at least three structurally and functionally distinct subdomains (9): i) the pellicular membrane that surrounds the cell body, ii) the flagellar membrane that covers the flagellum, and iii) the flagellar pocket membrane, and invagination of the plasma membrane that is located at the base of the flagellum. These membranes are physically contiguous and together constitute the plasma membrane surface of the parasite. However, currently little

is known about how these membranes differ in protein composition or how proteins are targeted to and retained within each subdomain.

We have shown previously (177) that two closely related isoforms of the major glucose transporter from the parasitic protozoan *Leishmania enriettii* are differentially localized. Isoform-1 (ISO1) is located primarily in the flagellar membrane, while isoform-2 (ISO2) is localized primarily to the pellicular membrane surrounding the cell body. Hence although these two membranes are contiguous, the differential localization of these glucose transporter isoforms underscores the fact that they have different protein compositions and constitute distinct domains of the plasma membrane. Both isoforms are also present in the membrane of the flagellar pocket, the functionally specialized domain of the plasma membrane that receives proteins that are ultimately destined for the pellicular and flagellar membranes or that are secreted into the extracellular medium (240). These two glucose transporter isoforms differ only in their cytosolic NH₂-terminal domains; ISO1 has a 130 amino acid domain which is completely different in sequence from the 48 amino acid NH₂-terminal domain of ISO2 (Fig. 2-1). Because the isoforms differ only in their NH₂-terminal domains and are identical in sequence throughout the rest of the protein, the NH₂-terminal region of ISO1 is likely to contain a flagellar targeting signal. The presence of a flagellar targeting signal is supported by experiments in this paper which demonstrate that chimeric proteins containing the NH₂-terminal domain of ISO1 are targeted to the flagellar membrane.

Leishmania and other members of the Kinetoplastida have unusual cytoskeletons comprised of subpellicular microtubules that are attached to the inner surface of the plasma membrane and which provide the cell with its characteristic shape (39, 201). The linkage between these subpellicular microtubules and the plasma membrane is likely to involve the direct or indirect

interaction of integral membrane proteins with the microtubules. The other surface membranes, those surrounding the flagellar pocket, the flagellar adhesion zone and the flagellum itself, are devoid of subpellicular microtubules. The flagellum also contains internal cytoskeletal elements including the flagellar axoneme and the paraflagellar rod (233). One potential explanation for the differential targeting of the two glucose transporter isoforms between these specialized membrane compartments is that each isoform interacts differently with various cytoskeletal components. To investigate this possibility, we have fractionated parasites into detergent insoluble cytoskeletons and detergent soluble supernatants and monitored the association of each glucose transporter isoform with each fraction. These experiments reveal that the pellicular membrane ISO2 tightly associates with the subpellicular microtubules, whereas the flagellar ISO1 is released into the supernatant by detergent solubilization. These results suggest that ISO2 anchors in the cell body membrane by tethering to the subpellicular microtubules, while ISO1 targets to the flagellar membrane by structural information present in its unique NH₂-terminal domain. Similar interactions may direct other parasite pellicular membrane or flagellar membrane proteins to their correct subcellular addresses.

Materials and Methods

Plasmid Constructs

The plasmid pX63Hyg (7) was used for expression of epitope tagged constructs in *L. enriettii*. The 13 COOH-terminal amino acids of rat GLUT2 (225) (TVQMEFLGSSETV), which were used as the epitope tag, were introduced into ISO1 and ISO2-containing plasmids as previously described (177). The polylinker 5' to ISO1 was modified to create a new *Bgl* II restriction site by digesting at the 5' *Sma* I site and ligating to a *Bgl* II linker. NH₂-terminal deletion constructs of ISO1 removing the first 10, 20, 25, 30, 50, and 100 amino acids were created. For these constructs, a primer containing a *Bgl* II restriction site, a Kozak sequence (AGCAGC), and encoding a methionine and the first 6 amino acids following the region to be deleted, was used as the forward primer and an antisense primer encoding the 6 amino acids upstream of the unique *Cla* I site within the coding region (35) and the *Cla* I site was used as the reverse primer to amplify the NH₂-terminal region of ISO1. The amplified fragments were gel purified, digested with *Bgl* II and *Cla* I, and cloned into a [*pX63 HYG ISO1*] vector containing the GLUT2 epitope tagged ISO1 (177) using the internal *Cla* I site and the *Bgl* II site in the upstream polylinker region. The regions containing the deletions were sequenced, as reported previously (177), to confirm that the correct constructs had been generated.

The plasmid [*pALT NEO*] (115) was used for expression of the chimeras containing the NH₂- terminal cytoplasmic domains of either ISO1 or ISO2 fused to the body of the D2 hexose transporter (120). A DNA sequence encoding the first 130 amino acids of *ISO1* or the first 48 amino acids of *ISO2* (the NH₂-terminal domains) followed by amino acids 108 to 112 of *D2* (a sequence encoding the beginning of the first predicted transmembrane domain and containing an *Nru* I site used for subcloning) were introduced into a *D2*

containing plasmid by polymerase-chain-reaction-based mutagenesis (177). The regions of these chimeras amplified by PCR were sequenced to ensure that no unintended sequence alterations had occurred during PCR.

Cell Culture and Transfection

Promastigotes of *L. enriettii* were cultured at 26°C in DME-L medium (93) containing 5% fetal calf serum and 5% bovine embryonic fluid. Parasites were transfected by electroporation (103) of plasmid DNA using a Gene Pulser (Bio Rad Laboratories, Richmond, CA) apparatus. One day after transfection, hygromycin (Calbiochem-Novabiochem Corp., La Jolla, CA) was added to a final concentration of 50 µg/ml to the culture, and the parasites were maintained under these conditions until drug-resistant parasites grew out (usually ~4 weeks). The hygromycin concentration was then increased to 200 µg/ml for maintenance of transfected parasites. Parasites transfected with pAlt-Neo based plasmids were selected with 10µg/ml of G418 (Gibco/BRL, Gaithersberg, MD) one day after transfection, and the drug concentration was increased to 200 µg/ml after parasites grew out.

Antibody Preparation

Polyclonal antiserum against the glutathione *S*-transferase fusion protein containing the 25 COOH-terminal amino acids of a rat GLUT2 was purchased from East Acres Biologicals (Southbridge, MA) and it was used for immunofluorescence at a dilution of 1:500. For Western blots, polyclonal antiserum against a maltose binding protein fusion protein (81, 134) (New England Biolabs, Beverly, MA) containing the 13 COOH-terminal amino acids of a rat GLUT2 was used. Cocalico Biologicals, Inc. (Reamstown, PA) prepared the antiserum and it was used at a dilution of 1:500.

The anti-P1C (PRO1 COOH-terminus antibody, directed against the 32 COOH-terminal amino acids of the PRO1 glucose transporters, has been

described previously (177). The anti-PIL (PRO1 loop) antiserum was raised against a glutathione S-transferase fusion protein containing amino acids 160-227 of ISO2 (35), which are contained within the first extracellular loop of PRO1. This antiserum was affinity purified (177) over a sepharose column (BioRad Laboratories) containing this fusion protein, concentrated by passing the affinity purified serum over a protein A sepharose column (Sigma Chemical Co., St. Louis, MO), and used at a dilution of 1:500 for protein blots. The specificity of each antiserum was confirmed using immunoblots by competition with the fusion protein used to raise the antiserum, as described previously (177); the same concentration of native glutathione S-transferase did not compete the signal from either antiserum.

The mouse anti- α -tubulin monoclonal antibody raised against native chick brain microtubules was obtained from Amersham Corp. (Arlington Heights, IL). The E7 mouse anti-human β -tubulin monoclonal antibody was prepared by Dr. Michael Klymkowsky and was obtained from the Developmental Studies Hybridoma Bank maintained by the Department of Pharmacology and Molecular Sciences, Johns Hopkins University School of Medicine, Baltimore, MD 21205, and the Department of Biological Sciences, University of Iowa, Iowa City, IA 52242, under contract N01-HD-2-3144 from the NICHD. The anti-D2 and anti-MIT affinity purified antibodies, which were directed against the COOH-terminal hydrophilic domains of each transporter, have been described previously (59, 121).

Cell Lysates and Immunoblots

For preparation of total cell lysates, parasites at a density of $1-2 \times 10^7$ /ml were pelleted, washed with PBS, resuspended in Laemmli sample buffer (190) to a density of $0.2-1 \times 10^9$ cells/ml and immediately heated to 65°C for 5 min. Samples containing 10 μ l of lysate were reheated to 65°C for 3 min, loaded onto

10% SDS-polyacrylamide gels, separated by standard methods (166), and electroblotted onto a nitrocellulose membrane using a Mini Trans-Blot apparatus (Bio Rad Laboratories) according to the manufacturer's instructions. Blots were developed using the ECL chemiluminescence system (Amersham Corp.) and goat anti-rabbit IgG coupled to horseradish peroxidase (Boehringer Mannheim Biochemicals, Indianapolis, IN), as detailed in the manufacturer's instructions, and the developed blots were exposed to XAR-5 film (Eastman Kodak Co., Rochester, NY).

Cytoskeleton Preparation

Leishmania cytoskeletons were prepared using the method of Schneider *et al.* (198). Briefly, parasites were grown to $1-2 \times 10^7$ cells/ml and washed 3x in ice cold PBS. The pellet of cells was resuspended in MME (10mM MOPS, pH 6.9, 0.1mM EGTA, 1mM MgSO₄, and 0.1% Triton X-100) plus protease inhibitors (1 μ M each of leupeptin, aprotinin, and chymostatin) at a concentration of 4×10^7 cells/ml. The cells were incubated on ice for 10 min and centrifuged at 3000 x g in an Eppendorf microcentrifuge (Brinkmann Instruments Inc., Westbury, NY) for 5 min. The pellet was washed once with PBS and resuspended to 1/20 of the MME volume in PBS/Laemmli Sample Buffer, at a 1:1 mix. The supernatant was concentrated to 1/10 of the original volume with a Microcon 10 microconcentrator (Amicon, Beverly, MA), to approximate the pellet concentration, and 0.25 volume of 4x Laemmli Sample Buffer was added to the supernatant. Both supernatant and pellet were heated at 60°C for 5 min. For protein gels and immunoblots, 10 μ l of pellet and 20 μ l of supernatant were run per lane. For immunofluorescence, the pellets were prepared as described above, except that they were resuspended in 1/2 the original volume of PBS following centrifugation and washing.

Immunofluorescence Microscopy

For immunofluorescence imaging, parasites were pelleted, washed twice in PBS, resuspended at a density of approximately 10^7 cells/ml, and attached to poly-L-lysine-coated coverslips. For cytoskeleton preps, pellets were prepared as described above, resuspended at a density of approximately 10^7 cytoskeletons/ml, and attached to poly-L-lysine-coated coverslips. The adherent parasites/cytoskeletons were fixed with 100% methanol at -20°C for 15 min. After fixation, coverslips were rinsed in PBS and then incubated in PBS plus 2% goat serum for 15 min. Antiserum was added at the appropriate dilution in PBS plus 2% goat serum and incubated for 1 h at room temperature. Coverslips were rinsed three times in PBS and then incubated for 1 h with a 1:200 dilution of goat anti-rabbit IgG coupled to FITC (fluorescein isothiocyanate) (Molecular Probes, Inc., Eugene, OR) or to rhodamine B (Biosource International, Camarillo, CA) or with goat anti-mouse IgG coupled to Bodipy Oregon Green (1200) or Texas Red (1:800)(both from Molecular Probes, Inc.) in PBS plus 2% goat serum. Coverslips were rinsed 5 times with PBS and then mounted on slides in 50 mM Tris, pH 8.0, 90% glycerol, and 20 mg/ml n-propyl-gallate (Sigma Chemical Co.). For confocal microscopy, samples were examined with a confocal laser scanning microscope as described previously (177).

Results

Fractionation of Glucose Transporter Isoforms into Detergent Soluble and Insoluble Phases

One possible explanation for the differential localization of the glucose transporter isoforms ISO1 and ISO2 is that each isoform interacts with the parasite cytoskeleton in a different way. The cytoskeleton of Kinetoplastid parasites, containing the subpellicular microtubules and the flagellar axoneme, can be separated from the cytosolic and membrane components of the cell by solubilization with non-ionic detergents such as Triton X-100 followed by centrifugation to quantitatively pellet the cytoskeletons (183). To test the possible association of each glucose transporter isoform with the detergent insoluble cytoskeleton, we prepared soluble and insoluble fractions from *L. enriettii* promastigotes and probed immunoblots of each fraction with the anti-P1C antibody directed against the COOH-terminal hydrophilic domain that is conserved in both isoforms (Fig. 2-1). Whereas immunoreactive proteins of ~50kD and ~65kD are present in the total cell lysates (Fig. 2-2A, lane 1), the ~50 kD protein is quantitatively associated with the detergent insoluble fraction (lane 2), and the ~65 kD protein is quantitatively associated with the supernatant (lane 3).

These results suggest that the major glucose transporter isoform, ISO2, fractionates quantitatively with the detergent insoluble pellet and is likely to be associated with the parasite cytoskeleton. This isoform has a predicted molecular mass of 61.4 kD but migrates more rapidly on SDS-PAGE (179), similar to the anomalously rapid mobility of mammalian glucose transporters (157). Conversely, the less intense slower mobility band present in the supernatant fraction is likely to represent the larger (~70 kD predicted molecular weight) and

less abundant ISO1 that is located in the flagellar membrane (177). These suggestions are confirmed by epitope tagging results discussed below. Similar fractionation results have also been obtained (data not shown) using the anti-PIL antibody directed against the first extracellular loop that is conserved in ISO1 and ISO2.

One potential artifact of the preceding fractionation experiments could arise from possible cross-reactivity of the anti-P1C and anti-PIL antibodies with the abundant α - and β -tubulin proteins present in the cytoskeletal pellet. To demonstrate that the ~50 kD band detected in the pellet is not a tubulin subunit, we probed immunoblots (Fig. 2-2B) of the pellet fraction with the anti-PIL antibody (lane 1), and with monoclonal antibodies directed against either chicken α -tubulin (lane 2) or human β -tubulin (lane 3). The distinctly slower mobility of the tubulin subunits compared to the band that reacts with the anti-PIL antibody demonstrates that this latter band does not represent tubulin.

To confirm the results of the immunoblots, we have also examined the detergent-extracted cytoskeletons by immunofluorescence using both the anti-P1C and anti- β -tubulin antibodies. The anti-P1C antibody reacts with the body of the parasite in these cytoskeletal preps but not with the flagella (Fig. 2-3, *P1C*), consistent with the notion that the pellicular membrane ISO2 is associated with the cytoskeleton but the flagellar ISO1 is not. In contrast, the control anti- α -tubulin antibody reacts with microtubules in both the cell body and the flagellum (Fig. 2-3, *α -tubulin*).

To further support the conclusion that the interaction between the parasite glucose transporter and components of the pellet is not the result of non-specific binding, we have also performed fractionations using lysis buffer containing high concentrations of Triton X-100 (1%), n-octyl-glucoside (0.5%), CHAPS (0.5%), Zwittergent (0.5%), Nonidet-P40 (0.5%), NaCl (1M), and β -mercaptoethanol (0.5

M). In each case, the ~50 kD glucose transporter band fractionated quantitatively with the pellet (data not shown). We have also attempted to specifically solubilize the parasite cytoskeleton to demonstrate that disruption of the microtubules releases the glucose transporter from the pellet. The subpellicular microtubules of Kinetoplastid parasites are impervious to classical microtubule disrupting treatments including alkaloids such as colchicine, cold, vinblastine, etc. ((201) and data not shown). The microtubules of the closely related parasite *Trypanosoma brucei* can be disrupted by 1 mM CaCl₂ or 1 M NaCl (159). However, we have found that the cytoskeletons of *L. enriettii* and other *Leishmania* species are resistant to 1 M NaCl, and are disorganized by 1-10 mM CaCl₂ but form amorphous aggregates that pellet upon centrifugation.

The tricyclic drug chlorpromazine disrupts cytoskeletons of trypanosomatid protozoa (200) including *Leishmania* (168) when live cells are incubated with drug. To determine whether this cytoskeletal disrupting drug releases ISO2 from the pellet of a detergent extract, we incubated *L. enriettii* cells with 1mM chlorpromazine for 30 minutes and then prepared fractionated detergent extracts. As shown in Fig. 2-4 (*lanes 3, 4*) this cytoskeletal disrupting agent releases ISO2 into the supernatant, whereas treatment of control cells with DMSO alone (Fig. 2-4 *lanes 1, 2*) or with a nonspecific cell poison, 0.5% sodium azide (not shown), does not release ISO2 from the detergent insoluble pellet. However, one complication with the preceding experiment is that the mechanism of action of chlorpromazine is not known. Although this drug removes pellicular microtubules from the plasma membrane (200), it clearly does not completely depolymerize these microtubules, as they still fractionate with the pellet of the detergent extract (Fig. 2-4 *lanes 7, 8*). The ability of this cytoskeletal disrupting drug to release ISO2 from the pellet is consistent with the interpretation that ISO2 interacts with the parasite cytoskeleton and not with some other component of the

detergent insoluble pellet; however, the absence of a drug that efficiently depolymerizes subpellicular microtubules in this parasite precludes a definitive interpretation of these pharmacological results.

Fractionation of Individual Epitope Tagged Glucose Transporter Isoforms

To examine the cytoskeletal association of each glucose transporter isoform, we used previously established (177) parasite lines that express either ISO1 (line pX63 HYG ISO1) or ISO2 (line pX63 HYG ISO 2) containing a COOH-terminal 13 amino acid epitope tag derived the COOH-terminus of the rat glucose transporter GLUT2 (225). Immunoblots of pellets and supernatants from each cell line probed with the anti-GLUT2 antiserum (Fig. 2-5) reveal that the ~50kD ISO2 fractionates quantitatively with the pellet (lanes 1,2), whereas the ~65 kD ISO1 fractionates quantitatively with the supernatant (lanes 3,4).

Examination of cytoskeletal pellets derived from each cell line using double label immunofluorescence (Fig. 2-6) confirms the cytoskeletal association of ISO2 but not ISO1. Thus cytoskeletons from the ISO1-expressing cell line incubated with the anti-GLUT2 antibody directed against the epitope tag show only background levels of staining (*ISO1 GLUT2*), confirming the absence of ISO1 in the cytoskeletons. However, the same cells incubated with the control anti- α -tubulin antibody stain on both the cell bodies and the flagella (*ISO1 α -tubulin*). In contrast, cytoskeletons from the ISO2-expressing cell line incubated with the anti-GLUT2 antibody stain intensely over the cell body but not the flagellum (*ISO2 GLUT2*), indicating the presence of ISO2 in this cytoskeletal fraction associated with the subpellicular microtubules. The control anti- α -tubulin antibody stains both the cell body and the flagellum (*ISO2 α -tubulin*).

Partial Characterization of a Flagellar Targeting Signal of ISO1

Because ISO1 and ISO2 differ only in their NH₂-terminal domains, these regions must contain the information required for differential targeting. One

possibility is that the NH₂-terminal domain of ISO1 contains a signal that causes trafficking of this isoform to the flagellum. To determine whether the NH₂-terminal domain of ISO1 was sufficient to target an integral membrane protein to the flagellar membrane, we created a chimeric construct which replaced the NH₂-terminal cytoplasmic domain of a different pellicular membrane transporter, the D2 hexose transporter from the related parasite *L. donovani* (121), with the NH₂-terminal domain of ISO1. This I1::D2 chimeric protein was expressed in *L. enriettii* cells, and the location of the chimera was determined by immunofluorescence microscopy using an antibody directed against the *L. donovani* D2 transporter. In contrast to the wild type D2 transporter, the I1::D2 chimera is targeted to the flagellar membrane (Fig. 2-7, *I1.D2*). Thus, the ISO1 NH₂-terminal domain contains a dominant flagellar targeting signal that is sufficient to redirect a pellicular membrane protein to the flagellum. As a complementary control, we also prepared a chimera containing the NH₂-terminal cytoplasmic domain of ISO2 fused to the body of the D2 hexose transporter. Immunofluorescence images of parasites expressing this I2::D2 chimera reveal that it is targeted to the pellicular membrane and does not appear in the flagellar membrane (Fig. 2-7, *I2.D2*), similar to the previously determined localization of ISO2 (177) and similar to the localization of the *L. donovani* D2 transporter when it is expressed in either *L. donovani* (121) or in *L. enriettii* (data not shown).

To begin to characterize the flagellar targeting signal, we created a series of NH₂-terminal deletions of ISO1 (Fig. 2-8A) as detailed in Materials and Methods. Each epitope tagged construct was transfected into *L. enriettii*, and the stably transfected cells were assayed by confocal immunofluorescence microscopy for localization of the ISO1 deletion mutants (Fig. 2-8B). NH₂-terminal deletions of 10 (not shown) and 20 (Fig. 2-8B, $\Delta 20$), amino acids result in ISO1 mutants that exhibit wild type localization in the flagellar membrane. Deleting five more

amino acids creates a protein that localizes primarily to the plasma membrane, but with some staining present on the flagella of some parasites (Fig. 2-8B, $\Delta 25$).

Deletion of five additional amino acids results in a protein that localizes exclusively to the plasma membrane (Fig. 2-8B, $\Delta 30$), identical to ISO2 targeting.

Deletions of 50 and 100 amino acids also exhibit the same pellicular membrane localization as $\Delta 30$ (data not shown). Thus, essential ISO1 flagellar targeting information begins at approximately amino acid 25. It is not yet clear whether this targeting information is contained in a discrete contiguous sequence of amino acids, as is the case for the internalization signal of the transferrin receptor (97), or whether it represents a three-dimensional recognition motif, as is the case for the signals for lysosomal enzyme targeting (13). Nonetheless, these results confirm that the NH₂-terminus of ISO1 contains a signal for flagellar targeting.

Fractionation of ISO1 NH₂ Domain Mutants in Detergent Soluble and Insoluble Phases

To examine whether the retargeted ISO1 deletion mutants associate with the cytoskeleton, we performed immunofluorescence of detergent extracted cytoskeletons. Examination of cytoskeletal pellets derived from each cell line using double label immunofluorescence (Fig. 2-9) confirms the cytoskeletal association of $\Delta 25$ and $\Delta 30$. Cytoskeletons from the $\Delta 10$ and $\Delta 20$ expressing cell line show only background levels of anti-GLUT2 staining (Fig. 2-9A, $\Delta 10$ and $\Delta 20$), consistent with the absence of these truncated transporters in the cytoskeletons. The same cells labeled with the control anti- α -tubulin antibody have staining on flagella and cell bodies (Fig. 2-9B), demonstrating that the cytoskeletons remain intact. In contrast, cytoskeletons of $\Delta 25$ and $\Delta 30$ expressing cells labeled with the anti-GLUT2 antibody stain intensely over the cell body, but not the flagellum (Fig. 2-9A, $\Delta 25$ and $\Delta 30$), indicating that these deletion mutants associate with the subpellicular microtubules. The control anti- α -tubulin

antibody stains both the cell body and flagellum (Fig 9B, $\Delta 25$ and $\Delta 30$). Thus, retargeting of ISO1 from the flagellar membrane to the pellicular membrane results in association of the mutant proteins with the cytoskeleton.

Cytoskeletal Tethering in other Leishmania Integral Membrane Proteins

To determine if the phenomenon of cytoskeletal association could be generalized to other integral membrane proteins and to other species of *Leishmania*, we prepared immunoblots of pellets and supernatants of *L. donovani* overexpressing the D2 hexose transporter (121) or the MIT *myo*-inositol transporter (59).

Previous studies have shown that D2 localizes to the plasma membrane (121), whereas MIT localizes to both the pellicular membrane and the flagellar membrane (59). Immunoblots of fractionated D2 hexose transporter and MIT overexpressing cell lines probed with anti-D2 and anti-MIT antibodies respectively (Fig. 2-10) reveal that the ~50kD D2 band fractionates exclusively with the pellet (lanes 1,2), while the ~50kD MIT band fractionates in both the pellet and supernatant (lanes 3,4). These immunoblot results were also confirmed with confocal immunofluorescence microscopy, which reveals that both the D2 and MIT transporters are retained in the detergent extracted cytoskeletons (Fig. 2-11). Thus another pellicular membrane transporter (D2) associates with the cytoskeleton, whereas a transporter (MIT) that is in both the pellicular membrane and the flagellar membrane fractionates with both the cytoskeletal pellet and the supernatant.

Discussion

Association with cytoskeletal components is often a way of targeting membrane proteins to specific locations in the cell. We have demonstrated that the pellicular membrane glucose transporter isoform of the parasitic protozoan *L. enriettii* is specifically bound to the parasite cytoskeleton and that this interaction may serve to constrain this isoform to the cell body domain of the plasma membrane. Conversely the flagellar glucose transporter isoform, which differs from the pellicular membrane isoform exclusively in the NH₂-terminal hydrophilic domain, does not associate with the cytoskeleton. The distinct fractionation properties of these two closely related isoforms underscores the specificity of the interaction between ISO2 and the cytoskeleton and argues strongly that this association is not simply an artifactual binding of a hydrophobic protein to a cytoskeletal component. This conclusion is reinforced by the fact that ISO2 fractionates quantitatively with the cytoskeleton and ISO1 fractionates quantitatively with the detergent soluble supernatant, a result which would be unlikely for a non-specific interaction. However, deletion of the first 25-30 amino acids from the flagellar isoform results in retargeting of this transporter to the pellicular membrane and concomitant association with the cytoskeleton. These results suggest that both isoforms contain the structural information required for cytoskeletal association, but that the flagellar isoform is prevented from establishing this interaction by physical separation into a compartment that does not contain the subpellicular microtubules. We do not yet know the molecular details of this cytoskeletal tethering. However, by analogy to other mammalian membrane proteins that are tethered to the cytoskeleton (AE1, Na⁺/K⁺-ATPase, and the glycine receptor), it is likely that some linker protein binds the transporter to the microtubules. Additional studies will be required to determine which parts

of the ISO2 protein are required for cytoskeletal tethering and to determine whether linker proteins mediate the association of these glucose transporters with the microtubules.

It is noteworthy that tethering to the subpellicular microtubules occurs for other integral membrane proteins that show complete (D2 hexose transporter) or partial (MIT *myo*-inositol transporter) localization to the plasma membrane. Although we do not know how many integral membrane proteins are associated with the cytoskeleton in these organisms, the linkage to microtubules of the three transporters studied here suggests that there may be a large family of such proteins. It is also worth noting that biochemical purification of many integral membrane proteins from Kinetoplastid parasites may require that these proteins be released from the cytoskeleton either before or after detergent extraction.

We have demonstrated, using deletion mutagenesis and chimeric constructs, that the unique NH₂-terminal domain of ISO1 is both necessary and sufficient for the trafficking to the flagellar membrane. Further deletion and point mutagenesis studies are currently in progress to determine whether the flagellar targeting signal is a discrete stretch of amino acids, beginning around amino acid 25, or whether it is structurally more complex. It is likely that this flagellar targeting signal interacts with another protein or proteins required for flagellar targeting, as has been shown for the interaction of the tyrosine-based sorting signal from the mammalian integral membrane protein TGN38 with two clathrin-associated proteins (159). However, this issue remains to be investigated.

The results reported here suggest a tentative model for differential targeting of the two glucose transporter isoforms. During biosynthesis, both proteins are presumably added to the external membrane of the flagellar pocket, the organelle to which integral membrane and secreted proteins are targeted (240) and a membrane that contains both ISO1 and ISO2 (177). Proteins such as ISO1 that

contain a flagellar targeting signal may be sorted to the contiguous flagellar membrane, presumably by interaction of a flagellar targeting signal with other proteins that are part of the sorting apparatus. Proteins such as ISO2 that do not contain a flagellar targeting signal may traffic to the plasma membrane, possibly by default, where they can then interact with the subpellicular microtubules. The cytoskeletal tethering would then constrain these proteins to remain in the cell body membrane. This model underscores the notion that proteins that are differently sorted into subdomains of a contiguous membrane system require not only signals for differential targeting during their trafficking to the membrane but also a mechanism for retention of each protein at its correct subcellular address. Proteins such as MIT that are present in both membranes might have a weak flagellar targeting signal that would sort only a fraction of the proteins to the flagellar membrane. Conversely, MIT might have a weak cytoskeletal tethering signal that would allow diffusion of some of these transporters into the flagellar membrane.

A major objective of future studies will be to identify structural components of each isoform that are involved in cytoskeletal tethering or flagellar targeting and to search for other proteins that may interact with these targeting signals to direct each isoform to its correct subcellular address. Since various proteins in different Kinetoplastid protozoa are restricted largely to the pellicular plasma membrane (e.g. the ISO2 and D2 glucose transporters in *Leishmania* species) or to the flagellar membrane (e.g. ISO1 in *L. enriettii* and the receptor adenylate cyclases in *Trypanosoma brucei* (166)), these targeting pathways may be of broad significance in these protozoa.

The authors wish to thank Jodi Engstrom and Ken Fish for performing the confocal microscopy presented in this paper. Xiaowen Xu prepared the anti-P1L and P1C antibodies. Marco Sanchez and Andreas Seyfang helped with cell transfections. We also wish to thank Caroline Enns, Eric Barklis, and Buddy Ullman for helpful discussions.

This work was supported by National Institutes of Health Grants AI25920 and AI01162 to S.M.L., as well as by a Tartar Fellowship and a NRSA Training Grant to E.L.S. S.M.L. is a recipient of the Molecular Parasitology Award from the Burroughs Wellcome Fund.

Figure 2-1. Schematic Diagram Showing the Putative Membrane Topology of PRO1 Glucose Transporters Isoforms, ISO1 and ISO2. Black boxes represent putative transmembrane domains. Loops above the boxes represent extracellular domains and the loops below the boxes represent intracellular domains. The hatched line of ISO1 and the bold black line for ISO2 indicate that the only sequence differences between the two isoforms occur within the NH₂-terminal domains. ISO1 has a 130 amino acid NH₂-terminal domain, while ISO2 has a 48 amino acid NH₂-terminal domain.

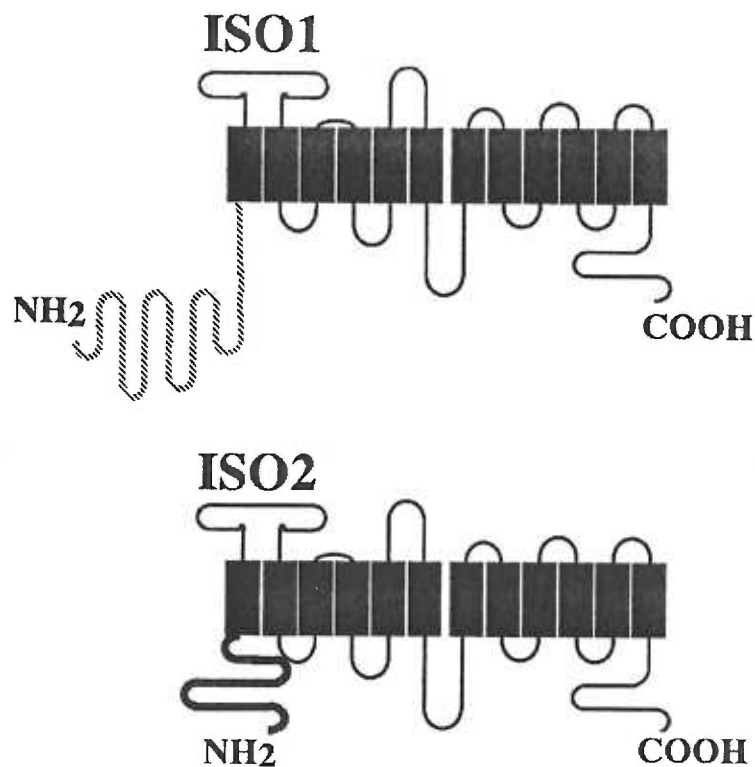
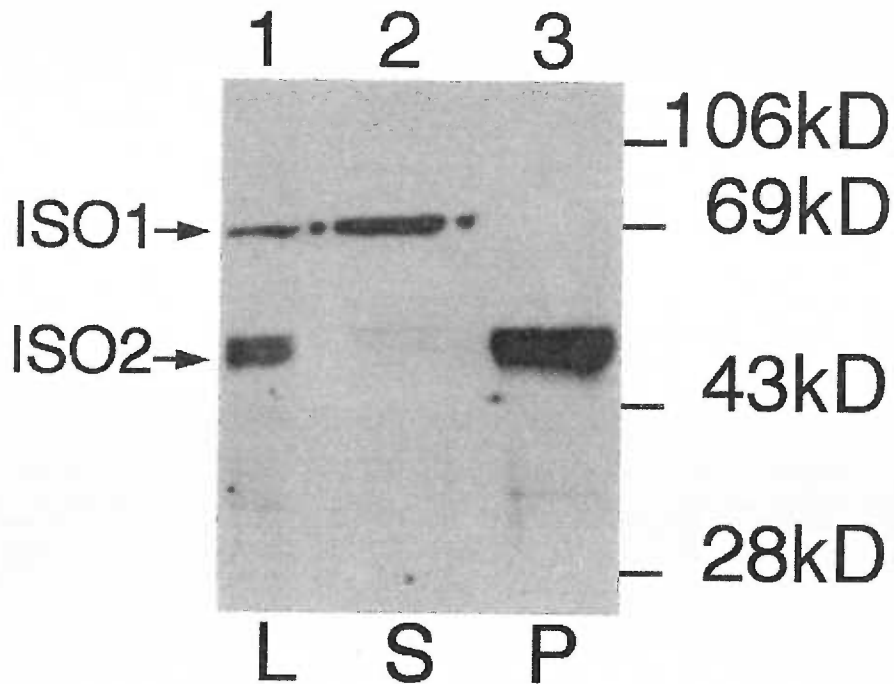


Figure 2-2. Immunoblots of Triton X-100 Extracted *L. enriettii* Fractions.

L designates total lysate, *S* designates the supernatant fraction, and *P* designates the cytoskeletal pellet. *iso-1* and *iso-2* indicate the bands on the blot that correspond to each of these two glucose transporter isoforms. Samples were separated on a 10% SDS-polyacrylamide gel, blotted onto nitrocellulose, and probed with the indicated antibodies. The blots in (A) were probed with affinity purified anti-P1C antibody, and the blots in (B) were probed with anti-P1L (*lane 1*), anti- α -tubulin (*lane 2*), or anti- β -tubulin (*lane 3*). Numbers at the left indicate the mobilities of molecular mass markers in kilodaltons.

A.



B.

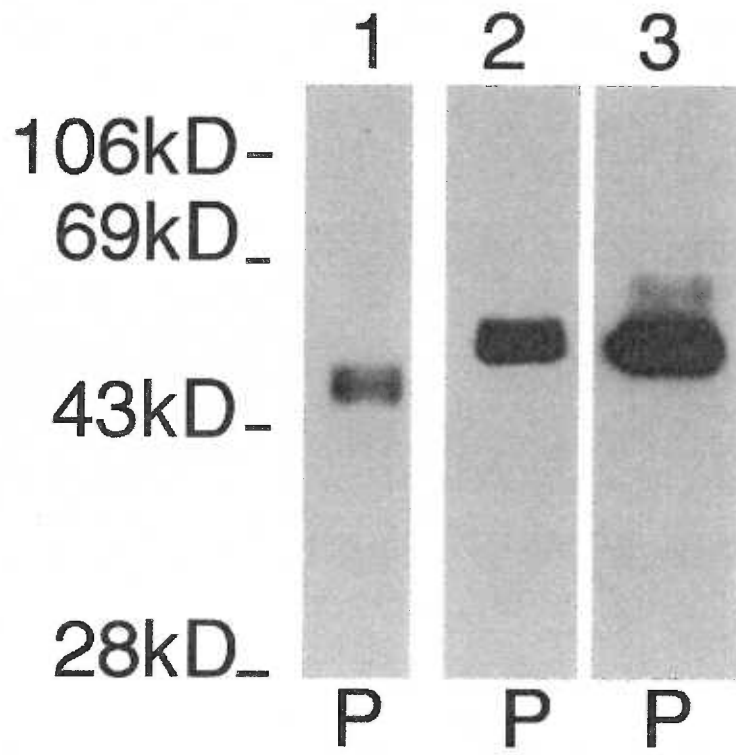


Figure 2-3. Confocal Micrographs of Triton X-100 Extracted *L. enriettii*

Cytoskeletons. Parasites were fixed with methanol, stained with 1:500 dilutions of the anti-P1C antibody and anti- β -tubulin antibody and then with an FITC-conjugated anti-rabbit IgG (*P1C*) and a rhodamine-conjugated anti-mouse IgG (α -*tubulin*) secondary antibodies. Parasites were examined by confocal microscopy using illumination at 488 nm to visualize the PRO1 glucose transporter complexed FITC antibody (*P1C*) or at 546 nm to visualize α -tubulin complexed with the rhodamine antibody (α -*tubulin*). Each micrograph represents a single 0.5- μ m section through each field.

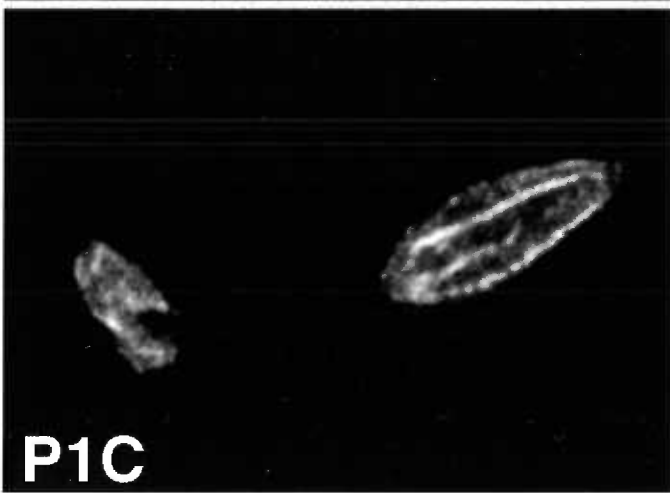
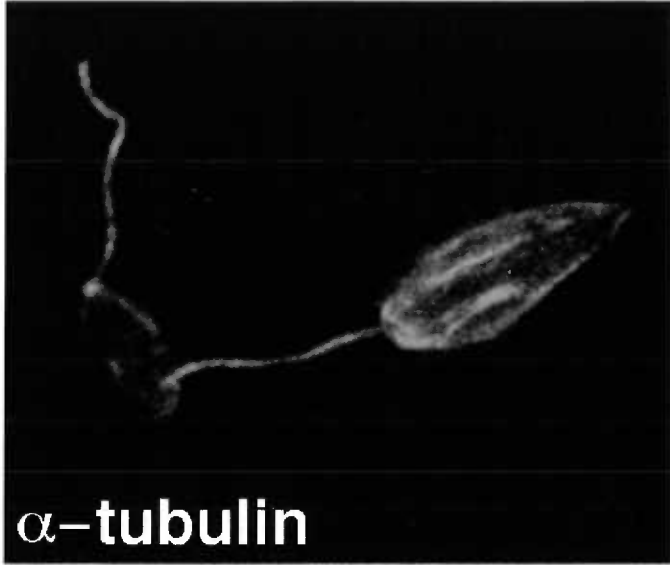


Figure 2-4. Immunoblot of Chlorpromazine Treated Detergent Extraction Fractions of *L. enriettii*. Immunoblot of pellet (*P*) and the supernatant (*S*) fractions from *L. enriettii* incubated with 10% DMSO (lanes 1, 2, 5, and 6) or 1mM chlorpromazine in 10% DMSO (lanes 3, 4, 7, and 8) followed by Triton X-100 extraction. The samples were run on an 8% acrylamide gel. The blot containing lanes 1-4 was probed with the anti-P1C antibody (1:100), and the blot containing lanes 5-8 was probed with the anti- α -tubulin antibody (1:1000). The solid arrow indicates the position of ISO1, and the open arrow indicates the position of ISO2. The numbers at the left indicate the migration of molecular mass markers, with molecular masses given in kD.

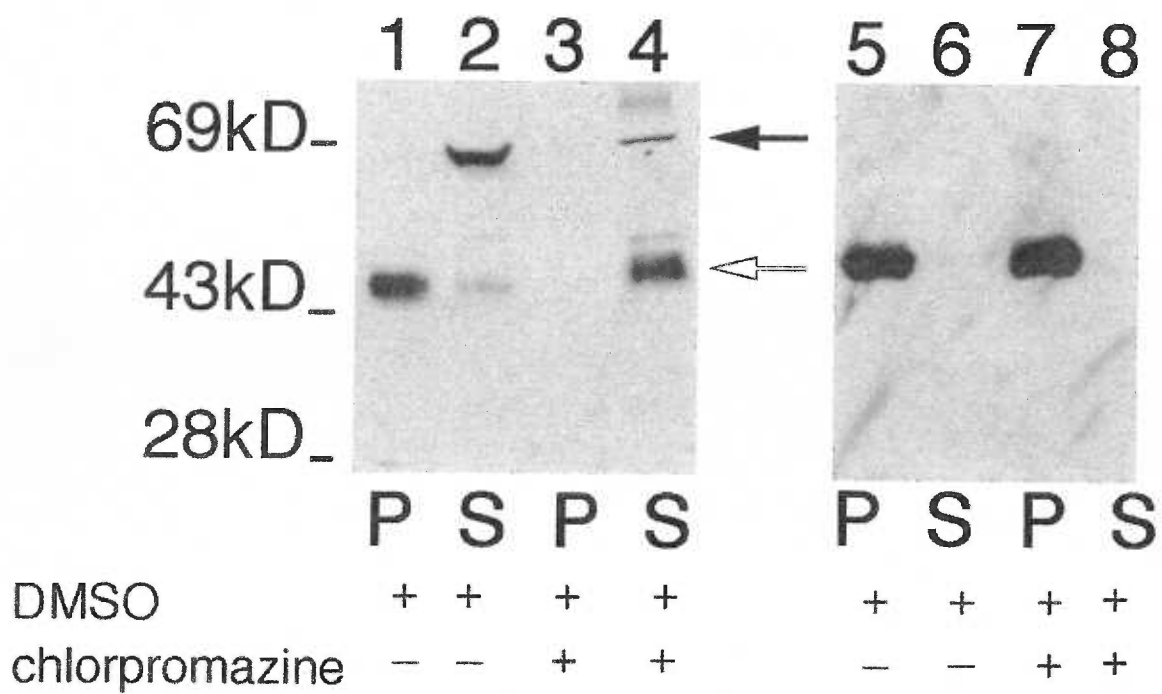


Figure 2-5. Immunoblot of Epitope Tagged ISO1 and ISO2 Detergent

Extraction Fractions. Immunoblot of pellet (P) and the supernatant (S) fractions from triton X-100 extracted *L. enriettii* transfected with plasmids encoding epitope tagged ISO2 (*lanes 1 and 2*) or epitope tagged ISO1 (*lanes 3 and 4*). The blot was probed with an anti-GLUT2 antibody. Other symbols are as indicated in Fig. 2-2.

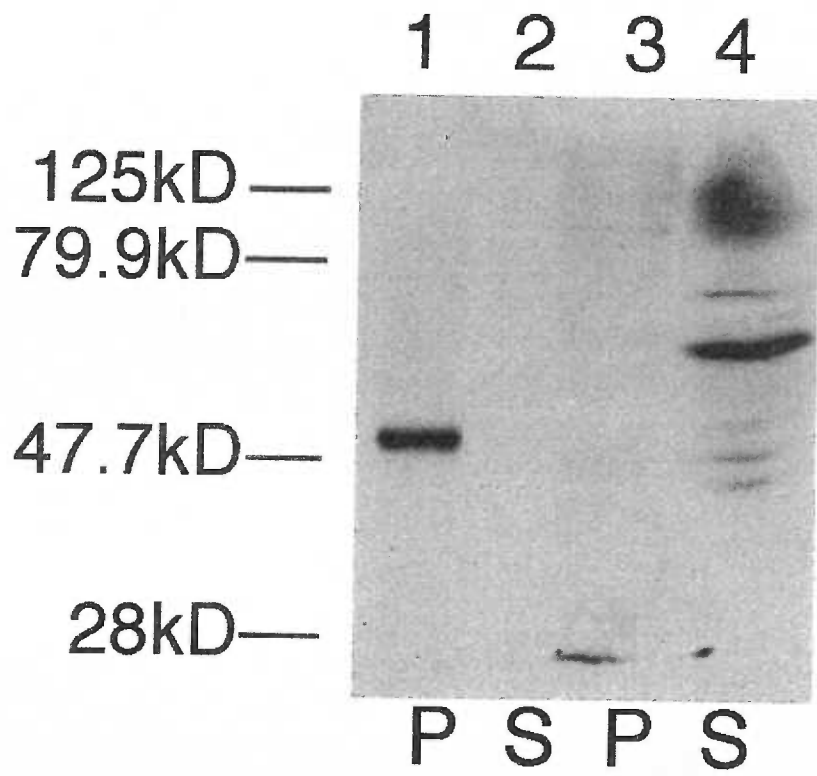


Figure 2-6. Confocal Micrographs of Detergent Extracted Cytoskeletons from Epitope Tagged ISO1 and ISO2 Expressing Cells. Double label confocal laser scanning micrographs of triton X-100 extracted *L. enriettii* promastigotes transfected with plasmid encoding epitope tagged ISO1 (top two images, marked *iso-1*) or epitope tagged ISO2 (bottom two images, marked *iso-2*) and stained with the rabbit anti-GLUT2 antibody directed against the epitope tag (*GLUT2*) and the murine anti- α -tubulin antibody (*α -tub*). Cytoskeletons were fixed with methanol, stained with 1:500 dilutions of the anti-GLUT2 antibody and anti- α -tubulin antibodies and then with an FITC-conjugated anti-rabbit IgG (*GLUT2*) and a rhodamine-conjugated anti-mouse IgG (*α -tub*) secondary antibodies. Parasites were examined by confocal microscopy. Each micrograph represents a single 0.5- μ m section through each field.

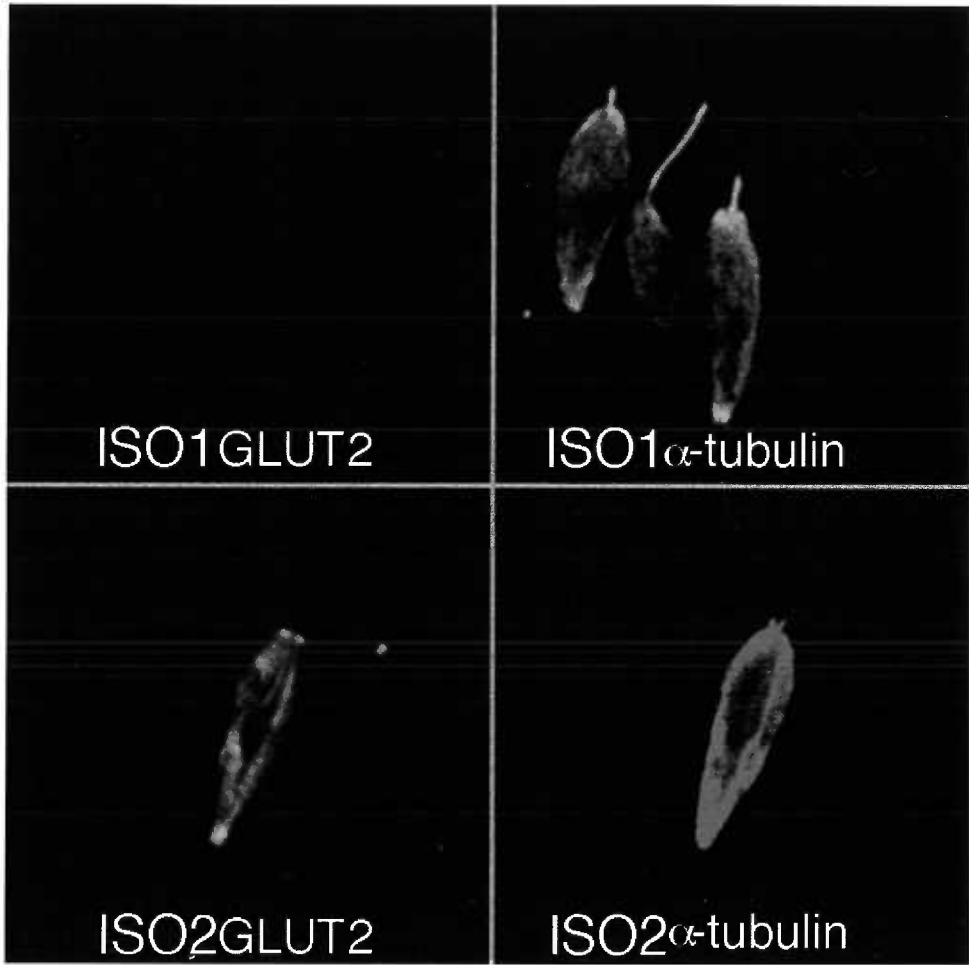


Figure 2-7. Confocal Micrographs of Cells Expressing ISO1::D2 or ISO2::D2 Chimeras. Confocal laser microscopy of *L. enriettii* parasites overexpressing chimeras of the D2 hexose transporter containing the NH₂-terminal domain of ISO1 (*I1.D2, top*) or ISO2 (*I2.D2, bottom*). Cells were double-stained with the anti- α -tubulin antibody (*α -tub*, 1:400) and the anti-D2 antibody (*D2*, 1:200), followed by goat anti-mouse Texas red and goat anti-rabbit Bodipy Oregon green. Each micrograph represents a single 0.5- μ m section through each field.

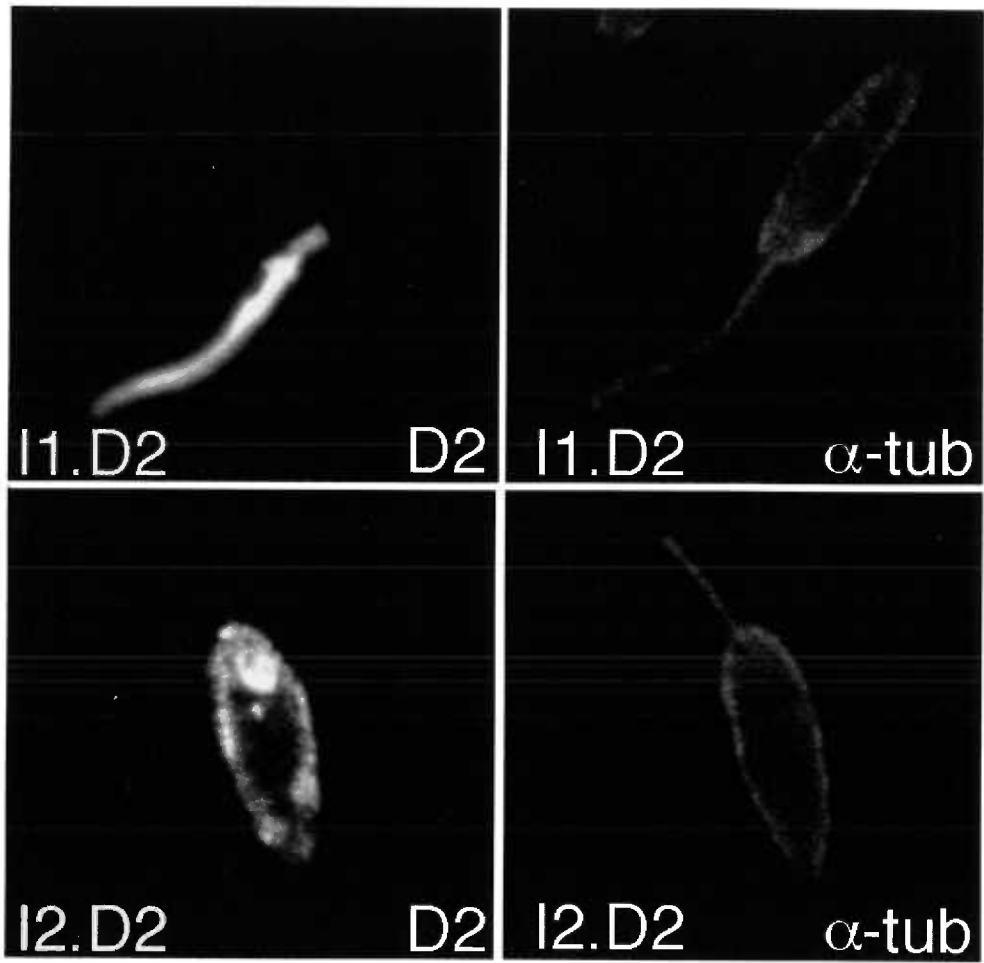


Figure 2-8. NH₂-terminal Deletions of ISO1. (A) Deletions of the NH₂-terminal domain of ISO1. WT represents the wild type sequence. The Δ numbers represent the number of NH₂-terminal amino acids deleted in each construct. The amino acid sequence (single letter code) of the relevant portion of the NH₂-terminal domain is indicated at the top with numbers designating the amino acid position starting with the initiating methionine at position 1. (B) Confocal laser scanning microscopy of *L. enriettii* promastigotes expressing epitope tagged deletion constructs Δ20, Δ25, and Δ30. Stable cell lines transfected with either pX63Hyg.Δ20, pX63Hyg.Δ25, or pX63Hyg.Δ30 were stained with a 1:500 dilution of the anti-GLUT2 antibody and a 1:200 dilution of FITC-conjugated secondary antibody and examined by confocal microscopy. Each micrograph represents a single 0.5-μm section through each field.

B.

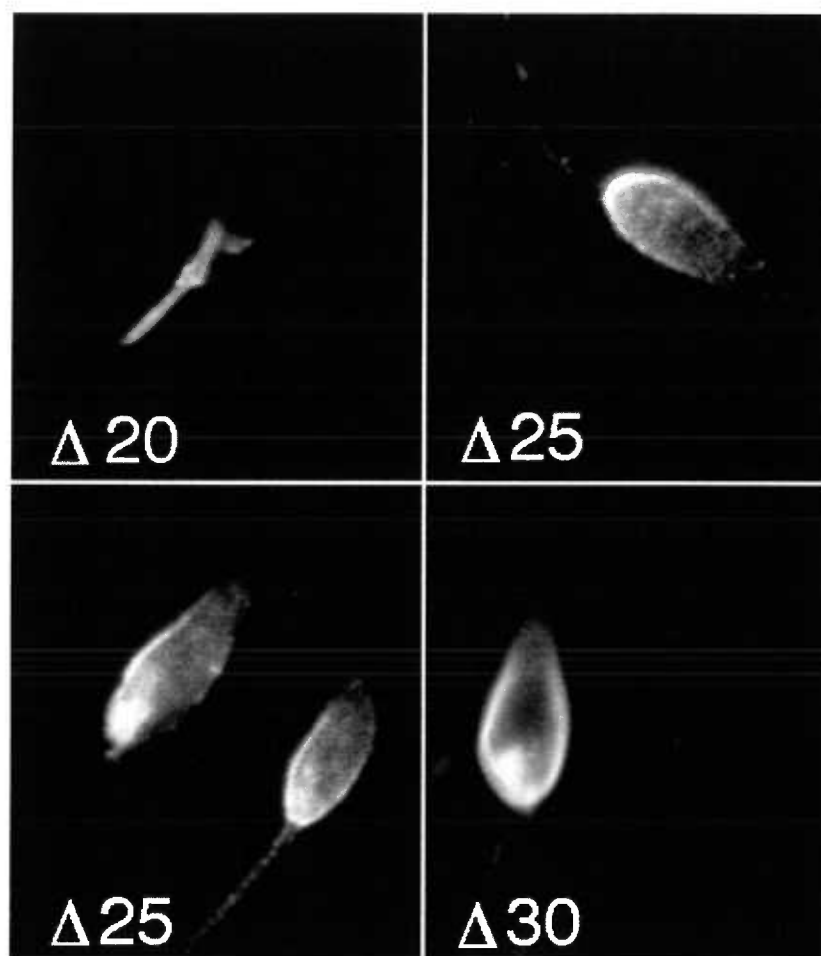
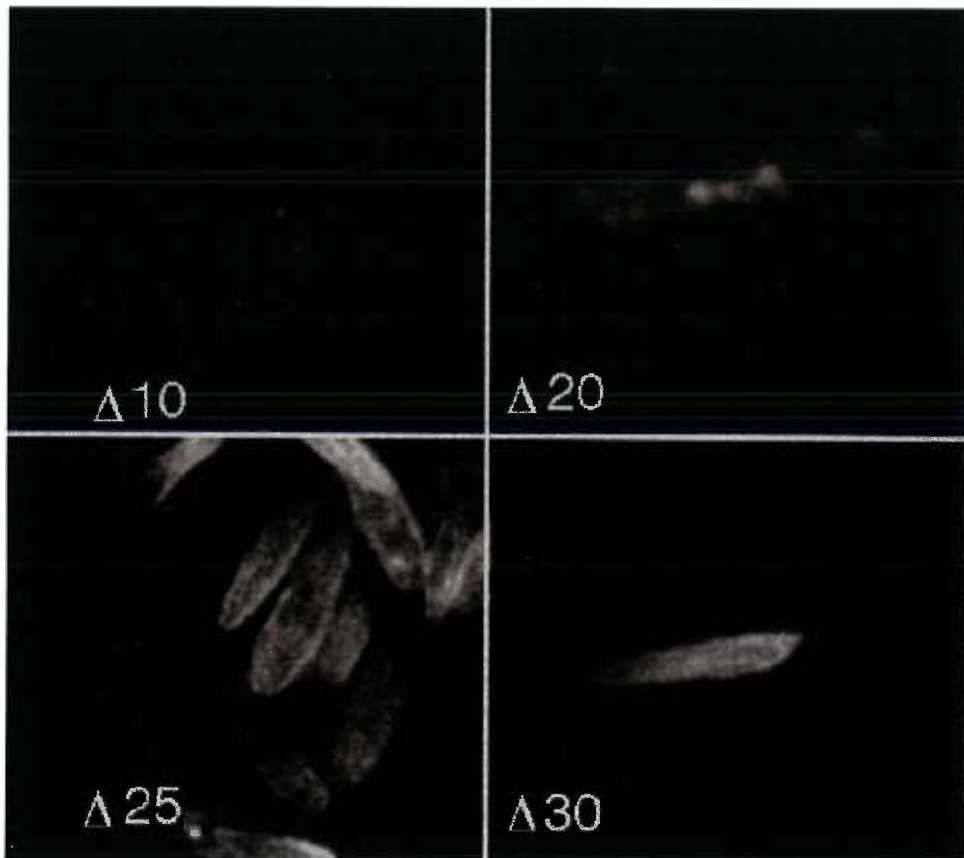


Figure 2-9. Confocal Micrographs of Detergent Extracted Cytoskeletons of ISO1 NH₂-terminal Deletion Expressing Cells. Confocal laser scanning microscopy of triton X-100 extracted *L. enriettii* promastigotes expressing epitope tagged deletion constructs $\Delta 10$, $\Delta 20$, $\Delta 25$, and $\Delta 30$. Stable cell lines transfected with pX63Hyg. $\Delta 10$, pX63Hyg. $\Delta 20$, pX63Hyg. $\Delta 25$, or pX63Hyg. $\Delta 30$ were stained with a 1:500 dilutions of the anti-GLUT2 antibody (A) and the anti- α -tubulin antibody (B) and an FITC-conjugated and a rhodamine conjugated secondary antibody and examined by confocal microscopy, as described in Fig. 2-4. Each micrograph represents a single 0.5- μ m section through each field.

A.



B.

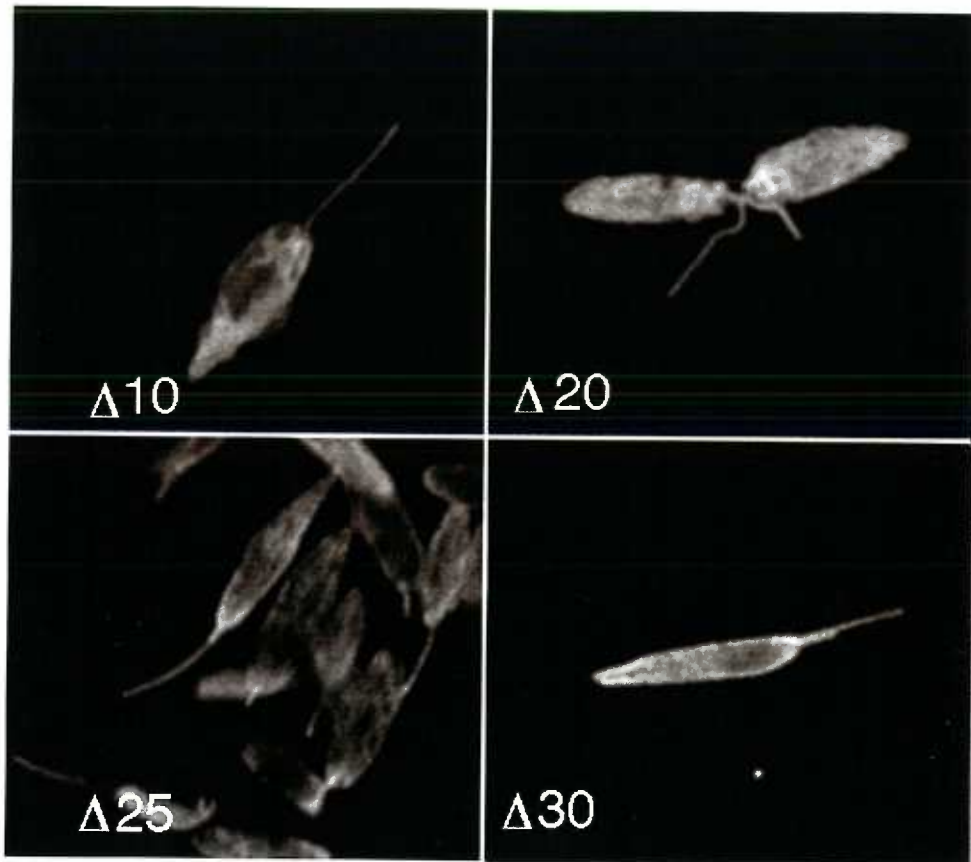


Figure 2-10. Immunoblots of Detergent Fractions of Cells Expressing D2 or MIT. Immunoblots of triton X-100 extracts from stably transfected *L. donovani* promastigotes overexpressing the D2 hexose transporter (lanes 1 and 2) or the MIT *myo*-inositol transporter (lanes 3 and 4). *P* designates the pellet (lanes 1 and 3) and *S* designates the supernatants (lanes 2 and 4) of the detergent extracts. Lanes 1 and 2 were stained with the anti-D2 antibody and lanes 3 and 4 were stained with the anti-MIT antibody. Numbers to the left indicate the mobilities of protein molecular weight mass markers in kilodaltons.

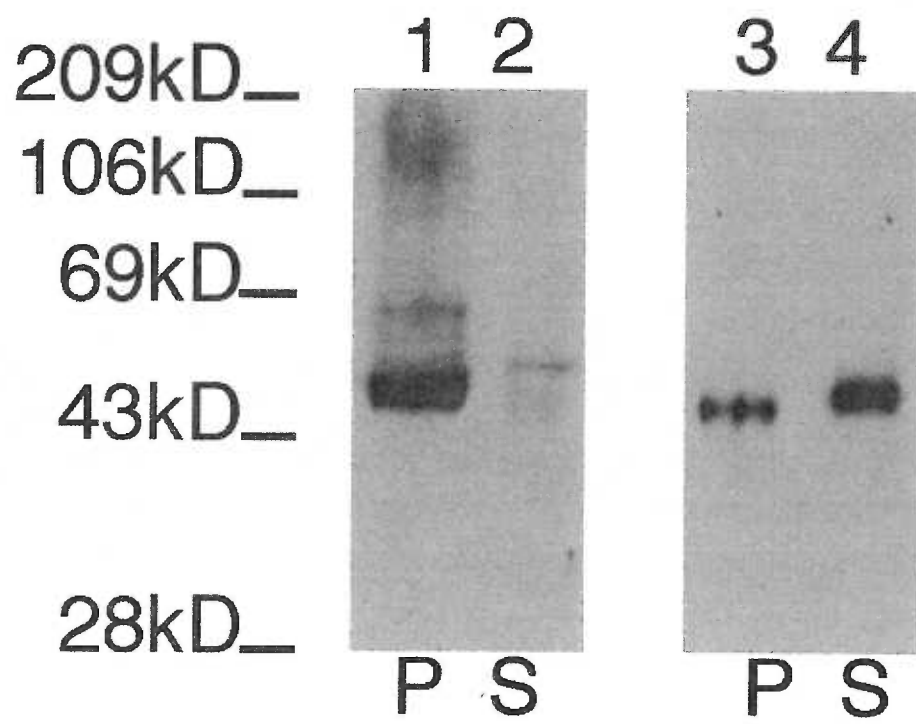
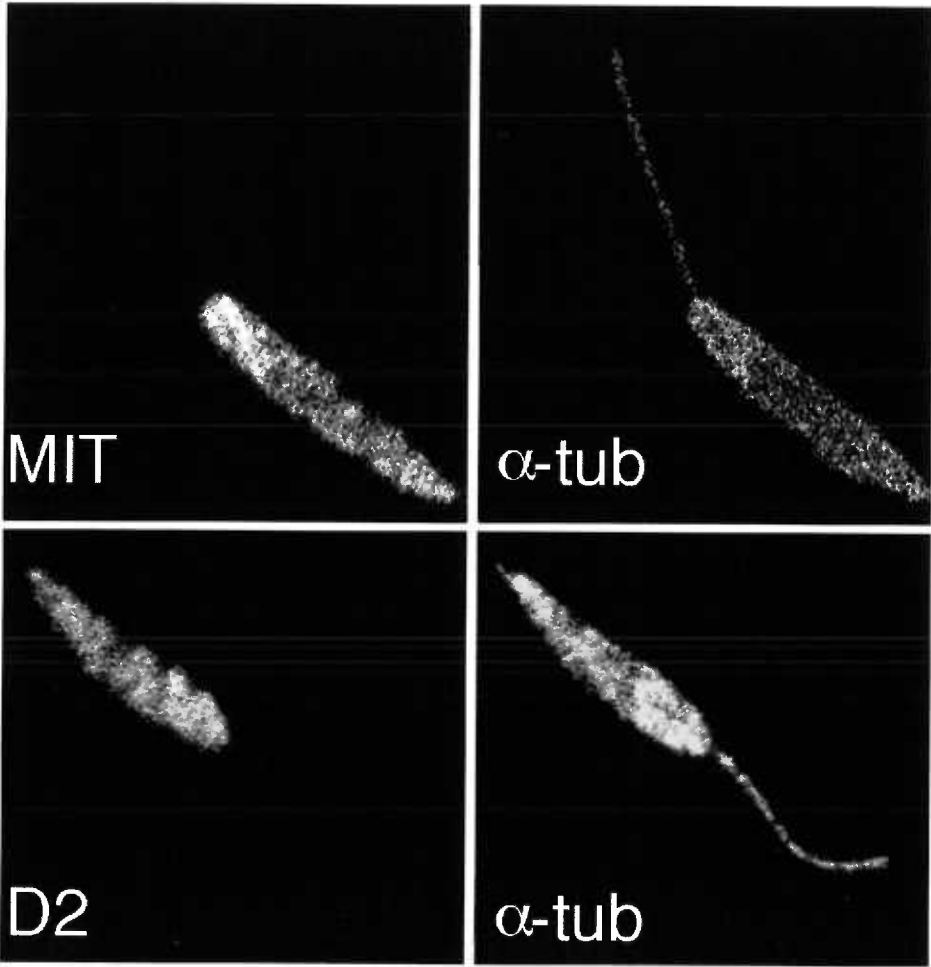


Figure 2-11. Confocal Micrographs of Detergent Extracted Cytoskeletons of Cells Expressing D2 or MIT. Confocal laser scanning microscopy of Triton X-100 extracted promastigotes of *L. donovani* overexpressing the MIT *myo*-inositol transporter (*top*) or the D2 hexose transporter (*bottom*). Each cytoskeleton was double-stained with either the anti-MIT antibody (*MIT*, 1:1,000) or the anti-D2 antibody (*D2*, 1:200), followed by the control α -tubulin antibody (*α -tub*, 1:500). Secondary FITC-conjugated or rhodamine-conjugated antibodies were used to reveal staining of the anti-transporter or anti- α -tubulin antibodies, respectively. Each micrograph represents a single 0.5 μ m section through each field.



Chapter 3

Characterization of a Flagellar Membrane Protein Targeting Motif in *Leishmania enriettii*

Erik L. Snapp and Scott M. Landfear

Department of Molecular Microbiology and Immunology, Oregon Health
Sciences University, Portland, Oregon 97201

Address correspondence to Scott M. Landfear, Department of Molecular
Microbiology and Immunology, Oregon Health Sciences University, 3181 S.W.
Sam Jackson Park Road, Portland, OR 97201. Tel: (503) 494-2426. Fax: (503)
494-6862.

Abstract

The surface membranes of eukaryotic flagella and cilia are contiguous with the plasma membrane. Despite the absence of obvious physical structures that could form a barrier between the two membrane domains, the lipid and protein compositions of flagella and cilia are distinct from the rest of the cell surface membrane. We have previously identified a flagellar isoform of a glucose transporter (ISO1) in the parasitic protozoan *Leishmania enriettii* and demonstrated that the 130 amino acid NH₂-terminal cytoplasmic domain of ISO1 was sufficient to target a nonflagellar integral membrane protein into the flagellar membrane. We have now determined that an essential flagellar targeting signal is located between amino acids 20-35 of the NH₂-terminal domain. We have further analyzed the role of specific amino acids in this region by alanine replacement mutagenesis and determined that single amino acid substitutions did not abrogate targeting to the flagellar membrane. However, individual mutations located within a cluster of five contiguous amino acids conferred differences in the degree of targeting to the flagellar membrane and the flagellar pocket, implying a role for these residues in the mechanism of flagellar trafficking. In addition, several flagellar membrane proteins from related trypanosomatids contain sequences similar to the flagellar targeting motif of ISO1, which suggests that the targeting sequence may be of general significance in this family of parasites. This paper describes the first flagellar membrane protein targeting motif in eukaryotic cells and provides a model system for the study of flagellar membrane protein targeting.

Introduction

Eukaryotic flagella and cilia are present throughout the evolution of eukaryotic cells from early flagellated protozoa to mammalian cilia. These specialized organelles contain an internal microtubule based axoneme that provides structure and generates movement (46, 127). Flagella and cilia play roles in cellular locomotion, trapping of food, and sensory functions (27). To carry out sensory functions, ciliary and flagellar membranes contain proteins unique to these organelles. For example, *C. elegans* expresses ODR-10 (a seven transmembrane domain receptor), OSM-9 (a cation channel), and ODR-3 (a $G\alpha$ protein) that localize to the cilia of AWA olfactory neurons (42, 63, 181, 202). Mammalian ependymal cells, oviduct, and trachea contain a G protein subtype (G_{12}) that localizes predominantly in cilia (207). In addition to distinct protein compositions, considerable evidence has accumulated that flagella and cilia exhibit lipid compositions distinct from other domains of the plasma membrane (102). For example, *Paramecium* cilia contain 1.5 times more sterols and five times more sphingolipids relative to the lipid composition of the whole cell (102). Despite lipid and protein compositions distinct from the rest of the plasma membrane, the membranes of these organelles are contiguous with the plasma membrane. How these membrane subdomains are generated is a question of general importance in cell biology.

Previously, several motile processes have been observed that could be responsible for movement of proteins into and within the flagellar membrane (27, 112, 186). Dwyer *et al.* have identified two proteins, ODR-4 and ODR-8, in *C.*

elegans, that are required for the localization of ODR-10 to the cilia of AWA olfactory neurons (63). However, little is known about the process by which specific membrane proteins are targeted to ciliary and flagellar membranes. To better study the mechanisms that generate the differential protein distributions in eukaryotic flagella, we have characterized a flagellar targeting motif for a flagellar integral membrane protein in the parasitic protozoan, *Leishmania enriettii*.

We have shown previously (177) that two closely related isoforms of the major glucose transporter from *L. enriettii* are differentially localized. Isoform-1 (ISO1) is located primarily in the flagellar membrane, while isoform-2 (ISO2) localizes primarily to the pellicular plasma membrane surrounding the cell body. Both isoforms are also present in the flagellar pocket membrane, the functionally specialized domain of the plasma membrane that receives proteins that are ultimately destined for the pellicular and flagellar membranes or that are secreted into the extracellular medium (9, 163, 240).

ISO1 and ISO2 differ only in the sequence of their cytosolic NH₂-terminal domains; ISO1 has a 130 amino acid domain that lacks similarity to the 48 amino acid NH₂-terminal domain of ISO2. The NH₂-terminus of ISO2 has a higher content of acidic amino acids (27.66% versus 7.7% for ISO1) that results in a predicted pI of 4.23, while ISO1 has a predicted pI of 6.69. In contrast to ISO1, ISO2 lacks leucine, isoleucine, cysteine, tyrosine, glycine, and histidine. In addition, ISO1 has more than twice the proline content of ISO2 (13.85% versus 6.38%). Thus, the NH₂- termini of the two isoforms resemble each other only in

the sense that both domains are hydrophilic and are predicted to be on the cytoplasmic side of the plasma membrane.

Previously, we have demonstrated that the NH₂-terminal domain of ISO1 is sufficient to target an integral pellicular plasma membrane protein to the flagellar membrane (211). Based on the combined results of the NH₂-terminal deletions and chimeric constructs, a critical flagellar targeting sequence has now been mapped to the region between amino acids 20-35. To further characterize the flagellar targeting sequence, we performed alanine scanning mutagenesis of amino acids 22-32 of ISO1. While no individual alanine replacement retargeted ISO1 away from the flagellum or to the pellicular plasma membrane, mutations in any one of amino acids 25-29 resulted in a quantitative redistribution of ISO1 within the plasma membrane, suggesting a role for these amino acids in flagellar targeting. Finally, we compare the flagellar targeting sequence of ISO1 with sequences of other known flagellar membrane proteins in related trypanosomatids to suggest that diverse trypanosomatid flagellar membrane proteins may use a similar sequence for flagellar localization.

Materials and Methods

Alanine Replacement Mutagenesis of the ISO1 NH₂-terminal Cytoplasmic Domain

In the following descriptions, all restriction sites followed by (P) indicate that these sites are in the polylinker cloning region of the plasmid. Alanine scanning mutagenesis and addition of new restriction sites to ISO1 was accomplished using a variation of the Promega Altered Sites II Mutagenesis Systems protocol (Promega, Madison, WI). Briefly, mutagenic oligomers (sense orientation and containing both a single mutated base to convert the encoded amino acid to an alanine and a change of one or two wobble bases to add or remove a restriction site for ease of screening, listed in Table 3-1, were phosphorylated with the T4 polynucleotide kinase (Promega) and annealed to single stranded phagemid DNA from a Bluescript based plasmid containing a fragment of ISO1 (bases 1-1432 of the open reading frame [ORF] terminating in the single *Cla* I site within the ORF) in the antisense orientation (215). DNA synthesis and ligation were performed, and the product was transformed into ES1301, a *mutS* strain of bacteria, and then into XL-1 blue bacteria (203). Mutants were screened by restriction digests, followed by sequencing of the mutated DNA, as described below. Mutagenized constructs were excised with *Bam*H I (P) and *Cla* I and ligated into the *Bgl* II (P)/*Cla* I site of the *pX63 HYG TΔ20* vector (211), which produced an expression vector encoding the mutant ISO1 protein containing a 13 amino acid epitope tag from rat GLUT2 at the COOH-terminus (see below).

Construction of Chimeras and Internal Deletion Mutants

The plasmid *pX63 HYG* (48) was used for expression of epitope tagged constructs in *L. enriettii*. The 13 COOH-terminal amino acids of rat GLUT2 (225) (TVQMEFLGSSETV), which were used as the epitope tag, were introduced into *ISO1* and *ISO2* containing plasmids as described previously (177).

For chimeric constructs (Fig. 3-1), a primer containing a *EcoR* I restriction site, the six nucleotides immediately preceding the initiating methionine of *ISO1* (a putative Kozak sequence, AGCAGC), and encoding a methionine and the first six amino acids of the region to be fused (amino acids 1-31, 10-31, 20-35, 20-31, 20-29, 21-31, or 21-29 of *ISO1*), was used as the forward primer, and an antisense primer encoding the final six amino acids of the *ISO1* sequence to be included in the construct followed by an *Asp* I site was used as the reverse primer to amplify regions near the NH₂-terminus of *ISO1* by PCR. The oligomers used are listed in Table 3-2. To create the *ISO1* (NH₂-terminal fragment)::*ISO2* chimeras (Fig. 3-1, Step 1), the PCR amplified fragments were gel purified, digested with *EcoR* I and *Asp* I, and cloned into *EcoR* I/*Asp* I digested *pBS ISO2 EcoR* I (P)/*Cla* I, a Bluescript plasmid containing the coding region of *ISO2* from the initiating methionine to the *Cla* I restriction site (35). Since the *ISO2* gene contains an *Asp* I site spanning bases 13-18 of the *ISO2* ORF, the resulting chimeric plasmid encodes a protein containing an NH₂-terminal fragment of *ISO1* fused to amino acid 4 of *ISO2*. Subsequently (Fig. 3-1, Step 2), the *Bam*H I (P)/*Cla* I fragment of this chimeric construct was cloned into the *Bgl* II (P)/ *Cla* I sites of the *pX63 HYG ISO1* vector containing the GLUT2 epitope tag (211) using the internal *Cla* I site and the *Bgl* II site in the upstream polylinker region. The regions containing the chimeras were sequenced, as reported previously (35), to confirm that the correct constructs had been generated. The *ISO1* (1-35)::*ISO2* construct was generated by cloning the *Bam*H I (P)/*Asp* I fragment of wild type *ISO1* (encoding amino

acids 1-35) into the *Bam*H I (P)/*Asp* I sites of *pBS ISO2 EcoR* I (P)/*Cla* I (removing the first four amino acids of ISO2, MSDR). The *Bam*H I (P)/*Cla* I fragment containing the chimera region was then cloned into the *pX63 HYG ISO1 Bgl* II (P)/*Cla* I sites, as above.

To create the Δ 30-46, Δ 46-73, Δ 46-101, and Δ 46-125 internal deletion constructs of *ISO1* (Fig. 3-2), pairs of unique restriction sites were introduced into the *ISO1* NH₂-terminal sequence. For each construct, a single *Spe* I site was introduced by mutating the nucleotides encoding amino acids 29,30TS, 46,47TT, TS72,73, 101,102ST, or SS125,126 using the method described above and oligomers listed in Table 3-3 to create *ISO1 TS**. After an initial *Spe* I site was created, single stranded DNA for the phagemid was generated, and the mutagenesis process was repeated to create a second *Spe* I site (*ISO1 TS***). Next, the *Bam*H I (P)/*Cla* I fragment of *ISO1 TS*** was cloned into *pSP72* (Promega), a plasmid that lacks any *Spe* I restriction sites. The *Spe* I/*Spe* I fragment within the *ISO1* coding region was removed by digesting with *Spe* I. The plasmid was gel purified, and religated to create *pSp72 ISO1 Δ TS**. Coding regions that contained deletions were then digested with *Bam*H I and *Cla* I and cloned into the *Bgl* II (P) and *Cla* I sites of the *pX63 HYG ISO1* vector described above to create *pX63 HYG ISO1 Δ* . Constructs were confirmed by sequencing as described above.

Table 3-1. Oligonucleotides Used to Generate Alanine and Glycine Mutants of ISO1

Oligo Name	Sequence
P22A <i>Kpn</i> I	TTCAGCTCAGCGCCTCGGGCGAACAGGT <u>ACCACGTCC</u>
P23A <i>Kpn</i> I	AGCTCACCGGCTCGGGCGAACAGGT <u>ACCACGTCC</u>
R24A <i>Kpn</i> I	TCACCGCCTGCGCGAACAGGT <u>ACCACGTCC</u>
R25A <i>Xho</i> I	ACCGCCTCGAG <u>CAACAGGAACCA</u>
T26A no new site	CCTCGGGCGAGCAGGAACCA
G27A no new site	CGGGCGAACAGCAACCACGT
T28A <i>Nar</i> I	CGGGCGAACAGGGCGCCACGTCCAC
T29A <i>Kpn</i> I	CGGGCGAACAGGT <u>ACCGCGTCCACGCA</u>
TT28,29AA - <i>Nar</i> I	TCGGCGAACAGGAGCCGCGTCCACGCAGCC
S30A <i>Kpn</i> I	CGAACAGGT <u>ACCACGGCCCACGCAGCC</u>
H31A <i>Kpn</i> I	CGAACAGGT <u>ACCACGTCCGCCGCAGCCCAT</u>
A32G <i>Kpn</i> I	CGAACAGGT <u>ACCACGTCCACGGAGCCCATAAC</u>
RR24,25AA - <i>Xho</i> I	AGCTCACCGCCTG <u>CAGCAACAGGAACC</u>

Table 3-2. Oligonucleotides Used to Generate ISO1::ISO2 Chimeras

Oligo Name	Sequence
ISO1 TΔ20 <i>Bgl</i> II	TCGATCAGATCTAGCAGCATGTCACCGCCTCGGGCGAAC
ISO1 F21 <i>EcoR</i> I	GACTGAATTCAGCAGCATGTCACCGCCTCGGGCGAAC
ISO1 F22 <i>EcoR</i> I	GACTGAATTCAGCAGCATGCCGCCTCGGGCGAACAGGA
ISO1 R29 <i>Asp</i> I	TCAGGACCCTGTCCGTGGTTCCTGTTTCG
ISO1 R30 <i>Asp</i> I	TCAGGACCCTGTCCGGACGTGGTTCCTGTTTCG
ISO1 R31 <i>Asp</i> I	TCAGGACCCTGTCCGTGGGACGTGGTTCCTGTTTCG

Table 3-3. Oligonucleotides Used to Generate Internal Deletions of ISO1

Oligo Name	Sequence
30 <i>Spe</i> I	AACAGGAACC <u>ACTAGT</u> CACGCAGCCCATAAC
46 <i>Spe</i> I	AACTTTGCCA <u>ACTAGT</u> CCACCGCTACCAAGC
73 <i>Spe</i> I	CTCCTTAACG <u>ACTAGT</u> CCGCCATCAGTCAAC
101 <i>Spe</i> I	CAACCCTGCA <u>ACTAGT</u> GGAAGACGATAACCACC
125 <i>Spe</i> I	ATCACTTTTCA <u>ACTAGT</u> CTCAACATTCGCGCT

Cell Culture and Transfection

Promastigotes of *L. enriettii* were cultured at 26°C in Dulbecco's Modified Eagle-L medium (DME-L) (GIBCO BRL Life Technologies, Grand Island, New York) (93) containing 5% fetal calf serum and 5% bovine embryonic fluid or RPMI medium (Gibco BRL Life Technologies) containing 10% fetal calf serum. Both types of medium contained xanthine (0.1 mM) and hemin (50 µg/ml) supplements. Parasites were transfected by electroporation (103) of plasmid DNA using a Gene Pulser (Bio Rad Laboratories, Richmond, CA) apparatus. One day after transfection, hygromycin (Calbiochem-Novabiochem Corp., La Jolla, CA) was added to a final concentration of 50 µg/ml to the culture, and the parasites were maintained under these conditions until drug-resistant parasites grew out (usually ~3-4 weeks). The hygromycin concentration was then increased to 200 µg/ml for maintenance of transfected parasites.

Antibody Preparation

Polyclonal antiserum against a glutathione *S*-transferase fusion protein containing the 25 COOH-terminal amino acids of rat GLUT2 was purchased from Biogenesis (Sandown, NH). Antibody was used for immunofluorescence at a dilution of 1:500 and at a dilution of 1: 2000 for immunoblots. The mouse anti- α -tubulin monoclonal antibody raised against native chick brain microtubules was obtained from Amersham Corp. (Arlington Heights, IL). The antibody was used at a dilution of 1:600 for immunofluorescence and 1:5000 for immunoblots.

Cell Lysates and Immunoblots

For preparation of total cell lysates, parasites at a density of $1-2 \times 10^7$ /ml were pelleted, washed with PBS, resuspended in Laemmli sample buffer (190) to a density of $0.2-1 \times 10^9$ cells/ml and immediately heated to 65°C for 5 min. Samples containing 10 µl of lysate were reheated to 65°C for 3 min, loaded onto 10% SDS-polyacrylamide gels, separated by standard methods (166), and

electroblotted onto a nitrocellulose membrane using a Mini Trans Blot apparatus (Bio Rad Laboratories) according to the manufacturer's instructions. Blots were developed using the ECL chemiluminescence system (Amersham Corp.) and goat anti-rabbit IgG coupled to horseradish peroxidase (Sigma, St. Louis, MO), as detailed in the manufacturer's instructions, and the developed blots were exposed to XAR-5 film (Eastman Kodak Co., Rochester, NY).

Immunofluorescence Microscopy

For immunofluorescence imaging, parasites were pelleted, washed twice in PBS, resuspended at a density of approximately 10^7 cells/ml, and attached to poly-L-lysine-coated coverslips. The adherent parasites were fixed with 100% methanol at -20°C for 15 min. After fixation, coverslips were rinsed in PBS and then incubated in PBS plus 2% goat serum for 15 min. Antiserum was added at the appropriate dilution in PBS plus 2% goat serum and incubated for 1 h at room temperature. Coverslips were rinsed three times in PBS and then incubated for 1 h with a 1:200 dilution of goat anti-rabbit IgG coupled to FITC (fluorescein isothiocyanate) (Sigma) or to Texas Red (1:800)(Molecular Probes, Inc., Eugene, OR) in PBS plus 2% goat serum. Coverslips were rinsed 5 times with PBS and then mounted on slides in 50 mM Tris, pH 8.0, 90% glycerol, and 20 mg/ml n-propyl-gallate (Sigma).

Images were acquired at the Oregon Hearing Research Center (at OHSU) with a Bio-Rad MRC 1024 ES laser scanning confocal imaging system attached to an inverted Nikon Eclipse TE300 microscope using a 60X oil immersion lens and a 2X zoom. The acquisition system (LaserSharp) uses a krypton/argon laser with excitation lines at 488, 568 and 647 nm, and simultaneous or sequential detection using one/two/three 8-bit photomultiplier tubes (PMTs). Images were processed using the LaserSharp (Bio-Rad) post-processing software.

Statistical Analysis of Flagellar Membrane Targeting Phenotypes

To characterize flagellar targeting phenotypes, 30 different confocal immunofluorescence images of each wild type or mutant ISO1 expressing cell line were obtained. Each 512x512 72 pixel per inch image was analyzed using NIH Image 1.61 for Power PC Macintosh on a Power Macintosh 7300. Images were opened as grayscale images and inverted (i.e. bright pixels become gray to black and dark pixels become gray to white) for ease of processing. The flagellar pocket was designated as the most intense 3x3 pixel area, inside the cell, within 6 pixels of the point at which the flagellum and pellicular plasma membrane join. Flagellar fluorescence values were taken as the average of three 3x3 pixel areas along the flagellum (specifically, the area within 2 pixels just before the flagellum joins the cell body, a point approximately in the middle of the flagellum, and the tip of the flagellum) (Figure 3-3). Fluorescence values for flagella and the flagellar pockets was normalized to a scale of 1-100 for each cell, in which the flagellar pocket value was designated as 100. The Relative Flagellar Fluorescence was defined as the average of the three flagellar fluorescence values divided by the flagellar pocket fluorescence value (Fig. 3-3). Since the data presented in the histograms (Fig. 3-7) do not fit a normal distribution, we used the Chi Square statistical test to determine whether differences in the relative flagellar fluorescence staining were significant. Because no specific criteria exist to divide relative flagellar intensities into high and low values, we compared the significance of the relative distributions of flagellar intensities at two different cutoffs (80% and 60% of relative flagellar pocket intensity). In all cases where statistically significant differences were found, distinct mutant phenotypes differed from the wild type epitope tagged ISO1 significantly in the amount of staining that occurred above both the 80% and 60% cutoff values ($p < 0.05$).

Results

One objective of the current study was to define a minimal protein sequence that results in the targeting of polypeptides to the flagellar membrane of trypanosomatid protozoa. Previous studies on the flagellar glucose transporter from *L. enriettii*, ISO1, demonstrated that the unique NH₂-terminal hydrophilic domain of this polytopic membrane protein contained a flagellar membrane targeting sequence. Thus, addition of the 130 amino acid cytoplasmic domain of ISO1 to the NH₂-terminus of the D2 hexose transporter was sufficient to retarget the D2 protein from the pellicular plasma membrane to the flagellar membrane (211). NH₂-terminal deletion mutagenesis of ISO1 further revealed that the first 20 amino acids of ISO1 were not necessary for flagellar targeting. In contrast, deletion of the first 25 amino acids retargeted most of ISO1 to the pellicular plasma membrane, while deletion of the first 30 amino acids completely retargeted ISO1 to the pellicular plasma membrane. Together, these results suggested that an essential flagellar targeting sequence was located near amino acid 25.

Studies with Chimeric Transporters

To define more precisely the flagellar membrane targeting sequence of ISO1, we prepared chimeric constructs that encode segments of the NH₂-terminal domain of ISO1 fused to amino acid 5 of ISO2, a protein normally targeted to the pellicular plasma membrane (Fig. 3-4). These constructs were transfected into *L. enriettii* promastigotes, and the location of each chimeric protein was assayed by confocal immunofluorescence microscopy. The data in Figure 3-4 indicate that

the chimera containing amino acids 1-35 of ISO1 fused to the NH₂-terminus of ISO2 largely retargets to the flagellar membrane. In contrast, the chimeras containing shorter segments of ISO1 remain in the pellicular plasma membrane (data not shown), as does the wild type ISO2 protein. Consequently, the shortest segment that is sufficient to cause flagellar retargeting, at least in the context of these particular chimeras, contains amino acids 1-35.

Internal Deletions

To test whether other regions of the ISO1 NH₂-terminus contain flagellar targeting information, we created internal deletion mutants that removed various segments of sequence (Fig. 3-5), as described in Materials and Methods. Deletion of amino acids 46-125, 46-100, and 46-73 retargeted ISO1 to the pellicular plasma membrane, while deletion of amino acids 30-46 produced a protein that gave diffuse staining over much of the cell (Fig. 3-5A). One possible explanation for the failure to detect the Δ 30-46 protein could be that it was either synthesized at a lower level or degraded more rapidly than the wild type ISO1. To test these possibilities, we performed immunoblots of cell lines expressing the wild type ISO1 and each deletion mutant (Fig. 3-5B). The results indicate that Δ 46-73 protein levels (Fig. 3-5B lane Δ 46-73) were similar to wild type ISO1 (Fig. 3-5B, lanes *ISO1*), while the protein level of Δ 30-46 (Fig. 3-5B, lane Δ 30-46) appeared to be barely detectable. It is unclear whether the reduced protein levels of Δ 30-46 resulted from defects in protein folding or mistargeting of the deletion mutant.

The retargeting of Δ 46-73, Δ 46-101 and Δ 46-125 deletions could be due to either removal of a targeting motif or to a substantial alteration of the three

dimensional conformation of the cytoplasmic domain. The fact that all the deletion mutants tested either failed to be expressed or failed to target to the flagellum raises the possibility that some flagellar targeting information could exist in the region between amino acids 35 and the beginning of the first transmembrane domain. Nonetheless, the observation that the 1-35 chimera does target to the flagellar membrane confirms that this region does contain all the essential flagellar targeting sequence. Furthermore, the observation that the first 20 amino acids of ISO1 could be deleted without affecting flagellar targeting (211) implies that the region between amino acids 20-35 (SSPPRRTGTTSHAAHN, Fig. 3-6) contains all of the essential flagellar targeting information.

Alanine Replacement Mutagenesis

To define more precisely which amino acids are required for flagellar targeting, we have individually mutated amino acids 22 to 31 to alanine and amino acid 32 from alanine to glycine and have used confocal immunofluorescence microscopy to determine the localization of each mutant protein. The results (Fig. 3-6) indicate that no single alanine mutation retargets ISO1 to the pellicular plasma membrane, implying that no single amino acid is essential for flagellar targeting. However, visual inspection of these images suggested that some mutants were not expressed as abundantly on the flagellar membrane as wild type ISO1, while others were expressed almost exclusively on the flagellar membrane and not in the flagellar pocket.

To determine whether ISO1 was quantitatively redistributed on the surface membrane in any of the mutants, confocal immunofluorescence images were obtained for 30 cells for each mutant cell line (Galleries in Appendices, Figures AP-11 through AP-22). Intensities were measured for the flagellar pocket and flagellum, as described in Materials and Methods, and the digitized images were analyzed using the computer program NIH Image to measure relative staining intensities. Histograms of the distributions of flagellar intensities relative to the flagellar pocket (Relative Flagellar Intensity, see Materials and Methods) are presented in Figure 3-7, and the results are summarized in Table 3-4. Mutants P22A, P23A, R24A, S30A, and A32G (Fig. 3-6A) localized with a similar distribution between the flagellar pocket and flagellar membrane compared to wild type ISO1. In contrast, mutants G27A, T28A and T29A (Fig. 3-6C) localized significantly more strongly to the flagellar pocket than the flagellum ($p < 0.05$ at both subgroups of cells with flagellar staining intensities of 80% or greater and 60% or greater than the flagellar pocket). These results suggest that G27A, T28A, and T29A either target inefficiently to the flagellar membrane, or the mutants are poorly retained in the flagellar membrane. The difference between localization of H31A compared to wild type ISO1 was at the borderline of statistical significance ($p = 0.049$ for the 60% cutoff and 0.055 for the 80% cutoff).

The assay for comparing flagellar membrane staining to flagellar pocket staining could not be performed for mutants R25A and T26A, because relatively few cells (11 cells out of 30 and 11 out of 27 for R25A and T26A respectively)

displayed significant flagellar pocket staining. However, the flagellar membranes for both mutants stain intensely and were analyzed using an alternative method (Table 3-4). Comparing relative flagellar staining to point 1 (where the flagellum meets the cell), R25A and T26A flagella do not differ significantly in intensity from wild type ISO1 flagella ($p > 0.05$ at both cutoffs for both mutants). In a different analysis, the numbers of cells with or without flagellar pocket staining were compared relative to wild type ISO1 (Table 3-5). The numbers of parasites lacking staining in the flagellar pocket was much greater for both R25A and T26A mutants than for wild type ISO1 (p value < 0.0002). The results suggest that R25A and T26A either enter the flagellar membrane from the flagellar pocket more efficiently than wild type ISO1 or that they are retained more efficiently in the flagellar membrane once they arrive there. Taken together, these results indicate that mutations in amino acids 25-29 significantly affect the targeting of ISO1 and suggest that these amino acids are important components of a flagellar targeting motif.

Double Alanine Mutants

One hypothesis that could account for the inability of any single alanine mutant to relocate to the pellicular plasma membrane is that redundancies exist in the flagellar targeting motif. Since two basic (R24, R25) and four hydroxyl amino acids (T26, T28, T29, and S30) are present within the region examined, it is possible that a neighboring amino acid could compensate functionally for an individual alanine replacement. To address this possibility, double alanine mutants were created for RR24,25AA and TT28,29AA. Confocal

immunofluorescence microscopy results in Figure 3-8 revealed that instead of retargeting ISO1 to the pellicular plasma membrane or flagellar pocket, the proteins stained poorly, and no distinct localization could be determined, although punctate structures did appear. However the structures were not bright, and it was unclear whether the staining was cytoplasmic or on the plasma membrane. To assess whether these proteins were expressed or degraded, immunoblotting was performed. Figure 3-9 contains an immunoblot of whole cell lysates of wild type and mutant expressing cells probed with an anti-GLUT2 epitope tag antibody. The wild type ISO1 lysate (lane 1) contains a band at approximately 65 kD, which corresponds to ISO1. Lane 2, which corresponds to RR24,25AA and Lane 3 which represents to TT28,29AA, both contain a band at the same molecular weight and of similar intensity as wild type ISO1. Thus, the double mutants were expressed, but the proteins appeared to be mistargeted in a way that was difficult to interpret and did not reveal useful information about the targeting signal.

Flagellar Membrane Localizing Mutants May Turn Over More Slowly than Wild Type Protein

We investigated relative protein expression levels for alanine mutants R25A, T26A, G27A, T28A, and T29A by immunoblotting (Fig. 3-10). While most alanine mutant proteins were present in similar amounts to wild type ISO1 (Fig. 3-10A), the R25A and T26A mutants appeared to express levels of protein higher than wild type ISO1. Immunoblots of the same samples probed with an anti- α -tubulin antibody controlled for equivalent loading and demonstrate that T26A has twice as much protein lysate loaded as wild type ISO1 (Fig 3-10B). To

quantify the amounts of R25A and T26A relative to the wild type ISO1 overexpressor, different amounts of protein lysates for both mutants were compared to ISO1 lysate on an immunoblot (Fig. 3-10C). T26A has twice as much mutant protein as ISO1 (Fig. 3-10C lanes 2, 6, 7, 8). However, the tubulin blot revealed that T26A was overloaded by a factor of two (Fig. 3-10B). Thus, T26A has similar levels of mutant protein compared to wild type ISO1. R25A has three to four times as much protein as ISO1 (Fig. 3-10C lanes 2, 3, 4, 5) and is not significantly overloaded relative to wild type ISO1. Thus, the R25A mutant cell line accumulates more ISO1 protein compared to cells expressing other alanine mutants or wild type ISO1. Since the mutant protein was located primarily in the flagellar membrane, one intriguing possibility was that the increased abundance of the R25A mutant polypeptide could reflect a reduced rate of turnover compared to wild type ISO1. It will be necessary to directly measure the half lives of the ISO1 and R25A proteins to determine whether or not this hypothesis is correct.

Other Leishmania Species are Capable of Targeting ISO1 to the Flagellar Membrane

To determine whether any of the other species of *Leishmania* could localize ISO1 to the flagellar membrane, *L. major*, *L. mexicana*, and *L. donovani* were transfected with [*pX63 HYG ISO1*]. The immunofluorescence results in Figure 3-11 demonstrate that all three *Leishmania* species can target ISO1 to the flagellar membrane and thus contain flagellar membrane targeting components that recognize the flagellar targeting signal of ISO1.

Alignment to Other Trypanosomatid Flagellar Membrane Proteins

To examine the possibility that other trypanosomatids might share a common flagellar membrane targeting sequence, we compared the region of ISO1 shown to be sufficient for flagellar targeting of ISO1 (amino acids 20-35) to the sequences of other known flagellar localized proteins from related trypanosomatids. Figure 3-12 aligns a portion of the sufficient flagellar targeting region of ISO1 (amino acids 24-32) with sequences from the flagellar calcium binding proteins of *Trypanosoma cruzi* (65) and *Trypanosoma brucei brucei* (244), and the flagellar receptor adenylate cyclase of *T. brucei brucei* (166). While no sequence is identical to the ISO1 flagellar membrane targeting region, common sequence elements are present and suggest that a related flagellar membrane targeting sequence might exist in these proteins. The sequence shown for the *T. cruzi* flagellar calcium binding protein is within the NH₂-terminal segment that has been shown to be required for flagellar targeting (74) further supporting its possible role in flagellar targeting, but the crucial targeting regions of the other proteins are unknown.

In these alignments, the most highly conserved amino acids are an R or K at position 3 and a T or S at position 6. Position 2 is polar (R/S) and sometimes basic. Position 4 varies (T, G, D, N, P), but is usually an amino acid that favors or does not disrupt predicted β -turn secondary structures, i. e. proline, glycine, serine, aspartic acid, or asparagine (40). Position 7 is polar (T, S, N). Position 9 is usually basic (histidine or lysine), but in the case of ESAG4, it is a polar threonine. Positions 1 (P, G, A, S, T), 5 (G, S, T, and A), 8 (S, D, P, V), and 10

(A, G, D, S) mostly consist of amino acids that favor β -turns. The entire region between positions 1-10 is mostly polar, suggesting these sequences are likely to be solvent exposed.

Based on the alignments and the alanine mutant data, we predict that R/K-B-B-S/T-S/T/N, where B represents β -turn favoring amino acids (P, G, S, D, and N; T is also allowed, because it is not considered β -turn destroying), could represent a common trypanosomatid flagellar membrane targeting sequence. However, we emphasize that this hypothesis is currently untested. Furthermore, the chimera experiments demonstrate that the common sequence alone is not sufficient to target another protein such as ISO2 to the flagellar membrane and suggest that the sequence is probably context dependent.

Discussion

Identification of a Flagellar Targeting Motif in ISO1

In this study, we have defined a minimal sequence capable of redirecting a pellicular plasma membrane protein, ISO2, to the flagellar membrane, amino acids 1-35 of ISO1. Furthermore, our previous study demonstrated that the first 20 amino acids of ISO1 were not necessary for flagellar membrane localization (211). These data imply that an essential flagellar targeting motif maps between amino acids 20-35 of ISO1. The inability of ISO1 fragments shorter than 1-35 to localize ISO2 to the flagellar membrane indicates that the surrounding sequences must influence the ability of region 20-35 to function in flagellar targeting. Potential context requirements include distance of sequence from the first transmembrane domain, charge of the sequence between the motif and the first transmembrane domain, and the effects on motif folding and solvent exposure. The inability of ISO1 internal deletions to localize to the flagellar membrane supports the hypothesis that the targeting motif must be a defined distance from the first transmembrane domain, or that proper folding or exposure of this motif is adversely affected by these deletions.

We performed alanine replacement scanning mutagenesis to identify amino acids that influence flagellar targeting. The inability of individual amino acid replacements to prevent targeting of ISO1 to the flagellar membrane indicates that the flagellar targeting sequence is not absolute and allows for amino acid substitutions. However, the ability of individual alanine replacement mutants, clustered between amino acids 25-29, to affect the distribution of ISO1

to the flagellar membrane and flagellar pocket strongly supports a role for that the amino acid cluster in flagellar targeting. The fact that some mutations (R25A and T26A) promote a greater degree of targeting to the flagellar membrane than wild type transporter while other mutations (G27A, T28A, T29A) provoke a greater degree of targeting to the flagellar pocket suggests that each of these two classes of mutation may be affecting a different aspect of flagellar targeting. For instance, G27, T28, and T29 might be important for anterograde transport into the flagellar membrane, while R25 and T26 might be important for retrograde transport from the flagellum to the flagellar pocket. The potential alignment of the ISO1 flagellar targeting motif with sequences from other flagellar trypanosomatid proteins further suggests that the other proteins in related organisms might utilize a similar flagellar targeting motif and mechanisms of flagellar localization.

Structure and Role of the ISO1 Flagellar Targeting Motif

Amino acid sequences involved in targeting of proteins are often responsible for interactions of the targeted protein with other proteins that are components of the targeting machinery. Thus, the tyrosine-containing sorting signals in the cytoplasmic domains of some integral membrane proteins interact with the μ_2 chain of the clathrin-associated protein complex AP-2 (159, 164), and phosphotyrosine-containing sequences in many proteins bind to structurally conserved SH2 domains of other interacting proteins (194). Such interactions may involve, at least in part, recognition of specific secondary structures or phosphorylated amino acids. Hence, it is reasonable to ask whether the proposed

flagellar targeting motif might assume a particular secondary structure or involve modification of a particular amino acid. Analysis by the Chou-Fasman algorithm (40) of the region including and surrounding the flagellar targeting motif suggests that amino acids 20-23 and 26-29 have a high propensity to form a β -turn, raising the possibility that this or some other secondary structure is an important component of the recognition of the flagellar targeting sequence by the targeting machinery. In addition, amino acids 25-28 of the sequence shown in Fig. 3-6 form a potential protein kinase A consensus sequence (R-R-X-S/T) (171), raising the possibility that recognition of the flagellar targeting motif could require phosphorylation. Determining whether such structures or modifications of the protein are important in the mechanism of flagellar targeting will require identification of possible interacting partners, structure determination of the hydrophilic NH₂-terminal domain of ISO1, and studies on the phosphorylation state of the targeting motif.

Potential Mechanisms for Addition and Retention of ISO1 in the Flagellar Membrane

One longterm goal is to characterize the mechanism and cellular components that direct proteins to and maintain the distinct protein composition of the flagellar membrane. Studies by Bloodgood and Kozminski *et al.* have described two distinct forms of protein transport specific to the flagellum (27, 112, 186). Bloodgood described gliding, the bidirectional Ca²⁺ dependent movement of polystyrene beads on the flagellar membrane of *Chlamydomonas reinhardtii* (27). Kozminski *et al.* characterized Intraflagellar Transport (IFT),

which differs from bead movement in that IFT is ATP dependent and has been correlated with a specific flagellar kinesin, Fla10 (111, 112). The kinesin colocalizes with electron dense "lollipop" structures in transmission electron micrographs of *C. reinhardtii* flagella. Studies in *C. elegans* and *Drosophila melanogaster* have characterized similar lollipop structures in cilia (186), which suggest that IFT has been evolutionarily conserved. IFT has been implicated in the movement of integral membrane proteins in *C. reinhardtii* (92). Although the mechanism of ISO1 transport to the flagellar membrane remains to be elucidated, it is possible that one of the two flagellar transport processes cited above could be involved in this trafficking event.

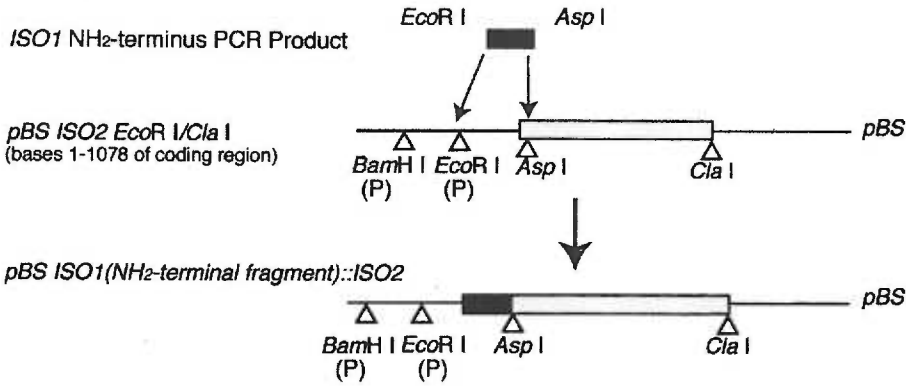
Acknowledgments

The authors wish to thank Aurelie Snyder for operating the confocal microscope for images presented in this paper. We also wish to thank Caroline Enns, Eric Barklis, and Buddy Ullman for helpful discussions.

This work was supported by National Institutes of Health Grants AI25920 and AI01162 to S.M.L., as well as by a Tartar Fellowship and a NRSA Training Grant to E.L.S. S.M.L. is a recipient of the Molecular Parasitology Award from the Burroughs Wellcome Fund.

Figure 3-1. Chimera Strategy. The figure illustrates the steps for the construction of *ISO1(NH₂-terminal sequence)::ISO2* plasmids used to characterize the minimal *ISO1* sequence necessary to retarget *ISO2* from the pellicular plasma membrane to the flagellar membrane. The cloning steps are described in the Materials and Methods section. Black shaded boxes indicate the PCR generated NH₂-terminal sequence of *ISO1*. Gray shaded boxes indicate *ISO2* coding sequence, and white boxes indicate coding sequence of *ISO1*. The hatched box represents the 13 amino acid GLUT2 epitope tag, described in Materials and Methods. Polylinker restriction sites are indicated by (P). The *Asp* I site spans bases 13-18 of the *ISO2* ORF and was used to subclone each *ISO1* NH₂-terminus PCR product to generate an *ISO1::ISO2* fusion ORF. The brackets at the bottom of the figure indicate the three components of this *ISO1::ISO2* ORF: i) the *ISO1* NH₂-terminal fragment, ii) the *ISO2* NH₂-terminal domain, and iii) the sequence that codes for the rest of the protein following the NH₂-terminal hydrophilic domain (identical for *ISO1* and *ISO2*)

Step 1



Step 2

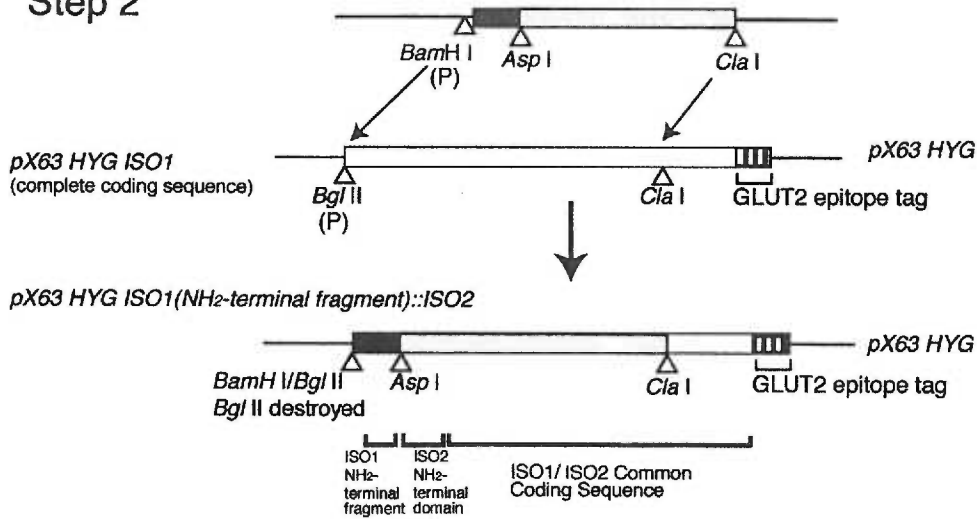
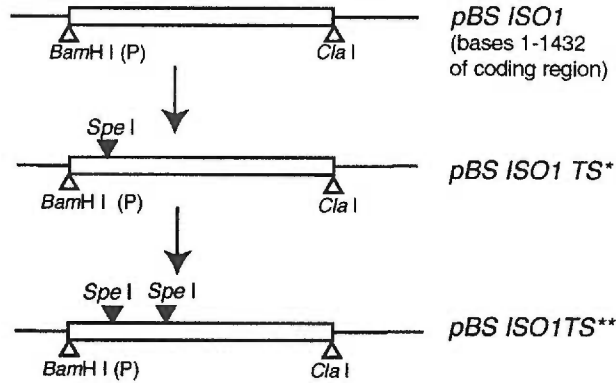


Figure 3-2. Internal Deletion Strategy. The figure illustrates the steps for the construction of internal deletions of the ISO1 NH₂-terminal domain, as described in Materials and Methods. Black triangles indicate unique *Spe* I restriction sites that were introduced by site-directed mutagenesis. Polylinker restriction sites are indicated by (P). The hatched box represents the 13 amino acid GLUT2 epitope tag, described in Materials and Methods.

Step 1

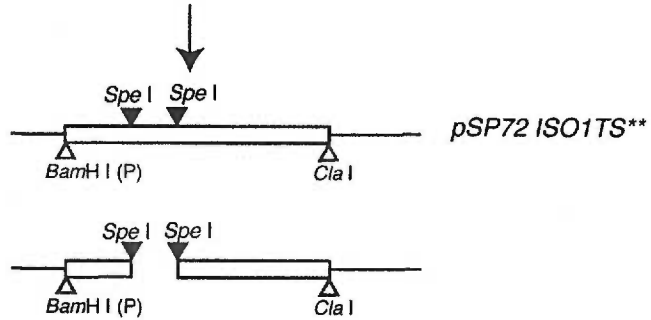
Mutate TS to TS* (*Spe*I site)
make ssDNA of TS* construct.

Mutate second TS to TS* → TS**
now two independent *Spe*I sites.



Step 2

Clone TS** into SP72
Digest with *Spe*I, gel purify, religate
to make Δ TS*.



Step 3

Clone *Bam*HI/*Cla*I Δ TS* into
pX63 HYG expression Vector

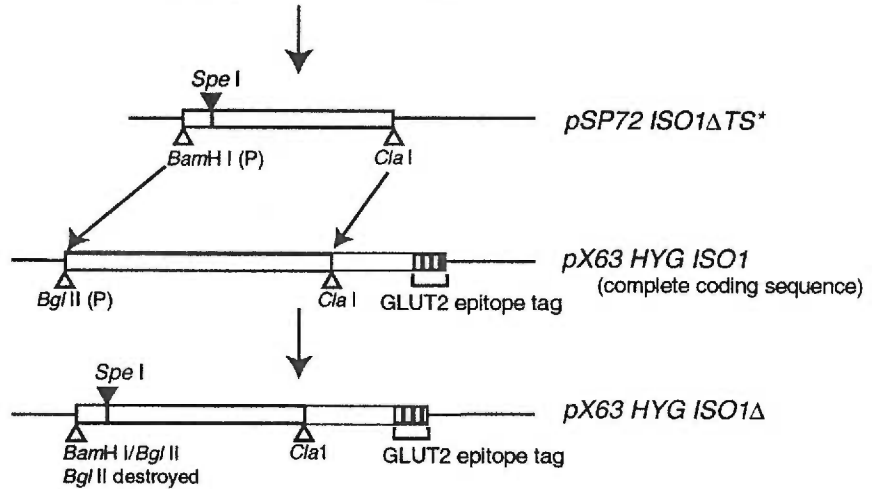
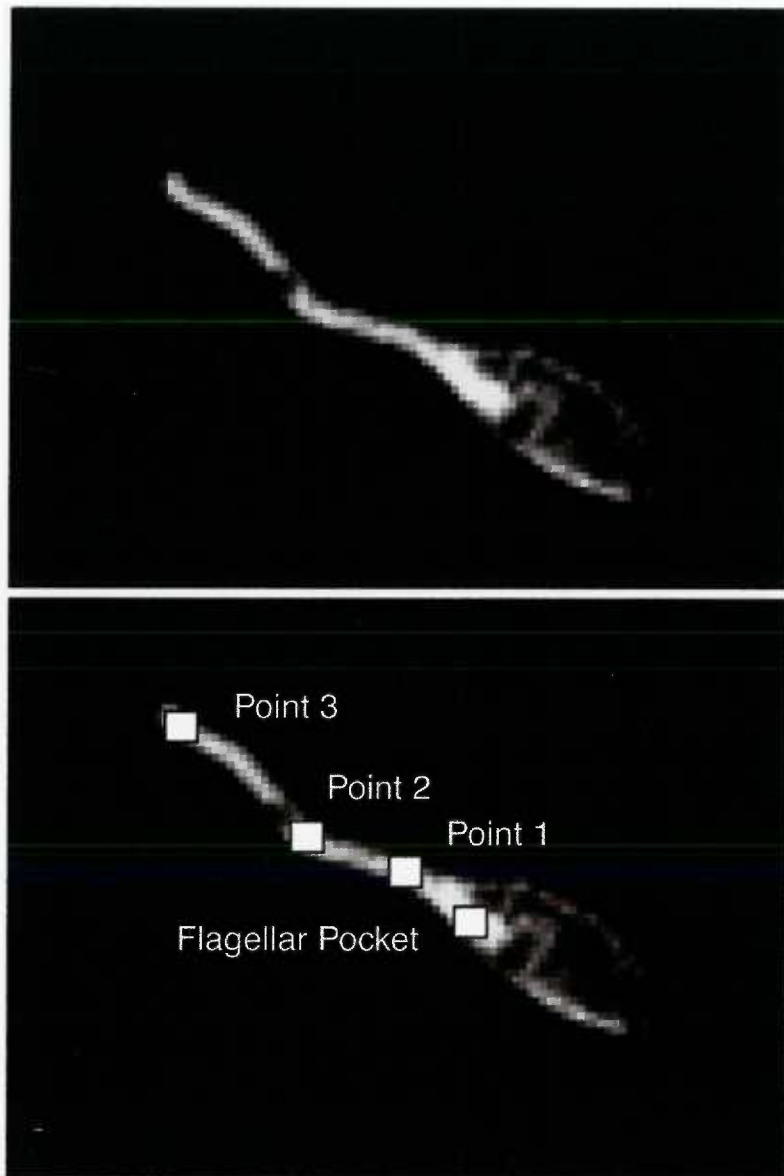


Figure 3-3. Analysis of Immunofluorescence Staining on the Flagellum and Flagellar Pocket. The figure demonstrates the method used to analyze confocal immunofluorescence images of ISO1 alanine mutants and to compare the staining intensity of the flagellar membrane relative to the flagellar pocket. The *upper* image is analyzed as represented in the *lower* image. Each box in the lower image represents a 3x3 pixel area whose average intensity was measured using the computer program NIH Image 1.6, as described in Materials and Methods. The bottom equation was used to calculate the intensity of flagellar staining relative to the flagellar pocket staining (Relative Flagellar Intensity).



$$\text{Relative Flagellar Intensity} = \frac{(P1+P2+P3)}{3(\text{Flagellar Pocket})}$$

Figure 3-4. Confocal Immunofluorescence Microscopy Image of ISO1 (1-35)::ISO2 Chimera Expressing Cells. Confocal laser scanning microscopy images of *L. enriettii* promastigotes expressing either epitope tagged *ISO2* (left) or the epitope tagged chimeric construct *ISO1(1-35)::ISO2* (right) are shown. Stable cell lines transfected with *pX63 HYG ISO2* or *pX63 HYG ISO1(1-35)::ISO2* were stained with a 1:500 dilution of the anti-GLUT2 antibody and a 1:200 dilution of FITC-conjugated secondary antibody and examined by confocal microscopy. Each micrograph represents a single 0.5- μ m section through each field.

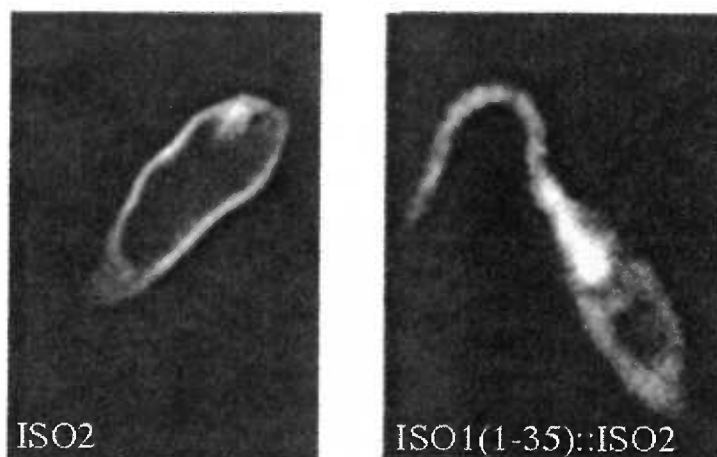
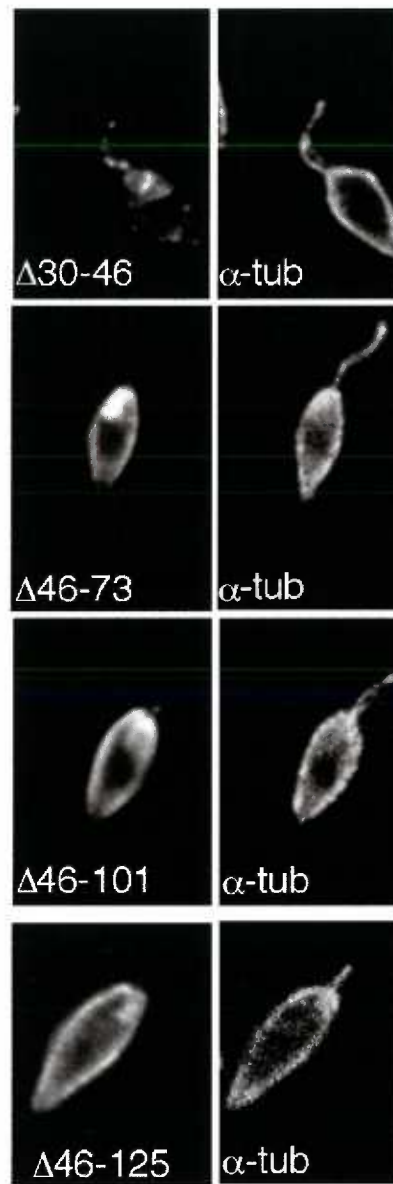


Figure 3-5. Confocal Immunofluorescence Microscopy Images and Immunoblot of Cells Expressing Internal Deletion Mutants of ISO1.

A. Confocal laser scanning microscopy images of *L. enriettii* promastigotes expressing epitope tagged deletion constructs ISO1 Δ 30-46, ISO1 Δ 46-73, ISO1 Δ 46-101, or ISO1 Δ 46-125 are shown. Stable cell lines transfected with either *pX63 HYG ISO1 Δ 30-46*, *pX63 HYG ISO1 Δ 46-73*, *pX63 HYG ISO1 Δ 46-101*, or *pX63 HYG ISO1 Δ 46-125* were stained with a 1:500 dilution of the anti-GLUT2 and anti- α -tubulin (1:500) antibodies and a FITC-conjugated anti-rabbit IgG (1:500) or a rhodamine-conjugated anti-mouse IgG (*α -tub*)(1:500) secondary antibody and examined by confocal microscopy. Each micrograph represents a single 0.5- μ m section through each field. B. An immunoblot of whole cell lysates from stably transfected *L. enriettii* promastigotes expressing the *pX63 HYG* vector, wild type ISO1, ISO1 Δ 30-46 or ISO1 Δ 46-73 is shown. The blot was stained with the anti-GLUT2 antibody (1:3000). Numbers to the right indicate the mobilities of protein molecular weight mass markers in kilodaltons.

A.



B.

vector ISO1 d30-46 d46-73

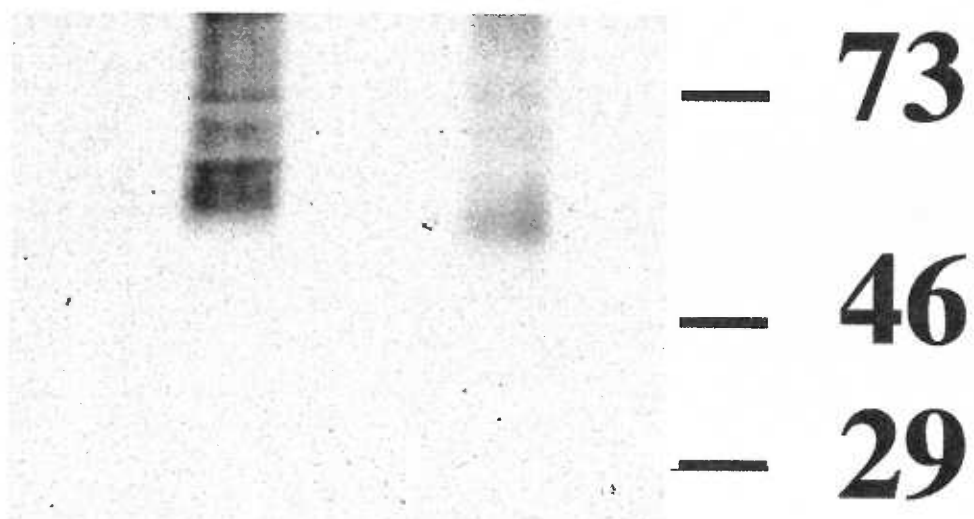


Figure 3-6. Confocal Immunofluorescence Microscopy Images of Alanine

Replacement Mutants of ISO1. Confocal microscopy images of *L. enriettii*

promastigotes expressing epitope tagged ISO1 alanine replacement mutants

P22A, P23A, R24A, R25A, T26A, G27A, T28A, T29A, S30A, H31A, or A32G are

shown. Stable cell lines transfected with one *pX63 HYG ISO1(Alanine Mutant)*

construct each were stained with a 1:500 dilution of the anti-GLUT2 antibody and

a 1:200 dilution of FITC-conjugated secondary antibody and examined by

confocal microscopy. Each micrograph represents a single 0.5- μ m section

through each field. *A.* The *P22A, P23A, R24A, S30A, H31A, and A32G* mutants

do not differ significantly in their pattern of ISO1 staining when compared to wild

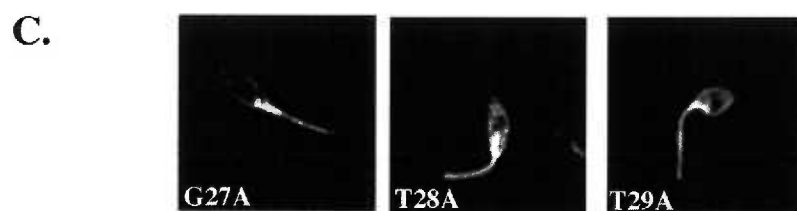
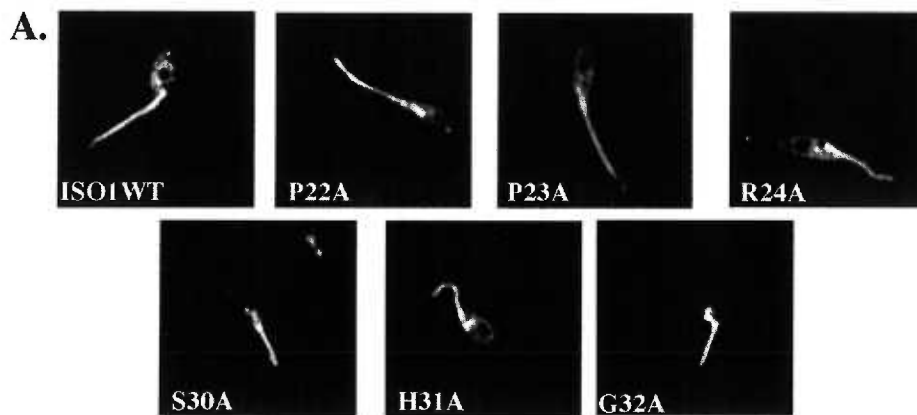
type ISO1. *B.* The *R25A* and *T26A* mutants stain strongly on the flagellum but

very weakly in the flagellar pocket. *C.* The *G27A, T28A, and T29A* mutants

exhibit less intense flagellar staining relative to flagellar pocket staining, when

compared to wild type ISO1. The sequence below *C.* illustrates the relative

position of each amino acid in the ISO1 sequence from amino acids 20-35.



D.

SSPPRRRTGTTSHA AHN

20 21 22 23 24 25 26 27 28 29 30 31 32 33 34 35

Figure 3-7. Histograms of Relative Flagellar Intensities of ISO1 Alanine

Replacement Mutants. Relative Flagellar Intensities of wild type ISO1 and ISO1 alanine replacement mutant expressing cells were analyzed as described in the Materials and Methods. For each cell line, flagellar intensities relative to the flagellar pocket were measured for 30 cells and expressed as a fraction of flagellar pocket staining (1.0). The histograms indicate the numbers of cells with each level of Relative Flagellar Intensity plotted in increments of 0.1. *Relative Flagellar Intensities for R25A and T26A were not possible to measure, because most cells lacked flagellar pocket staining. For these two mutants, mean flagellar intensities were normalized against the value at point 1 (illustrated in Fig. 3-3) for each cell.

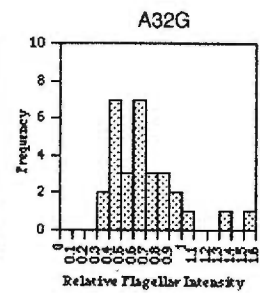
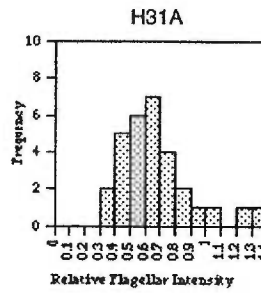
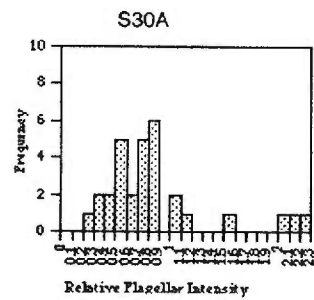
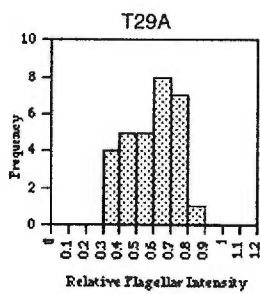
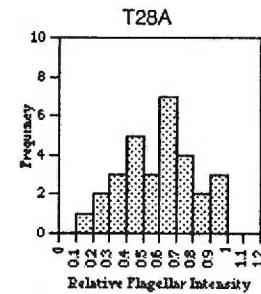
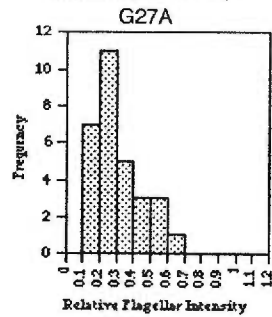
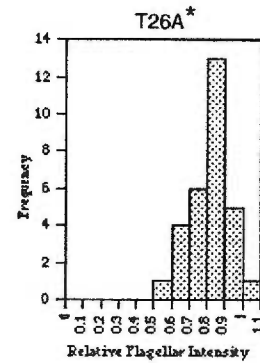
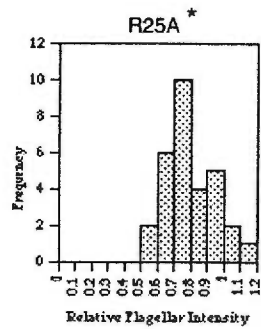
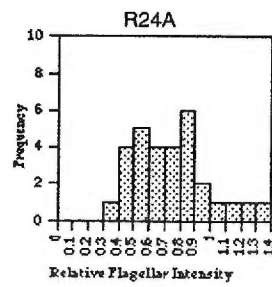
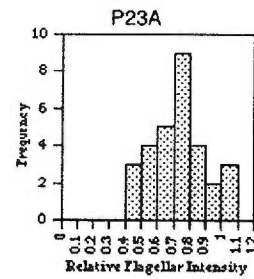
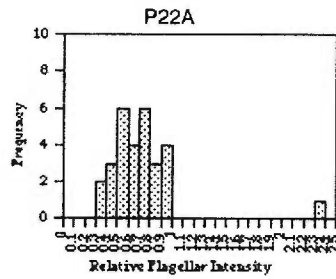
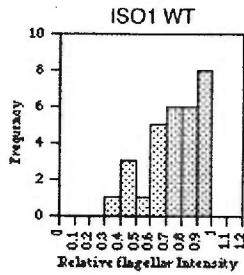


Figure 3-8. Confocal Immunofluorescence Microscopy Images of Double Alanine Replacement Mutants of ISO1. Confocal microscopy images were recorded for *L. enriettii* promastigotes expressing epitope tagged ISO1 double alanine mutants. Stable cell lines transfected with either *pX63 HYG ISO1 RR24,25AA* or *pX63 HYG ISO1 TT28,29AA* were stained with the anti-GLUT2 antibody (1:500) and the anti- α -tubulin antibody (1:500) and then with an FITC-conjugated anti-rabbit IgG (1:200) (*RR24,25AA* and *TT28,29AA*) and a rhodamine-conjugated anti-mouse IgG (1:500) (*α -tub*) secondary antibodies and examined by confocal microscopy. Each micrograph represents a single 0.5- μ m section through each field.

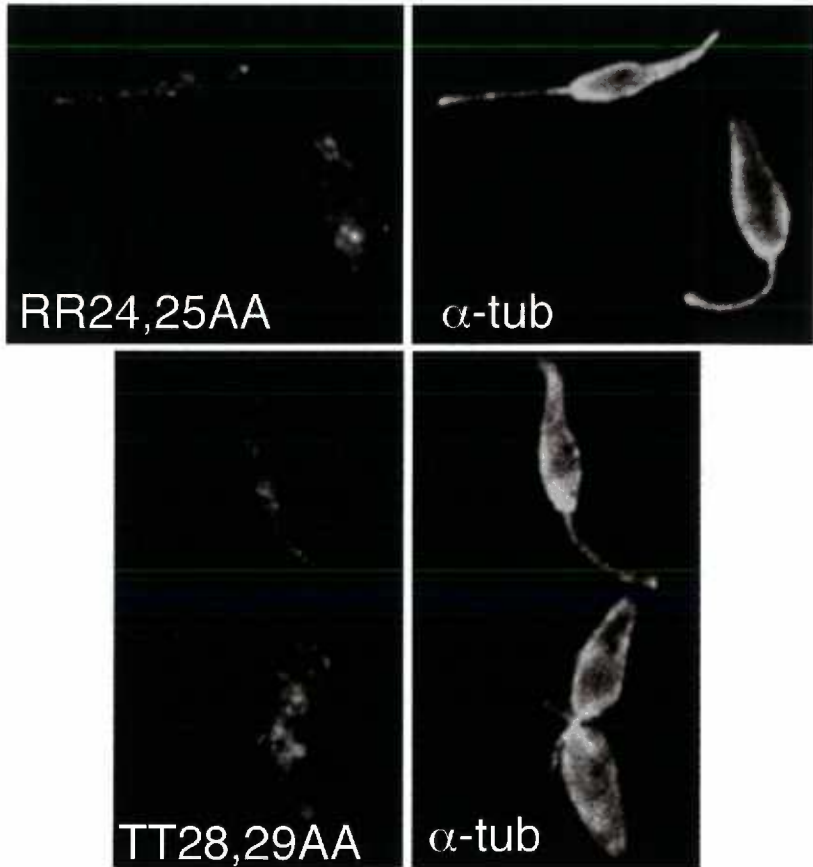


Figure 3-9. Immunoblot of ISO1 Double Alanine Mutants. Whole cell lysates from stably transfected *L. enriettii* promastigotes expressing, the *pX63 HYG* vector, epitope tagged ISO1, ISO1 RR24,25AA, or ISO1 TT28,29AA were immunoblotted. Each lane was equally loaded with lysate of 5×10^6 cells. The blot was stained with the anti-GLUT2 antibody (1:3000) followed by a goat anti-rabbit horse radish peroxidase antibody (1:5000). Numbers to the left indicate the mobilities of protein molecular weight mass markers in kilodaltons. The arrow to the right indicates the band that corresponds to wild type ISO1 protein.

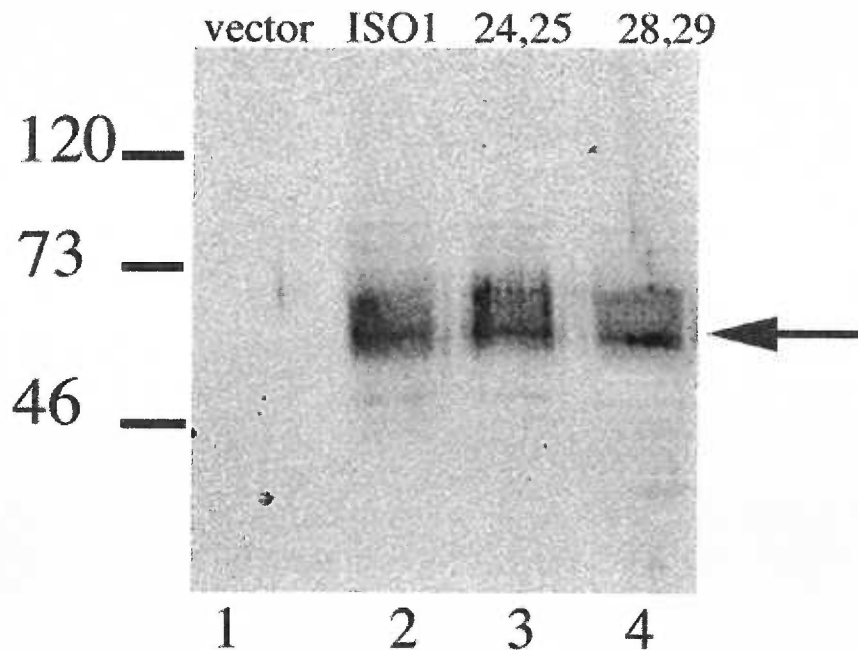
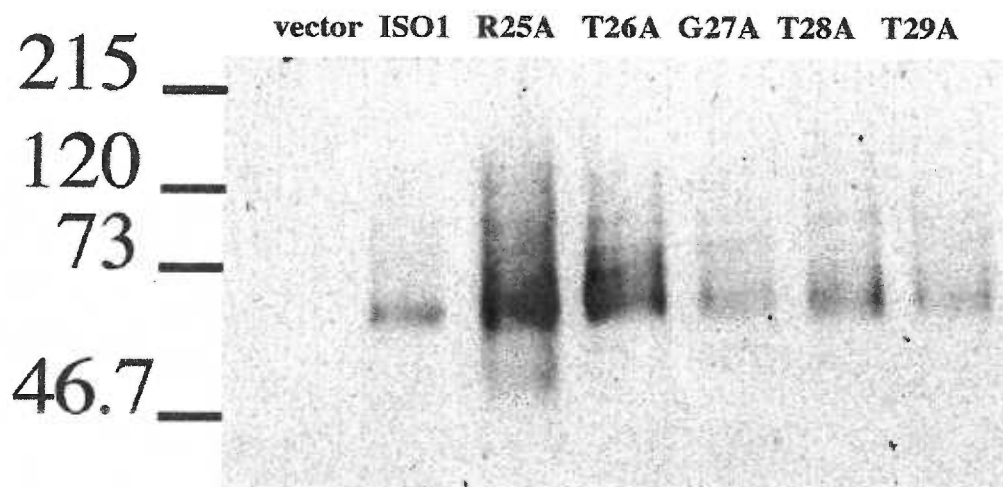
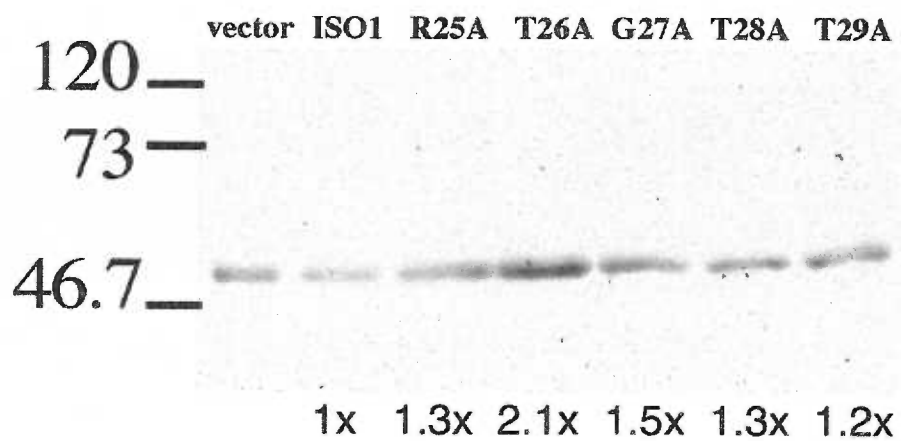


Figure 3-10. Immunoblot of Single Alanine Mutants. The figure shows immunoblots of whole cell lysates from stably transfected *L. enriettii* promastigotes transfected with the pX63 HYG vector or overexpressing epitope tagged ISO1 or epitope tagged ISO1 alanine replacement mutants (*R25A*, *T26A*, *G27A*, *T28A*, *T29A*). *A* and *C*. The blots were stained with the anti-GLUT2 antibody (1:3000) followed by a goat anti-rabbit horse radish peroxidase antibody (1:5,000). *B*. The sample lysates used in *A* were immunoblotted using an anti- α -tubulin antibody (1:500) followed by a goat anti-mouse IgG horseradish peroxidase antibody (1:5000). Band intensities were quantitated using NIH image 1.61. Intensities values were normalized by setting the intensity of wild type ISO1 as the 1X value. Numbers to the left indicate the mobilities of protein molecular weight mass markers in kilodaltons. *C*. Relative levels of *R25A* and *T26A* compared to wild type ISO1 were determined by loading 1X, 1/2 X and 1/5 X of mutant cell lysate. The arrow indicates the band that corresponds to wild type ISO1 protein.

A.



B.



C.

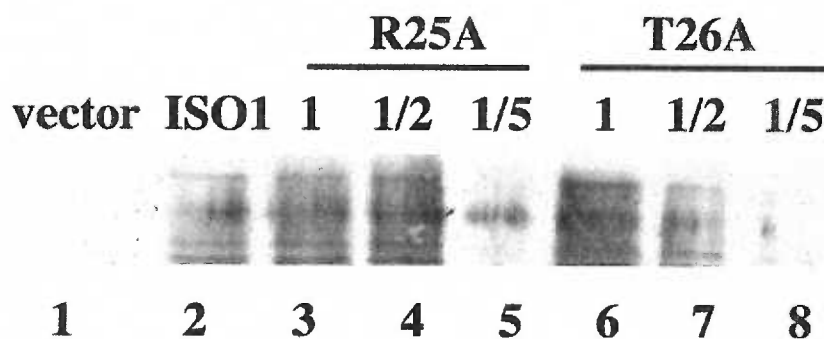


Figure 3-11. Localization of *L. enriettii* ISO1 Expressed in Other *Leishmania* Species. Confocal microscopy was performed on *L. major* (*L. maj.*), *L. mexicana* (*L. mex.*), and *L. donovani* (*L. don.*) promastigotes expressing epitope tagged ISO1. Stable cell lines transfected with *pX63 HYG ISO1* were stained with a 1:500 dilution of the anti-GLUT2 antibody and a 1:200 dilution of FITC-conjugated secondary antibody and examined by confocal microscopy. Each micrograph represents a single 0.5- μ m section through each field.

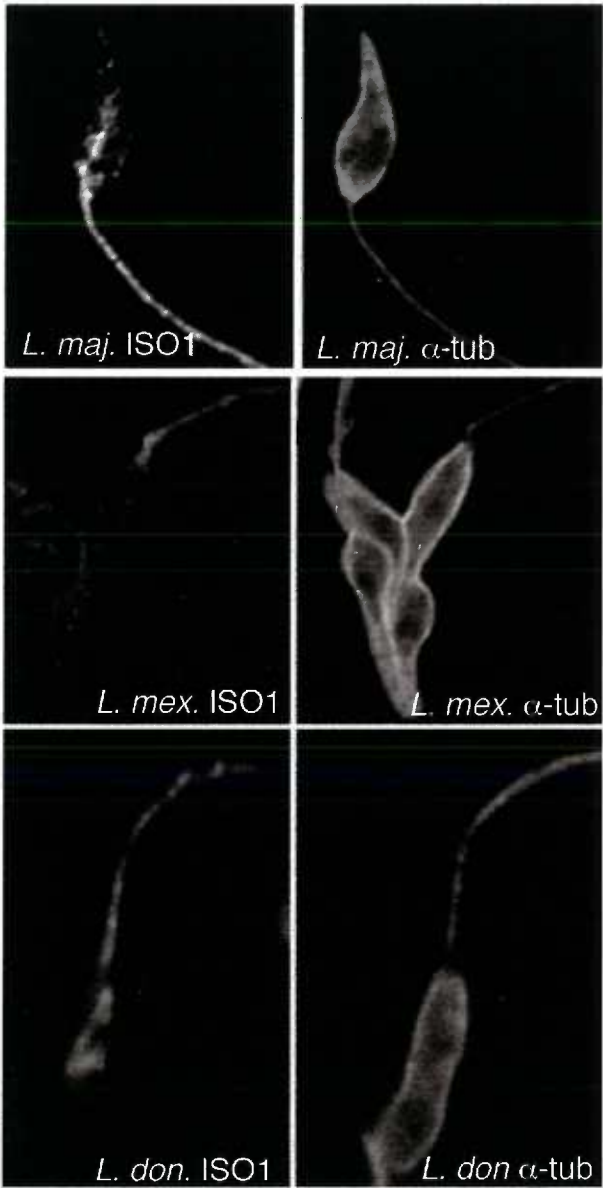


Figure 3-12. Alignment of ISO1 Flagellar Targeting Motif to Other

Trypanosomatid Flagellar Proteins. The putative ISO1 flagellar targeting motif was compared to amino acid sequences of other known flagellar membrane proteins from the related trypanosomatids *T. cruzi* and *T. brucei*. The relative position of each sequence is indicated in the left-most column in parentheses, next to each protein's function. Each amino acid position has been numbered between 1 and 10 for reference. Bold amino acids (R and K in position 3 and T and S in position 6) are identical or similar between all of the sequences.

Alignment of Trypanosomatid Flagellar Proteins with ISO1

<u>Species</u>	<u>Protein</u>	<u>Sequence</u>	<u>Function (sequence of amino acids)</u>
<i>L. enriettii</i>	ISO1	1 2 3 4 5 6 7 8 9 10 P R R T G T T S H A	Glucose transporter (22-32)
<i>T. cruzi</i>	FCABP	G S K G S T S D K G	Flagellar calcium binding protein (5-14)
<i>T. brucei</i>	TB44A	A S K D T T N S K D	Flagellar calcium binding protein (5-14)
<i>T. brucei</i>	TB17	S S K N A S N P K D	Flagellar calcium binding protein (5-14)
<i>T. brucei</i>	ESAG4	T R K P S S S V T S	Receptor adenylate cyclase (1211-1220)

Table 3-4. IS01 Relative Flagellar Intensities of Alanine Scan Mutants Compared to IS01. This table was assembled from the data in the histograms in Fig. 3-7. The number of cells with flagella staining at least 80% as intensely and at least 60% as intensely as the flagellar pocket are listed in each column. The number of cells above the cutoff and below the cutoff were compared to the numbers for wild type IS01. Significance was determined by performing a Chi-square test for each set of comparisons. P values less than 0.05 were considered significant. G27A, T28A, and T29A were determined to be significant for both cutoff values and are in bold.

Mutant	Intensity > 80% Flagellar Pocket (p value)		Intensity > 60% Flagellar Pocket (p value)	
	number out of 30 cells		number out of 30 cells	
ISO1	14		25	
P22A	8 (0.18)		18 (0.086)	
P23A	9 (0.29)		23 (0.75)	
R24A	12 (0.79)		20 (0.23)	
R25A	12 (0.79)*		28 (0.65)*	
T26A	19 (0.29)*		29 (0.20)*	
G27A	0 (0.<0.001)		1 (<0.001)	
T28A	5 (0.026)		16 (0.026)	
T29A	1 (0.<0.001)		16 (0.026)	
S30A	13 (0.61)		21 (0.36)	
H31A	6 (0.055)		17 (0.049)	
A32G	8 (0.18)		18 (0.086)	

* Most of the R25A and T26A cells lacked significant flagellar pocket staining for measuring the relative flagellar intensity. Instead, the mean flagellar intensity was compared to the intensity of point 1 (as illustrated in Fig. 3-3) for each cell.

Table 3-5. Comparison of Flagellar Pocket Staining and Flagellar Staining. Each cell of the 30 collected images for each alanine mutant was analyzed for flagellar pocket staining. Positive flagellar pockets stained at least as intensely as the flagellum. Negative flagellar pockets displayed no obvious staining in the region subtending the base of the flagellum. Numbers of positive and negative flagellar pockets for each alanine mutant were compared to the number of positive and negative flagellar pockets using the Chi-square test. A P value of 0.05 or less was considered significant. The two significant mutants, R25A and T26A are in bold print.

Mutant	Positive Flagellar Pocket	Negative Flagellar Pocket (p value)
ISO1	29	1
P22A	27	3 (0.60)
P23A	29	1 (0.47)
R24A	30	0 (1.0)
R25A	11	19 (<0.001)
T26A	11	16*(<0.001)
G27A	30	0 (1.0)
T28A	29	1 (0.47)
T29A	29	1 (0.47)
S30A	30	0 (1.0)
H31A	30	0 (1.0)
A32G	29	1 (0.47)

a. Three cell images were discarded because background staining obscured the flagellar pocket and the ability to score.

Chapter 4: Discussion

Parasitic protozoa, much like highly specialized polarized cells such as epithelial cells and neurons, need to target specific membrane proteins to discrete domains of the plasma membrane or elsewhere. While some of the mechanisms responsible for the differential localization have been studied extensively in mammalian cells, there is still little known about how differential subcellular targeting occurs in trypanosomatid protozoa. The two isoforms of the major *L. enriettii* plasma membrane glucose transporter present an ideal example of such differential trafficking, since one isoform is localized to the flagellar membrane and the other resides in to the pellicular plasma membrane. The overall objective of these studies has been to begin to analyze the requirements and mechanisms involved in this discrete targeting of each isoform.

I have demonstrated by constructing chimeras with another integral membrane protein that the only region that differs between ISO1 and ISO2, the NH₂-terminal hydrophilic domain, is responsible for the flagellar targeting of ISO1. I also have demonstrated that ISO2 is tethered to the cytoskeleton that underlies the pellicular plasma membrane. Hence, there seem to be two different aspects to the differential targeting, one specifically inducing targeting to the flagellar membrane and the other, presumably a retention mechanism, that anchors proteins in the pellicular membrane.

Cytoskeletal Tethering

Cytoskeletal tethering for integral membrane proteins in the pellicular plasma membrane has been demonstrated for three 12 transmembrane domain

transporters, ISO2, MIT, and D2, in two different species of *Leishmania*, and it is likely that other *Leishmania* integral membrane proteins are restricted to the pellicular plasma membrane by cytoskeletal tethering. Since there are pronounced dissimilarities between the amino acid sequences of the cytoplasmic domains of ISO2, MIT, and D2, it is unclear from sequence comparisons alone which motifs are essential for pellicular plasma membrane targeting. In addition, no charged 18-40 amino acid repeats characteristic of microtubule binding proteins (87) are present in ISO2, MIT, or D2. The absence of known microtubule binding motifs and the precedence for integral membrane proteins in higher eukaryotes binding to cytoskeletal elements *via* a linker protein makes it plausible that the twelve transmembrane domain proteins interact indirectly with the cytoskeleton. Despite the dissimilarity of transport functions, ISO2, MIT, and D2 may bind *via* a common linker protein, similar to the Glycine Receptor and the GABA receptor binding to microtubules *via* gephyrin (144, 226), and Na⁺/K⁺-ATPase and AE1 binding to the spectrin cytoskeleton through ankyrin (57, 100).

The absence of clearly homologous motifs between ISO2, MIT, and D2 suggests that some intelligent guesswork will have to be done to identify potential tethering sequences. In an initial approach, I speculated that the COOH-terminal hydrophilic domain of ISO2 might be required for cytoskeletal tethering. However, the observation that truncation of this domain did not disrupt cytoskeletal tethering (see Figure AP-8) indicated that the interaction domain must lie elsewhere. Since the largest intracellular loops in some mammalian transporters (e.g. Na⁺/K⁺-ATPase and AE1) are involved in linkage to the

cytoskeleton, the large loop between transmembrane domains 6 and 7 of ISO2 is another potential candidate for this interaction. Construction of chimeric proteins may prove useful for examining this possibility. Specifically, it is possible that heterologous transporter proteins from an evolutionarily distant organism, i. e. the mammalian glucose transporters, will not contain a tethering sequence recognized by *Leishmania* parasites. Chimeras exchanging the large intracellular loops from ISO2 and GLUT1 could be constructed, transfected into *Leishmania*, and assayed for tethering by subcellular fractionation and by immunofluorescence microscopy.

It is not clear why *Leishmania* prevents ISO2 and other transporters from diffusing into the flagellar membrane. Two nonexclusive hypotheses could explain the presence of the cytoskeletal tethering mechanism. First, tethering could affect transport function, as in the case of the ATP sensitive K⁺ channel activity which becomes insensitive to ATP induced inhibition in response to actin disruption by cytochalasin or DNase I treatments (148, 222). In another example, a Na⁺ channel's activity in A6 cells increased in response to the actin disrupting drug cytochalasin (148). Thus, tethering to the promastigote cytoskeleton could modulate transporter activity. Second, tethering may be unrelated to transport function. For example, AE1 tethering to actin is essential for adherence of the red blood cell membrane to the disc shaped actin cytoskeleton (173). The microtubule cytoskeleton imparts the thin bullet-like shape to the promastigote stage of *Leishmania*. For the plasma membrane to conform to the bullet shape, the pellicular plasma membrane must be tethered to the cytoskeleton, and Dwyer *et al.* have demonstrated that the subpellicular microtubules associate with the

pellicular plasma membrane (62). It is possible that the parasite utilizes the abundant transporters as membrane anchors that attach the pellicular plasma membrane to the cytoskeleton, similar to the role of AE1 in the red blood cell. The presence of several transmembrane domains in transporters makes such proteins attractive candidates for membrane anchors.

The Flagellar Membrane Targeting Motif

This thesis describes the first characterization of a flagellar membrane targeting sequence in an eukaryotic cell. The results of these thesis studies and future studies may provide insights into the mechanism(s) of flagellar/ciliary membrane targeting in other eukaryotic cells. The flagellar targeting chimera data (Fig. 3-4) demonstrate that the sequence of amino acids 1-35 is critical for targeting ISO1 to the flagellar membrane. NH₂-terminal deletions of ISO1 (Fig. 2-8A) demonstrate that amino acids 1-20 are not necessary for the flagellar targeting of ISO1 (211). Thus, an essential targeting sequence maps between amino acids 20-35. Furthermore, mutation of any one of five contiguous amino acids (RTGTT) within this essential targeting region was shown to affect the relative distribution of ISO1 between the flagellum and the flagellar pocket. The core flagellar targeting sequence contains potential similarities to sequences in other flagellar membrane targeted proteins in other trypanosomatids. In addition, other species of *Leishmania* contain the necessary components to target ISO1 to the flagellar membrane (Chapter 3).

To determine whether the proposed common motif is found in proteins that do not reside within the flagellar membrane, we searched the Swiss Prot

database using PatternFind¹ for proteins containing the sequence [RSKT]-[RK]-[PGSDTN]-[PGSTDN]-[ST]-[STN]. The search results for trypanosomatid proteins identified the known flagellar proteins used in the alignment, a group of mucin-like proteins, three kinases related to MAP kinases, a surface sialidase, a secreted acid phosphatase, two putative potassium channels, a glycosomal glycolysis enzyme, two groups of cyclophilins, two variable surface glycoproteins, a P-type ATPase, and a U5 (a small nuclear ribonucleoprotein) homologue. The potassium channels and the P-type ATPase meet the criterion of being membrane proteins, and the putative flagellar targeting sequences map to predicted cytoplasmic domains. The other proteins are either not membrane proteins, or the putative flagellar targeting sequence maps to predicted extracellular domains. Thus, despite the degeneracy of the two B positions, the flagellar targeting motif is not ubiquitous for most proteins, and requirements that the sequence be associated with a membrane protein and that the sequence must be cytoplasmic may provide additional specificity.

Targeting mechanisms

No studies to date have described the mechanism(s) by which membrane proteins are added to and removed from the flagellar membrane in trypanosomatids. It is unlikely that the trafficking mechanism involves vesicular transport, because no vesicles have been identified in the flagella or cilia of any organisms (27). Two flagellar membrane trafficking mechanisms have been characterized in the algal flagellate *Chlamydomonas reinhardtii*, intraflagellar

1. (http://www.isrec.isbsib.ch/software/PATFND_form.html)

trafficking (IFT) and gliding (186). IFT is mediated by the Fla10 kinesin along flagellar microtubules (111). Fla10 is incorporated into "raft" structures that transport soluble flagellar proteins and have been suggested to mediate the trafficking of flagellar membrane proteins (111, 186). Gliding is a distinct mechanism of bi-directional Ca^{2+} dependent flagellar surface movement that can be demonstrated by attaching polystyrene beads to the flagellar membrane (27). IFT and the associated raft structures have been observed in the cilia of *C. elegans* and *Drosophila melogaster* which suggests that IFT has been evolutionarily conserved (186). It is possible that IFT or a related mechanism could be involved in the trafficking of ISO1 and other flagellar membrane proteins.

It is unclear if ISO1 targets first to the flagellar pocket or the flagellar membrane, but the flagellar pocket is a likely first step, since both ISO1 and ISO2 are located within this organelle. The initial sorting step may occur at the flagellar pocket. A speculative model is that after addition of ISO1 to the flagellar pocket membrane, a receptor protein will associate with the flagellar targeting sequence of ISO1. The receptor either has a kinesin motor or binds to a kinesin that drags ISO1 into the flagellar membrane, similar to the IFT mechanism. Eventually ISO1 dissociates from the kinesin and either associates with a new kinesin that could direct retrograde trafficking or diffuses along the flagellar membrane back to the flagellar pocket.

The Possible Functions of ISO1

The selective pressure for maintaining a flagellar glucose transporter remains unclear. Hypotheses for the role of ISO1 include: 1) a mechanism for

obtaining extra nutrients, 2) a function as a glucose sensor, and 3) *in vivo* transport properties that are different from ISO2. All three hypotheses are consistent with indirect evidence, but will require additional experiments including “gene knockouts” to differentiate between the hypotheses. An additional complication arises because the insect host of *L. enriettii* has not been identified making it difficult to assess the full range of the phenotypes of knockout mutants in the insect stage of the life cycle. A subtle phenotype may be difficult to detect in tissue culture conditions, and the relevance of a phenotype may not be apparent. Thus, if ISO1 serves a sensory function, it is not immediately clear what the “readout” of the sensing process would be (chemotaxis towards glucose, induction or repression of glucose regulated genes, or some other unknown effect), and it is thus not obvious what phenotype to examine in an ISO1 knockout parasite.

The extra nutrients hypothesis is the simplest interpretation consistent with the data. Adding glucose transporters to the extra ~20% of the plasma membrane surface area present on the flagellum could provide a selective advantage for the parasite during conditions of low glucose. A flagellar isoform could conceivably arise through a series of mutations in the NH₂-terminal domain that could create a flagellar membrane targeting motif. The necessary components for flagellar targeting might already exist for other critical flagellar membrane proteins such as the flagellar calcium binding protein in trypanosomes (65). However, two pieces of evidence weaken the extra nutrients hypothesis. First, studies by others indicate that glucose transport is not limiting for uptake of glucose or for

glycolysis in these parasites, at least under the ideal conditions of a chemostat (219-221). Second, and more importantly, the NH₂-terminal domains of ISO1 and ISO2 contain no apparent sequence similarities. It seems unlikely that the NH₂-terminal domain of ISO1 arose through a series of point mutations. In addition, the chimera studies demonstrate that the first 35 amino acids of ISO1 are sufficient for flagellar targeting. Yet, ISO1 contains an additional 100 amino acids that do not align with the sequence in the ISO2 NH₂-terminal cytoplasmic domain. While the simplicity of the “extra nutrients” hypothesis is appealing, the dramatic sequence differences between ISO1 and ISO2 suggest functional differences.

A non-glucose related function seems intuitively unlikely, because the glucose transport function has been conserved to the extent that ISO1 and ISO2 are identical in sequence (after the NH₂-terminal cytoplasmic domain) and at least very similar in biochemical properties. However, several transporter like proteins in yeast have been identified that have high homology with glucose transporters, but do not transport glucose (37, 165, 178). Rather, they sense the presence of glucose and relay this information, *via* a sensor motif in the COOH-terminal cytoplasmic domain, which leads to an induction of the expression of *bona fide* glucose transporters and other glucose-regulated genes (178). Özcan *et al.* have added the COOH-terminus of a sensor domain to a functional yeast glucose transporter and demonstrated that this chimeric protein retains both transport and sensor functions (165). Thus, precedence exists for functional glucose sensor-transporters. The phenomenon of sensors is not limited to *Saccharomyces*, as a

candidate glucose sensor that is also a transporter has been identified in *Neurospora* (*rco-3*) (133). Furthermore, sensing is not limited to carbohydrate sensors, as Iragui *et al.* have characterized an amino acid sensor (*SSY1*) in *S. cerevisiae* (94).

Hypotheses 2 (possible receptor function) is intriguing because the limited number of flagellar membrane proteins identified in trypanosomatids include several that probably perform sensory functions, including receptor-adenylate cyclases and calcium binding proteins. These observations suggest that the flagellum serves as a sensory organelle. Furthermore, ISO1 contains a region in the NH₂-terminal cytoplasmic domain (amino acids 42-61) that contains potential homology to the sensor domain of yeast glucose sensor proteins (Fig. AP-9). Eight out of 20 amino acids are identical or highly similar between the ISO1 sequence and the yeast sensor motifs. Because significant differences exist between the sequences in other regions, we investigated whether these amino acid differences affected predicted secondary structure. Figure AP-10 compares two secondary structure algorithms for the relevant regions of SNF3.1 and ISO1. Both algorithms predict very similar secondary structures common to the two proteins. The common sequences and predicted structures acquire more strength when another common sensor characteristic is considered, the length of the domain containing the sensor region relative to the length of the homologous region in other transporters. The sensor proteins have an unusually long cytoplasmic domain (yeast sensor COOH-termini are longer than 200 amino acids, while yeast glucose transporter COOH-termini are less than 50 amino

acids) (99, 165). While the alignments do not prove that ISO1 has a sensor function, the similarity suggests a possible sensor role and should be investigated.

Hypothesis 3 (different *in vivo* transport properties) highlights the drawback of expressing ISO1 in a heterologous system (*Xenopus* oocytes). While innate properties of a transporter can be characterized in oocytes, the heterologous system may not reveal *in vivo* properties of the protein that depend upon interactions that occur only in the homologous cell system. If ISO1 binds to a specific *Leishmania* protein that modifies transporter function or is post-translationally modified (i.e. phosphorylated), then the true role or properties of ISO1 could be obscured in a heterologous expression system. In principle, it may be possible to test for distinct functional properties of ISO1 and ISO2 by "knocking out" the entire *PRO1* gene cluster by homologous recombination and then transfecting this knockout line separately with *ISO1* and *ISO2* genes. This experiment would generate *L. enriettii* lines that express each isoform in the absence of the other, allowing the measurement of various functional parameters (e. g. K_m s and substrate specificities) of each isoform in a homologous system. Furthermore, testing for post-translational modifications, such as phosphorylation or a difference in protein stability of ISO1 compared to ISO2 and searching for interacting proteins by the yeast two-hybrid method should be possible.

Precedence exists for transporters having properties in their native environment that are not manifest in a heterologous system. For example, the erythrocyte Anion Exchanger 1 transporter can be expressed in a renal epithelial cell line and can target to either the apical or basolateral membrane under specific

conditions (228). Antibodies that recognize the basolateral AE1 can not recognize AE1 in the apical membrane (228). In addition, the apical transporter had a reduced sensitivity to a normally potent inhibitor of AE1 activity (228). Because the flagella and cilia of other eukaryotic organisms have demonstrably different lipid compositions from the rest of the plasma membrane (similar to the apical membrane of polarized epithelial cells) (102), ISO1 could have transport properties that differ from ISO2 or from the properties characterized by uptake studies in the *Xenopus* oocyte system.

Future Directions

Future studies will include identifying the cytoskeletal tethering sequence of ISO2 and any potential binding proteins, testing for cytoskeletal tethering *in vivo*, further characterizing the flagellar targeting signal, identifying the proteins that interact with the flagellar targeting motif of ISO1, and characterizing the mechanism and components of flagellar localization.

Some of these studies are in progress. To test for cytoskeletal tethering *in vivo* I am creating green fluorescent protein chimeras of ISO1 or ISO2. I will perform fluorescence recovery after photobleaching (FRAP) experiments to compare the mobilities of ISO1 and ISO2. These experiments will test the hypothesis that ISO2 is tethered to the cytoskeleton and thus constrained in mobility while ISO1 is freer to diffuse within the flagellar membrane.

To identify proteins that interact with the ISO1 targeting motif, I have created constructs containing the ISO1 NH₂-terminal domain fused to the activator domain of the *S. cerevisiae Gal4* gene to screen for interacting proteins

in a yeast two-hybrid system. Other approaches will include protein affinity chromatography and coimmunoprecipitations to search for proteins that may interact with the flagellar targeting motif (174). A similar approach could be used to characterize putative linker proteins that could tether ISO2 to the cytoskeleton.

Further characterization of the flagellar targeting motif will be needed to address several questions: 1) Does phosphorylation play a role in flagellar membrane targeting? Amino acids 25-28, RTGT, constitute a putative protein kinase A site (171), and phosphorylation at this site might be required for flagellar targeting. 2) Which amino acids are sufficient for flagellar targeting? Chimeras may prove useful in answering this question. Mutating amino acids in the 1-35 chimera may present more dramatic phenotypes than the alanine mutants in wild type ISO1. 3) Does the putative glucose sensor domain have a function? Will mutations in this domain alter targeting of ISO1 and/or cause other phenotypes? 4) Can the ISO1 flagellar targeting motif target proteins to the flagellum in trypanosomes, suggesting that these related parasites contain the same flagellar targeting machinery as *Leishmania*? 5) What are the contextual requirements for function of the flagellar targeting motif (i.e. how close can the sequence be to the membrane, and can the sequence be at the COOH-terminus or in an intracellular loop)?

Currently, we are attempting to crystallize the cytoplasmic NH₂-terminal domain of ISO1 to determine its structure. Such structural studies could reveal whether the core flagellar targeting motif, RTGTT, is present in some specific secondary structure or surface fold that might promote interaction with other

proteins involved in targeting. The chimeras, alignments, and alanine mutant studies hint that the essential flagellar targeting motif may be a β -turn and should be solvent exposed. Furthermore, determining the structure may provide clues for future site-directed mutagenesis studies.

Summary

A fundamental question of cell biology is how proteins are targeted and localized to different subcellular domains. My thesis describes and begins to characterize targeting signals and mechanisms for integral membrane proteins of the flagellar membrane and pellicular plasma membrane of *Leishmania enriettii*.

The two isoforms of PRO1 (ISO1 and ISO2) are identical except for their NH₂-terminal cytoplasmic domains, which lack any apparent homology. ISO1 has a 130 amino acid NH₂-terminal cytoplasmic domain, while ISO2 has a 48 amino acid domain. ISO1 targets to both the flagellar membrane and the flagellar pocket, while ISO2 targets to the pellicular plasma membrane and the flagellar pocket. We have exploited ISO1 and ISO2 as a model system for the study of differential targeting of integral membrane proteins in a contiguous membrane.

The first aim of my studies characterized the flagellar targeting sequence for ISO1. We postulated that the necessary information for flagellar targeting should be contained in the NH₂-terminal domain of ISO1. We tested this hypothesis by creating chimeric proteins of the pellicular plasma membrane targeted hexose transporter D2, in which the NH₂-terminus of D2 was replaced by the NH₂-terminus of ISO1 or ISO2. Confocal immunofluorescence microscopy revealed that the ISO2::D2 chimera targeted to the pellicular plasma membrane,

like the wild type D2 protein. However, the ISO1::D2 chimeric protein targeted to the flagellar membrane, demonstrating that the NH₂-terminus of ISO1 is **sufficient** to retarget a pellicular plasma membrane protein to the flagellar membrane. A series of NH₂-terminal deletion mutants identified a **necessary** flagellar targeting sequence that mapped to the region near amino acid 25. A chimera in which the first 35 amino acids of ISO1 were added to ISO2 retargeted ISO2 to the flagellar membrane, demonstrating that the region between amino acids 1-35 contains a **sufficient** flagellar targeting signal. The combined results of these chimera and deletion studies imply that a sequence involved in flagellar targeting falls between amino acids 20 and 35 of ISO1. However, smaller chimeras of amino acids 21-29, 20-29, 22-30 and 22-35 of ISO1 can not redirect ISO2 to the flagellar membrane, which suggests that amino acids 21 and/or 22 may be important for flagellar targeting or may affect the secondary structure of the flagellar targeting sequence.

In an attempt to identify the essential amino acids of the flagellar targeting sequence, amino acids 22 through 32 were individually mutagenized and replaced with alanines (or a glycine at A32). No single amino acid substitution completely disrupted flagellar targeting of ISO1. We hypothesized that redundancies may exist in the targeting sequence and that individual amino acid substitutions are insufficient to retarget ISO1 from the flagellar membrane to the pellicular plasma membrane. However, individual alanine replacement mutants of amino acids 25-29 displayed quantitatively different flagellar distributions relative to wild type ISO1. The cluster of mutants displayed two distinct phenotypes. R25A and

T26A conferred strong flagellar staining and minimal flagellar pocket localization. In contrast, G27A, T28A, and T29A localized primarily to the flagellar pocket and more weakly to the flagellar membrane. The results suggest that G27A, T28A, and T29A target less efficiently to the flagellar membrane or are not retained efficiently in the flagellar membrane and traffic in a retrograde manner to the flagellar pocket. R25A and T26A appear either to target more efficiently to the flagellar membrane or to be trapped or compromised in their ability to traffic in a retrograde direction to the flagellar pocket. The latter interpretation is supported by immunoblot data which demonstrates that R25A (and less dramatically T26A) cells contain dramatically higher levels of mutant protein, consistent with the idea the mutants may be sequestered away from proteolytic degradation pathways. The observation that clathrin-mediated endocytosis probably occurs in the flagellar pocket (163, 240) could provide a link between flagellar "trapping" and the reduced rate of turnover of these two mutant proteins. It will be necessary to measure the half lives of wild type ISO1 and of the R25A and T26A mutants to determine whether these mutants do experience a reduced rate of turnover.

The second aim of this thesis was to characterize the nature of pellicular plasma membrane targeting of ISO2. We tested the hypothesis that ISO1 or ISO2 might differentially associate with the parasite cytoskeleton. We performed Triton X-100 extractions followed by low speed centrifugation to separate the cytoskeleton-containing pellet from the supernatant. Immunoblots with three different antibodies against the two isoforms demonstrated that ISO1 fractionated

exclusively with the supernatant, while ISO2 fractionated quantitatively with the cytoskeletal pellet. Confocal immunofluorescence microscopy of detergent extracted cytoskeletons from wild type *L. enriettii* and from parasites expressing each epitope tagged isoform confirmed the immunoblot results. Parasite cytoskeletons displayed intense staining over the subpellicular microtubules and background staining of flagellar microtubules. Cytoskeletal tethering was demonstrated for other integral membrane proteins including the D2 hexose transporter and the MIT *myo*-inositol transporter, both from another species, *L. donovani*. Interestingly, NH₂-terminal deletion mutants of ISO1 that retarget to the pellicular plasma membrane also tether to the subpellicular microtubules. The phenomenon of cytoskeletal tethering may act to anchor and restrict ISO2 and other pellicular plasma membrane proteins away from the flagellar pocket and the flagellar membranes.

Flagellar targeting and cytoskeletal tethering represent two distinct but complementary mechanisms that result in the differential distribution of two glucose transporters with similar properties. The reason why the parasite has evolved the differential targeting mechanisms for ISO1 and ISO2 is still not clear. ISO1 could have multiple functions besides transporting glucose, such as acting as a sensor of extracellular glucose concentrations.

In this thesis, two different mechanisms of protein targeting/localization in *Leishmania* have been identified and partially characterized. A class of integral membrane proteins, members of the glucose transporter superfamily, that target to the pellicular plasma membrane are anchored and restricted to that membrane

domain by tethering of the transporters to the parasite cytoskeleton. Another member of the glucose transporter superfamily, ISO1, and possibly three unrelated flagellar membrane proteins, the FCaBPs and the receptor adenylate cyclase ESAG4, target to the flagellar membrane by a flagellar targeting sequence. These two targeting mechanisms complement each other to create differential distributions of integral membrane proteins within different domains of a contiguous membrane.

References

1. (1999) Leishmaniasis control. 1999, World Health Organization.
2. Adosraku, R. K., Anderson, M. M., Anderson, G. J., Choi, G., Croft, S. L., Yardley, V., Phillipson, J. D. & Gibbons, W. A. (1993). Proton NMR lipid profile of *Leishmania donovani* promastigotes. *Mol. Biochem. Parasitol.* 62:251-262.
3. Agabian, N. (1990). *Trans* splicing of nuclear pre-mRNAs. *Cell* 61:1157-1160.
4. Alberts, B., Bray, D., Lewis, J., Raff, M., Roberts, K. & Watson, J. D. (1994). third. New York: Garland Publishing, Inc.
5. Alexander, J. & Russell, D. G. (1992). The interaction of *Leishmania* species with macrophages. *Adv. Parasitol.* 31:175-253.
6. Alper, S. L., Stuart-Tilley, A., Simmons, C. F., Brown, D. & Drenckhahn, D. (1994). The fodrin-ankyrin cytoskeleton of choroid plexus preferentially colocalizes with apical Na⁺K⁺-ATPase rather than with basolateral anion exchanger AE2. *J. Clin. Invest.* 93:1430-1438.
7. Ameisen, J. C., Idziorek, T., Billaut-Mulot, O., Loyens, M., Tissier, J.-P., Potentier, A. & Ouaiissi, A. (1995). Apoptosis in a unicellular eukaryote (*Trypanosoma cruzi*) implications for the evolutionary origin and role of programmed cell death in the control of cell proliferation, differentiation and survival. *Death and Diff.* 2:285-300.

8. Ashford, D. W., Desjeux, P. & deRaadt, P. (1992). Estimation of population at risk of infection and number of cases of leishmaniasis. *Parasitol. Today* 8:104-5.
9. Balber, A. E. (1990). The pellicle and the membrane of the flagellum, flagellar adhesion zone, and flagellar pocket: Functionally discrete surface domains of the bloodstream form of African trypanosomes. *Crit. Rev. Immuno.* 10:177-201.
10. Bangs, J. D., Brouch, E. M., Ransom, D. M. & Roggy, J. L. (1996). A soluble secretory reporter system in *Trypanosoma brucei*. *J. Biol. Chem.* 271:18387-18393.
11. Bangs, J. D., Ransom, D. M., McDowell, M. A. & Brouch, E. M. (1997). Expression of bloodstream variant surface glycoproteins in procyclic stage *Trypanosoma brucei*: role of GPI anchors in secretion. *EMBO Journal* 16:4285-4294.
12. Baranski, T. J., Cantor, A. B. & Kornfeld, S. (1992). Lysosomal enzyme phosphorylation: I. Protein recognition determinants in both lobes of procathepsin D mediate its interaction with UDP-GlcNAc:Lysosomal N-acetylglucosamine-1-phosphotransferase. *J. Biol. Chem.* 267:23342-23348.
13. Baranski, T. J., Koelsch, G., Hartsuck, J. A. & Kornfeld, S. (1991). Mapping and molecular modeling of a recognition domain for lysosomal enzyme targeting. *J. Biol. Chem.* 266:23365-23372.
14. Bard, E. (1989). Molecular biology of *Leishmania*. *Biochem. Cell Biol.* 67:516-524.

15. Bartles, J. R. (1995). The spermatid plasma membrane comes of age. *Trends Cell Biol.* 5:400-404.
16. Bastin, P., Matthews, K. R. & Gull, K. (1998). Paraflagellar rod is vital for trypanosome motility. *Nature* 391:548.
17. Bates, P. A. (1994). The developmental biology of *Leishmania* promastigotes. *Exp. Parasitol.* 79:215-218.
18. Bates, P. A., Robertson, C. D., Tetley, L. & Coombs, G. H. (1992). Axenic cultivation and characterization of *Leishmania mexicana* amastigote-like forms. *Parasitology* 105:193-202.
19. Bennett, V. & Stenbuck, P. J. (1979). The membrane attachment protein for spectrin is associated with band 3 in human erythrocyte membranes. *Nature* 280:468-473.
20. Berman, J. D. (1997). Human leishmaniasis: clinical, diagnostic, and chemotherapeutic developments in the last 10 years. *Clin. Infect. Dis.* 24:684-703.
21. Beverley, S. M. (1996). Hijacking the cell: Parasites in the driver's seat. *Cell* 87:787-789.
22. Beverley, S. M., Ismach, R. B. & McMahon Pratt, D. (1987). Evolution of the genus *Leishmania* as revealed by comparisons of nuclear DNA restriction fragment patterns. *Proc. Natl. Acad. Sci. U.S.A.* 84:484-488.
23. Bibi, E. & Kaback, H. R. (1990). *In vivo* expression of the *lacY* gene in two segments leads to functional *lac* permease. *Proc. Natl. Acad. Sci. U.S.A.* 87:4325-4329.

24. Blattner, J., Helfert, S., Michels, P. & Clayton, C. (1998). Compartmentation of phosphoglycerate kinase in *Trypanosoma brucei* plays a critical role in parasite energy metabolism. *Proc. Natl. Acad. Sci. U.S.A.* 95:11596-11600.
25. Blattner, J., Swinkels, B., Dorsam, H., Prospero, T., Subramani, S. & Clayton, C. (1992). Glycosome assembly in trypanosomes: variations in the acceptable degeneracy of a COOH-terminal microbody targeting signal. *J. Cell Biol.* 119:1129-1136.
26. Blenis, J. & Resh, M. D. (1993). Subcellular localization specified by protein acylation and phosphorylation. *Curr. Opin. Cell Biol.* 5:984-989.
27. Bloodgood, R. A. (1992). Directed movements of ciliary and flagellar membrane components: a review. *Biol. Cell* 76:291-302.
28. Blum, J. J. (1993). Intermediary metabolism of *Leishmania*. *Parasitol. Today* 9:118-122.
29. Bordier, C., Garavito, R. M. & Armbruster, B. (1982). Biochemical and structural analyses of microtubules in the pellicular membrane of *Leishmania tropica*. *J. Protozool.* 29:560-565.
30. Bretscher, A. (1991). Microfilament structure and function in the cortical cytoskeleton. *Ann. Rev. Cell Biol.* 7:337-374.
31. Bretscher, M. S. & Munro, S. (1993). Cholesterol and the Golgi apparatus. *Science* 261:1280-1281.

32. Bringaud, F. & Baltz, T. (1992). A potential hexose transporter gene expressed predominantly in the bloodstream form of *Trypanosoma brucei*. *Mol. Biochem. Parasitol.* 52:111-121.
33. Burchmore, R. J. S. & Hart, D. T. (1995). Glucose transport in amastigotes and promastigotes of *Leishmania mexicana mexicana*. *Mol. Biochem. Parasitol.* 74:77-86.
34. Burchmore, R. J. S. & Landfear, S. M. (1998). Differential regulation of multiple glucose transporter genes in the parasitic protozoan *Leishmania mexicana*. *J. Biol. Chem.* 273:29118-29126.
35. Cairns, B. R., Collard, M. W. & Landfear, S. M. (1989). Developmentally regulated gene from *Leishmania* encodes a putative membrane transport protein. *Proc. Natl. Acad. Sci. U.S.A.* 85:2130-2134.
36. Cantor, A. B., Baranski, T. J. & Kornfeld, S. (1992). Lysosomal enzyme phosphorylation: II. Protein recognition determinants in either lobe of procathepsin D are sufficient for phosphorylation of both the amino and carboxyl lobe oligosaccharides. *J. Biol. Chem.* 267:23349-23356.
37. Celenza, J. L., Marshall-Carlson, L. & Carlson, M. (1988). The yeast SNF3 gene encodes a glucose transporter homologous to the mammalian protein. *Proc. Natl. Acad. Sci. U.S.A.* 85:2130-2134.
38. Chakkalath, H. R. & Titus, R. G. (1994). *Leishmania major*-parasitized macrophages augment Th2-type t-cell activation. *J. Immunol.* 153:4378-4387.
39. Chang, K.-P. Cell biology of *Leishmania*. In *Modern Parasite Biology*, (ed. Wyler, D. J.), pp. 79-90. New York: W.H. Freeman and Co.

40. Chou, P. Y. & Fasman, G. D. (1978). Prediction of the secondary structure of proteins from their amino acid sequence. *Adv. Enzymol. Rel. Areas Mol. Biol.* 47:45-148.
41. Chow, M., Newman, J. F., Filman, D., Hogle, J. M. & Rowlands, D. J. (1987). Myristylation of picornavirus capsid protein V4 and its structural significance. *Nature* 327:482-486.
42. Colbert, H. A., Smith, T. L. & Bargmann, C. I. (1997). OSM-9, a novel protein with structural similarity to channels, is required for olfaction, mechanosensation, and olfactory adaptation in *Caenorhabditis elegans*. *J. Neuroscience* 17:8259-8269.
43. Collawn, J. F., Stangel, M., Kuhn, L. A., Esekogwu, V., Jing, S., Trowbridge, I. S. & Tainer, J. A. (1990). Transferrin receptor internalization sequence YXRF implicates a tight turn as the structural recognition motif for endocytosis. *Cell* 63:1061-1072.
44. Cook, G. C. (1996). Twentieth. London, England: W. B. Saunders Company Ltd.
45. Coppens, I., Opperdoes, F. R., Courtoy, P. J. & Baudhuin, P. (1987). Receptor-mediated endocytosis in the bloodstream form of *Trypanosoma brucei*. *J. Protozool.* 34:465-473.
46. Cosson, J. (1996). A moving image of flagella: news and views on the mechanisms involved in axonemal beating. *Cell Biol. Internat.* 20:83-94.

47. Croan, D. G. & Morrison, D. A. (1997). Evolution of the genus *Leishmania* revealed by comparison of DNA and RNA polymerase gene sequences. *Mol. Biochem. Parasit.* 89:149-159.
48. Cruz, A., Coburn, C. M. & Beverley, S. M. (1991). Double targeted gene replacement for creating null mutants. *Proc. Natl. Acad. Sci. U.S.A.* 88:7170-7174.
49. Cuozzo, J. W., Tao, K., Cygler, M., Mort, J. S. & Sahagian, G. G. (1998). Lysine-based structure responsible for selective mannose phosphorylation of cathepsin D and cathepsin L defines a common structural motif for lysosomal enzyme targeting. *J. Biol. Chem.* 33:21067-21076.
50. Dagger, F., Dunia, I., Hernandez, A. G., Pradel, L. A. & Benedetti, E. L. (1989). Plasma membrane and cytoskeletal constituents in *Leishmania mexicana*. *Mol. Biol. Reports* 13:197-206.
51. Dahms, N. M., Lobel, P. & Kornfeld, S. (1989). Mannose-6-phosphate receptors and lysosomal enzyme targeting. *J. Biol. Chem.* 264:12115-12118.
52. Davies, A., Meeran, K., Cairns, M. T. & Baldwin, S. (1987). Peptide-specific antibodies as probes of the orientation of the glucose transporter in the human erythrocyte membrane. *J. Biol. Chem.* 262:9347-9352.
53. de Arruda, M. V. & Matsudaira, P. (1994). Cloning and sequencing of the *Leishmania major* actin-encoding gene. *Gene* 139:123-125.
54. Deflorin, J., Rudolf, M. & Seebeck, T. (1994). The major components of the paraflagellar rod of *Trypanosoma brucei* are two similar, but distinct proteins which are encoded by two different gene loci. *J. Biol. Chem.* 269:28745-28751.

55. Dell'Angelica, E. C., Klumperman, J., Stoorvogel, W. & Bonifacino, J. S. (1998). Association of the AP-3 adaptor complex with clatharin. *Science* 280:431-434.
56. Dierks, T., Volkmer, J., Schlenstedt, G., Jung, C., Sandholzer, U., Zachmann, K., Schlotterhose, P., Neifer, K., Schmidt, B. & Zimmermann, R. (1996). A microsomal ATP-binding protein involved in efficient protein transport into the mammalian endoplasmic reticulum. *EMBO Journal* 15:6931-6942.
57. Ding, Y., Kobayashi, S. & Kopito, R. (1996). Mapping of ankyrin binding determinants on the erythroid anion exchanger, AE1. *J. Biol. Chem.* 271:22494-22498.
58. Drenckhahn, D., Schülter, K., Allen, D. P. & Bennett, V. (1985). Colocalization of band 3 with ankyrin and spectrin at the basal membrane of intercalated cells in the rat kidney. *Science* 230:1287-1289.
59. Drew, M. E., Langford, C. K., Klamo, E. M., Russell, D. G., Kavanaugh, M. P. & Landfear, S. M. (1995). Functional expression of a *myo*-inositol/H⁺ symporter from *Leishmania donovani*. *Mol. Cell. Biol.* 15:5508-5515.
60. Drewes, G., Ebnet, A. & Mandelkow, E.-A. (1998). MAPs, MARKs, and microtubule dynamics. *Trends in Biochem. Sci.* 23:307-311.
61. Duszenko, M. & Seyfang, A. VSG traffic in Trypanosomes. In *Membrane Traffic in Protozoa*, 2B (ed. Plattner, H.), pp. 227-258.
62. Dwyer, D. (1980). Isolation and partial characterization of surface membranes from *Leishmania donovani* promastigotes. *J. Protozool.* 27:176-182.

63. Dwyer, N. D., Troemel, E. R., Sengupta, P. & Bargmann, C. I. (1998). Odorant receptor localization to olfactory cilia is mediated by ODR-4, a novel membrane-associated protein. *Cell* 93:455-466.
64. Engelman, D. M., Steitz, T. A. & Goldman, A. (1986). Identifying nonpolar transbilayer helices in amino acid sequences of membrane proteins. *Ann. Rev. Biophys. Biophysical Chem.* 15:321-353.
65. Engman, D. M., Krause, K.-H., Blumin, J. H., Kim, K. S., Kirchhoff, L. V. & Donelson, J. E. (1989). A novel flagellar Ca⁺²-binding protein in trypanosomes. *J. Biol. Chem.* 264:18627-18631.
66. Erdmann, R., Veenhuis, M. & Kunau, W.-H. (1997). Peroxisomes: organelles at the crossroads. *Trends in Cell Biol.* 7:400-407.
67. Ersfeld, K. & Gull, K. (1997). Partitioning of large and minichromosomes in *Trypanosoma brucei*. *Science* 276:611-614.
68. Eul, J., Graessmann, M. & Graessmann, A. (1995). Experimental evidence for RNA trans-splicing in mammalian cells. *EMBO Journal* 14:3226-3235.
69. Fernandes, A. P., Nelson, K. & Beverley, S. M. (1993). Evolution of nuclear ribosomal RNAs in kinetoplastid protozoa: perspective on the age and origins of parasitism. *Proc. Natl. Acad. of Sci. U.S.A.* 90:11608-11612.
70. Feugas, J.-P., Neel, D., Pavia, A. A., Laham, A., Goussault, Y. & Derappe, C. (1990). Glycosylation of the human erythrocyte glucose transporter is essential for glucose transport activity. *Biochim. Biophys. Acta* 1030:60-64.
71. Fong, D. & Chang, K.-P. (1981). Tubulin biosynthesis in the developmental cycle of a parasitic protozoan, *Leishmania mexicana*: Changes during

- differentiation of motile and nonmotile stages. *Proc. Natl. Acad. Sci. U.S.A.* 78:7624-7628.
72. Friedrichson, T. & Kurzchalia, T. V. (1998). Microdomains of GPI-anchored proteins in living cells by crosslinking. *Nature* 394:802-805.
73. Garippa, R. J., Judge, T. W., James, D. E. & McGraw, T. E. (1994). The amino terminus of GLUT4 functions as an internalization motif but not an intracellular retention signal when substituted for the transferrin receptor cytoplasmic domain. *J. Cell Biol.* 124:707-715.
74. Godsel, L. M. & Engman, D. M. (1999). Flagellar protein localization mediated by a calcium-myristoyl/palmitoyl switch mechanism. *EMBO* in press:
75. Gould, G. & Holman, G. D. (1993). The glucose transporter family: structure, function and tissue-specific expression. *Biochem. J.* 295:329-341.
76. Gould, G. W., Thomas, H. M., Jess, T. J. & Bell, G. I. (1991). Expression of human glucose transporters in *Xenopus* oocytes: Kinetic characterization and substrate specificities of the erythrocyte, liver, and brain isoforms. *Biochem.* 30:5139-5145.
77. Gould, S. J., Keller, G. A. & Subramani, S. (1987). Identification of a peroxisomal targeting signal at the carboxy terminus of firefly luciferase. *J. Cell Biol.* 105:2923-2931.
78. Grab, D. J., Shaw, M. K., Wells, C. W., Verjee, Y., Russo, D. C., Webster, P., Naessens, J. & Fish, W. R. (1993). The transferrin receptor in African trypanosomes: identification, partial characterization and subcellular localization. *Eur. J. Cell Biol.* 62:114-126.

79. Green, S. J., Meltzer, M. S., Hibbs, J. B. J. & Nacy, C. A. (1990). Activated macrophages destroy intracellular *Leishmania major* amastigotes by an L-arginine-dependent killing mechanism. *J. Immunol.* 144:278-283.
80. Grevelink, S. A. & Lerner, E. A. (1996). Leishmaniasis. *J. Amer. Acad. Dermatol.* 34:257-272.
81. Guan, C., Li, P., Riggs, D. & Inouye, H. (1987). Vectors that facilitate the expression and purification of foreign peptides in *Escheria coli* by fusion to maltose binding protein. *Gene* 67:21-30.
82. Haft, C. R., De La Luz Sierra, M., Hamer, I., Carpentier, J. L. & Taylor, S. I. (1998). Analysis of the juxtamembrane dileucine motif in the insulin receptor. *Endocrinol.* 139:1618-1629.
83. Hart, D. T., Vickerman, K. & Coombs, G. H. (1981). Transformation *in vitro* of *Leishmania mexicana* amastigotes to promastigotes: nutritional requirements and the effects of drugs. *Parasitol.* 83:529-541.
84. Hartmann, E., Rapoport, T. A. & Lodish, H. F. (1989). Predicting the orientation of eukaryotic membrane-spanning proteins. *Proc. Natl. Acad. Sci. U.S.A.* 86:5786-5790.
85. Häusler, T., Stierhof, Y.-D., Blattner, J. & Clayton, C. (1997). Conservation of mitochondrial targeting sequence function in mitochondrial and hydrogenosomal proteins from the early-branching eukaryotes *Crithidia*, *Trypanosoma* and *Trichomonas*. *Eur. J. Cell Biol.* 73:240-251.

86. Hediger, M. A., Coady, M. J., Ikeda, T. S. & Wright, E. M. (1987). Expression cloning and cDNA sequencing of the Na⁺/glucose co-transporter. *Nature* 330:379-381.
87. Hemphill, A., Affolter, M. & Seebeck, T. (1992). A novel microtubule-binding motif identified in a high molecular weight microtubule-associated protein from *Trypanosoma brucei*. *J. Cell Biol.* 117:95-103.
88. High, S. & Laird, V. (1997). Membrane protein biosynthesis- all sewn up? *Trends Cell Biol.* 7:206-210.
89. Hille-Rehfeld, A. (1995). Mannose 6-phosphate receptors in sorting and transport of lysosomal enzymes. *Biochim. Biophys. Acta* 1241:177-194.
90. Honing, S., Sandoval, I. V. & von Figura, K. (1998). A di-leucine-based motif in the cytoplasmic tail of LIMP II and tyrosinase mediates selective binding of AP-3. *EMBO* 17:1304-1314.
91. Hresko, R. C., Kruse, M., Strube, M. & Mueckler, M. (1994). Topology of the GLUT1 glucose transporter deduced from glycosylation scanning mutagenesis. *J. Biol. Chem.* 269:20482-20488.
92. Hunnicutt, G. R., Kosfischer, M. G. & Snell, W. J. (1990). Cell body and flagellar agglutinins in *Chlamydomonas reinhardtii*: the cell body plasma membrane is a reservoir for agglutinins whose migration to the flagella is regulated by a functional barrier. *J. Cell Biol.* 111:1605-1616.
93. Iovannisci, D. M. & Ullman, B. (1983). High efficiency plating method for *Leishmania* promastigotes in semidefined or completely defined medium. *J. Parasitol.* 69:633-636.

94. Iraqui, I., Vissers, S., Bernard, F., De Craene, J.-O., Boles, E., Urrestrazu, A. & Andre', B. (1999). Amino acid signaling in *Saccharomyces cerevisiae*: a permease-like sensor of external amino acids and F-box protein Grr1p are required for transcriptional induction of the *AGPI* gene, which encodes a broad-specificity amino acid permease. *Mol. Cell. Biol.* 19:989-1001.
95. James, D. E. & Piper, R. C. (1993). Targeting of mammalian glucose transporters. *J. Cell Sci.* 104:607-612.
96. James, D. E., Strube, J. & Mueckler, M. (1989). Molecular cloning and characterization of an insulin-regulatable glucose transporter. *Nature* 338:83-87.
97. Jing, S., Spencer, T., Miller, K., Hopkins, C. & Trowbridge, I. S. (1990). Role of the human transferrin receptor cytoplasmic domain in endocytosis: Localization of a specific signal sequence for internalization. *J. Cell Biol.* 110:283-294.
98. Jing, S. Q. & Trowbridge, I. S. (1987). Identification of the intermolecular disulfide bonds of the human transferrin receptor and its lipid-attachment site. *EMBO Journal* 6:327-331.
99. Johnston, M. (1999). Feasting, fasting, and fermenting: glucose sensing in yeast and other cells. *Trends in Genet.* 15:29-33.
100. Jordan, C., Püschel, Koob, R. & Drenckhahn, D. (1995). Identification of a binding motif for ankyrin on the α -subunit of Na^+, K^+ -ATPase. *J. Biol. Chem.* 270:29971-29975.

101. Kable, M. L., Seiwert, S. D., Heidmann, S. & Stuart, K. (1996). RNA editing: a mechanism for gRNA-specified uridylyate insertion into precursor mRNA. *Science* 273:1189-1195.
102. Kaneshiro, E. S. Lipids of ciliary and flagellar membranes. In *Ciliary and Flagellar Membranes*, (ed. Bloodgood, R. A.), pp. 241-265. New York: Plenum Press.
103. Kapler, G. M., Coburn, C. M. & Beverley, S. M. (1990). Stable transfection of the human parasite *Leishmania major* delineates a 30-kilobase region sufficient for extrachromosomal replication and expression. *Mol. Cell. Biol.* 10:1084-1094.
104. Keller, G.-A., Krisans, S., Gould, S. J., Sommer, J. M., Wang, C. C., Schliebs, W., Kunau, W., Brody, S. & Subramani, S. (1991). Evolutionary conservation of a microbody targeting signal that targets proteins to peroxisomes, glyoxysomes, and glycosomes. *J. Cell Biol.* 114:893-904.
105. Kendall, G., Wilderspin, A. F., Ashall, F., Miles, M. A. & Kelly, J. M. (1990). *Trypanosoma cruzi* glycosomal glyceraldehyde-3-phosphate dehydrogenase does not conform to the "hotspot" topogenic signal model. *EMBO Journal* 9:2751-2758.
106. Kirsch, J. & Betz, H. (1995). The postsynaptic localization of the glycine receptor-associated protein gephyrin is regulated by the cytoskeleton. *J. Neurosci.* 15:4148-4156.

107. Kirsch, J., Langosch, D., Prior, P., Littauer, U. Z., Schmitt, B. & Betz, H. (1991). The 93-kDa glycine receptor-associated protein binds to tubulin. *J. Biol. Chem.* 266:22242-22245.
108. Kirsch, J., Wolters, I., Triller, A. & Betz, H. (1993). Gephyrin antisense oligonucleotides prevent glycine receptor clustering in spinal neurons. *Nature* 366:745-748.
109. Kohl, L. & Gull, K. (1998). Molecular architecture of the trypanosome cytoskeleton. *Mol. Biochem. Parasitol.* 93:1-9.
110. Koob, R. M., Zimmerman, M. & Schonert, W. (1988). Colocalization and coprecipitation of ankyrin and Na⁺, K⁺-ATPase in kidney epithelial cells. *Eur. J. Cell Biol.* 45:230-237.
111. Kozminski, K. G., Beech, P. L. & Rosenbaum, J. L. (1995). The Chlamydomonas Kinesin-like Protein FLA10 is involved in motility associated with the flagellar membrane. *J. Cell Biol.* 131:1517-1527.
112. Kozminski, K. G., Johnson, K. A., Forscher, P. & Rosenbaum, J. L. (1993). A motility in the eukaryotic flagellum unrelated to flagellar beating. *Proc. Natl. Acad. Sci. U.S.A.* 90:5519-5523.
113. Krause, M. & Hirsh, D. (1987). A trans-spliced leader sequence on actin mRNA in *C. elegans*. *Cell* 49:753-761.
114. Kyte, J. & Doolittle, R. F. (1982). A simple method for displaying the hydropathy of a protein. *J. Mol. Biol.* 157:105-132.

115. Laban, A., Tobin, J. F., de Lafaille, M. A. C. & Wirth, D. F. (1990). Stable expression of the bacterial neo^r gene in *Leishmania enriettii*. *Nature* 343:572-574.
116. Lainson, R. (1997). On *Leishmania enriettii* and other enigmatic *Leishmania* species of the neotropics. *Memorias do Instituto Oswaldo Cruz* 92:377-387.
117. Landfear, S. M., McMahon-Pratt, D. & Wirth, D. F. (1983). Tandem arrangement of tubulin genes in the protozoan parasite *Leishmania enriettii*. *Mol. Cell. Biol.* 3:1070-1076.
118. Landfear, S. M. & Wirth, D. F. (1984). Control of tubulin gene expression in the parasitic protozoan *Leishmania enriettii*. *Nature* 309:716-717.
119. Langford, C. K., Burchmore, R. J. S., Hart, D. T., Wagner, W. & Landfear, S. M. (1994). Biochemistry and molecular genetics of *Leishmania* glucose transporters. *Parasitol.* 108:S73-S83.
120. Langford, C. K., Ewbank, S. A., Hanson, S. A., Ullman, B. & Landfear, S. M. (1992). Molecular characterization of two genes encoding members of the glucose transporter superfamily in the parasitic protozoan *Leishmania donovani*. *Mol. Biochem. Parasitol.* 55:51-64.
121. Langford, C. K., Kavanaugh, M. P., Stenberg, P. E., Zhang, W. & Landfear, S. M. (1995). Functional expression and subcellular localization of a high K_m hexose transporter from *Leishmania donovani*. *Biochem.* 34:11814-11821.

122. Langford, C. K., Little, B. M., Kavanaugh, M. P. & Landfear, S. M. (1994). Functional expression of two glucose transporter isoforms from the parasitic protozoan *Leishmania enriettii*. *J. Biol. Chem.* 269:17939-17943.
123. Lawyer, P. G., Young, D. G., Butler, J. F. & Akin, D. E. (1987). Development of *Leishmania mexicana* in *Lutzomyia diabolica* and *Lutzomyia shannoni* (Diptera: Psychodidae). *J. Med. Entom.* 24:347-355.
124. Lebowitz, J. H., Smith, H. Q., Rusche, L. & Beverley, S. M. (1993). Coupling of poly(A) site selection and *trans*-splicing in *Leishmania*. *Genes Dev.* 7:996-1007.
125. Letourner, F. & Klausner, R. D. (1992). A novel di-leucine motif and a tyrosine-based motif independently mediate lysosomal targeting and endocytosis of CD3 chains. *Cell* 69:1143-1157.
126. Levy, D. (1996). Membrane proteins which exhibit multiple topological orientations. *Essays in Biochem.* 31:49-60.
127. Lindemann, C. B. & Kanous, K. S. (1997). A model for flagellar motility. *Int. Rev. Cytol.* 173:1-72.
128. Lippincott-Schwartz, J. (1998). Cytoskeletal proteins and Golgi dynamics. *Curr. Opin. Cell Biol.* 10:52-59.
129. Lisanti, M. P. & Rodriguez-Boulan, E. (1990). Glycophospholipid membrane anchoring provides clues to the mechanism of protein sorting in polarized epithelial cells. *Trends in Biochem. Sci.* 15:113-118.

130. Lithgow, T. & Schatz, G. Targeting precursor proteins to mitochondria. In *Protein Targeting*, 16 (ed. Hurtley, S.), pp. 1-24. New York: Oxford University Press.
131. Machamer, C. E. ER-Golgi membrane traffic and protein targeting. In *Protein Targeting*, 16 (ed. Hurtley, S.), pp. 123-151. New York: Oxford University Press.
132. MacRae, T. H. & Gull, K. (1990). Purification and assembly *in vitro* of tubulin from *Trypanosoma brucei brucei*. *Biochem.* 265:87-93.
133. Madi, L., McBride, S. A., Bailey, L. A. & Ebbole, D. J. (1997). *rco-3*, a gene involved in glucose transport and conidiation in *Neurospora crassa*. *Genetics* 146:499-508.
134. Maina, C. V., Riggs, P. D., Grandea, A. G., Slatko, B. E., Moran, L. S., Tagliamonte, J. A., McReynolds, L. A. & Guan, C. (1988). A vector to express and purify foreign proteins in *Escherichia coli* by fusion to and separation from maltose binding protein. *Gene* 74:365-373.
135. Marks, M. S., Woodruff, L., Ohno, H. & Bonifacino, J. S. (1996). Protein targeting by tyrosine- and di-leucine-based signals: evidence for distinct saturable components. *J. Cell Biol.* 135:341-354.
136. Marsden, P. D. & Jones, T. C. Clinical manifestations, diagnosis and treatment of leishmaniasis. In *Leishmaniasis*, 1 (ed. Chang, K. P. & Bray, R. S.), pp. Elsevier Science Publishers B. V.
137. Maslov, D. A., Lukes, J., Jirku, M. & Simpson, L. (1996). Phylogeny of trypanosomes as inferred from the small and large subunits rRNAs: implications

- for the evolution of parasitism in the trypanosomatid protozoa. *Mol. Biochem. Parasit.* 75:197-205.
138. Matlack, K. E. S., Mothes, W. & Rapoport, T. A. (1998). Protein translocation: tunnel vision. *Cell* 92:381-390.
139. Matter, K. & Mellman, I. (1994). Mechanisms of cell polarity: sorting and transport in epithelial cells. *Curr. Opin. Cell Biol.* 6:545-554.
140. Mauel, J. (1990). Macrophage-parasite interactions in *Leishmania* infections. *J. Leuk. Biol.* 47:187-193.
141. McDowell, M. A., Ransom, D. M. & Bangs, J. D. (1998). Glycophosphatidylinositol secretory transport in *Trypanosoma brucei*. *Biochem.* 335:681-689.
142. McHugh, C. P., Melby, P. C. & LaFon, S. G. (1996). Leishmaniasis in Texas: Epidemiology and clinical aspects of human cases. *Am. J. Trop. Med. Hyg.* 55:547-555.
143. McIlhinney, R. A. (1990). The fats of life: the importance and function of protein acylation. *TIBS* 15:387-391.
144. Meyer, G., Kirsch, J., Betz, H. & Langosch, D. (1995). Identification of a gephyrin binding motif on the glycine receptor β -subunit. *Neuron* 15:563-572.
145. Michels, P. A. M., Poliszczak, A., Osinga, K. A., Misset, O., Van Beeumen, J., Wierenga, R. K., Borst, P. & Opperdoes, F. R. (1986). Two tandemly linked identical genes code for the glycosomal glyceraldehyde-phosphate dehydrogenase in *Trypanosoma brucei*. *EMBO Journal* 5:1049-1056.

146. Miller, S. I., Landfear, S. M. & Wirth, D. F. (1986). Cloning and characterization of a *Leishmania* gene encoding a RNA spliced leader sequence. *Nucleic Acids Res.* 14:7341-7360.
147. Miller, S. I. & Wirth, D. F. (1988). *trans* Splicing in *Leishmania enriettii* and identification of ribonucleoprotein complexes containing the spliced leader and U2 equivalent RNAs. *Mol. Cell. Biol.* 8:2597-2603.
148. Mills, J. W. & Mandel, L. J. (1994). Cytoskeletal regulation of membrane transport events. *FASEB J.* 8:1161-1165.
149. Moore, L. M., Santrich, C. & LeBowitz, J. H. (1996). Stage-specific expression of the *Leishmania mexicana* paraflagellar rod protein PFR-2. *Mol. Biochem. Parasitol.* 80:125-135.
150. Moreira, M. E., Del Portillo, H. A., Milder, R. V., Balanco, J. M. & Barcinski, M. A. (1996). Heat shock induction of apoptosis in promastigotes of the unicellular organism *Leishmania (Leishmania) amazonensis*. *J. Cell. Physiology* 167:305-313.
151. Morrow, J. S., Cianci, C. D., Ardito, T., Mann, A. S. & Cashgarian, M. (1989). Ankyrin links fodrin to the alpha subunit of Na,K-ATPase in Madin-Darby canine kidney cells and in intact renal tubule cells. *J. Cell Biol.* 108:455-465.
152. Mortara, R. A. (1989). Studies of trypanosomatid actin
I. Immunochemical and biochemical identification. *J. Protozool.* 36:8-13.

153. Mostov, K. E. & Cardone, M. H. (1995). Regulation of protein traffic in polarized epithelial cells. *Bioessays* 17:129-138.
154. Mueckler, M. (1994). Facilitative glucose transporters. *Eur. J. Biochem.* 219:713-725.
155. Mueckler, M., Caruso, C., Baldwin, S. A., Panico, M., Blench, I., Morris, H. R., Allard, W. J., Lienhard, G. E. & Lodish, H. F. (1985). Sequence and structure of a human glucose transporter. *Science* 229:941-945.
156. Munro, S. (1991). Sequences within and adjacent to the transmembrane segment of alpha-2,6-sialyltransferase specify Golgi retention. *EMBO Journal* 10:3577-3588.
157. Nelson, W. J. & Hammerton, R. W. (1989). A membrane-cytoskeletal complex containing Na⁺, K⁺-ATPase, ankyrin, and fodrin in Madin-Darby canine kidney (MDCK) cells; implications for the biogenesis of epithelial cell polarity. *J. Cell Biol.* 108:893-902.
158. Odorizzi, G., Cowles, C. R. & Emr, S. D. (1998). The AP-3 complex: a coat of many colours. *Trends in Cell Biol.* 8:282-288.
159. Ohno, H., Stewart, J., Fournier, M.-C., Bosshart, H., Rhee, I., Miyatake, S., Saito, T., Gallusser, A., Kirchhausen, T. & Bonifacino, J. S. (1995). Interaction of tyrosine-based signals with clathrin-associated proteins. *Science* 269:1872-1875.
160. Olivares, L., Aragon, C., Gimenez, C. & Zafra, F. (1995). The role of N-glycosylation in the targeting and activity of the GLT1 glycine transporter. *J. Biol. Chem.* 270:9437-9442.

161. Opperdoes, F. R. Glycosomes. In *Biochemical Protozoology*, (ed. Coombs, G. & North, M.), pp. 134-144. London and Washington: Taylor and Francis.
162. Opperdoes, F. R. & Michels, P. A. M. (1993). The glycosomes of the Kinetoplastida. *Biochimie* 75:231-234.
163. Overath, P., Stierhof, Y.-D. & Wiese, M. (1997). Endocytosis and secretion in trypanosomatid parasites - tumultuous traffic in a pocket. *Trends in Cell Biol.* 7:27-33.
164. Owen, D. J. & Evans, P. R. (1998). A structural explanation for the recognition of tyrosine-based endocytic signals. *Science* 282:1327-1332.
165. Özcan, S., Dover, J. & Johnston, M. (1998). Glucose sensing and signaling by two glucose receptors in the yeast *Saccharomyces cerevisiae*. *EMBO* 17:2566-2573.
166. Paindavoine, P., Rolin, S., Van Assel, S., Geuskens, M., Jauniaux, J., Dinsart, C., Huet, G. & Pays, E. (1992). A gene from the variant surface glycoprotein expression site encodes one of several transmembrane adenylate cyclases located on the flagellum of *Trypanosoma brucei*. *Mol. Cell. Biol.* 12:1218-1225.
167. Pao, S. S., Paulsen, I. T. & Saier, M. H. J. (1998). Major facilitator superfamily. *Microbio. Mol. Biol. Rev.* 62:1-34.
168. Parson, R. D., Manian, A. A., Marcus, J. L., Hall, D. & Hewlett, E. L. (1982). Lethal effect of phenothiazine neuroleptics on the pathogenic protozoan *Leishmania donovani*. *Science* 217:369-371.

153. Mostov, K. E. & Cardone, M. H. (1995). Regulation of protein traffic in polarized epithelial cells. *Bioessays* 17:129-138.
154. Mueckler, M. (1994). Facilitative glucose transporters. *Eur. J. Biochem.* 219:713-725.
155. Mueckler, M., Caruso, C., Baldwin, S. A., Panico, M., Blench, I., Morris, H. R., Allard, W. J., Lienhard, G. E. & Lodish, H. F. (1985). Sequence and structure of a human glucose transporter. *Science* 229:941-945.
156. Munro, S. (1991). Sequences within and adjacent to the transmembrane segment of alpha-2,6-sialyltransferase specify Golgi retention. *EMBO Journal* 10:3577-3588.
157. Nelson, W. J. & Hammerton, R. W. (1989). A membrane-cytoskeletal complex containing Na⁺, K⁺-ATPase, ankyrin, and fodrin in Madin-Darby canine kidney (MDCK) cells; implications for the biogenesis of epithelial cell polarity. *J. Cell Biol.* 108:893-902.
158. Odorizzi, G., Cowles, C. R. & Emr, S. D. (1998). The AP-3 complex: a coat of many colours. *Trends in Cell Biol.* 8:282-288.
159. Ohno, H., Stewart, J., Fournier, M.-C., Bosshart, H., Rhee, I., Miyatake, S., Saito, T., Gallussner, A., Kirchhausen, T. & Bonifacino, J. S. (1995). Interaction of tyrosine-based signals with clathrin-associated proteins. *Science* 269:1872-1875.
160. Olivares, L., Aragon, C., Gimenez, C. & Zafra, F. (1995). The role of N-glycosylation in the targeting and activity of the GLT1 glycine transporter. *J. Biol. Chem.* 270:9437-9442.

161. Opperdoes, F. R. Glycosomes. In *Biochemical Protozoology*, (ed. Coombs, G. & North, M.), pp. 134-144. London and Washington: Taylor and Francis.
162. Opperdoes, F. R. & Michels, P. A. M. (1993). The glycosomes of the Kinetoplastida. *Biochimie* 75:231-234.
163. Overath, P., Stierhof, Y.-D. & Wiese, M. (1997). Endocytosis and secretion in trypanosomatid parasites - tumultuous traffic in a pocket. *Trends in Cell Biol.* 7:27-33.
164. Owen, D. J. & Evans, P. R. (1998). A structural explanation for the recognition of tyrosine-based endocytic signals. *Science* 282:1327-1332.
165. Özcan, S., Dover, J. & Johnston, M. (1998). Glucose sensing and signaling by two glucose receptors in the yeast *Saccharomyces cerevisiae*. *EMBO* 17:2566-2573.
166. Paindavoine, P., Rolin, S., Van Assel, S., Geuskens, M., Jauniaux, J., Dinsart, C., Huet, G. & Pays, E. (1992). A gene from the variant surface glycoprotein expression site encodes one of several transmembrane adenylate cyclases located on the flagellum of *Trypanosoma brucei*. *Mol. Cell. Biol.* 12:1218-1225.
167. Pao, S. S., Paulsen, I. T. & Saier, M. H. J. (1998). Major facilitator superfamily. *Microbio. Mol. Biol. Rev.* 62:1-34.
168. Parson, R. D., Manian, A. A., Marcus, J. L., Hall, D. & Hewlett, E. L. (1982). Lethal effect of phenothiazine neuroleptics on the pathogenic protozoan *Leishmania donovani*. *Science* 217:369-371.

169. Parsons, M., Nelson, R. G., Watkins, K. P. & Agabian, N. (1984). Trypanosome mRNAs share a common 5' spliced leader sequence. *Cell* 38:309-316.
170. Parsons, M. & Smith, J. M. (1989). Trypanosome glycosomal protein P60 is homologous to phosphoenolpyruvate carboxykinase (ATP). *Nucleic Acids Res.* 17:6411.
171. Pearson, R. B. & Kemp, B. E. (1991). Protein Kinase Phosphorylation Site Sequences and Consensus Specificity Motifs: Tabulations. *Methods Enzymol.* 200:62-81.
172. Pessin, J. E. & Bell, G. I. (1992). Mammalian facilitative glucose transporter family: structure and molecular regulation. *Ann. Rev. Physiol.* 54:911-930.
173. Peters, L. L., Shivdasani, R. A., Liu, S.-C., Hanspal, M., John, K. M., Gonzalez, J. M., Bruggera, C., Gwynn, B., Mohandas, N., Alper, S. L., Orkin, S. H. & Lux, S. E. (1996). Anion exchanger 1 (Band 3) is required to prevent erythrocyte membrane surface loss but not to form the membrane skeleton. *Cell* 86:917-927.
174. Phizicky, E. M. & Fields, S. (1995). Protein-protein interactions: methods for detection and analysis. *Microbiol. Rev.* 59:94-123.
175. Pimenta, P. F. P., Saraiva, E. M. B., Rowton, E., Modi, G. B., Garraway, L. A., Beverley, S. M., Turco, S. J. & Sacks, D. L. (1994). Evidence that the vectorial competence of phlebotomine sand flies for different species of

Leishmania is controlled by structural polymorphisms in the surface lipophosphoglycan. *Proc. Natl. Acad. Sci. U.S.A.* 91:9155-9159.

176. Piper, R. C., Tai, C., Slot, J. W., Hahn, C. S., Rice, D., Huang, H. & James, D. E. (1992). The efficient intracellular sequestration of the insulin-regulatable glucose transporter (GLUT4) is conferred by the N terminus. *J. Cell Biol.* 117:729-743.

177. Piper, R. C., Xu, X., Russell, D. G., Little, B. M. & Landfear, S. M. (1995). Differential targeting of two glucose transporters from *Leishmania enriettii* is mediated by an NH₂-terminal domain. *J. Cell Biol.* 128:499-508.

178. Prior, C., Fukuhara, H., Blaisonneau, J. & Wesolowski-Louvel, M. (1993). Low-affinity glucose carrier gene LGT1 of *Saccharomyces cerevisiae*, a homologue of the *Kluyveromyces lactis* RAG1 gene. *Yeast* 9:1373-1377.

179. Quest, A. F., Harvey, D. J. & McIlhinney, R. A. (1997). Myristoylated and nonmyristoylated pools of sea urchin sperm flagellar creatine kinase exist side-by-side: myristoylation is necessary for efficient lipid association. *Biochem.* 36:6993-7002.

180. Rajkovic, A., Davis, R. E., Simonsen, J. N. & Rottmann, F. M. (1990). A spliced leader is present on a subset of mRNA's from the human parasite *Schistosoma mansoni*. *Proc. Natl. Acad. of Sci. U.S.A.* 87:8879-8883.

181. Roayaie, K., Crump, J. G., Sagasti, A. & Bargmann, C. I. (1998). The G α protein ODR-3 mediates olfactory and nociceptive function and controls cilium morphogenesis in *C. elegans* olfactory neurons. *Neuron* 20:55-67.

182. Roberts, L. S. & Janovy, J. J. (1996). *Foundations of Parasitology*. Fifth Edition. Wm. C. Brown Publishers.
183. Robinson, D., Beattie, P., Sherwin, T. & Gull, K. (1991). Microtubules, tubulin, and microtubule-associated proteins of trypanosomes. *Methods Enzymol.* 196:285-299.
184. Robinson, D. R., Sherwin, T., Ploubidou, A., Byard, E. H. & Gull, K. (1995). Microtubule polarity and dynamics in the control of organelle positioning, segregation, and cytokinesis in the trypanosome life cycle. *J. Cell Biol.* 128:1163-1172.
185. Romisch, K. & Corsi, A. Protein translocation into the endoplasmic reticulum. In *Protein Targeting*, 16 (ed. Hurlley, S.), pp. 101-122. New York: Oxford University Press.
186. Rosenbaum, J. L., Cole, D. G. & Diener, D. R. (1999). Intraflagellar transport: the eyes have it. *J. Cell Biol.* 144:385-388.
187. Russell, D. G. (1995). *Mycobacterium* and *Leishmania*: stowaways in the endosomal network. *Trends in Cell Biol.* 5:125-128.
188. Russell, D. G. & Dubremetz, J.-F. (1986). Microtubular cytoskeletons of parasitic protozoa. *Parasitol. Today* 2:177-179.
189. Russell, D. G. & Wilhelm, H. (1986). The involvement of the major surface glycoprotein (gp63) of *Leishmania* promastigotes in attachment to macrophages. *J. Immunol.* 136:2613-2620.
190. Sambrook, J., Fritsch, E. F. & Maniatis, T. (1989). 2nd. Cold Spring Harbor, N.Y.: Cold Spring Harbor Laboratory.

191. Santrich, C., Moore, L., Sherwin, T., Bastin, P., Brokaw, C., Gull, K. & LeBowitz, J. H. (1997). A motility function for the paraflagellar rod of *Leishmania* parasites revealed by PFR-2 gene knockouts. *Mol. Biochem. Parasitol.* 90:95-109.
192. Sasse, R. & Gull, K. (1988). Tubulin post-translational modifications and the construction of microtubular organelles in *Trypanosoma brucei*. *J. Cell Sci.* 90:577-589.
193. Sato, M., Hresko, R. & Mueckler, M. (1998). Testing the charge difference hypothesis for the assembly of a eucaryotic multispinning membrane protein. *J. Biol. Chem.* 273:25203-25208.
194. Schaffhausen, B. (1995). SH2 domain structure and function. *Biochim. Biophys. Acta* 1242:61-75.
195. Schlein, Y. (1986). Sandfly diet and *Leishmania*. *Parasitol. Today* 2:175-177.
196. Schlein, Y., S., B. & Greenblatt, C. L. (1987). Development of sandfly forms of *Leishmania major* in sucrose solutions. *J. Parasitol.* 73:797-805.
197. Schneider, A., Plessmann, U. & Weber, K. (1997). Subpellicular and flagellar microtubules of *Trypanosoma brucei* are extensively glutamylated. *J. Cell Sci.* 110:431-437.
198. Schneider, A., Sherwin, T., R., S., Russell, D. G., Gull, K. & Seebeck, T. (1987). Subpellicular and flagellar microtubules of *Trypanosoma brucei brucei* contain the same alpha tubulin isoforms. *J. Cell Biol.* 104:431-438.

199. Scott, V., Sherwin, T. & Gull, K. (1997). γ -Tubulin in trypanosomes: molecular characterisation and localisation to multiple and diverse microtubule organising centres. *J. Cell Sci.* 110:157-168.
200. Seebeck, T. & Gehr, P. (1983). Trypanocidal action of neuroleptic phenothiazines in *Trypanosoma brucei*. *Mol. Biochem. Parasitol.* 9:197-208.
201. Seebeck, T., Hemphill, A. & Lawson, D. (1990). The cytoskeleton of trypanosomes. *Parasitol. Today* 9:201-206.
202. Sengupta, P., Chou, J. H. & Bargmann, C. I. (1996). *odr-10* encodes a seven transmembrane domain olfactory receptor required for responses to the odorant diacetyl. *Cell* 84:899-909.
203. Seyfang, A., Kavanaugh, M. P. & Landfear, S. M. (1997). Aspartate 19 and glutamate 121 are critical for transport function of the *myo*-inositol/H⁺ symporter from *Leishmania donovani*. *J. Biol. Chem.* 272:24210-24215.
204. Shapiro, S. Z. & Webster, P. (1989). Coated vesicles from the protozoan parasite *Trypanosoma brucei*: purification and characterization. *J. Protozool.* 36:344-349.
205. Sherwin, T. & Gull, K. (1989). The cell division cycle of *Trypanosoma brucei brucei*: timing of event markers and cytoskeletal modulations. *Phil. Trans. Soc. Lond.* 323:573-588.
206. Sherwin, T. & Gull, K. (1989). Visualization of detyrosination along single microtubules reveals novel mechanisms of assembly during cytoskeletal duplication in trypanosomes. *Cell* 57:211-221.

207. Shinohara, H., Asano, T., Kato, K., Kameshima, T. & Semba, R. (1998). Localization of a G protein Gi2 in the cilia of rat ependyma, oviduct and trachea. *Eur. J. Neurosci.* 10:699-707.
208. Simons, K. & Ikonen, E. (1997). Functional rafts in cell membranes. *Nature* 387:569-572.
209. Simpson, L. & Maslov, D. A. (1994). RNA editing and the evolution of parasites. *Science* 264:1870-1871.
210. Simpson, L. & Thiemann, O. H. (1995). Sense from nonsense: RNA editing in mitochondria of kinetoplastid protozoa and slime molds. *Cell* 81:837-840.
211. Snapp, E. L. & Landfear, S. M. (1997). Cytoskeletal association is important for differential targeting of glucose transporter isoforms in *Leishmania*. *J. Cell. Biol.* 139:1775-1783.
212. Sommer, B., Kohler, M., Sprengel, R. & Seeburg, P. H. (1991). RNA editing in brain controls a determinant of ion flow in glutamate-gated channels. *Cell* 67:11-19.
213. Sommer, J. M., Cheng, Q.-L., Keller, G.-A. & Wang, C. C. (1992). In vivo import of firefly luciferase into the glycosomes of *Trypanosoma brucei* and mutational analysis of the C-terminal targeting signal. *Mol. Biol. Cell* 3:749-759.
214. Sommer, J. M., Peterson, G., Keller, G.-A., Parsons, M. & Wang, C. C. (1993). The C-terminal tripeptide of glycosomal phosphoglycerate kinase is both necessary and sufficient for import into the glycosomes of *Trypanosoma brucei*. *FEBS Letts.* 316:53-58.

215. Stack, S. P., Stein, D. R. & Landfear, S. M. (1990). Structural isoforms of a membrane transport protein from *Leishmania*. *Mol. Cell. Biol.* 10:6785-6790.
216. Stein, D. R., Cairns, B. R. & Landfear, S. M. (1990). Developmentally regulated transporter in *Leishmania* is encoded by a family of clustered genes. *Nucleic Acids Res.* 18:1549-1547.
217. Steverding, D., Stierhof, Y.-D., Fuchs, H., Tauber, R. & Overath, P. (1995). Transferrin-binding protein complex is the receptor for transferrin uptake in *Trypanosoma brucei*. *J. Cell Biol.* 131:1173-1182.
218. Sugrue, P., Hirons, M. R., Adam, J. U. & Holwill, M. E. J. (1988). Flagellar wave reversal in the kinetoplastid flagellate *Crithidia oncopelti*. *Biology of the Cell* 63:127-131.
219. ter Kuile, B. H. (1993). Glucose and proline transport in kinetoplastids. *Parasitol. Today* 9:206-210.
220. ter Kuile, B. H. & Cook, M. (1994). The kinetics of facilitated diffusion followed by enzymatic conversion of the substrate. *Biochim. Biophys. Acta* 1193:235-239.
221. ter Kuile, B. H. & Opperdoes, F. R. (1993). Uptake and turnover of glucose in *Leishmania donovani*. *Mol. Biochem. Parasitol.* 60:313-322.
222. Terzic, A. & Kurachi, Y. (1996). Actin microfilament disrupters enhance K(ATP) channel opening in patches from guinea-pig cardiomyocytes. *J. Physiol.* 492:395-404.

223. Tessier, L. H., Keller, M., Chan, R. L., Fournier, R., Weil, J. H. & Imbault, P. (1991). Short leader sequences may be transferred from small RNAs to premature mRNAs by trans-splicing in *Euglena*. *EMBO Journal* 10:2621-2625.
224. Tetaud, E., Barrett, M. P., Bringaud, F. & Baltz, T. (1997). Kinetoplastid glucose transporters. *Biochem. J.* 325:569-580.
225. Thorens, B., Charron, M. J. & Lodish, H. F. (1990). Molecular physiology of glucose transporters. *Diabetes Care* 13:209-218.
226. Todd, A. J., Watt, C., Spike, R. C. & Sieghart, W. (1996). Colocalization of GABA, glycine, and their receptors at synapses in the rat spinal cord. *J. Neurosci.* 16:974-982.
227. Turner, A. (1994). PIG-tailed membrane proteins. *Essays Biochem.* 28:113-127.
228. van't Hof, W., Malik, A., Vijayakumar, S., Qiao, J., van Adelsberg, J. & Al-Awqati, Q. (1997). The effect of apical and basolateral lipids on the function of the band 3 anion exchange protein. *J. Cell Biol.* 139:941-949.
229. Varma, R. & Mayor, S. (1998). GPI-anchored proteins are organized in submicron domains at the cell surface. *Nature* 394:798-801.
230. Verhey, K. J. & Birnbaum, M. J. (1994). A Leu-Leu sequence is essential for COOH-terminal targeting signal of GLUT4 glucose transporter in fibroblasts. *J. Biol. Chem.* 269:2353-2356.
231. Verhey, K. J., Hausdorff, S. F. & Birnbaum, M. J. (1993). Identification of the carboxy terminus as important for the isoform-specific subcellular targeting of glucose transporter proteins. *J. Cell. Biol.* 123:137-147.

232. Verhey, K. J., Yeh, J.-I. & Birnbaum, M. J. (1995). Distinct signals in the GLUT4 glucose transporter for internalization and for targeting to an insulin-responsive compartment. *J. Cell Biol.* 130:1071-1079.
233. Vickerman, K. (1974). The ultrastructure of pathogenic flagellates. *Ciba Found. Symp.* 20:171-190.
234. Vickerman, K. (1994). The evolutionary expansion of the trypanosomatid flagellates. *Internat. J. Parasitol.* 24:1317-1331.
235. Wade, R. H. & Hyman, A. A. (1997). Microtubule structure dynamics. *Curr. Opin. Cell Biol.* 9:12-17.
236. Waitumbi, J. N., Tetaud, E. & Baltz, T. (1996). Glucose uptake in *Trypanosoma vivax* and molecular characterization of its transporter gene. *Eur. J. Biochem.* 237:234-239.
237. Walton, P. A., Wendland, M., Subramani, S., Rachubinski, R. A. & Welch, W. J. (1994). Involvement of 70-kD heat shock proteins in peroxisomal import. *J. Cell Biol.* 125:1037-1046.
238. Wang, W., Hansen, P. A., Marshall, B. A., Holloszy, J. O. & Mueckler, M. (1996). Insulin unmasks a COOH-terminal GLUT4 epitope and increases glucose transport across T-tubules in skeletal muscle. *J. Cell Biol.* 135:415-430.
239. Warburg, A. & Schlein, Y. (1986). The effect of post-bloodmeal nutrition of *Phlebotomus papatasi* on the transmission of *Leishmania major*. *Am. J. Trop. Med. Hyg.* 35:926-930.
240. Webster, P. & Russell, D. G. (1993). The flagellar pocket of trypanosomatids. *Parasitol. Today* 9:201-206.

241. Welburn, S. C., Dale, C., Ellis, D., Beecroft, R. & Pearson, T. (1996). Apoptosis in procyclic *Trypanosoma brucei rhodiense* in vitro. *Death and Differentiation* 3:229-236.
242. Wong, A. K., de Lafaille, M. A. & Wirth, D. F. (1994). Identification of a cis-acting gene regulatory element from the lemDr1 locus of *Leishmania enriettii*. *J. Biol. Chem.* 269:26497-26502.
243. Woods, A., Baines, A. J. & Gull, K. (1992). A high molecular mass phosphoprotein defined by a novel monoclonal antibody is closely associated with the intermicrotubule cross bridges in the *Trypanosoma brucei* cytoskeleton. *J. Cell Sci.* 103:665-675.
244. Wu, Y., Deford, J., Benjamin, R., Lee, M. G.-S. & Ruben, L. (1994). The gene family of EF-hand calcium-binding proteins from the flagellum of *Trypanosoma brucei*. *Biochem.* 304:833-841.
245. Yeagle, P. L. (1985). Cholesterol and the cell membrane. *Biochim. Biophys. Acta* 822:267-287.
246. Yokoyama, K., Trobridge, P., Buckner, F. S., Van Voorhis, W. C., Stuart, K. D. & Gelb, M. H. (1998). Protein farnesyltransferase from *Trypanosoma brucei*. *J. Biol. Chem.* 273:26497-26505.
247. Zhang, J.-T., Lee, C. H., Duthie, M. & Ling, V. (1995). Topological determinants of internal transmembrane segments in P-glycoprotein sequences. *J. Biol. Chem.* 270:1742-1746.

248. Zilberstein, D. & Dwyer, D. (1985). Proton force-driven active transport of D-glucose and L-proline in the protozoan parasite *Leishmania donovani*. *Proc. Natl. Acad. Sci. U.S.A.* 82:1716-1720.

Appendices

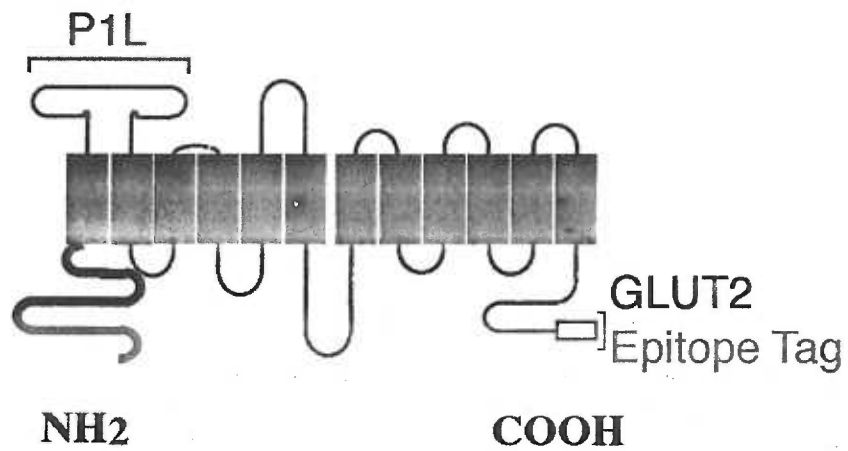
The Appendices contain figures for experiments and data that were not essential for the two manuscript chapters. However, each experiment in the Appendix reveals information that enhances the general understanding of ISO1 and ISO2 targeting or consists of data not shown in the manuscript chapters. Materials and Methods for each figure are listed in the figure legend.

AP1. Immunofluorescence Testing of the Predicted Topology of ISO2

Considerable work has been performed by other laboratories to define the topology of several members of the major facilitator superfamily (MFS)(167) that are 12 transmembrane domain proteins. Since antibodies were available against two hydrophilic domains of the PRO1 transporters, we have used them to partially confirm the Kyte-Doolittle (114) predicted topology of PRO1. To do this we used the anti-P1L antibody that recognizes an external epitope (the first extracellular loop)(211) and the anti-GLUT2 antibody that recognizes the COOH-terminal peptide on the GLUT2 epitope tagged form of ISO2 (Fig. AP-1). Cells expressing the epitope tagged ISO2 were fixed in 4% paraformaldehyde in PBS (pH 7.2) for 30 minutes on ice, washed in 2X in PBS containing 50 mM glycine, and either permeabilized with 0.2% Triton X-100 for 15 minutes or left untreated. Cells were then washed 2X with PBS and stained as previously described (Chapter 2, Materials and Methods). Permeabilized and nonpermeabilized cells were stained using P1L or anti-GLUT2 antiserum. The results (Fig. AP-2) indicate that P1L stains both permeabilized and nonpermeabilized cells, while

anti-GLUT2 stains only permeabilized cells. The staining patterns are consistent with the predicted topology of ISO2.

Figure AP-1. Topology of ISO2 and the regions of ISO2 recognized by the P1L and anti-GLUT2 antibodies. The figure is a model of the predicted membrane topology of the GLUT2 epitope tagged form of ISO2. The sequences recognized by each antibody are bracketed and labeled accordingly.



AP2. Biochemical Characterization of the Cytoskeletal Tethering of ISO2.

In Chapter 2, we tested the ability of ISO1 and ISO2 to associate with the parasite cytoskeleton. Several controls were performed and described as data not shown. Several of these controls are shown in the figures below. In all cases, buffers and procedures were the same as those described in the Materials and Methods in Chapter 2.

Figure AP-2. Immunofluorescence of permeabilized and nonpermeabilized ISO2 expressing *L. enriettii*.

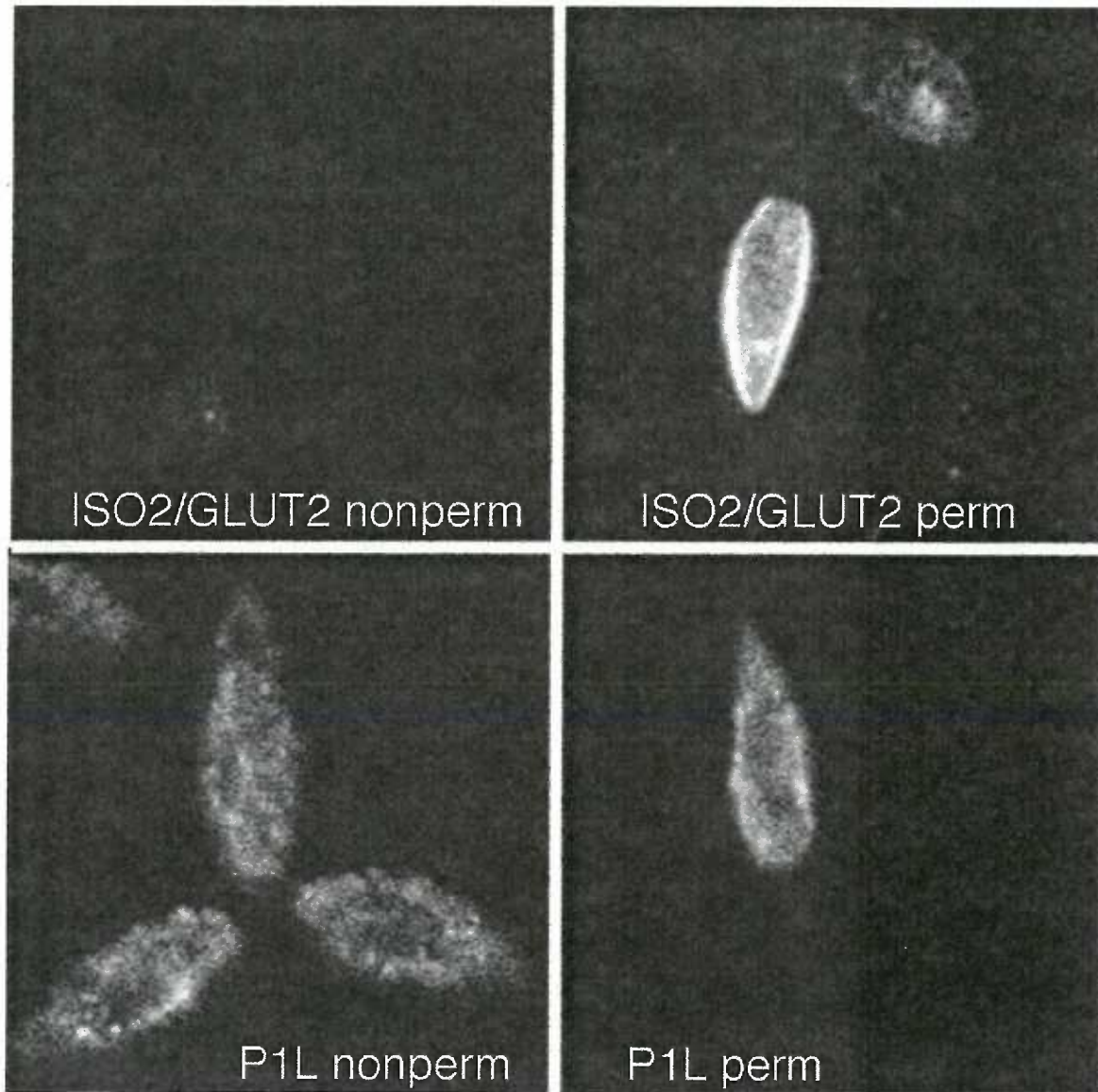


Fig. AP-3 Detergent Extraction of GP63. For this experiment, we wanted to demonstrate that detergent extraction of cytoskeletons had successfully remove all membrane components from the cytoskeletal pellets, allowing us to conclude that proteins present in the cytoskeletal pellet were likely to be associated with the cytoskeleton. For this control experiment, we required a non-tethered membrane protein that should be completely solubilized by detergent. Due to the relative paucity of other characterized integral plasma membrane proteins in *Leishmania*, we used GP63, the major GPI-anchored plasma membrane protein (189). The detergent extracted cytoskeletal pellet and detergent soluble supernatant of wild type *L. donovani* were separated by SDS-PAGE and immunoblotted using a monoclonal murine anti-GP63 antibody, generously provided by Dr. Rob McMaster, and a goat anti-mouse IgG horseradish peroxidase conjugate. The supernatant (*S*) contained a band at approximately 63 kD that was present in the unfractionated lysate (*L*) but was absent in the cytoskeletal pellet (*P*). This result suggests that the detergent extraction was complete enough to quantitatively release any plasma membrane proteins that were not tethered to the cytoskeleton or some other detergent insoluble complex.

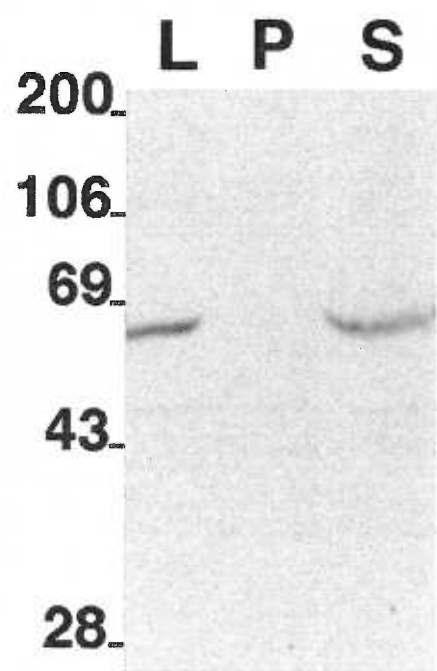


Fig. AP-4. Triton X-100 Extractions. To determine the degree of resistance of ISO2 to detergent extraction by triton X-100, wild type *L. enriettii* were extracted in buffer containing 0.1%, 0.2%, 0.5%, and 1.0% triton X-100, and the pellets and supernatants were immunoblotted and probed with the P1L antibody. In all cases, the 50 kD band that corresponds to ISO2 quantitatively fractionated into the cytoskeletal pellet. This experiment demonstrates that ISO2 could not be released from the pellet by high concentrations (1%) of nonionic detergent, further confirming the association of ISO2 with the cytoskeleton.

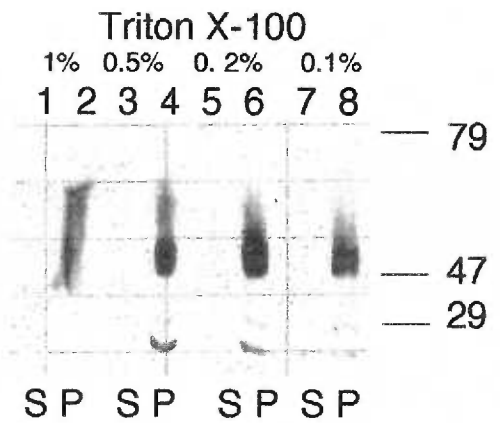
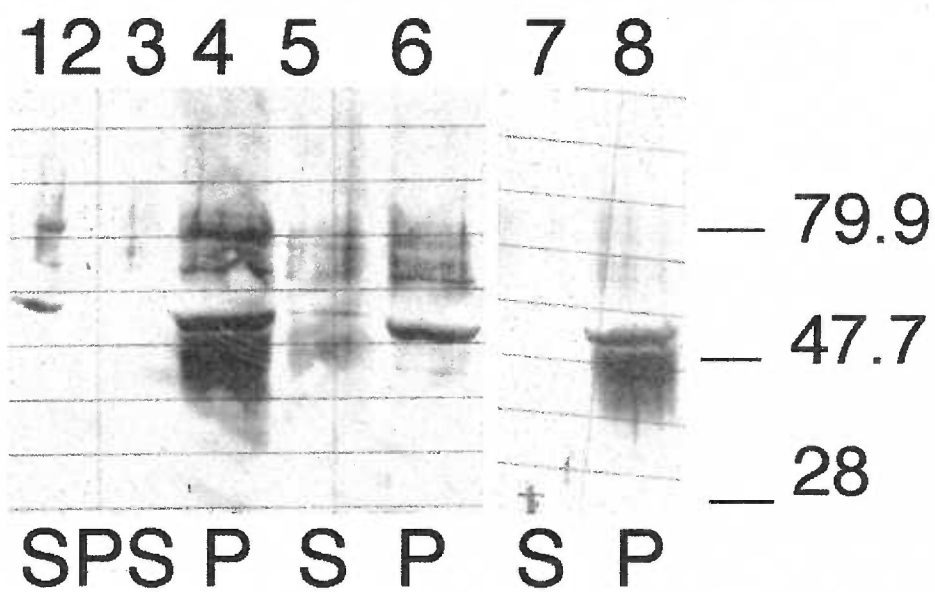


Fig. AP-5. Other Detergent Extractions. A potential caveat of triton X-100 extractions is that certain lipids remain insoluble in triton X-100. Such lipids can form membrane patches that remain associated with the cytoskeleton. To control for this possibility, the detergent used in the extraction buffer was changed to 0.5% octylglucoside (*lanes 3, 4*), 0.5% zwittergent (*lanes 5, 6*), 0.5% NP40 (*lanes 7, 8*), or 2M guanidine with 0.5% CHAPS (*lanes 1, 2*) (a previous experiment had demonstrated that 0.5% CHAPS does not disassociate ISO2 from the cytoskeletal pellet). Extractions were performed with wild type *L. enriettii*, and blots were probed with the PIL antibody. None of the detergents alone disassociated ISO2 from the cytoskeletal pellet. However, the combined detergent/guanidine solution completely disassociated ISO2 from the cytoskeletal pellet. The requirement for the combination of a chaotropic agent and a detergent further suggests that ISO2 forms a tight association with the cytoskeleton.



1, 2 2M Guanidine + 0.5% CHAPS

3, 4 0.5% Octylglucoside

5, 6 0.5% Zwittergent

7, 8 0.5% NP40

Fig. AP-6. SDS extractions. To assess whether ISO2 could be released into the supernatant by a strong ionic detergent, wild type *L. enriettii* cells were extracted with 0.1% (lanes 3, 4) or 1.0% (lanes 5, 6) SDS, and immunoblots were probed with the P1L antibody. Concentrations of SDS as low as 0.1% were sufficient to release the majority of ISO2 into the supernatant, whereas cytoskeletal pellets extracted with 0.5% triton X-100 (lanes 1, 2) quantitatively retained ISO2. *P* refers to the insoluble pellet and *S* the supernatant of each fractionation.

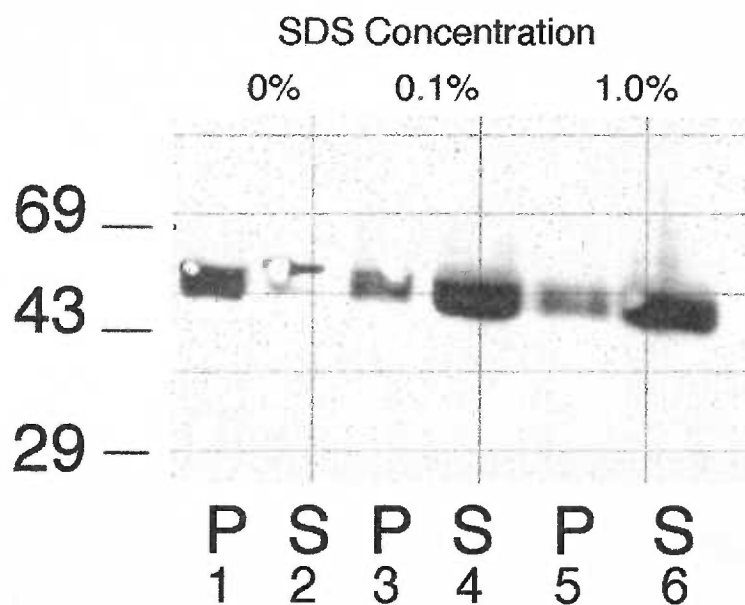
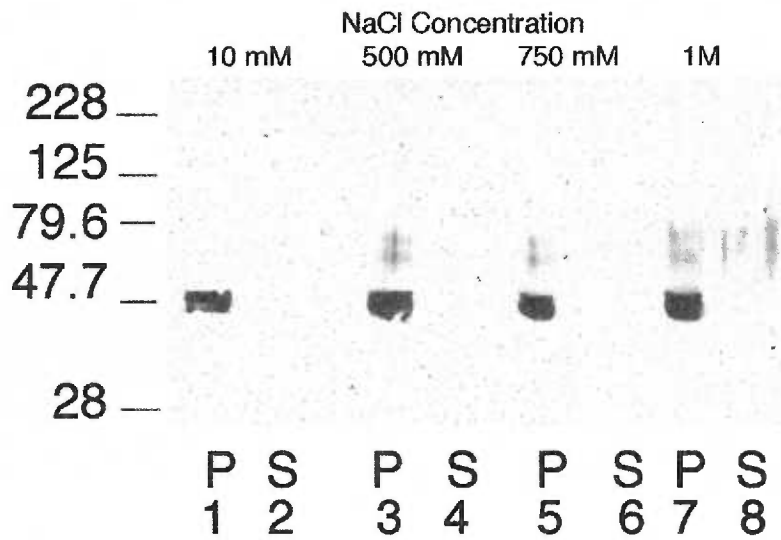


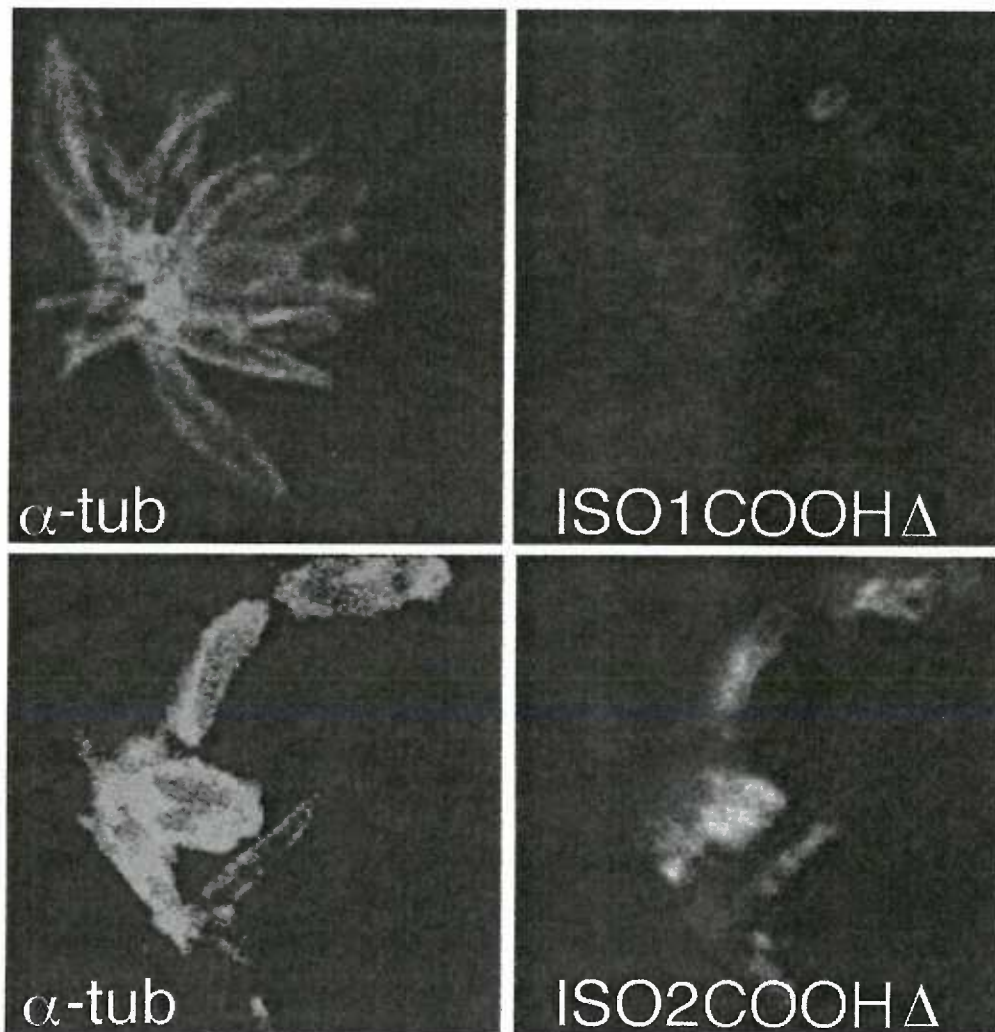
Fig. AP-7. NaCl Extractions. To determine whether high salt could release ISO2 from the cytoskeletal pellet, wild type *L. enriettii* were extracted with increasing concentrations of NaCl. Concentrations ranging from 10 mM to 1 M NaCl did not release ISO2 into the supernatant. *P* indicates the pellet and *S* the supernatant of each fractionation.



AP3. COOH-terminal Deletions of ISO1 and ISO2

One significant, but unresolved, question is whether a specific sequence of ISO2 is involved in interaction with the cytoskeleton and is thus essential for tethering. Studies on mammalian Na⁺/K⁺-ATPase (100) and the "Band 3" anion exchanger (AE1) (57) have revealed that a short sequence of amino acids located within the largest intracellular hydrophilic loop is required for binding each transporter to ankyrin and thus attachment to the spectrin cytoskeleton. We tested whether the COOH-terminal hydrophilic domain of ISO2 might contain sequences important for cytoskeletal tethering. PCR generated constructs of *ISO1* and *ISO2* lacking the COOH-terminal cytoplasmic domain (*ISO1-COOHΔ* and *ISO2-COOHΔ* respectively) and containing the *GLUT2* epitope tag at the COOH terminus were cloned into the [*pX63 HYG*] expression vector and transfected into *L. enriettii*. Confocal immunofluorescence microscopy using the anti-GLUT2 and anti- α -tubulin antibodies (Fig. AP-8) demonstrated that detergent extracted cytoskeletons of the *ISO2-COOHΔ* expressing cells stained intensely for ISO2, while the *ISO1-COOHΔ* expressing cells displayed only background level staining. We conclude that the COOH-terminal hydrophilic domain of ISO2 does not play a significant role in cytoskeletal tethering.

Figure AP-8. Immunofluorescence of Detergent Extracted Cytoskeletons from Cells Expressing ISO1 or ISO2 with COOH-terminal Deletions.



AP4. Alignment of ISO1 NH₂-terminus with Yeast Glucose Sensors.

Several glucose transporters in fungi serve as glucose sensors. The transporters (or transporter-like proteins in some cases) sense glucose in the extracellular environment and induce changes in the level of transcription of hexose transporter genes and other genes (99). The sensing function has been mapped to conserved amino acid sequences in the COOH-terminal hydrophilic domain of the sensor proteins.

Many membrane proteins that localize to the flagellar membrane have environmental sensing functions. The Receptor Adenylate Cyclases in *T. brucei brucei* are the best characterized example (166). The flagellar localization of ISO1 suggests the speculative possibility that it might have a role in sensing glucose. We decided to examine the ISO1 NH₂-terminal hydrophilic sequence for potential homologies to the fungal sensor consensus. The sensor domains of *S. cerevisiae* glucose sensors SNF3, SNF3.2, RGT2, and *K. lactis* KLRAG4 were aligned against amino acids 42-61 of ISO1 (Fig. AP-9). A space between the first two positions for the yeast sensor domains was added to improve the alignment with ISO1. Amino acids that are identical between ISO1 and most or all of the yeast proteins are indicated in capitalized bold lettering. Common amino acids between the four yeast sensors are in lowercase italicized letters.

Although a possible homology has been found, this similarity is still highly speculative and will require testing for a sensor function. In particular, it is noteworthy that the level of identity between the four yeast sensor domains is considerably higher than that between the yeast and *Leishmania* sequences.

Possible experimental approaches to address a potential sensor function for the ISO1 protein are described in Chapter 4.

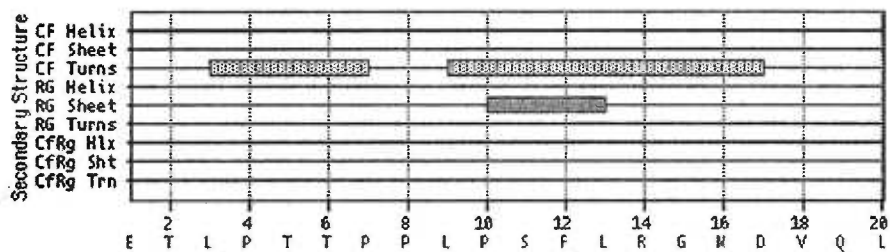
Figure AP-9. Alignment of Yeast Sensor Domains and the NH₂-terminus of ISO1.

	<i>S. cerevisiae</i>	
	SNF3	D - L g n G I a L n A Y N R R G G p p p S I - L
	SNF3.2	D - L g n G I a L n A Y N R R G G p p p S - - L
	<i>K. lactis</i>	
	KLRAG4	D - L g n T I g I t T Y Q R R G G p p p S V - L
	<i>L. enriettii</i>	
	ISO1	E t L p t T p p L p S F L R R G n - - V q L

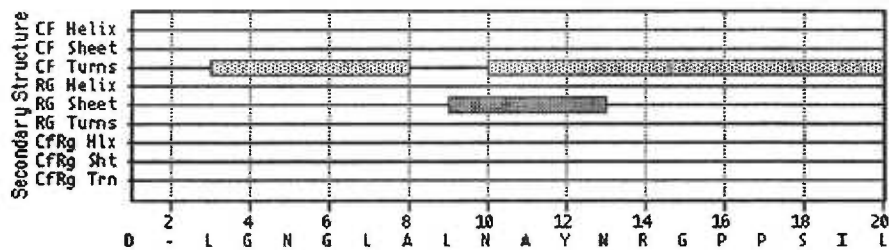
A clear difference in the ISO1 alignment exists in the nonconserved amino acids. However, differences in the amino acid sequences may not necessarily affect the secondary structures. We used computer analysis to compare the potential secondary structures of the consensus sensor domain and the corresponding domain of ISO1. The sensor domain of SNF3.1 and amino acids 42-61 of ISO1 were analyzed for potential secondary structure motifs using two different prediction algorithms in MacVector 5.0 (Chou Fasman and Robson-Garnier) (Fig. AP-10). For both proteins, the Chou Fasman (CF) analysis predicts two turn-rich domains that partially align with each other. The Robson-Garnier (RG) algorithm predicts a β -sheet domain over common aligned sequences between the two proteins. Although the sequences of the yeast and *Leishmania* proteins do not align exactly, the similarities in predicted secondary structures do suggest that the nonconserved amino acids do not contribute to dramatically different folding patterns between the various sequences. The secondary structure predictions do not demonstrate a sensor function for ISO1, but the predictions do support the plausibility of this speculative hypothesis.

Figure AP-10. Comparison of the Predicted Secondary Structures of ISO1 and the SNF3.1 Sensor Domain.

ISO1 AA 42-60



SNF3.1 AA 776-795



AP5. Galleries of Alanine Mutants of ISO1

The following figures are the galleries of confocal immunofluorescence images of 30 cells from wild type ISO1 and each alanine mutant (P22A, P23A, R24A, R25A, T26A, G27A, T28A, T29A, S30A, H31A, and A32G) referred to in Chapter 3 and analyzed in Tables 3-4 and 3-5. Staining and confocal immunofluorescence microscopy were performed as described in the Materials and Methods section of Chapter 3.

Figure AP-11. ISO1 Gallery.

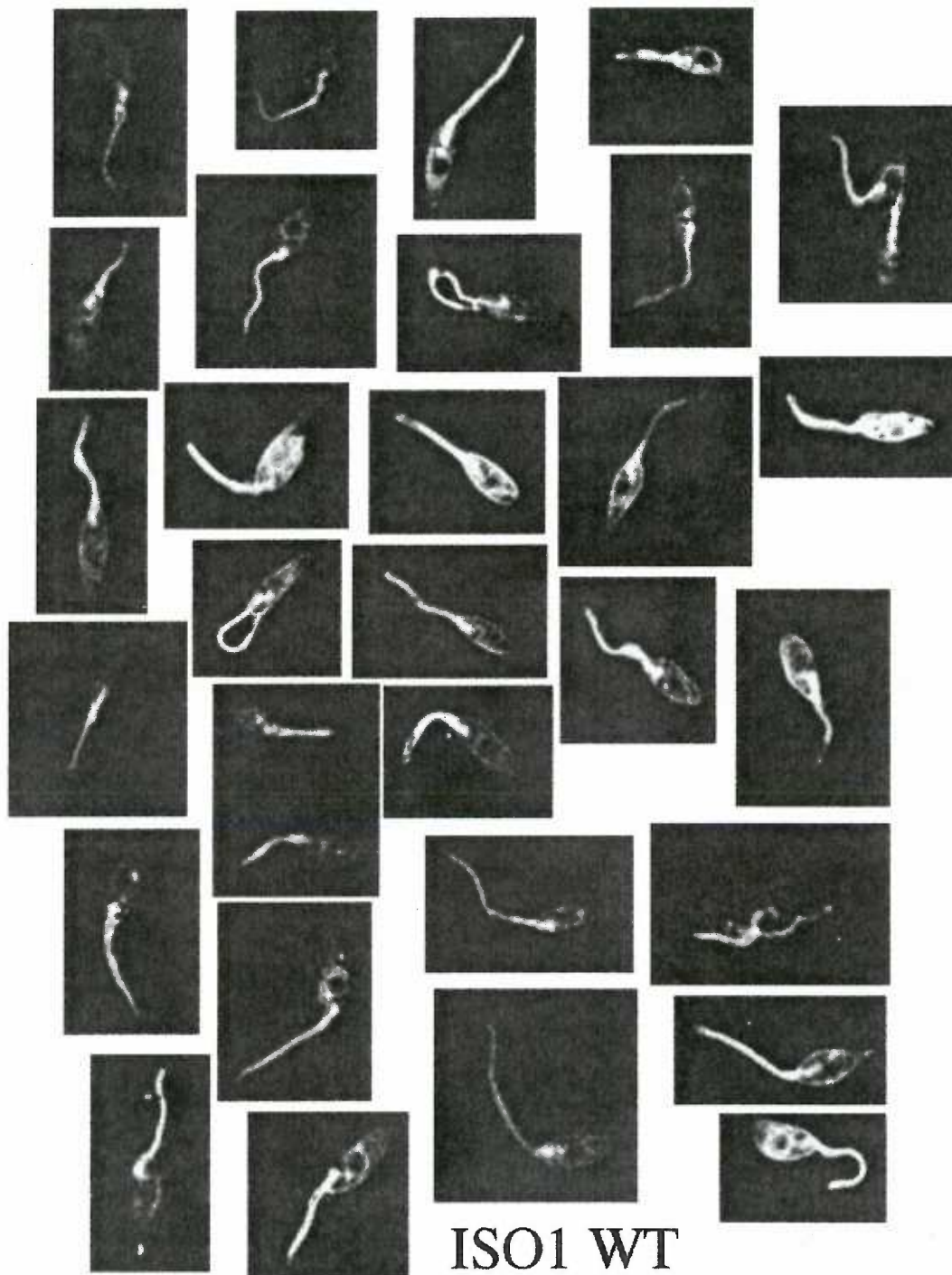


Figure AP-12. P22A Gallery.

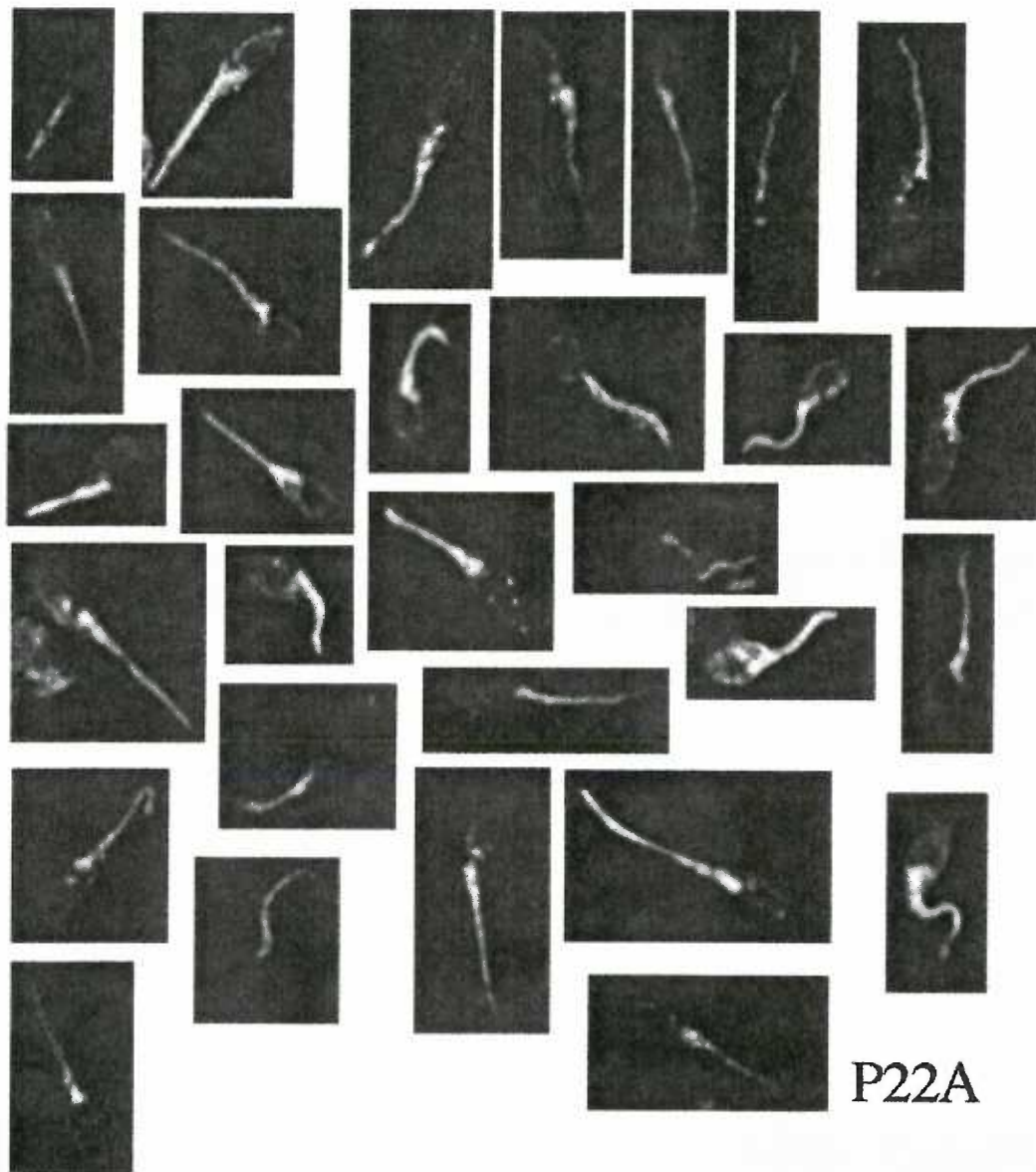


Figure AP-13. P23A Gallery.



Figure AP-14. R24A Gallery.

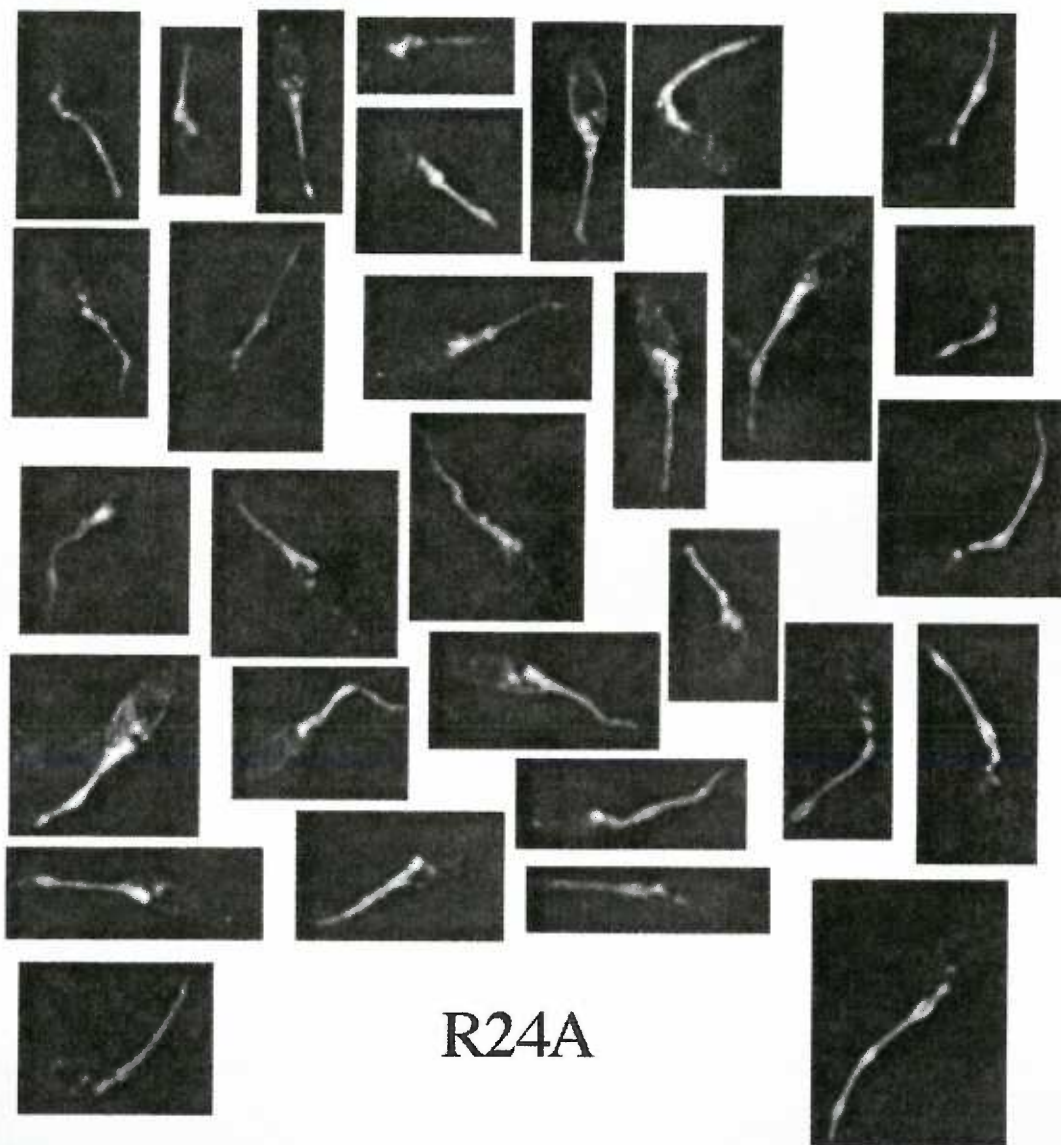


Figure AP-15. R25A Gallery.



Figure AP-16. T26A Gallery.

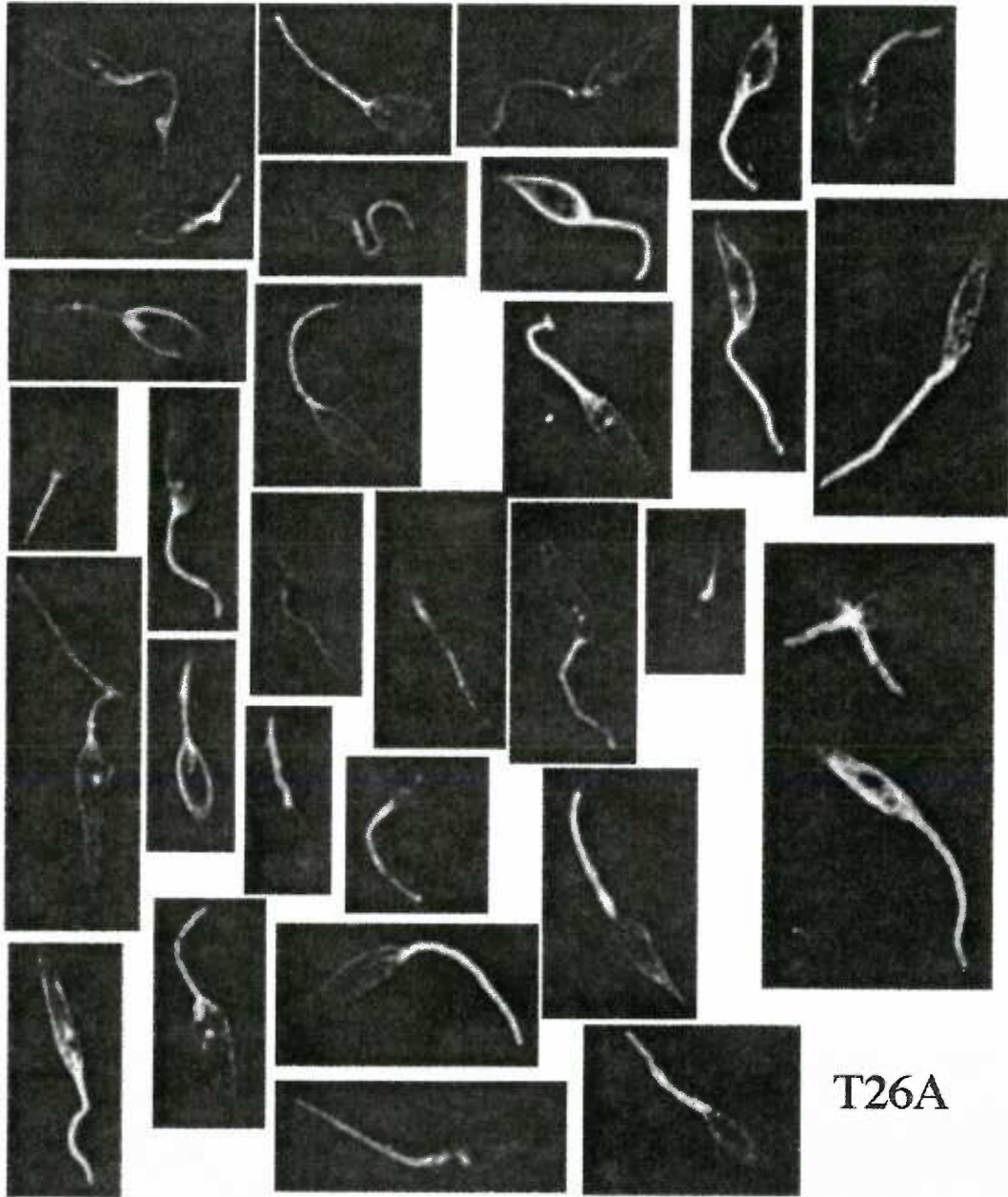


Figure AP-17. G27A Gallery.

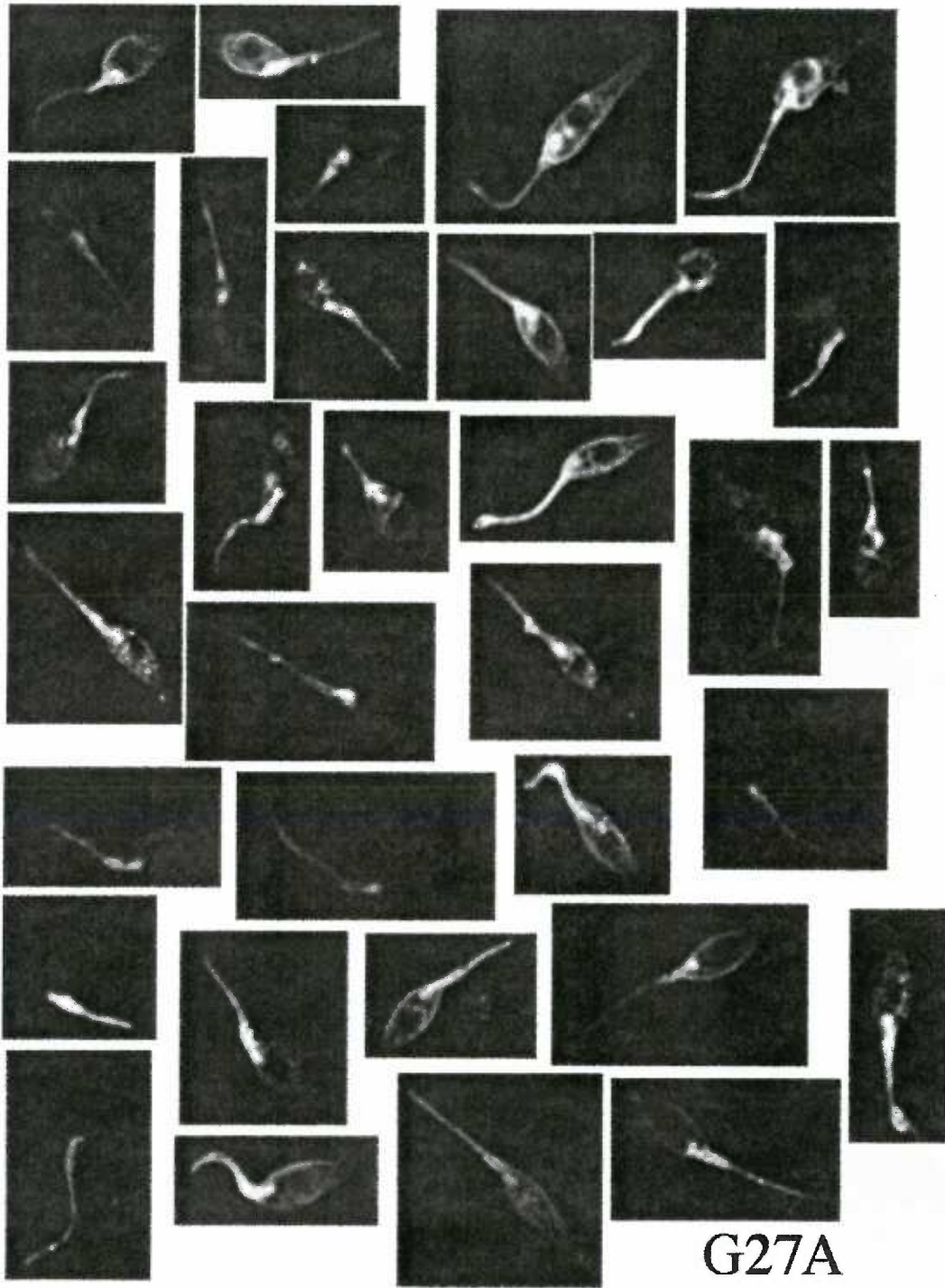


Figure AP-18. T28A Gallery.

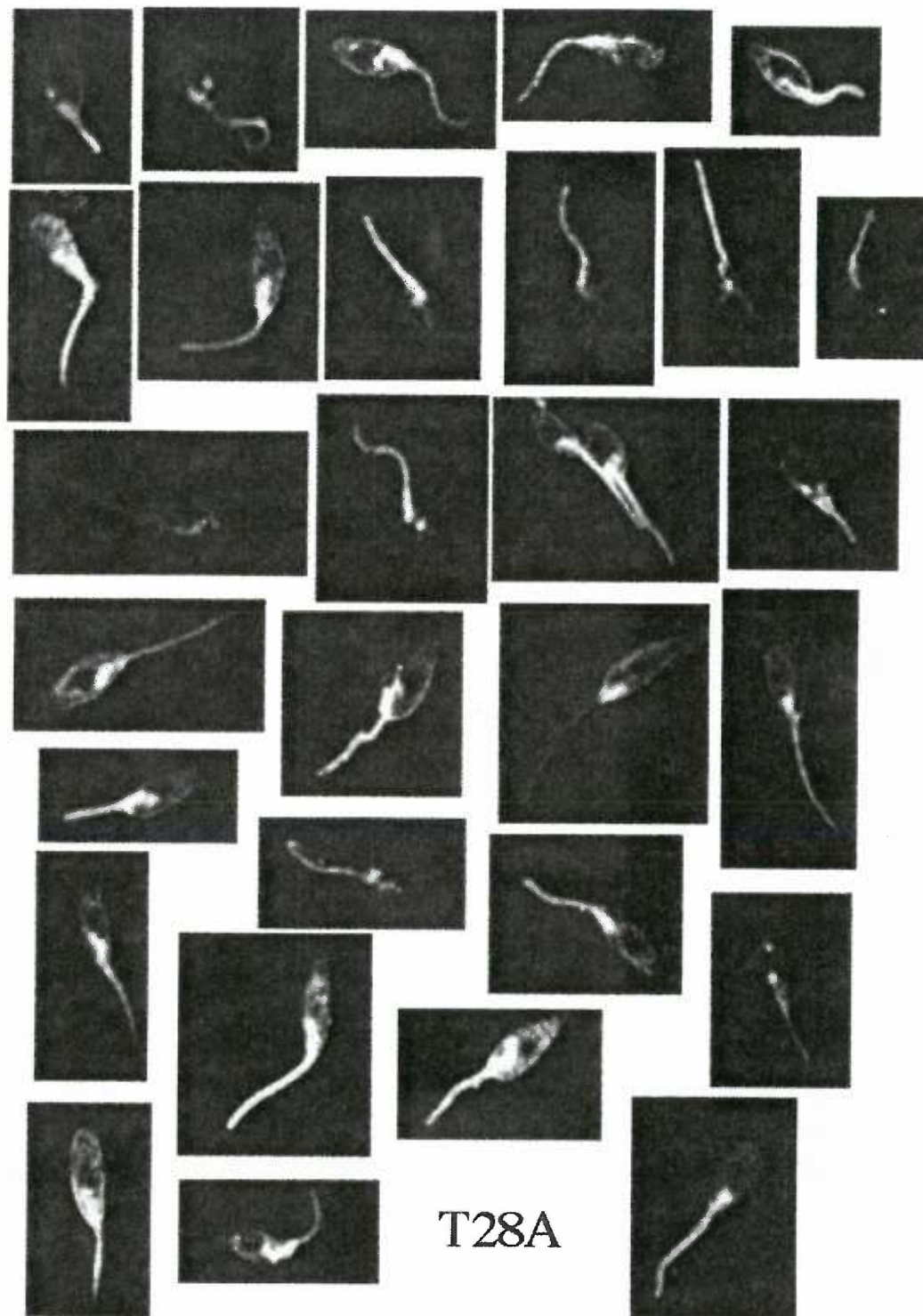


Figure AP-19. T29A Gallery.

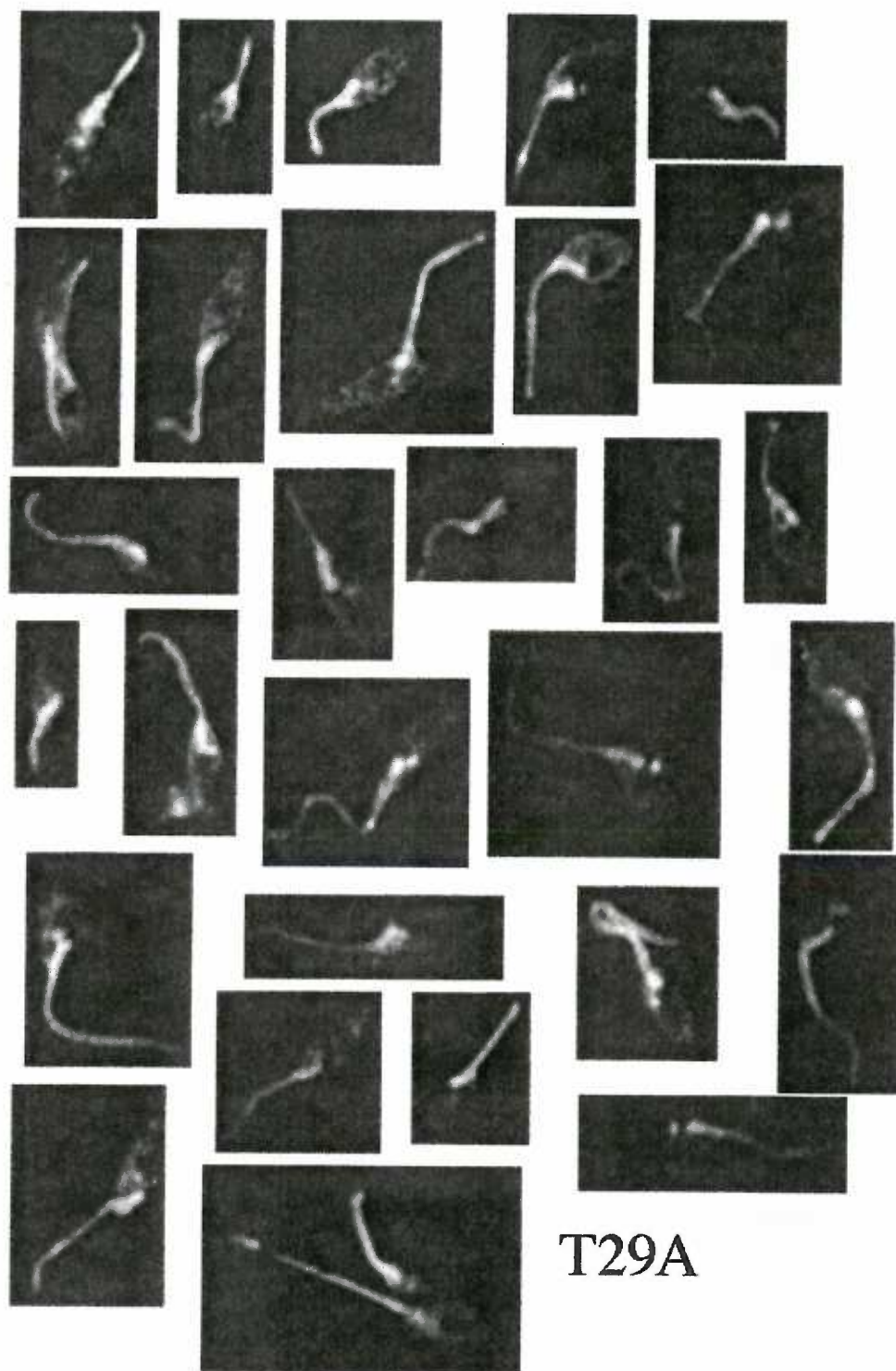


Figure AP-20. S30A Gallery.

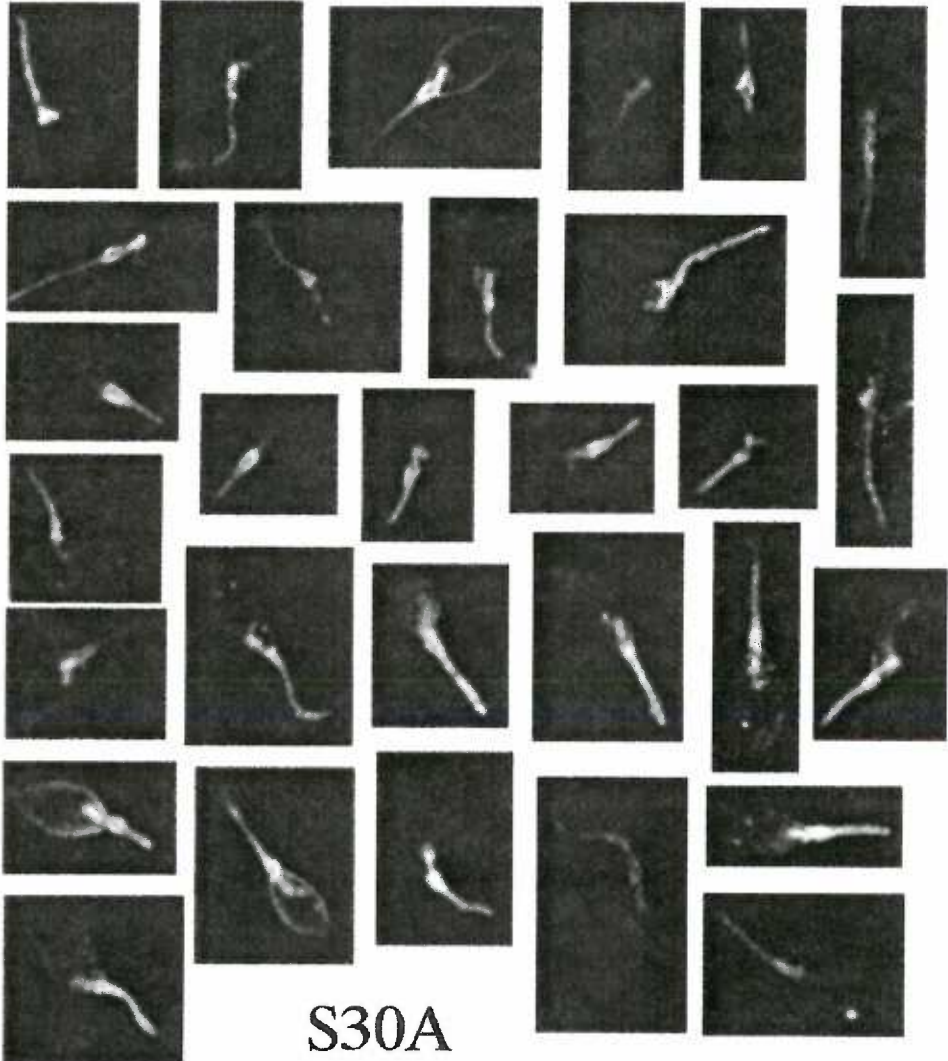
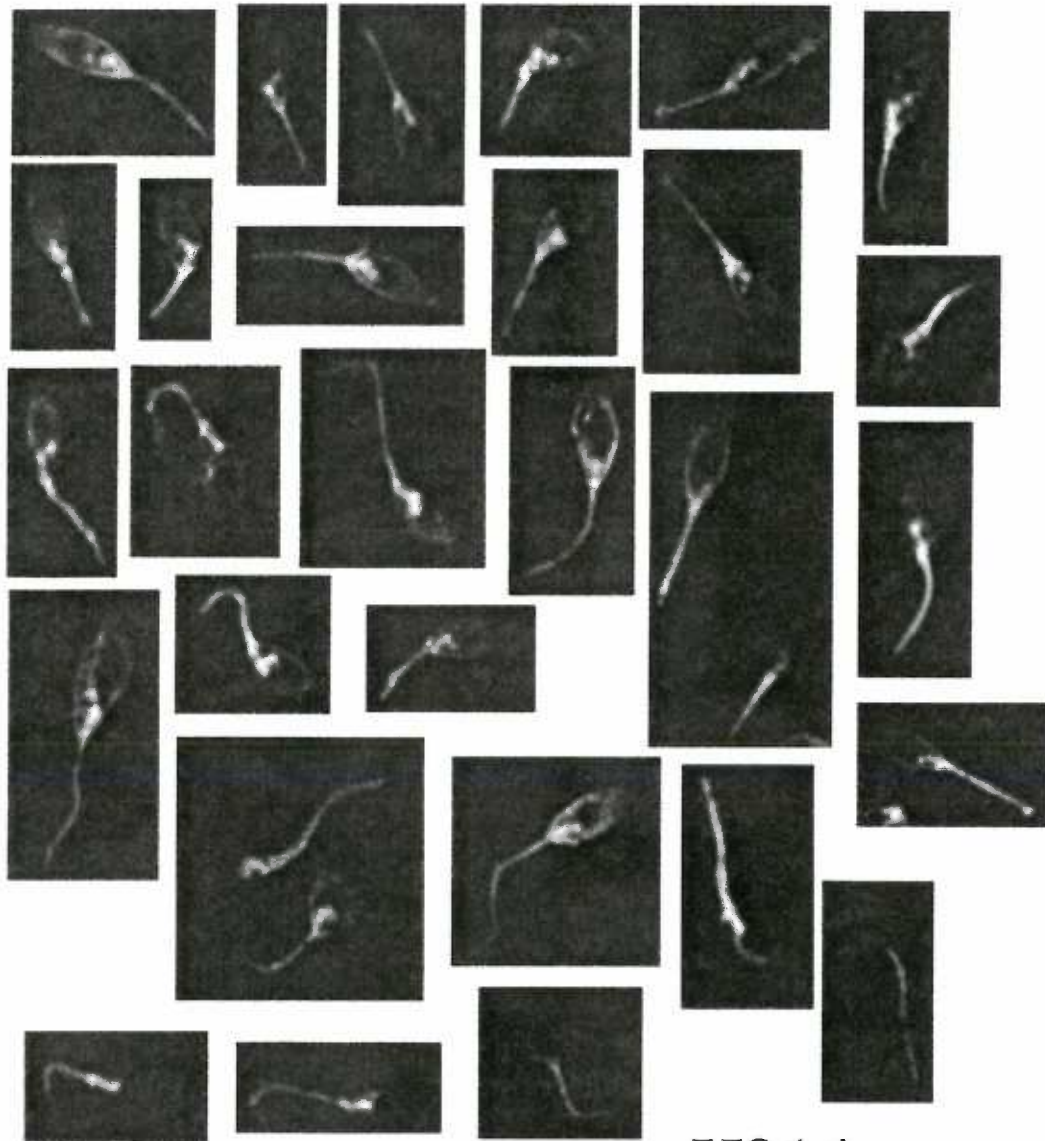


Figure AP-21. H31A Gallery.



H31A

Figure AP-22. A32G Gallery.

